

*VŠB – Technical University of Ostrava
Nanotechnology Centre*

NanoOstrava 2019



6th Nanomaterials and Nanotechnology Meeting

*May 13-16, 2019
Ostrava*

ISBN 978-80-248-4290-5

Book of Abstracts, Programme and General Information
(International conference)

NanoOstrava 2019 – 6th Nanomaterials and Nanotechnology Meeting

VŠB – Technical University of Ostrava, Czech Republic

May 13-16, 2019

Published by Vydavatelství VŠB – TU Ostrava

17. listopadu 2172/15, 708 00 Ostrava

Czech Republic

Proceedings were designed by

Ing. Sylva Holešová, Ph.D.

ISBN 978-80-248-4290-5

PROJECT PARTNERS

The Statutory City of Ostrava financially supported realization of conference NanoOstrava 2019.

OSTRAVA!!!

Conference **NanoOstrava 2019** was supported by following projects:

Nanotechnology – the basis for international cooperation project, reg. no. **CZ.1.07/2.3.00/20.0074**, supported by Operational Programme Education for Competitiveness funded by Structural Funds of the European Union and state budget of the Czech Republic.



Dear Conference participants, Visitors and Colleagues,

We welcome you to the NanoOstrava 2019 - 6th international biennial 'Nanomaterials and Nanotechnology Meeting' in Ostrava, which is the centre of the Moravian-Silesian region and, at the same time, the third largest city in the Czech Republic. The symposium will be held at VŠB-Technical University of Ostrava, which has more than 170 years of existence. The University provides world class education in 7 Faculties offering Bachelor's, Master's, PhD, and exchange programmes to students from six continents.

The conference is organized under cooperation of scientists from the Nanotechnology Centre (VŠB-TU of Ostrava) and Institute of Geonics AS CR.

The meeting is a platform to facilitate open discussions between scientists, students and representatives from companies with a vested interest in furthering the development of nanomaterials and nanotechnology. Conference supports young scientist and enthusiastic students helping them to open doors to scientific career.

Five scientific sessions in field of nanoscience will be introduced by eminent world-known lecturers and number of scientist and one session for presenters from the industry.

1. Advanced Nanomaterials
2. Nanomaterials Characterizations and Devices
3. Nanotech for Energy
4. Nanotech for Medicine and Pharmacy
5. Nanotech for Environmental Solution
6. Industrial Forum

We wish you successful and fruitful conference – and enjoy Ostrava!

Organizing committee of NOM 2019

Organizing Committee:

Jaromír Pištora (Chairman of Conference)

Nanotechnology Centre, VŠB-Technical University of Ostrava, Czech Republic

Karla Čech Barabaszová

Nanotechnology Centre, VŠB-Technical University of Ostrava, Czech Republic

Sylva Holešová

Nanotechnology Centre, VŠB-Technical University of Ostrava, Czech Republic

Marianna Hundáková

Nanotechnology Centre, VŠB-Technical University of Ostrava, Czech Republic

Gabriela Kratošová

Nanotechnology Centre, VŠB-Technical University of Ostrava, Czech Republic

Lenka Pazourková

Nanotechnology Centre, VŠB-Technical University of Ostrava, Czech Republic

Daniela Plachá

Nanotechnology Centre, VŠB-Technical University of Ostrava, Czech Republic

Grażyna Simha Martynková

Nanotechnology Centre, VŠB-Technical University of Ostrava, Czech Republic

Vlastimil Matějka

Department of Chemistry, VŠB-Technical University of Ostrava, Czech Republic

Radim Škuta

Department of Chemistry, VŠB-Technical University of Ostrava, Czech Republic

Eva Plevová

Institute of Geonics of CAS, Ostrava

Lenka Vaculíková

Institute of Geonics of CAS, Ostrava

Věra Valovičová

Institute of Geonics of CAS, Ostrava

Scientific Committee:

Alicja Bachmatiuk

Centre of Polymer and Carbon Materials, Polish Academy of Sciences, Poland

Miroslav Boča

Institute of Inorganic Chemistry, Slovak Academy of Sciences, Slovakia

Michael Cada

Dalhousie University, Halifax, Canada

Pavla Čapková

University of J. E. Purkyně, Ústí nad Labem, Czech Republic

Josef Jampílek

Comenius University, Bratislava, Slovakia

Dušan Kimmer

SPUR, a.s., Zlín, Czech Republic

Yafei Lyu

Beijing University of Chemical Technology, Beijing, China

Lucie Obalová

Institute of Environmental Technology, VŠB-Technical University of Ostrava, Czech Republic

Jaromír Pištora

Nanotechnology Centre, VŠB-Technical University of Ostrava, Czech Republic

Petr Praus

Faculty of Materials Science and Technology, VŠB-Technical University of Ostrava, Czech Republic

Daniela Predoi

NIMP, Magurele, Romania

Vijay Ramani

ICARES, Washington University in St. Louis, USA

Mark Rümmeli

Institute for Solid State Research, IFW Dresden, Germany

Ivo Šafařík

Palacky University, České Budějovice, Czech Republic

Marta Valášková

Institute of Environmental Technology, VŠB-Technical University of Ostrava, Czech Republic

Welcome from NanoOstrava 2019 Organizing Committee Chair

On behalf of NanoOstrava 2019 Organizing Committee, it is my honour and pleasure to welcome you to the NanoOstrava 2019, 6th Nanomaterials and Nanotechnology Meeting. The conference is aimed to scientists, students and representatives from companies, which deal with nanomaterials and nanotechnology.

Our Program Committee has tried to prepare an interesting and informative technical program outlining current progress and activities in many research areas of nanotechnology. Over 100 abstracts from more than 10 countries have been accepted and scheduled for the 3-day conference.

Participants of the conference are cordially invited to contribute original research papers to Special Issue of Open Access Journal by MDPI – *Nanomaterials* and also to Special Issue of Open Access Journal by MDPI – *Materials*.

Conference is organized at VŠB – Technical University of Ostrava campus, where study and research is closely related to the fact that Ostrava, the third largest city in the Czech Republic, is an important industrial part of Central Europe. Our University draws on 170 years of research and academic excellence to provide world class education in 7 Faculties offering Bachelor's, Master's, PhD, and exchange programmes to students from six continents.

I wish you to have beneficial conference and I hope that you will enjoy both scientific and cultural aspects of the conference programme as well as your stay in Ostrava.


Jaromír Pistora
Chairman, NanoOstrava 2019

SPONSORS

The organizers would like to thank the following companies for generously sponsoring this meeting:

ANAMET



ANTON PAAR



CHROMSPEC



EDLIN



MĚŘÍČÍ TECHNIKA MORAVA



NANO CHEMI GROUP



NICOLET



OPTIK INSTRUMENTS



NENOVISION



RIGAKU



SPECION



TESCAN



CONFERENCE PAPERS

Conference full papers should present these substantial conditions: high quality research, original ideas, not published anywhere else. Conference full papers will be published in following journals.

Special papers in Open Access Journals:

Nanomaterials

is an international and interdisciplinary scholarly open access journal. It publishes reviews, regular research papers, communications, and short notes that are relevant to any field of



nanomaterials

an Open Access Journal by MDPI

study that involves nanomaterials, with respect to their science and application. Thus, theoretical and experimental articles will be accepted, along with articles that deal with the synthesis and use of nanomaterials. **Nanomaterials** is dedicated to a high scientific standard. All manuscripts undergo a rigorous reviewing process and decisions are based on the recommendations of independent reviewers.

Current IF= 3.504

Participants of the conference are cordially invited to contribute original research papers or reviews to special issue "Nanotech for Medicine and Pharmacy: Selected Papers from Nano Ostrava Meeting 2019".

For publication in Nanomaterials, please contact: **Daniela Plachá** (daniela.placha@vsb.cz).

Deadline for manuscript submissions: **30 June 2019**

Materials

is an open access journal of related scientific research and technology development. It publishes reviews, regular research papers and short communications. **Materials** provides a



materials

an Open Access Journal by MDPI

forum for publishing papers which advance the in-depth understanding of the relationship between the structure, the properties or the functions of all kinds of materials.

Current IF= 2.467

Participants of the conference are cordially invited to contribute original research papers or reviews to special issue "Research in Nanostructures, Interfaces and Nanocomposites of Functional Ceramics".

For publication in Materials, please contact: **Grazyna Simha Martynkova** (grazyna.simha@vsb.cz)

Deadline for manuscript submissions: **20 December 2019**

The agreement established between conference organizers and MDPI publisher allows for manuscripts submission to these special issues discount on the APCs.

Conference proceedings:

Materials Today: Proceedings

Materials Today: Proceedings provides the materials science community with a fast and flexible route to the publication of research presented at leading scientific conferences spanning the field of materials science, technology and engineering.

For publication in Materials Today: Proceedings send your manuscript to: **Grażyna Simha Martynková** (grazyna.simha@vsb.cz).

Deadline for manuscript submissions: **20 June 2019**



Conference papers:

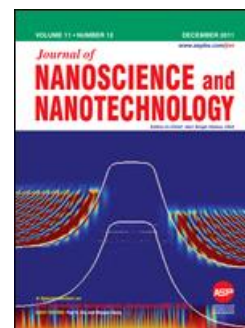
Journal of nanoscience and nanotechnology (JNN)

JNN is a multidisciplinary peer-reviewed journal covering fundamental and applied research in all disciplines of science, engineering and medicine. JNN publishes all aspects of nanoscale science and technology dealing with materials synthesis, processing, nanofabrication, nanoprobe, spectroscopy, properties, biological systems, nanostructures, theory and computation, nanoelectronics, nano-optics, nano-mechanics, nanodevices, nanobiotechnology, nanomedicine, nanotoxicology.

Current IF= 1.354

For publication in Journal of nanoscience and nanotechnology send your manuscript to: **Grażyna Simha Martynková** (grazyna.simha@vsb.cz).

Deadline for manuscript submissions: **20 June 2019**



PROGRAMME

NanoOstrava 2019	9:00 am	10:30 am	1:15 pm	3:30 pm
Monday 13				Registration till 6:30pm Welcome Party
Tuesday 14	Registration Opening ceremony <u>Plenary lecture</u> <i>Ewa Serwicka</i>	TOPIC 1	TOPIC 2 <u>Invited lecture</u> <i>Frank DelRio</i>	Trip – Landek Park Ostrava
Wednesday 15	TOPIC 2 <u>Invited lecture</u> <i>Des Richardson</i>	TOPIC 4	TOPIC 1 <u>Invited lecture</u> <i>Jaroslav Šesták</i>	Posters Section 7:00 pm Conference Evening
	TOPIC 5 <u>Invited lecture</u> <i>Inga Zinicovskaia</i>		TOPIC 3 <u>Invited lecture</u> <i>Jan Macák</i>	
Thursday 16	TOPIC 3 <u>Invited lecture</u> <i>Hatem Akbulut</i>	TOPIC 3	Closing ceremony	

May 13 - 16, New aula, VŠB-TU Ostrava

NanoOstrava 2019

Monday, May 13**16:00-18:00****Registration and Welcome party** (new aula, in front of room NA1 and room NA2)**Tuesday, May 14****from 8:00****Registration** (new aula, in front of room NA1)**9:00 - 9:30****Opening ceremony, Chairman's Welcome** (room NA2)**9:30 - 10:00****Plenary lecture** (room NA2)**E. M. Serwicka**: *Nanostructural catalysts derived from clay minerals***10:00 - 10:15****Coffee break** (in front of room NA2)**Topic 1 – Advanced Nanomaterials** (room NA3)**10:15 - 10:30****P. Piotrowski**, A. Kielczewska, K. Zarębska, M. Skompska, A. Kaim: *New C₆₀ and C₇₀ fullerene derivatives designed for HOMO-LUMO gap tuning in photovoltaic devices***10:30 - 10:45****M. Sandomierski**, B. Strzemiecka, A. Voelkel: *The influence of thin aryl layers on the surface of fillers on the properties of composites***10:45 - 11:00****M. Foda**, C. Zou, H. Bahlol, H. Han: *New insights of dual-emission fluorescent nanoprobes for imaging metal ions in living cells***11:00 - 11:15****L. Bardoňová**, A. Kotzianová, K. Mamulová Kutláková, S. Holešová, J. Klemeš: *Electrospinning of nanofibrous layers containing antibacterial vermiculite***11:15 - 11:30****P. Ryšánek**, P. Čapková, M. Malý, M. Kormunda, Z. Kolská, M. Munzarová: *Antibacterial functionalization of electrospun nanofibrous membranes***11:30 - 11:45****M. Bílý**, K. Čech Barabaszová, S. Holešová, M. Hundáková: *CuO nanoparticles in antibacterial PVAc/vermiculite nanocomposite*

12:00 - 13:00

Lunch (room NA2)

Topic 2 - Nanomaterials Characterizations and Devices (room NA3)

13:00 - 13:30

Invited lecture

B.-C. Tran Khac, K.-H. Chung, **F. W. DelRio**: *Friction and fracture of 2D materials*

13:30 - 13:45

B. Strzemiecka, A. Jamrozik, Ł. Klapiszewski, P. Jakubowska, D. Matykiewicz, M. Sandomierski, T. Jesionowski, A. Voelkel: *The importance of adhesion between fillers and polymer matrix on the utility macro-properties of the composites materials*

13:45 - 14:00

G. Simha Martynková, G. Kratošová, R. Škuta, S. Sathish, K. Lafdi: *Structural study of thin films of graphene oxide with biosilver nanoparticles*

14:00 - 14:15

G. Jandieri, J. Pistora, M. Lesnak: *Interaction of electromagnetic waves with plasmonic structures in the terrestrial atmosphere*

14:15 - 14:30

M. Tokarčíková, L. Bardoňová, J. Seidlerová, K. Drobíková, O. Motyka: *Magnetically modified montmorillonite - characterization, sorption properties and stability*

14:30 - 14:45

J. Vlček, J. Pištora, M. Lesňák: *Resonance states in plasmonic-waveguiding structures*

14:45 - 15:00

M. Mičica, S. Eliet, M. Vanwolleghem, R. Motiyenko, A. Pienkina, L. Margulès, K. Postava, J. Pištora, J.-F. Lampin: *Measurement of THz gain in optically pumped ammonia gas*

15:00 - 15:15

A. Babusenar, S. Mondal, S. Ramaswamy, S. Dutta, M. Gopalakrishnan, J. Bhattacharyya: *Phenomenological and experimental investigation of exciton dissociation mechanism in organic semiconductor blends*

15:15 - 15:30

Coffee break (in front of room NA2)

16:15 - 19:00

Trip - Landek Park Ostrava

Wednesday, May 15 - Part1

Topic 4 - Nanotech for Medicine and Pharmacy (room NA3)

9:00 - 9:40

Invited lecture

Q. Miao, D. Xu, Z. Wang, L. Xu, T. Wang, Y. Wu, D. B. Lovejoy, D. S. Kalinowski, G. Nie, Y. Zhao, **D. R. Richardson**: *Amphiphilic hyper-branched co-polymer nanoparticles for the controlled delivery of novel anti-tumor agents*

9:40 - 9:55

M. Serda, M. J. Ware, J. M. Newton, M. Krzykawska-Serda, K. Malarz, A. Mrozek-Wilczkiewicz, R. Musioł, S. J. Corr, S. A. Curley, Lon J. Wilson: *The water-soluble [60]fullerene derivatives for anti-cancer studies*

9:55 - 10:20

D. Plachá: *Graphenic materials for biomedical applications*

10:20 - 10:45

J. Jampilek: *Nanomaterials for management of toxigenic fungi*

10:45 - 10:55

Coffee break (in front of room NA2)

10:55 - 11:20

W. Musiał, T. Urbaniak: *The influence of technical procedure on the hydrodynamic diameter of conjugates of lamivudine with biodegradable poly- ϵ -caprolactone microspheres for controlled drug delivery via cellular uptake*

11:20 - 11:45

A. Voelkel, B. Strzemiecka, M. Sandomierski: *Applications of Inverse Gas Chromatography and Dynamic Vapor Sorption for the physicochemical characterization of nanomaterials*

11:45 - 12:10

J. Silberring, A. Drabik, J. Ner-Kluza, A. Bodzoń-Kuśakowska, P. Suder: *Identification of biomolecules – a frustrating nano-business*

12:10 - 12:25

J. Bednář, P. Mančík, L. Svoboda, V. Foldyna, R. Dvorský: *Antimicrobial Silicate Nanomaterial with High Specific Surface Area*

12:25 - 12:40

D. Lazecká, S. Holešová, G. Simha Martynková: *Polymeric nanocomposites as a prevention of biofilm formation*

12:40 - 13:30

Lunch (room NA2)

Topic 1 – Advanced Nanomaterials (room NA3)

13:30 - 14:00

Invited lecture

J. Šesták: *Thermal Physics of Nanostructured Materials: Thermodynamic (Top-Down) and Quantum (Bottom-Up) Issues*

14:00 - 14:15

D. Gültekin, E. Duru, H. Akbulut: *Nanoceria reinforced Ni/CeO₂ nanocomposite production by electroless coating*

14:15 - 14:30

D. Gültekin, **F. Kayis,** H. Akbulut: *Morphological Evaluation of Zinc Oxide Nanostructures Synthesized by Solution Based Methods*

Topic 3 – Nanotech for Energy (room NA3)

14:30 - 15:00

Invited lecture

J. M. Macák: *One dimensional anodic nanostructures for energy applications*

15:00 - 15:15

Ubeyd Toçoğlu, Hatem Akbulut: *Towards high capacity rGO/MWCNT/ yolk-shell structured silicon composite anodes for li-ion batteries*

15:15 - 15:30

Coffee break (in front of room NA2)

Wednesday, May 15 - Part2

Topic 5 – Nanotech for Environmental Solution (room NA4)

9:00 - 9:30

Invited lecture

I. Zinicovskaia: *Neutron Activation Analysis and Related Analytical Techniques in the Assessment of Nanoparticle Uptake in Organisms*

9:30 - 9:45

O. Motyka, K. Štrbová, I. Zinicovskaia: *Chlorophyll content in two medicinal plant species following nano-TiO₂ exposure*

9:45- 10:00

K. Drobíková, **K. Štrbová**, M. Tokarčíková, O. Motyka, J. Seidlerová: *Magnetically modified bentonite: characterization and stability*

10:0- 10:15

I. Safarik, J. Prochazkova, E. Baldikova, K. Pospiskova, K. Drobikova, J. Seidlerova: *Progressive magnetically responsive materials for pollutants detection and removal*

10:15- 10:30

Z. Jankovská, M. Vaštyl, G. J. F. Cruz, L. Matějová: *Microwave preparation of activated carbons from residual agricultural biomass*

10:30 - 10:45

Coffee break (in front of room NA2)

10:45 - 11:00

G. Kratošová, S. Teplická, J. Klusák, M. Večeř: *Preparation of tailored nanoparticles using flow microreactors and green synthesis*

11:00- 11:15

Z. Konvičková, V. Holíšová, M. Kolenčík, K. Dědková, E. Dobročka, H. Otoupalíková, G. Kratošová, J. Seidlerová: *Effects of Biomass Heterogeneous Composition in Silver Nanoparticles Phytosynthesis Using Tilia sp. Leachate*

11:15- 11:45

M. Baláž: *Mechanochemistry as a versatile tool for nanomaterials synthesis*

12:00 - 13:00

Lunch (room NA2)

Topic 6 – Industrial Forum (room NA4)**13:00 - 13:15**

NenoVision: *AFM-in-SEM LiteScope™: Tool for comprehensive sample surface analysis*

13:15 - 13:30

Nicolet: *Scattering-Type Scanning Near-field Optical Microscopy and Spectroscopy of Low Dimensional and nanostructured materials*

13:30 - 13:45

Rigaku: *Rigaku SAXS and XRF instrumentation*

13:45 - 14:00

Anton Paar: *Metody charakterizace nanomateriálů*

14:00 - 14:15

Edlin: *Advanced ion milling of SEM and TEM samples*

14:15 - 14:30

NANO CHEMI GOUP: *Industrial Applications of Nanotechnologies*

14:30 - 14:45

Měřící technika Morava: *Chemistry at the Nanoscale with AFM-IR*

14:45 - 15:00

Contipro: A. Kotzianová, J. Klemeš, M. Pokorný, V. Velebný: *Research and development of nanotechnologies and nanomaterials*

15:00 - 15:30

Coffee break (in front of room NA2)

15:30 - 16:45

Poster section (new aula, between rooms NA1 and NA4)

19:00 - 23:30

Conference evening (room NA2)

Thursday, May 16

Topic 3 – Nanotech for Energy (room NA3)

9:00 - 9:30

Invited lecture

H. Akbulut, M. Tokur, T. Çetinkaya: *Nanocomposite Ceramic Based Negative Electrodes for Li-ion Batteries*

9:30 - 9:45

M. Michalska, J.-Y. Lin: *Li₄Ti₅O₁₂ spinel modified with carbon or oxide coatings as an advanced anode material for high-rate lithium-ion batteries*

9:45 - 10:00

S. K. Sathish, B. Novosad, K. Chrobáček, G. Simha Martynková: *Study of Clay-PEO system as application as solid electrolyte in Li-ion batteries*

10:00 - 10:15

S. Prabu, H.-W. Wang: *Nanocatalysts for hydrolysis of Al and H₂O reaction: Efficient synthesis of graphite-derived thin layer with Al(OH)₃ based nanoparticles*

10:15 - 10:30

Coffee break (in front of room NA2)

10:30 - 11:00

D. Legut, H. Tian, Z. W. Seh, K. Yan, Z. Fu, P. Tang, Y. Lu, R. F. Zhang, Y. Cui, and Q. Zhang:
Flexible anode materials and their protection

11:00- 11:20

J. Seidlerová, M. Valášková: *Several ways of FexOy/phyllsilicate composite preparation*

11:20 - 11:30

Closing ceremony (room NA3)

12:00 - 13:00

Lunch (room NA2)

LIST OF POSTER PRESENTATIONS**Topic 1 – Advanced Nanomaterials****P1**

K. Bahranowski, A. Klimek, A. Gaweł, A. Tomczyk, E. M. Serwicka: *Pillared montmorillonites as carbon dioxide nanosorbents*

P2

P. Čapková, P. Ryšánek, J. Štojdl, J. Trögl, O. Benada, M. Kormunda, Z. Kolská, M. Munzarová: *Functionalization and stability testing of nanofibrous PA6/DTAB membranes for air filtration*

P3

K. Čech Barabaszová, S. Holešová, K. Švábová, L. Chlebíková: *PVDF/vermiculite nanocomposite films*

P4_S

P. Grussmann, I. Martausová, Z. Lacný, A. Martaus, D. Cvejn: *Towards Clay Nanoreactors: Modified Clays as Catalysts for Baeyer-Villiger Reaction*

P5_S

D. Kędra, A. Baliś, Sz. Zapotoczny: *Photoactive mesoporous nanoparticles as photochemical reactors*

P6

K. Kopecká, L. Beneš, K. Melánová, P. Knotek, V. Zima, K. Zetková: *Layered double hydroxides: synthesis, exfoliation and dispersion in polymer systems*

P7_S

T. Kuciel, P. Nalepa, W. Górka, M. Szuwarzyński, S. Zapotoczny: *Nanocomposite systems based on polymer brushes and superparamagnetic iron oxide nanoparticles*

P8

M. Michalska, V. Matejka, J. Pavlovsky, P. Praus, G. S. Martynkova: *Comparison of TiO₂ and g-C₃N₄-based materials modified with Ag NPs utilized as a photocatalyst for degradation of model dye acid orange 7*

P9_S

P. Nalepa, W. Górka, T. Kuciel, M. Szuwarzyński, S. Zapotoczny: *Magnetically-responsive polymeric scaffolds for cell cultures*

P10

P. Otipka, J. Vlček: *Shape dependent model of EMA for nanostructured anisotropic materials*

P11

Z. Posel, P. Posocco: *Tuning the properties of nanogel surface coatings by grafting weak cationic polyelectrolyte brushes*

P12

A. Michalik, B. D. Napruszewska, A. Walczyk, J. Kryściak-Czerwenka, D. Duraczyńska, R. Dula, R. Karcz, **E. M. Serwicka**: *Starch as template for synthesis of nanocrystalline hydrotalcites*

P13

M. Valášková, P. Leštinský: α -Fe₂O₃ nanoparticles/vermiculite for catalytic decomposition of polystyrene

Topic 2 - Nanomaterials Characterizations and Devices**P14**

I. Jendrzejewska, Z. Barsova, T. Goryczka, E. Pietrasik, J. Goraus, J. Czerniewski, J. Jampilek: *Synthesis and structural, thermal and magnetic properties of Mn-doped CuCr₂Se₄ nanoparticles*

P15

J. Krček: *Surface polaritons at periodic interface – near field analysis*

P16

E. Plevova, L. Vaculikova, V. Valovicova, G. Simha Martynkova: *Thermal behaviour of organically modified smectites*

P17

A. Slíva, R. Brázda, K. Čech Barabaszová, G. Simha Martynková: *Gyromixer of nanostructured systems and method of mixing thereof*

P18_S

M. Słowikowska, A. Wójcik, K. Wolski, S. Zapotoczny: *Structural characterization of ladder-like conjugated polymer brushes*

P19

B. Thomasová, J. Thomas, L. Gembalová, V. Tomášek: *Preparation and characterization of fly ash based membranes for microfiltration and ultrafiltration*

P20

V. Valovičová, L. Vaculíková, E. Plevová, S. Dolinská, I. Znamenáčková, Z. Danková: *Characterization of fine-grained montmorillonite fractions suitable for composite preparation*

P21_S

Z. Vilamová, Z. Konvičková, P. Mikeš, V. Holíšová, P. Mančík, E. Dobročka, G. Kratošová, J. Seidlerová: *Ag-AgCl Nanoparticles Fixation on Electrospun PVA Fibers: Technological Concept and Progress*

Topic 3 – Nanotech for Energy**P22_S**

S. Prabu, H.-W. Wang: *Nanocatalysts for hydrolysis of Al and H₂O reaction: Efficient synthesis of graphite-derived thin layer with Al(OH)₃ based nanoparticles*

P23

Monika Michalska, Jeng-Yu Lin: *Synthesis and electrochemical properties of LiNi_{0.5}Mn_{1.5}O₄ surface modified with NiO coating as a cathode material for lithium-ion batteries*

P24_S

O. Skurikhina, R. Tarasenko, V. Tkáč, M. Orendáč, M. Fabián, M. Senna, V. Šepelák, E. Tóthová: *Fe(III) source-dependent properties of mechano/thermally synthesized $\text{LiFeSi}_2\text{O}_6$*

P25_S

A. J. Wójcik, M. Słowikowska, K. Wolski, S. Zapotoczny: *New acetylene and pyridine derivatives as monomers for conductive polymer brushes fabrication*

Topic 4 - Nanotech for Medicine and Pharmacy

P26

M. Dołowy, P. Perez Martinez, A. Pyka-Pająk, J. Jampilek: *Nanoparticles as effective delivery systems for steroidal drugs*

P27

M. Gasztych, W. Musiał: *Variability of electrokinetic potential of N-isopropylacrylamide derivatives in function of particles composition*

P28

A. Gola, A. Niżniowska, W. Musiał: *The influence of initiator concentration on physico-chemical properties on n-vinylcaprolactam derivatives*

P29

S. Holešová, K. Čech Barabaszová, M. Hundáková, M. Ščuková: *Synthesis and antimicrobial activity of ciclopiroxolamine/ZnO/vermiculite nanocomposites*

P30

S. Holešová, Y. Tarasiuk, M. Hundáková, E. Pazdziora: *Determination and characterization of metronidazole/imidazole/clay interaction*

P31

V. Kozik, A. Bąk, A. Świetlicka, A. Środa, **J. Jampilek**, W. Priebe, J. Jazowiecka-Rakus, A. Sochanik: *Potential Anticancer Drug Nanocarriers*

P32

M. Gargulák, N. Štrofová, M. Kepinska, H. Milnerowicz, A. E. Ofomaja, B. Hosnedlová, C. Fernandez, P. Vašíčková, **R. Kizek**: *CdTe QDs-based electrochemical assay for sensitive detection of African swine fever virus*

P33

N. Štrofová, M. Gargulák, K. Sehnal, M. Kepinska, H. Milnerowicz, C. Fernandez, J. Sochor, B. Hosnedlová, **R. Kizek**: *Effect of silver nanoparticles (AgNPs) prepared by green synthesis from sage leaves (*Salvia officinalis*) on maize plants*

P34

S. Vallová, B. Sokolová, V. Valovičová, **E. Plevová**: *Adsorption of pharmaceuticals from aqueous solutions onto clay minerals*

P35_S

M. Sandomierski, Z. Buchwald, M. Zielińska, A. Voelkel: *Micro- and mesoporous zeolites with high ion exchange capacity as materials with potential biomedical applications*

P36

K. Piechura, P. Mielczarek, **J. Silberring**: *The novel inhibitor of cysteine proteases*

P37_S

K. Škrlová, Z. Rybková, K. Malachová, D. Plachá: *Biocompatible polymer materials with antimicrobial properties for preparation of stents*

P38

M. Masár, **P. Troška**, J. Hradski, I. Talian: *Application of silver nanoparticles for analysis of pharmaceutical samples by microchip isotachopheresis with Raman spectroscopy*

P39_S

A. Verner, J. Tokarský: *Molecular modeling study of antibacterial molecules on nylon 6,6 surface*

Topic 5 – Nanotech for Environmental Solution

P40_S

A. Behal, V. D. Rajput: *Effect of titanium dioxide nanoparticles on extracellular polymeric substances under sunlight*

P41_S

K. Foniok, A. Smýkalová, V. Matějka, P. Praus: *A synthesis of composites of kaolin/g-C₃N₄ and metakaolin/g-C₃N₄*

P42

Z. Jankovská, M. Večeř, I. Koutník, L. Matějová: *A case study of waste scrap tyre-derived carbon blacks tested for nitrogen, carbon dioxide and cyclohexane adsorption*

P43

M. Kolenčík, D. Ernst, M. Šebesta, M. Urík, G. Kratošová, Z. Konvičková, M. Bujdoš, I. Černý, E. Dobročka, I. Vávra, H. Feng, Y. Qian, R. Illa: *Effect of different type of nanoparticles on crop production*

P44_S

M. Kováčová, M. Baláž, E. Dutková: *Bio-mechanochemical synthesis of silver nanoparticles using *Thymus vulgaris* L. plant*

P45

S. Rebilasová, **V. Matějka**, K. Foniok, K. Mamulová Kutláková, J. Vlček: *Utilization of photoactive clay/TiO₂ and quartz/TiO₂ composites in cement pastes*

P46

P. Matějková, V. Matějka, J. Vlček: *Activation of granulated blast furnace slag using powder activator*

P47

H. Ovčáčíková, J. Vlček, M. Klarová, M. Topinková: *Non-traditional glaze from iron waste*

P48_S

L. Procházka, P. Mec: *Possibility of Using Fly Ash After Denitrification by SNCR as Admixture in Alkali-activated Materials*

P49

M. Šihor, M. Valášková, M. Edelmannová, K. Kočí: *Ceramic cordierite/CeO₂ for photocatalytic reduction of CO₂*

P50_S

A. Smýkalová, B. Sokolová, K. Foniok, V. Matějka, P. Praus: *Degradation of pharmaceuticals by using three different photocatalysts*

P51

J. Tokarský, K. Mamulová Kutláková, R. Podlipná, T. Vaněk: *Phytotoxicity of ZnO / kaolinite nanocomposite - is the anchoring the right way to lower environmental risk?*

P52

S. Dolinská, I. Znamenáčková, J. Tomčová, V. Valovičová, **L. Vaculíková**, E. Plevová: *Application of bentonite-manganese oxide composites in removal of heavy metals*

GENERAL INFORMATION ABOUT POSTER SECTION

Wednesday, May 15

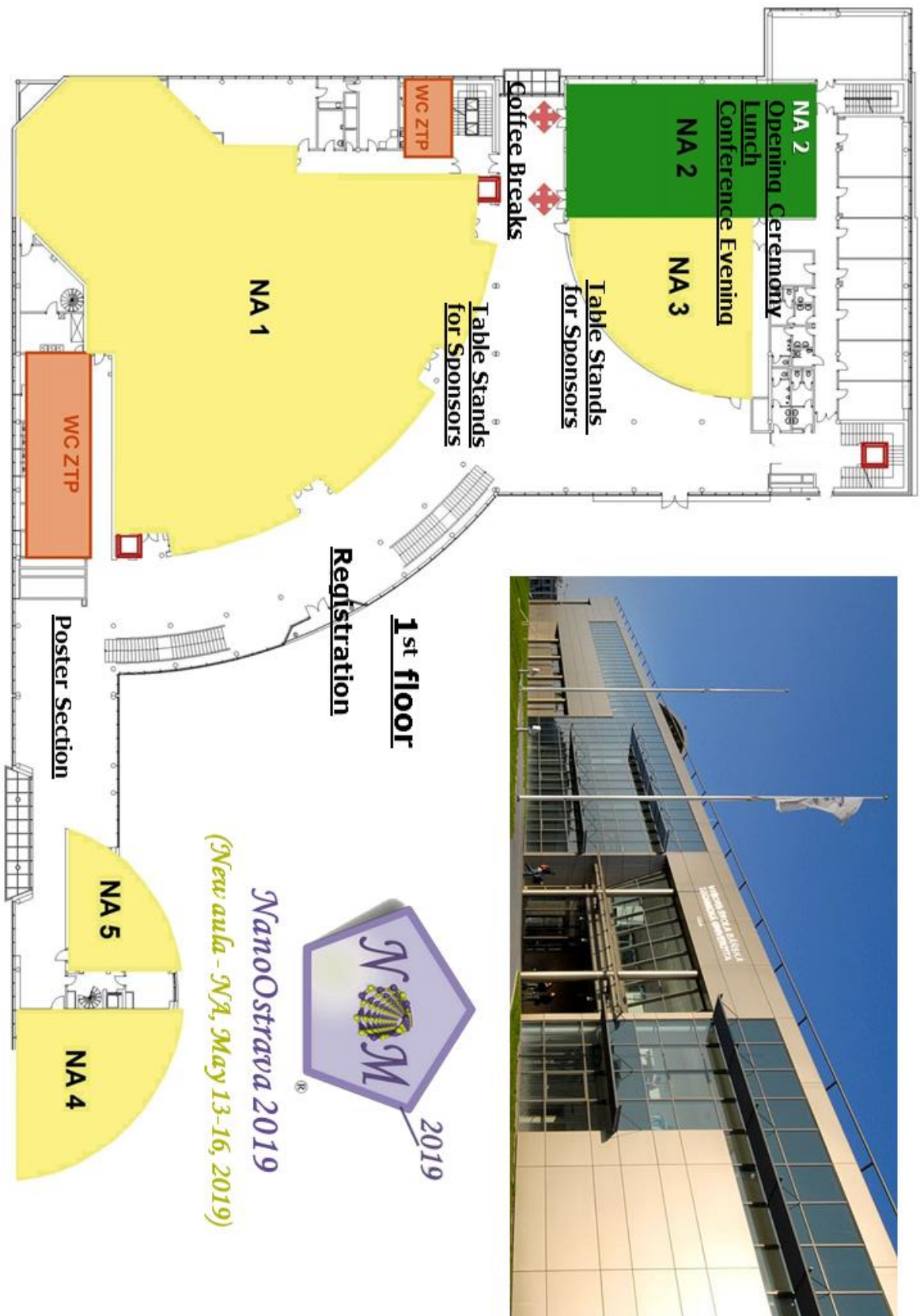
15:30 - 16:45

(new aula, between rooms NA1 and NA4)

You can set up your poster from Wednesday morning time.

Posters should be prepared in format A0 approx. 90 x 120 cm or smaller. The best **3 students posters** will be awarded. Special evaluation committee will be established and during the poster section all student's posters will be evaluate and best 3 awarded with diploma and practical price.

We kindly ask all students to take a part in the evaluation of poster competition during the conference evening.



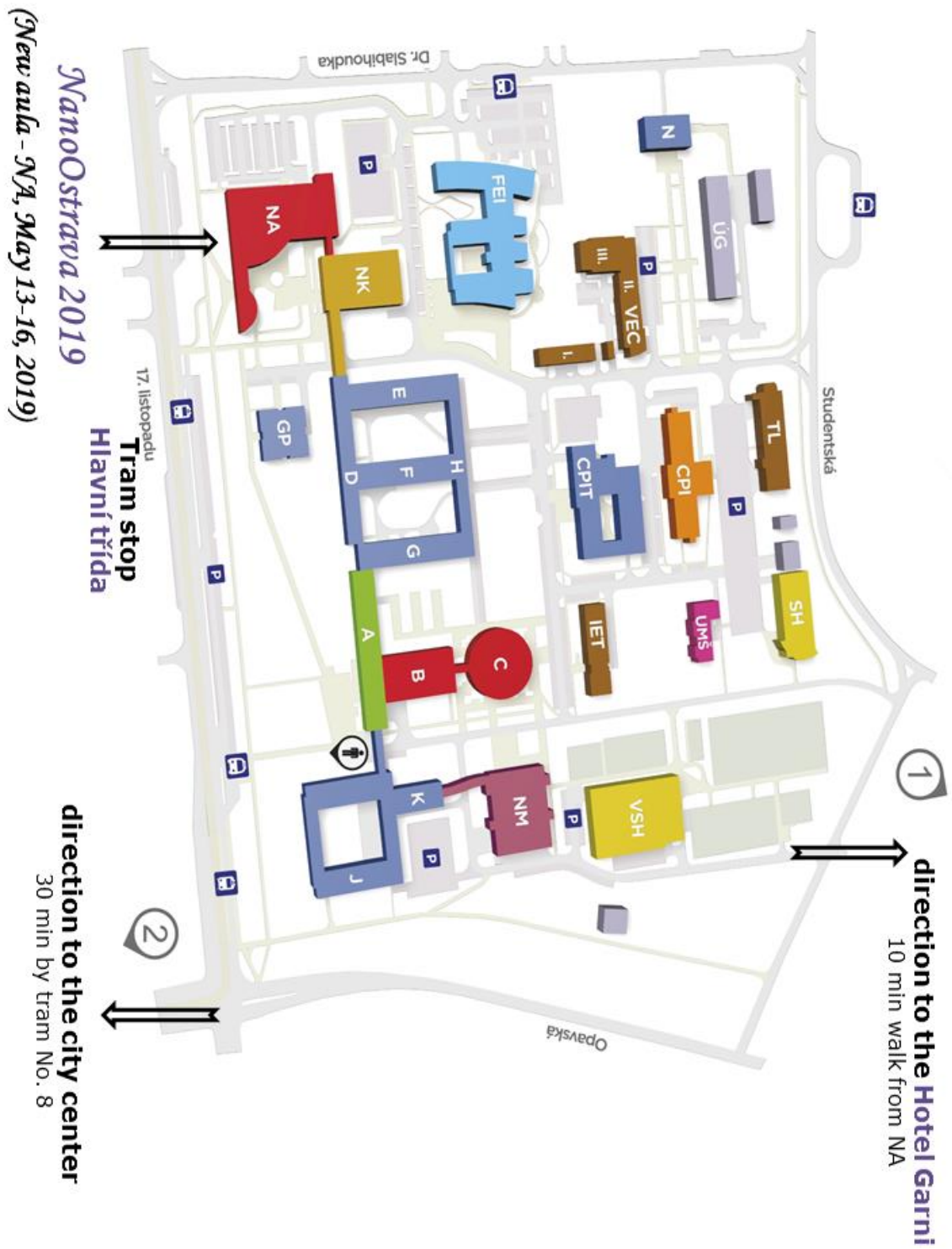


Table of content

Topic 1 – Advanced Nanomaterials

Invited lectures (IL):

E. M. Serwicka: <i>Nanostructural catalysts derived from clay minerals</i>	33
J. Šesták: <i>Thermal Physics of Nanostructured Materials: Thermodynamic (Top-Down) and Quantum (Bottom-Up) Issues</i>	33

Oral presentations (OP):

L. Bardoňová, A. Kotzianová, K. Mamulová Kutláková, S. Holešová, J. Klemeš: <i>Electrospinning of nanofibrous layers containing antibacterial vermiculite</i>	35
M. Bílý, K. Čech Barabaszová, S. Holešová, M. Hundáková: <i>CuO nanoparticles in antibacterial PVAc/vermiculite nanocomposite</i>	38
M. Foda, C. Zou, H. Bahlol, H. Han: <i>New insights of dual-emission fluorescent nanoprobe for imaging metal ions in living cells</i>	40
D. Gültekin, E. Duru, H. Akbulut: <i>Nanoceria reinforced Ni/CeO₂ nanocomposite production by electroless coating</i>	41
D. Gültekin, F. Kayış, H. Akbulut: <i>Morphological Evaluation of Zinc Oxide Nanostructures Synthesized by Solution Based Methods</i>	43
P. Piotrowski, A. Kielczewska, K. Zarębska, M. Skompska, A. Kaim: <i>New C₆₀ and C₇₀ fullerene derivatives designed for HOMO-LUMO gap tuning in photovoltaic devices</i>	45
P. Ryšánek, P. Čapková, M. Malý, M. Kormunda, Z. Kolská, M. Munzarová: <i>Antibacterial functionalization of electrospun nanofibrous membranes</i>	47
M. Sandomierski, B. Strzemieska, A. Voelkel: <i>The influence of thin aryl layers on the surface of fillers on the properties of composites</i>	47

Poster presentations (PP):

K. Bahranowski, A. Klimek, A. Gaweł, A. Tomczyk, E. M. Serwicka: <i>Pillared montmorillonites as carbon dioxide nanosorbents</i>	50
P. Čapková, P. Ryšánek, J. Štojdl, J. Trögl, O. Benada, M. Kormunda, Z. Kolská, M. Munzarová: <i>Functionalization and stability testing of nanofibrous PA6/DTAB membranes for air filtration</i>	52
K. Čech Barabaszová, S. Holešová, K. Švábová, L. Chlebíková: <i>PVDF/vermiculite nanocomposite films</i>	53
P. Grussmann, I. Martausová, Z. Lacný, A. Martaus, D. Cvejn: <i>Towards Clay Nanoreactors: Modified Clays as Catalysts for Baeyer-Villiger Reaction</i>	53
D. Kędra, A. Baliś, Sz. Zapotoczny: <i>Photoactive mesoporous nanoparticles as photochemical reactors</i>	55
K. Kopecká, L. Beneš, K. Melánová, P. Knotek, V. Zima, K. Zetková: <i>Layered double hydroxides: synthesis, exfoliation and dispersion in polymer systems</i>	57

T. Kuciel , P. Nalepa, W. Górka, M. Szuwarzyński, S. Zapotoczny: <i>Nanocomposite systems based on polymer brushes and superparamagnetic iron oxide nanoparticles</i>	59
M. Michalska , V. Matejka, J. Pavlovsky, P. Praus, G. S. Martynkova: <i>Comparison of TiO₂ and g-C₃N₄-based materials modified with Ag NPs utilized as a photocatalyst for degradation of model dye acid orange 7</i>	61
P. Nalepa , W. Górka, T. Kuciel, M. Szuwarzyński, S. Zapotoczny: <i>Magnetically-responsive polymeric scaffolds for cell cultures</i>	62
P. Otipka , J. Vlček: <i>Shape dependent model of EMA for nanostructured anisotropic materials</i>	64
Z. Posel , P. Posocco: <i>Tuning the properties of nanogel surface coatings by grafting weak cationic polyelectrolyte brushes</i>	67
A. Michalik, B. D. Napruszewska, A. Walczyk, J. Kryściak-Czerwenka, D. Duraczyńska, R. Dula, R. Karcz, E. M. Serwicka : <i>Starch as template for synthesis of nanocrystalline hydrotalcites</i> .	69
M. Valášková , P. Leštinský: <i>α-Fe₂O₃ nanoparticles/vermiculite for catalytic decomposition of polystyrene</i>	71

Topic 2 – Nanomaterials Characterizations and Devices

Invited lecture (IL):

B.-C. Tran Khac, K.-H. Chung, F. W. DelRio : <i>Friction and fracture of 2D materials</i>	74
--	----

Oral presentations (OP):

A. Babusen , S. Mondal, S. Ramaswamy, S. Dutta, M. Gopalakrishnan, J. Bhattacharyya: <i>Phenomenological and experimental investigation of exciton dissociation mechanism in organic semiconductor blends</i>	77
G. Jandieri , J. Pistora, M. Lesnak: <i>Interaction of electromagnetic waves with plasmonic structures in the terrestrial atmosphere</i>	78
M. Mičica , S. Eliet, M. Vanwolleghe, R. Motiyenko, A. Pienkina, L. Margulès, K. Postava, J. Pištora, J.-F. Lampin: <i>Measurement of THz gain in optically pumped ammonia gas</i>	80
G. Simha Martynková , G. Kratošová, R. Škuta, S. Sathish, K. Lafdi: <i>Structural study of thin films of graphene oxide with biosilver nanoparticles</i>	82
B. Strzemiecka , A. Jamrozik, Ł. Kłapiszewski, P. Jakubowska, D. Matykiewicz, M. Sandomierski, T. Jesionowski, A. Voelkel: <i>The importance of adhesion between fillers and polymer matrix on the utility macro-properties of the composites materials</i>	83
M. Tokarčíková , L. Bardoňová, J. Seidlerová, K. Drobíková, O. Motyka: <i>Magnetically modified montmorillonite - characterization, sorption properties and stability</i>	85
J. Vlček , J. Pištora, M. Lesňák: <i>Resonance states in plasmonic-waveguiding structures</i>	87

Poster presentations (PP):

I. Jendzejewska , Z. Barsova, T. Goryczka, E. Pietrasik, J. Goraus, J. Czerniewski, J. Jampilek: <i>Synthesis and structural, thermal and magnetic properties of Mn-doped CuCr₂Se₄ nanoparticles</i>	89
J. Krček : <i>Surface polaritons at periodic interface – near field analysis</i>	91

E. Plevová , L. Vaculikova, V. Valovicova, G. Simha Martynkova: <i>Thermal behaviour of organically modified smectites</i>	93
A. Slíva , R. Brázda, K. Čech Barabaszová, G. Simha Martynková: <i>Gyromixer of nanostructured systems and method of mixing thereof</i>	94
M. Słowikowska , A. Wójcik, K. Wolski, S. Zapotoczny: <i>Structural characterization of ladder-like conjugated polymer brushes</i>	96
B. Thomasová , J. Thomas, L. Gembalová, V. Tomášek: <i>Preparation and characterization of fly ash based membranes for microfiltration and ultrafiltration</i>	96
V. Valovičová , L. Vaculíková, E. Plevová, S. Dolinská, I. Znamenáčková, Z. Danková: <i>Characterization of fine-grained montmorillonite fractions suitable for composite preparation</i>	97
Z. Vilamová , Z. Konvičková, P. Mikeš, V. Holíšová, P. Mančík, E. Dobročka, G. Kratošová, J. Seidlerová: <i>Ag-AgCl Nanoparticles Fixation on Electrospun PVA Fibers: Technological Concept and Progress</i>	99

Topic 3 – Nanotech for Energy

Invited lectures (IL):

H. Akbulut , M. Tokur, T. Çetinkaya: <i>Nanocomposite Ceramic Based Negative Electrodes for Li-ion Batteries</i>	103
J. M. Macak : <i>One dimensional anodic nanostructures for energy applications</i>	104

Oral presentations (OP):

D. Legut , H. Tian, Z. W. Seh, K. Yan, Z. Fu, P. Tang, Y. Lu, R. F. Zhang, Y. Cui, Q. Zhang: <i>Flexible anode materials and their protection</i>	105
M. Michalska , J.-Y. Lin: <i>Li₄Ti₅O₁₂ spinel modified with carbon or oxide coatings as an advanced anode material for high-rate lithium-ion batteries</i>	106
S. Prabu , H.-W. Wang: <i>Nanocatalysts for hydrolysis of Al and H₂O reaction: Efficient synthesis of graphite-derived thin layer with Al(OH)₃ based nanoparticles</i>	107
S. K. Sathish , B. Novosad, K. Chrobáček, G. Simha Martynková: <i>Study of Clay-PEO system as application as solid electrolyte in Li-ion batteries</i>	107
U. Toçoğlu , H. Akbulut: <i>Towards high capacity rGO/MWCNT/ yolk-shell structured silicon composite anodes for li-ion batteries</i>	108

Poster presentations (PP):

M. Michalska , J.-Y. Lin: <i>Synthesis and electrochemical properties of LiNi_{0.5}Mn_{1.5}O₄ surface modified with NiO coating as a cathode material for lithium-ion batteries</i>	109
S. Prabu , H.-W. Wang: <i>Nanocatalysts for hydrolysis of Al and H₂O reaction: Efficient synthesis of graphite-derived thin layer with Al(OH)₃ based nanoparticles</i>	110
O. Skurikhina , R. Tarasenko, V. Tkáč, M. Orendáč, M. Fabián, M. Senna, V. Šepelák, E. Tóthová: <i>Fe(III) source-dependent properties of mechano/thermally synthesized LiFeSi₂O₆</i>	110
A. J. Wójcik , M. Słowikowska, K. Wolski, S. Zapotoczny: <i>New acetylene and pyridine derivatives as monomers for conductive polymer brushes fabrication</i>	112

Topic 4 – Nanotech for Medicine and Pharmacy

Invited lecture (IL):

Q. Miao, D. Xu, Z. Wang, L. Xu, T. Wang, Y. Wu, D. B. Lovejoy, D. S. Kalinowski, G. Nie, Y. Zhao, D. R. Richardson : <i>Amphiphilic hyper-branched co-polymer nanoparticles for the controlled delivery of novel anti-tumor agents</i>	116
---	-----

Oral presentations (OP):

J. Bednář , P. Mančík, L. Svoboda, V. Foldyna, R. Dvorský: <i>Antimicrobial Silicate Nanomaterial with High Specific Surface Area</i>	117
J. Jampilek : <i>Nanomaterials for management of toxigenic fungi</i>	117
D. Lazecká , S. Holešová, G. S.Martynková: <i>Polymeric nanocomposites as a prevention of biofilm formation</i>	119
W. Musiał , T. Urbaniak: <i>The influence of technical procedure on the hydrodynamic diameter of conjugates of lamivudine with biodegradable poly-ε-caprolactone microspheres for controlled drug delivery via cellular uptake</i>	119
D. Plachá : <i>Graphenic materials for biomedical applications</i>	122
M. Serda , M. J. Ware, J. M. Newton, M. Krzykawska-Serda, K. Malarz, A. Mrozek-Wilczkiewicz, R. Musioł, S. J. Corr, S. A. Curley, Lon J. Wilson: <i>The water-soluble [60]fullerene derivatives for anti-cancer studies</i>	122
J. Silberring , A. Drabik, J. Ner-Kluza, A. Bodzoń-Kuśakowska, P. Suder: <i>Identification of biomolecules – a frustrating nano-business</i>	124
A. Voelkel , B. Strzemiecka, M. Sandomierski: <i>Applications of Inverse Gas Chromatography and Dynamic Vapor Sorption for the physicochemical characterization of nanomaterials</i>	124

Poster presentations (PP):

M. Dołowy , P. Perez Martinez, A. Pyka-Pająk, J. Jampilek: <i>Nanoparticles as effective delivery systems for steroidal drugs</i>	127
M. Gasztych , W. Musiał: <i>Variability of electrokinetic potential of N-isopropylacrylamide derivatives in function of particles composition</i>	128
A. Gola , A. Niżniowska, W. Musiał: <i>The influence of initiator concentration on physico-chemical properties on n-vinylcaprolactam derivatives</i>	130
S. Holešová , K. Čech Barabaszová, M. Hundáková, M. Ščuková: <i>Synthesis and antimicrobial activity of ciclopiroxolamine/ZnO/vermiculite nanocomposites</i>	133
S. Holešová , Y. Tarasiuk, M. Hundáková, E. Pazdziora: <i>Determination and characterization of metronidazole/imidazole/clay interaction</i>	134
M. Gargulák, N. Štrofová, M. Kepinska, H. Milnerowicz, A. E. Ofomaja, B. Hosnedlová, C. Fernandez, P. Vašíčková, R. Kizek : <i>CdTe QDs-based electrochemical assay for sensitive detection of African swine fever virus</i>	134
N. Štrofová, M. Gargulák, K. Sehnal, M. Kepinska, H. Milnerowicz, C. Fernandez, J. Sochor, B. Hosnedlová, R. Kizek : <i>Effect of silver nanoparticles (AgNPs) prepared by green synthesis from sage leaves (Salvia officinalis) on maize plants</i>	137

V. Kozik , A. Bağ, A. Świetlicka, A. Środa, J. Jampílek, W. Priebe, J. Jazowiecka-Rakus, A. Sochanik: <i>Potential Anticancer Drug Nanocarriers</i>	139
S. Vallová, B. Sokolová, V. Valovičová, E. Plevová : <i>Adsorption of pharmaceuticals from aqueous solutions onto clay minerals</i>	140
M. Sandomierski , Z. Buchwald, M. Zielińska, A. Voelkel: <i>Micro- and mesoporous zeolites with high ion exchange capacity as materials with potential biomedical applications</i>	142
K. Piechura, P. Mielczarek, J. Silberring : <i>The novel inhibitor of cysteine proteases</i>	144
K. Škrlová , Z. Rybková, K. Malachová, D. Plachá: <i>Biocompatible polymer materials with antimicrobial properties for preparation of stents</i>	145
M. Masár, P. Troška , J. Hradski, I. Talian: <i>Application of silver nanoparticles for analysis of pharmaceutical samples by microchip isotachopheresis with Raman spectroscopy</i>	146
A. Verner , J. Tokarský: <i>Molecular modeling study of antibacterial molecules on nylon 6,6 surface</i>	149

Topic 5 – Nanotech for Environmental Solution

Invited lecture (IL):

I. Zinicovscaia : <i>Neutron Activation Analysis and Related Analytical Techniques in the Assessment of Nanoparticle Uptake in Organisms</i>	153
---	-----

Oral presentations (OP):

M. Baláž : <i>Mechanochemistry as a versatile tool for nanomaterials synthesis</i>	154
K. Drobíková , K. Štrbová, M. Tokarčíková, O. Motyka, J. Seidlerová: <i>Magnetically modified bentonite: characterization and stability</i>	156
Z. Jankovská , M. Vaštyl, G. J. F. Cruz, L. Matějová: <i>Microwave preparation of activated carbons from residual agricultural biomass</i>	158
Z. Konvičková , V. Holíšová, M. Kolenčík, K. Dědková, E. Dobročka, H. Otoupalíková, G. Kratošová, J. Seidlerová: <i>Effects of Biomass Heterogeneous Composition in Silver Nanoparticles Phytosynthesis Using Tilia sp. Leachate</i>	160
G. Kratošová , S. Teplická, J. Klusák, M. Večeř. <i>Preparation of tailored nanoparticles using flow microreactors and green synthesis</i>	163
O. Motyka , K. Štrbová, I. Zinicovscaia: <i>Chlorophyll content in two medicinal plant species following nano-TiO₂ exposure</i>	163
I. Safarik , J. Prochazkova, E. Baldikova, K. Pospiskova, K. Drobikova, J. Seidlerova: <i>Progressive magnetically responsive materials for pollutants detection and removal</i>	166
J. Seidlerová , M. Tokarčíková, K. Mamulová Kutláková, O. Životský: <i>Several ways of Fe_xO_y/phyllosilicate composite preparation</i>	168

Poster presentations (PP):

A. Behal , V. D. Rajput: <i>Effect of titanium dioxide nanoparticles on extracellular polymeric substances under sunlight</i>	170
K. Foniok , A. Smýkalová, V. Matějka, P. Praus: <i>A synthesis of composites of kaolin/g-C₃N₄ and metakaolin/g-C₃N₄</i>	172
Z. Jankovská , M. Večeř, I. Koutník, L. Matějová: <i>A case study of waste scrap tyre-derived carbon blacks tested for nitrogen, carbon dioxide and cyclohexane adsorption</i>	174
M. Kolenčík , D. Ernst, M. Šebesta, M. Urík, G. Kratošová, Z. Konvičková, M. Bujdoš, I. Černý, E. Dobročka, I. Vávra, H. Feng, Y. Qian, R. Illa: <i>Effect of different type of nanoparticles on crop production</i>	176
M. Kováčová , M. Baláž, E. Dutková: <i>Bio-mechanochemical synthesis of silver nanoparticles using Thymus vulgaris L. plant</i>	178
S. Rebilasová, V. Matějka , K. Foniok, K. Mamulová Kutláková, J. Vlček: <i>Utilization of photoactive clay/TiO₂ and quartz/TiO₂ composites in cement pastes</i>	181
P. Matějková , V. Matějka, J. Vlček: <i>Activation of granulated blast furnace slag using powder activator</i>	183
H. Ovčáčíková , J. Vlček, M. Klarová, M. Topinková: <i>Non-traditional glaze from iron waste</i>	184
L. Procházka , P. Mec: <i>Possibility of Using Fly Ash after Denitrification by SNCR as Admixture in Alkali-activated Materials</i>	186
M. Šihor , M. Valášková, M. Edelmannová, K. Kočí: <i>Ceramic cordierite/CeO₂ for photocatalytic reduction of CO₂</i>	186
A. Smýkalová , B. Sokolová, K. Foniok, V. Matějka, P. Praus: <i>Degradation of pharmaceuticals by using three different photocatalysts</i>	187
J. Tokarský , K. Mamulová Kutláková, R. Podlipná, T. Vaněk: <i>Phytotoxicity of ZnO / kaolinite nanocomposite - is the anchoring the right way to lower environmental risk?</i>	189
S. Dolinská, I. Znamenáčková, J. Tomčová, V. Valovičová, L. Vaculíková , E. Plevová: <i>Application of bentonite-manganese oxide composites in removal of heavy metals</i>	191

Topic 6 – Industrial Forum

Oral presentations (OP):

J. Neuman , Z. Novacek, V. Novotna, V. Hegrova, M. Pavera: <i>AFM-in-SEM LiteScope™: Tool for comprehensive sample surface analysis</i>	195
A. Cernescu, S. Amarie, J. Vávra : <i>Scattering-Type Scanning Near-field Optical Microscopy and Spectroscopy of Low Dimensional and nanostructured materials</i>	197
L. Lyapeikov , A. Chepak: <i>Industrial Applications of Nanotechnologies</i>	197
A. Kotziánová , J. Klemeš, M. Pokorný, V. Velebný: <i>Research and development of nanotechnologies and nanomaterials</i>	1978

TOPIC 1

Advanced Nanomaterials

Chair: Pavla Čapková

Nanoparticles – natural and synthetic
Nanocarbons, Nanoclays and Nanoceramics
Functionalization of nanomaterials
Nanocomposites and nanocatalysis



Invited lectures (IL):**Nanostructural catalysts derived from clay minerals**

E. M. Serwicka

Jerzy Haber Institute of Catalysis and Surface Chemistry, Polish Academy of Sciences, Poland

ncservicr@cyf-kr.edu.pl

ABSTRACT

The unique structural and compositional properties of cationic (layered silicates) and anionic (hydrotalcites) clays are discussed in light of the versatility and potential of these materials in manufacturing of catalytically active nanostructures. Here, the concept of atom-by-atom or molecule-by-molecule strategy in the catalyst design is extended to the use of individual silicate lamellae as prefabricated building blocks, ready to be fitted into the desired nano-construction. Alternatively, the hydrotalcite layer compositional flexibility may be used for design of catalysts with unique properties. The use of clay minerals for design and synthesis of catalytic materials is illustrated by examples from author's own works. Presentation focuses on manufacturing of catalytic materials relevant for environmental catalysis, with particular attention to the novel preparative strategies. The main interest lies in finding relation between the physico-chemical properties of the catalysts and their performance in the catalytic reaction.

Acknowledgments: Financial support from the National Science Center Poland, project OPUS 2017/27/B/ST5/01834, is gratefully acknowledged.

Thermal Physics of Nanostructured Materials: Thermodynamic (Top-Down) and Quantum (Bottom-Up) Issues

J. Šesták

New Technology - Research Centre in the Westbohemian Region, West Bohemian University, Universitní 8, CZ-30114 Pilsen

sestak@fzu.cz

ABSTRACT

The subject is focusing on the newly adjusted thermodynamic degree of freedom which is *dimension*. Nanoworld thermodynamic groundwork unfolds from a single phase division into α and β separated by interface the curvature of which request the higher pressure on the concave side with respect to the surrounding, p , i.e., $p_\alpha > p_\beta = p$ (Young-Laplace effect). It can happen by splitting up (division, cleavage) or nucleation, as well as by elastic deformation (strain) of already existing surface due to the impact if isotropic or nonisotropic stress, $dw_{\text{surf}} = \gamma dA$, where the scalar parameter γ (defined as a specific surface energy) is always positive (due to the stability criteria) and is independent on the surface, A . Performed work, $dw_{\text{surf}} = f dA_{\text{elast}} = f A d\varepsilon$, causes elastic deformation (*strain* ε) of the original surface assuming $d\varepsilon = dA/A$. Unite specific surface work is called surface stress, f , and possesses generally tensor denomination but for isotropous environment become scalar following $w_{\text{surf}} = f A_{\text{elast}}$. As a result we can say that any nanosystem possesses its size as an extra degree of freedom, equilibrium of which requires a modification of traditional macroscopic thermodynamics. Everything factually originates from the Kelvin historical relation,

$p/p_{\infty} = 2V\gamma/(RTr)$, and the related equation for temperatures, $T/T_{\infty} = 2V\gamma/(\Delta H r)$. In the other words it means that if we want to create any equilibrium modification for a variation of curvature upon the change of external conditions (T, p) we have to change either pressure (from $p_{\beta\infty}$ to $p_{\beta r}$ under constant T_{∞}) or temperature (from T_{∞} to T_r under constant p_{∞}) so that the change in the difference of bulk chemical potentials $\Delta\mu$ is compensated by negative $2\gamma V_{\text{am}}(1/r)$. It associates similar effect as rapidly changed temperature when observing real shapes kinetic phase diagrams (temperature shifts) providing a new space for novel thermophysical studies including impact of eccentricity of heat transfer, heat capacities or phase relations in nanodimensional space. Modern description came with the paper introducing the term ‘microcluster’ as a new phase of matter and book showing that they cannot be formed fully accidentally but the atoms are combined according some ‘magic numbers’ (e.g. Fibonacci following the calcium clusters series 561, 923, 1415, 2057, etc). The particle is in order of size ($\sqrt[3]{N}d$) where N is the number of atoms and d is their diameter showing that for $d \sim 2-3$ Å is $N \sim 2-10$ nm. There exists metal model clusters describing systems up to 80 atoms. The number of atoms of a nanoparticle can be derived from the Loschmidt number giving 2.6×10^{19} atoms in a cubic cm of a substance so that about 10^4 atoms are contained in nanoparticle cube with a side of 100 nm. It associates with a notion of the so-cooled Planck’s mass amounting 2.17×10^5 g and specifying the boundary of quantum world. In a crystallographic view spheres of a given radius or regular tetrahedral with a given edge can be assumed as the most closely packed in space, i.e., crowded so that the ratio between the filled part of the space and the unfilled part would be as large as possible. Using polyhedra the whole space could be filled by appropriate packing of the congruent specimens of these polyhedra starting e.g. from a cube, edge, a , (surface/volume: $A/V \cong 6/a$), tetrahedron, via penta-, hexa-, hepta-, nona-, deca-, dodeca-, icosahedron, triacontahedron, hexacontahedron, up to an infinite faceted ultimate sphere of radius, r , ($A/V \cong 2/r$). Another important process of covering a space with polyhedra is the so called stellation, following the historical Kepler constructions (year 1611) of the first two other stellar polyhedron from dodecahedron. This multiplication process of self-repetition yields the specificity of a self-similar system which shows statistically the same properties at many scales and which is well known as sourced on the Koch curves (i.e. snowflakes), further defining the *self-similarity dimension* in the sphere of fractals expressing thus the complexity of an object and giving the intermediary to chaos (supposing both ways from the top to bottom and vice versa). Similarly assumed clustering is close to the real pattern of a structure evolution from disorder (chaos), local ordering up to periodic structures sometimes including structural code or even inorganic gene and became close to the topic of chemistry beyond the molecule and special associated as superatoms exhibiting the quantum properties of nanoclusters (i.e. quantum nature of nanostes).

REFERENCES

1. V. Y. Schevchenko, Search in Chemistry, Biology and Physics of Nanostate, Lema, St. Petersburg, 2011.
2. J. Leitner, Struktura nanomateriálů - skriptá VŠChT, Praha, 2011.
3. J. J. Mareš, J. Šesták, J. Thermal Anal. Cal. 82 (2005) 681-686.
4. J. Šesták, *Composite materials and nano-structured systems: generalized description*. Invited lecture, ICCE-22: International conference on composites and nano-engineering, Malta, 2014.
5. J. Šesták, *Thermal physics of nanostructured materials: Thermodynamic (top-down) and quantum (bottom-up) issues*. Invited lecture, GNC-18: 4th Global Nanotechnology Congress and Expo, Dubai 2018, 2014.
6. J. Šesták, J. Thermal Anal. Calor. 120 (2015) 129-137.

Oral presentations (OP):**Electrospinning of nanofibrous layers containing antibacterial vermiculite**

L. Bardoňová¹, A. Kotzianová², K. Mamulová Kutláková¹, S. Holešová¹, J. Klemeš²

¹Nanotechnology Centre, VŠB – Technical University of Ostrava, Czech Republic; ²Contipro a.s., Czech Republic

lenka.bardonova.st@vsb.cz

ABSTRACT

The aim of this study was to describe electrospinning method for preparation of self-supporting homogenous nanofibrous layers with a presence of pristine vermiculite and vermiculite containing antibacterial agent chlorhexidine acetate in its interlayer space (CH/Ver). Nanofibers were made of hydrophobic polymers, polyurethane and polycaprolactone, to gain water stable and durable layers. Polymer solutions for electrospinning contained 2, 5 and 8 wt. % (according to the total weight of the solution) of vermiculite or chlorhexidine/vermiculite. These suspensions were homogenized and immediately spun using 4SPIN LAB. Morphology was characterized using scanning electron microscopy (SEM) and presence of clay minerals in the layer was confirmed by digital microscopy and EDX mapping. From SEM images, diameter of the fibres was evaluated. Fibre diameter decreased after adding the clay and was ranging from 600 nm to 1200 nm. Clay particles were present both in fibres and on the surface. Antibacterial chlorhexidine was found in the vermiculite matrix as well as separately in the fibres (result of imperfect intercalation). Antibacterial activity was evaluated by disc diffusion test against *Staphylococcus aureus* and *Pseudomonas aeruginosa*. Layers containing CH/Ver had good antibacterial activity against *S. aureus* and was dependent upon CH/Ver concentration and chlorhexidine release ability.

Keywords: Clay, nanofibers, electrospinning, chlorhexidine

INTRODUCTION

In order to prepare clay-nanofiber nanocomposites, wide range of polymers have been used with clay such as montmorillonite and hydroxyapatite. Added clay affected morphology and processability of prepared nanofibers^{1,2,3}, enhanced filtrating ability¹, increased thermal stability^{2,4}, improved tensile strength^{3,4} and chemical stability⁵ of the nanofiber mats. After intercalating drugs into the clay interlayer space nanofiber mats obtained antibacterial properties^{6,7} with drug sustained release activity⁶. Prepared materials have a potential in wound healing applications⁵, drug delivery systems^{6,7}, as an antioxidant product in food and pharmaceutical industries⁸ or filtration^{9,10}.

EXPERIMENTAL

Two basic polymer solutions were prepared – 10 wt. % polyurethane (PU) in *N,N*-dimethylformamide (DMF) and tetrahydrofuran (1:1) and 10 wt. % polycaprolactone (PCL) in DMF and chloroform (2:8). Suspensions for electrospinning contained 2, 5 and 8 wt. % of vermiculite (Ver) from Brazil (particle size fraction < 40 µm) or chlorhexidine acetate/vermiculite (prepared through intercalation process). The weight percent of added clay was with respect to the weight of the final suspension. Each suspension was stirred first in hand and then homogenized for 5 min by homogenizer IKA® T25 digital Ultra Turrax. Prepared suspension was immediately spun.

Electrospinning was performed using the 4SPIN LAB device (Contipro, Czech Republic) with two moving needles as an emitter and rotating cylinder (width 10 cm, 1000 rpm) covered by substrate (aluminium foil) as a collector. Each sample have been spun for 120 min, but after 60 min the suspension was changed for newly homogenized one. Other electrospinning conditions are mentioned in Table 1. The notation *wt.%Clay_polymer* is used in the following text.

Table 1. Electrospinning conditions.

Emitter-collector distance (cm)	18
Feed rate (μl/min)	20, 30 (8CH/Ver in PCL)
Applied voltage (kV)	25 (PU), 20 (PCL)
Ambient conditions	RH 30-43 %, 23-28 °C

Prepared samples were characterized by digital microscopy (VHX Multi Scan Keyence), scanning electron microscopy (Zeiss Ultra Plus, Carl ZEISS, applied voltage 3,5 kV), energy-dispersive X-ray spectroscopy mapping (Zeiss Ultra Plus, Oxford X-MAXN 80, accelerating voltage 10 kV, magnification of 1800). From SEM images (1000 x), diameter of fibres was evaluated using ImageJ 1.48 (average of 30 fibres). Disc diffusion test (cultivation at 30–35 °C for 24 hours) was carried out to evaluate antibacterial activity against *S. aureus* and *P. aeruginosa*. Qualitative chlorhexidine release was evaluated using leaching test according to the Council Decision 2003/33/EC, i.e. 30 mg of nanofiber layer was added into 30 ml of demineralized water, the solution was shaken for 24 h at 20 °C and, finally, by measuring the absorbance of CH by UV-VIS spectrophotometry (CINTRA 303, GBC Scientific Equipment).

RESULTS AND DISCUSSION

Digital microscopy imaging showed increasing clay content in the nanofibrous layers with higher clay concentration in the suspension. Some agglomerates exceeded the size of 100 μm even though vermiculite size fraction was under 40 μm. This trend was visible especially in samples with PCL. From SEM images, morphology of the nanofibrous layers could be observed. Neat polymer nanofibers were smooth and continuous with inhomogeneous diameter which decreased after adding the clay. Clay particles were probably incorporated into the PCL fibres as there were not many visible particles on their surface. PU fibres were thinner than PCL fibres and there were more clay particles visible on the surface of the fibres. Diameter of clay/PU fibres was also more homogeneous compared to clay/PCL fibres.

In EDX maps (Fig. 1), major elements contained in vermiculite are blue-coloured (Si, Al and Mg) and Cl (recognizable element for CH) is red-coloured. Clay particles were mostly concentrated along the fibres and some bigger particles (size exceeding fibre diameter multiple times) were between the fibres. Chlorhexidine was not always situated with vermiculite, there were many spots, where only chlorhexidine or only vermiculite could be found. This means that the intercalation process was not perfect and not all the chlorhexidine was intercalated into interlayer space of vermiculite.

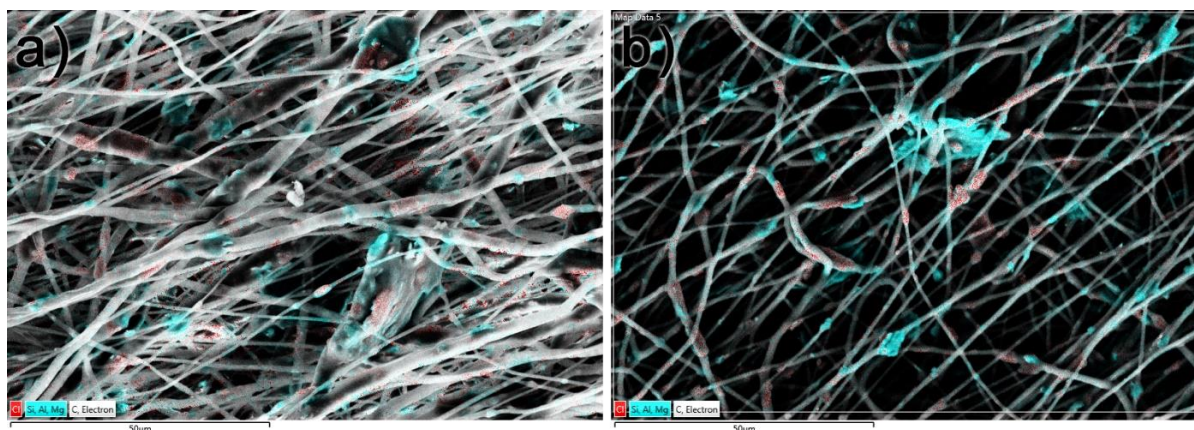


Fig. 1. EDX maps, blue coloured: Si, Al, Mg, red coloured: Cl: a) 5CH/Ver_PCL, b) 5CH/Ver_PU.

Samples containing CH/Ver showed good antibacterial activity against *S. aureus*. Inhibition zones were wider the higher CH/Ver concentration. In addition, CH/Ver_PU layers were more effective than CH/Ver_PCL layers. Even the highest CH/Ver concentration had no effect on *P. aeruginosa* bacteria. Chlorhexidine release test showed that more CH was released from CH/Ver_PU mats than from CH/Ver_PCL mats. This correlates with antibacterial activity test results – the more CH was released the more effective sample was against bacteria.

CONCLUSION

Nanofibrous layers with different weight concentration of vermiculite or chlorhexidine/vermiculite were successfully prepared under the same electrospinning conditions as neat polymers. Fibre diameter decreased after adding the clay and was 600–1200 nm. Clay content in the layer increased with concentration and clay particles were incorporated into the polymer fibres. Antibacterial chlorhexidine was found in the vermiculite matrix as well as separately in the fibres (as a result of imperfect intercalation). Samples with CH/Ver had good antibacterial activity against *S. aureus* which was related to CH release – samples possessed better antibacterial effect when more CH was released. Prepared CH/Ver/polymer layers seem to be promising, relatively inexpensive, and easy-to-produce material in the field of antibacterial applications.

Acknowledgments: This study was funded by projects No. CZ.02.1.01/0.0/0.0/17_049/0008441 "Innovative therapeutic methods of musculoskeletal system in accident surgery" within the Research and Development for Innovations Operational Programme financed by the European Union, was created in cooperation with Contipro a.s. and in the frame of the SP2019/31 project while financially supported by the Ministry of Education, Youth and Sports of the Czech Republic.

REFERENCES

1. ISARANKURA NA AYUTHAYA, S., TANPICHAI, S., SANGKHUN, W., WOOTTHIKANOKKHAN J. International Journal of Biological Macromolecules. 2016. vol. 85, pp. 585-595.
2. PARK, J. H., LEE, H. W., CHAE, D. K., WEONTAE, O., YUN, J. D., DENG, Y., YEUM, J. H. Colloid Polym Sci. 2009. vol. 287, pp. 943-950.
3. KIM, S. W., HAN, S. O., SIM, I. N., CHEON, J. Y., PARK, W. H. Journal of Nanomaterials. vol. 2015, Article ID 275230.
4. ALMUHAMED, S., BONNE, M., KHENOUSSE, N., BRENDLE, J., SCHACHER, L., LEBEAU, B., ADOLPHE, D. C. Journal of Industrial and Engineering Chemistry. 2016. vol. 25, pp. 146-152.
5. HEYDARY, A. H., KARAMIAN, E., POORAZIZI, E., KHANDAN, A., HEYDARIPOUR, J. Procedia Materials Science. 2015. vol. 11, pp. 176-182.
6. SAHA, K., BUTOLA, B. S., JOSHI, M. Journal of Applied Polymer Science. 2014. vol. 131, no. 10.

7. RAMÍREZ-AGUDELO, R., SCHUERMANN, K., GALA-GARCÍA, A., MONTEIRO, A. P. F., PINZÓN-GARCÍA, A. D., CORTÉS, M. E., SINISTERRA, R. D. *Materials Science and Engineering: C*. 2018. vol. 83, pp. 25-34.
8. SANGEETHA, K., ALSHARANI, F. A., VIJAYALAKSHMI, K., ANIL, S., SUDHA, P.N. *Journal of Pharmacy*. 2017. vol. 7, pp 7-12.
9. ZHU, Y., CHEN, D. *Ceramics International*. 2017. vol. 43, pp. 9465-9471.
10. PRINCE, J.A., SINGH, G., RANA, D., MATSUURA, T., ANBHARASI, V., SHANMUGASUNDARAM, T.S. *Journal of Membrane Science*. 2012. vol. 397-398, pp. 80-86.

CuO nanoparticles in antibacterial PVAc/vermiculite nanocomposite

M. Bílý, K. Čech Barabaszová, S. Holešová, M. Hundáková

Nanotechnology Centre, VŠB - TU Ostrava, Czech Republic

ABSTRACT

The purpose of this study was to investigate the antibacterial behavior of polyvinyl acetate (PVAc) with nanofiller in the form of CuO nanoparticles and CuO/vermiculite nanocomposite. The CuO nanoparticles and CuO/vermiculite nanocomposites were prepared by sonochemical synthesis. Since vermiculite is antibacterial itself, the expected outcome was the improvement of antibacterial properties. Concerning their antibacterial activity in PVAc thin films, they were measured against *Staphylococcus aureus* and *Enterococcus faecalis*, respectively. Results showed that the most efficient PVAc nanocomposite was that with 0.5 wt% of CuO/vermiculite, however other samples also exhibited decent antibacterial behavior.

Keywords: Copper oxide, vermiculite, PVAc, antibacterial activity

INTRODUCTION

Among all transition metal oxide nanoparticles (TMO NPs), copper oxide (CuO) nanoparticles have not been considered as promising as others, such as zinc oxide or titanium dioxide. However, the growing popularity of CuO shows a slight change in application potential. CuO is a semiconductive material with toxic properties that are dependent on the size and morphology of nanoparticles. Copper oxide nanoparticles can be grown on vermiculite layered structure, which can result in significant improvement of the antibacterial behavior and reduction of toxic activity. When incorporated in the polyvinyl acetate matrix, they can be prevented from free movement around the environment. Antibacterial activity issues, such as the resistance of certain bacterial species against antibacterial nanoparticles (Ag, ZnO, ...) can be addressed with the development of novel materials. PVAc thin films could be employed in antibacterial coatings and materials depending on the antibacterial activity against specific bacterial species.

EXPERIMENTAL STUDY

CuO nanoparticles and CuO/vermiculite nanocomposite particles have been both prepared by sonochemical synthesis method. 2,5 g of copper nitrate have been dissolved in 0,1M solution of sodium hydroxide. For CuO/V, 1 g of vermiculite has been added to the solution. After 15 minutes exposure to ultrasound, solutions were treated in centrifuge and precipitates were formed and then dried at 75 °C and calcinated at 350 °C. For PVAc nanocomposite preparation, radical polymerization has been used. Electron microscopy, confocal microscopy, X-Ray powder diffraction and particle size distribution methods were used for characterization of nanocomposites.

In addition, electrophoretic mobility (μ), specific surface area (SSA), conductivity (E) and ξ -potential were measured, too^{1,2}. As far as the evaluation of antibacterial behavior is concerned, nanocomposites were tested against two bacterial species - *Staphylococcus aureus* and *Enterococcus faecalis*.

RESULTS AND DISCUSSION

X-Ray powder diffraction confirmed successful fabrication of CuO nanoparticles and CuO/V nanocomposites. Based on the Scherrer equation, the crystalline size was around 100 nm. Particle size distribution has shown that the average particle size was dependent on the overall composition (less than 10 μm for CuO/V/350 and slightly over 10 μm in case of CuO/350). Based on electron microscopy observations, CuO nanoparticles formed agglomerates, whereas CuO/V nanocomposites exhibited CuO nanoparticle growth on the vermiculite layer edge. After the polymer sample preparation, these films were characterized by confocal microscopy. The results showed decent nanofiller dispersion within the polymer. As for antibacterial activity, polyvinyl acetate itself did not exhibit any antibacterial activity at all. After incorporation of nanofiller, antibacterial behavior was observed. The number of colony forming units (CFU) was calculated 24 h, 48 h and 72 h after exposure in order to evaluate antibacterial activity. Generally, the more efficient antibacterial agent was CuO/V nanocomposite, where only 0.5 wt% was sufficient for decreasing the number of CFU of bacteria. In case of pure CuO, the number of CFU of *Staphylococcus aureus* dropped down significantly after as soon as 48 h. Table 1 shows the efficiency of all prepared samples.

Table 1: Efficiency of individual antibacterial agents.

Samples	Time to presence of less than 200 CFU (h)	
	<i>S. aureus</i>	<i>E. faecalis</i>
PVAc	>72	>72
PVAc_0.1CuO_350	48	>72
PVAc_0.5CuO_350	48	>72
PVAc_1CuO_350	48	72
PVAc_0.1CuO/V_350	48	>72
PVAc_0.5CuO/V_350	24	72
PVAc_1CuO/V_350	48	48

CONCLUSION

Well-defined CuO nanoparticles and CuO/V nanocomposite particles have been prepared. Their shape and size were characterized by electron microscopy and particle size distribution, respectively. Based on the antibacterial activity observations, both CuO and CuO/V exhibited antibacterial behavior dependent on the origin of bacterial species. This could prove to be a significant step in developing novel antibacterial materials, considering the possibility of bacteria becoming resistant against specific compounds. However, further examination is necessary to determine antibacterial effect against other bacterial species as well as the sufficient concentration of nanofiller in the PVAc polymer nanocomposite before these compounds can be successfully implemented as antibacterial agents.

These results could be exploited in the preparation of novel antibacterial materials and coatings.

Acknowledgements: This work was supported by the project No: SP2019/24 "Hybrid and biodegradable clay nanocomposite materials". Authors thank to Dr. Erich Pazdziora for antibacterial tests performing.

REFERENCES

1. Bílý M.: Effect of the filler size on the PVAc nanocomposite preparation. Bachelor thesis, 2017, 49 p.
2. Čech Barabaszová K., Kalivoda P.: Journal of nanocomposites and nanoceramics 4(1), 2013, 7-13.

New insights of dual-emission fluorescent nanoprobe for imaging metal ions in living cells

M. Foda^{1,2,3}, C. Zou¹, H. Bahlol^{1,3}, H. Han^{1*}

¹State Key Laboratory of Agricultural Microbiology, College of Science, Huazhong Agricultural University, China; ²State Key Laboratory of Agricultural Microbiology, College of Veterinary Medicine, Huazhong Agricultural University, China; ³Department of Biochemistry, Faculty of Agriculture, Benha University, Egypt

m.frahat@fagr.bu.edu.eg

ABSTRACT

Fluorescent probes have grasped a huge attention throughout the last 2 eras in distinguishing diverse categories of metal ions based on two main conditions, the target prompted fluorescent improvement and/or the quenching mechanism of the nanoprobe^{1,2}. Meanwhile, The two-color emission fluorescent nanoparticles (NPs) in particular quantum dots (QDs) and carbon dots (CDs) have involved considerable research devotion in contrast to the single emission fluorescent NPs, which had some defects related to the ecological conditions, probe molecule concentration, and instrumental proficiency. Presently, heavy metals have triggered serious environmental damage due to its indestructibility as well as their toxicity effect on living creatures. Although the physiological essential of copper ions (Cu^{2+}) to the human body, however, the extreme quantity of Cu^{2+} might display high toxicity and cause severe damage to human body central nervous system, resulting in permanent diseases, for instance, Alzheimer's disease^{3,4}. Therefore, the detection and imaging of Cu^{2+} ions in biological fluids have become progressively vital.

In this study, a fluorescence nanohybrid complex ($\text{SiO}_2@\text{QDs}@\text{CDs}$) that include a well-defined silica SiO_2 for the detection and imaging of Cu^{2+} ions were fabricated via a carbodiimide-mediated method, where the SiO_2 represented the core-satellite followed by the coating of the as-prepared CdTe/CdS QDs and finally a compact outer layer of CDs. In this nanohybrid complex, QDs were quenched upon the exposure to Cu^{2+} ions in the aqueous solution which led to a significant ratiometric response in living cells. The fluorescence signal intensity and constancy can be improved due to the core silica nanospheres as a nanocarrier loaded with QDs on the outer surface as a signal label. More interestingly, carbon dots were compactly packed around the $\text{SiO}_2@\text{QDs}$ nanospheres which significantly condensed the toxicity of the nanosensor and the validation for the intracellular imaging of Cu^{2+} in HeLa cells as well as further biological applications⁵.

Keywords: Dual-emission fluorescent nanoprobe, Nanohybrid complex, Metal ions, Cell imaging

Acknowledgments: We gratefully acknowledge the financial support from National Natural Science Foundation of China (Grants 31750110464, 21778020); Huazhong Agricultural University, Talented Young Scientist Program (TYSP Grant No.42000481-7)

REFERENCES

1. Formica M., Fusi V., Giorgi L., Micheloni M. *Coord. Chem. Rev.* **2012**, 256, 170–192.
2. Jeong Y., Yoon J. *Inorg. Chim. Acta* **2012**, 381, 2–14.
3. Emerit J., Edeas M., Bricaire F. *Biomed. Pharmacother.* **2004**, 58, 39–46.
4. Viles J. H. *Coord. Chem. Rev.* **2012**, 256, 2271–2284.
5. Zou C., Foda M.F., Tan X., Shao K., Wu L., Lu Z., Bahlol H.S. and Han H. *Anal. Chem.* **2016**, 88, 7395–7403.

Nanoceria reinforced Ni/CeO₂ nanocomposite production by electroless coating

D. Gültekin, E. Duru, H. Akbulut

Sakarya University, Metallurgy and Materials Engineering Department, Turkey

dkurt@sakarya.edu.tr

ABSTRACT

Ni/CeO₂ composite coatings have been deposited by electroless deposition technique from a nickel sulfate solution containing nano CeO₂ particles. The pure Ni and CeO₂ reinforced Ni composite coatings tribological behaviour has been examined under dry sliding circumstances. The effects of CeO₂ on the friction and wear behavior have been discussed. The surface morphologies of electroless Ni and Ni/CeO₂ coatings have been observed with EDS equipped SEM and XRD.

Keywords: Nanocomposite, Nickel, CeO₂, Tribology

INTRODUCTION

Metal matrix nanocomposite coatings consist of a metallic matrix strengthened by the addition of nano-sized metallic or nonmetallic particles (or whiskers). These materials often exhibit enhanced physical, mechanical, and chemical properties compared with those of the bulk material coatings [1]. Nickel is one of the most commonly used structural metals for various engineering applications, and nickel coating can be used to provide resistance to corrosion, erosion and abrasion. To improve these properties, reinforced nickel composite coatings have been developed for particles [1]. Development of nickel boride composite coatings by co-deposition of secondary particles from electroless bath has received a great interest owing to the enhancement of properties over electroless nickel boron alloy coating. The electroless composite coatings formed using different particles has different effects [2]. Cerium oxide with different valence states and various crystalline structures have been explored for various applications such as electrical, electronic, catalytic, adsorption, optical, electrochemical, batteries, functional materials, energy storage, magnetic data storage and sensing properties [3]. In the present study, Ni/CeO₂ composite coatings have been deposited by electroless deposition technique from a nickel sulfate solution containing nano CeO₂ particles. The pure Ni and CeO₂ reinforced Ni composite coatings tribological behaviour has been examined under dry sliding circumstances. The effects of CeO₂ on the friction and wear behavior have been discussed. The surface morphologies of electroless Ni and Ni/CeO₂ coatings have been observed with EDS equipped SEM and XRD.

EXPERIMENTAL

Steel substrates with 30×30×3mm dimension have been used for electroless coating. The substrates have been polished with abrasive paper and cleaned in acetone. The cleaned substrate has been

etched with HCl solutions 30 sec for the removal of surface impurities. The bath constituents and process parameters used for coating are given in Table 1.

Table 1. Electroless coating bath contents

Electroless bath contents	
Nickel sulfate $\text{NiSO}_4(\text{H}_2\text{O})_6$	30g/L
DMAB	3 g/L
Sodium acetate (CH_3COONa)	4.4 g/L
Thiourea	0.1 g/L
Ceria	2.5 g/L
Bath temperature	70 °C
pH	6

RESULTS AND DISCUSSION

Fig.1 shows SEM images of electroless Ni and Ni/CeO₂ composite coating. The incorporation of nanoparticles at the boundaries of nickel crystallites can reduce the nodular grain size and become denser than the electroless Ni-B coating [2].

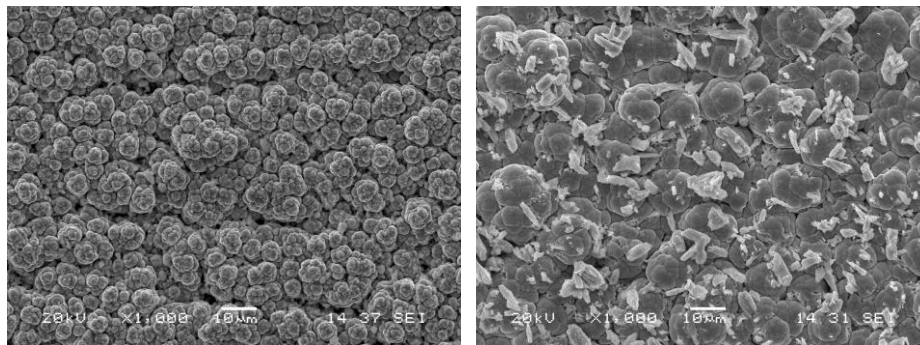


Fig.1 shows SEM images of electroless Ni and Ni/CeO₂ composite coating.

CONCLUSION

Ni and Ni/CeO₂ nanocomposite coatings have been deposited on steel substrates by the electroless coating process. The friction and wear behaviors of Ni–CeO₂ composite coatings are closely related with CeO₂ content [4]. Wear test shows that the reinforced CeO₂ particles decrease the friction coefficient and reduce the wear weight loss.

REFERENCES

1. N.S Qu, W.H. Qian, X.Y. Hu, Z.W. Zhu, Int. J. Electrochem. Sci., 8 (2013) 11564-11577.
2. J. K. Pancrecious, J.P. Deepa, V. Jayan, U.S. Bill, T.P.D. Rajan, B.C. Pai, Surface & Coatings Technology 356 (2018) 29-37.
3. M. Farahmandjou, M. Zarinkamar and T.P. Firoozabadi, Revista Mexicana de Física, 62 (2016) 496-499.
4. Yu-Jun Xue, Xian-Zhao Jia, Yan-Wei Zhou, Wei Ma, Ji-Shun Li, Surface & Coatings Technology 200 (2006) 5677-5681.

Morphological Evaluation of Zinc Oxide Nanostructures Synthesized by Solution Based Methods

D. Gültekin, F. Kayış, H. Akbulut

Sakarya University, Metallurgy and Materials Engineering Department, Turkey

dkurt@sakarya.edu.tr

ABSTRACT

In this study, ZnO nanostructures have been produced by solution based methods. Zinc acetate dihydrate and Zinc nitrate have been used as precursors whereas monoethanolamine, glycerol and hexamethylenetetramine have been used as additives to obtain nanostructures with different morphologies. General morphologies and detailed structural characterizations have been performed by scanning electron microscope, X-ray diffractometer.

Keywords: ZnO, Nanostructure, Solution, Hydrothermal.

INTRODUCTION

Zinc oxide with its unique physical and chemical properties, such as high chemical stability, high electrochemical coupling coefficient, broad range of radiation absorption and high photostability, is a multifunctional and important semiconductor which has a range of applications in electronics and electrotechnology [1]. ZnO is a wide band gap (3.37 eV) semiconductor and has a large binding energy (60 meV) [1, 2], low resistivity and high transparency in the visible range and high light trapping characteristics [3] mean that zinc oxide can be used in photoelectronic and electronic equipment, in devices emitting a surface acoustic wave, in field emitters, in sensors, in UV lasers, and in solar cells [1]. In recent years, lots of research has been focused on the synthesis, characteristics, growth mechanism, device fabrication, and performance improvement of ZnO nanostructures with various morphologies including nanowires, nanorods, nanobelts, nanotubes, nanosheets, nanopyramids, hollow nanospheres, and quantum dots [4], which have been fabricated via different methods, such as chemical vapor deposition, sol-gel method, hydrothermal method, and solvothermal method [4, 5]. Growth of ZnO nanostructures mainly depends on process conditions such as concentration of precursor solution, reaction temperature and pH value of the solvents [5].

In this study, ZnO nanostructures have been synthesized by solution based methods. Zinc acetate dihydrate and Zinc nitrate hexahydrate have been used as precursors whereas monoethanolamine (MEA), glycerol and hexamethylenetetramine (HMT) have been used as additives to obtain nanostructures with different morphologies. Distilled water and ethanol have been used as solvent. General morphologies and detailed structural characterizations have been performed by scanning electron microscope, X-ray diffractometer.

EXPERIMENTAL STUDY

Several zinc precursors have been used: nitrate, chloride, perchlorate, acetylacetonate and alkoxides such as ethoxide and propoxide, but the most often used is the acetate dihydrate and nitrate. Because of their low cost, facility of use, and commercial availability, metal salts are interesting as precursors and could be more appropriate for large-scale applications [6]. In our work, ZnO nanostructures synthesized by the preparation of ZnO sols in the liquid phase from homogeneous solutions with precursor of zinc acetate dihydrate ($\text{Zn}(\text{CH}_3\text{COO})_2 \cdot 2\text{H}_2\text{O}$) and zinc nitrate

hexahydrate ($\text{Zn}(\text{NO}_3)_2 \cdot 6\text{H}_2\text{O}$). MEA or HMT was added to adjust pH of solutions. Detailed structural characterizations of the ZnO films were obtained using (SEM) and XRD were used to determine preferred crystal orientation and particle size of the thin films.

RESULTS AND DISCUSSION

Fig.1 presents the X-ray diffraction patterns of synthesized ZnO nanorods. We only gave ZnO nanorods patterns for brevity. The peak positions in each product agree well with the reflections of ZnO with all peaks corresponding well to standard crystallographic data (ZnO: JCPDS 01-075-0576). (♦) symbol represents the diffraction peaks comes from FTO coated glass substrate. Furthermore, no other peak related to impurities was detected in the spectrum, which further confirms that the synthesized products are high purity. There have been changes in orientation and peaks intensities with the using different seed layer.

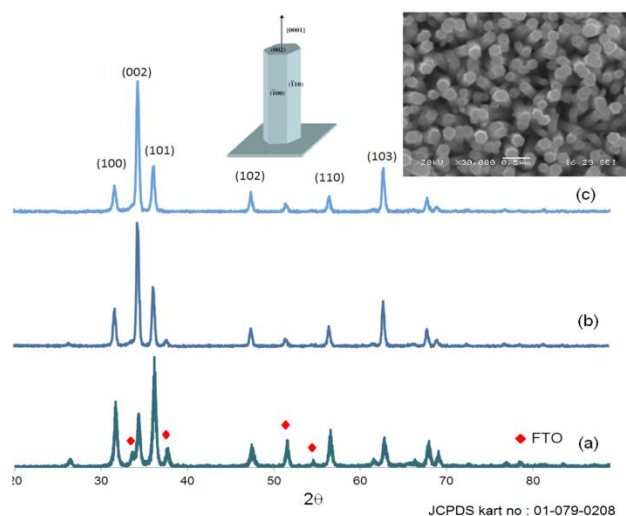


Fig. 1. XRD and SEM results of ZnO nanorods XRD analysis of ZnO nanorods a) with no seed layer, b) growth on one seed layer coated substrate, c) growth on five seed layer coated substrate

CONCLUSION

ZnO nanostructures with different morphologies have been produced by solution based methods. ZnO nanorods have been obtained by using Zinc nitrate precursor and HMT whereas ZnO nanopackets synthesized by using Zinc acetate, MEA and glycerol. Also ZnO nanosheets and nanoflowers have been successfully obtained under different circumstances.

REFERENCES

1. A. Kołodziejczak-Radzimska, T. Jesionowski, *Materials*, 7 (2014) 2833-2881.
2. S. Ilican, Y. Caglar, M. Caglar, F. Yakuphanoglu, *Appl. Surf. Sci.*, 255 (2008) 2353-2359.
3. Y. Caglar, S. Ilican, M. Caglar, F. Yakuphanoglu, *Spectrochimica Acta Part A*, 67, (2007) 1113-1119.
4. E. Emil, G. Alkan, S. Gurmen, R. Rudolf, D. Jenko, B. Friedrich, *Metals* 8 (2018) 569.
5. A. Rayerfrancis, P. B. Bhargav, N. Ahmed, B. Chandra, S. Dhara, *Physica B* 457 (2015) 96-102.
6. L. Znaidi, *Mater. Sci. and Eng.B*, 174 (2004) 18-30.

New C₆₀ and C₇₀ fullerene derivatives designed for HOMO-LUMO gap tuning in photovoltaic devices

P. Piotrowski, A. Kielczewska, K. Zarębska, M. Skompska, A. Kaim

Faculty of Chemistry, University of Warsaw, Poland

ppiotrowski@chem.uw.edu.pl

ABSTRACT

Series of new C₆₀ and C₇₀ fullerene derivatives have been synthesized and characterized with numerous analytical techniques. Electrochemical measurements allowed to calculate the HOMO-LUMO band gap revealing that obtained functionalized fullerenes largely retain favorable redox electronic properties, showing multiple reversible sequential 1e electrode processes. In addition, experimental results were supported by quantum mechanical calculations made by DFT B3LYP/6-31G(d) and PBEPBE/6-311G(d,p) methods.

Keywords: fullerenes, photovoltaics, HOMO-LUMO gap

INTRODUCTION

Bulk heterojunction solar cells combine an electron-deficient compound (acceptor) and electron rich material i.e. conjugated polymer (donor) with high content of interfacial areas. Resulting material shows photovoltaic effect when placed between suitable electrodes. In recent years development of novel polymer donor materials has drawn big attention and was the main route of investigation in organic photovoltaics. However, the electron accepting compounds are of the same great importance as they can allow construction of photovoltaic devices of higher efficiency too.

Among numerous nanomaterials, functionalized fullerenes are attractive candidates for photovoltaic applications^{1,2} due to their outstanding electron accepting properties and various possible functionalization methods. One of the most promising electron acceptor molecules for photovoltaic cells are C₆₀ and C₇₀ fullerenes and their derivatives due to their capacity for reduction with up to six electrons per single fullerene cage³ and high visible light absorption. Moreover, functionalization of fullerenes allows to introduce plenty of different electron withdrawing or donating groups, allowing to tune the location of HOMO/LUMO levels as well as the visible light absorption. Those groups not only can improve the electronic properties of the final molecule and their solubility but also modify morphology of resulting bulk heterojunction material.

For this purpose, we have designed and synthesized number of thiophene, naphthalene, fluorene and pyrene functionalized fullerenes. Each compound HOMO-LUMO gap was investigated using both electrochemical measurements and corresponding theoretical calculations. All presented functionalized fullerenes can be employed as acceptor materials in fullerene-polymer based photovoltaic cells.

EXPERIMENTAL/THEORETICAL STUDY

C₆₀ and C₇₀ fullerene derivatives were synthesized using modified Bingel-Hirsch procedure⁴. Obtained products were characterized using spectroscopic techniques: ESI-MS, ¹H and ¹³C NMR and FT-IR. Subsequently electrochemical properties of functionalized fullerenes were analyzed using cyclic voltammetry. Resulting HOMO-LUMO band gaps were compared with the values calculated using density functional theory (DFT) B3LYP/6-31G(d) and PBEPBE/6-311G(d,p) methods.

RESULTS AND DISCUSSION

Series of C_{60} and C_{70} fullerene malonates bearing diverse aromatic rings (Figure 1) designed for acceptor materials in photovoltaic cells has been synthesized. For this purpose, modified Bingel-Hirsch method resulting in methanofullerene monoadduct was used. Identification and detailed characterization of the newly obtained compounds was made using spectroscopic methods: mass spectrometry (ESI-MS), magnetic resonance spectroscopy 1H and ^{13}C NMR, IR spectroscopy (FT-IR).

Investigation of electronic properties of synthesized compounds was done by means of cyclic voltammetry (CV). Electrochemical measurements allowed to calculate the HOMO-LUMO band gap revealing at the same time that obtained functionalized fullerenes largely retain favourable redox electronic properties and show multiple reversible sequential 1e electrode processes. In addition, experimental results of electrochemical measurements were followed by quantum mechanical calculations using DFT B3LYP/6-31G(d) and PBEPBE/6-311G(d,p) methods.

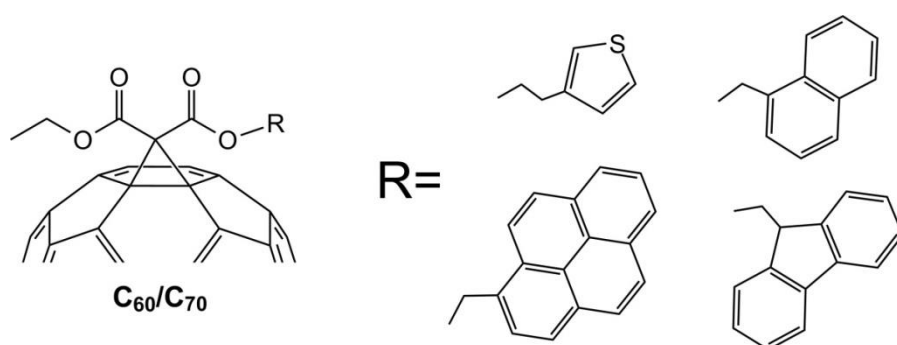


Fig. 1. Structure of synthesized C_{60}/C_{70} fullerene malonates.

CONCLUSION

We have synthesized a series of novel C_{60} and C_{70} fullerene malonates functionalized with diverse aromatic molecules. All compounds were characterized and their structure was confirmed with necessary spectroscopic techniques. Experimental and theoretical HOMO-LUMO levels were determined using cyclic voltammetry and quantum mechanical calculations DFT methods.

Obtained results show that theoretical studies can be very good tool for prediction of the HOMO-LUMO gap properties of fullerene based acceptor materials. Selected synthesized fullerene derivatives with the most adequate HOMO-LUMO levels to the donor polymer applied will be employed in construction of BHJ solar cells in the near future.

Acknowledgments: The authors gratefully acknowledge the financial support of the project TECHMATSTRATEG1/347431/14/NCBR/2018 by National Centre for Research and Development (NCBR) of Poland. For theoretical calculations, we have used computational resources of the Interdisciplinary Center for Mathematical and Computational Modeling at Warsaw University (Grant G 15-11).

REFERENCES

1. J. Nelson, Mater. Today, 14 (2011) 462-470.
2. P.R. Berger, M. Kim, J. Renewable Sustainable Energy, 10 (2018) 013508.
3. Q. Xie, E. Perez-Cordero, L. Echegoyen, 114 (1992) 3978-3980
4. Hirsch, M. Brettreich, Fullerenes: Chemistry and Reactions, Wiley-VCH: Weinheim, Germany, 2005.

Antibacterial functionalization of electrospun nanofibrous membranes

P. Ryšánek¹, P. Čapková¹, M. Malý¹, M. Kormunda¹, Z. Kolská¹, M. Munzarová²

¹Faculty of Science, J. E. Purkyně University, České mládeže 8, 400 96 Ústí nad Labem, Czech Republic;

²Nanovia, Ltd, Podkrušnohorská 271, 436 03 Litvínov - Chudeřín, Czech Republic

petr.rysanek@ujep.cz

ABSTRACT

One-step procedure (i.e. modifying agent in spinning solution) is the most common way of functionalization of electrospun polymeric nanofibrous structures. In such a case the key question is: How efficient is the modifying agent in the nanofibrous composites? For the maximum efficiency, we need modifying substance (antimicrobial, wound healing agent...) on the surface of nanofibers. For special purposes like air/water filtration the stability of composite is crucial. In this research, we analyze in details the effect of modifying substance in spinning solution on structure, phase composition, morphology of nanofibers and on permeability and antimicrobial activity of polyamide 6 (PA6) and polyvinylidene fluoride (PVDF) electrospun nanofibrous membranes modified by Chlorhexidine (CHX), 1-dodecyltrimethylammonium bromide (DTAB) and benzyltrimethylammonium bromide (BTAB).

XPS spectroscopy and electrokinetic measurements confirmed the presence of modifying substances on the surfaces of PA6 and PVDF nanofibers. XRD profile analysis showed that modifying agent in spinning solution did not affect significantly the crystallographic phase composition of PA6 and PVDF. Chemical modification resulted in increase of nanofiber diameters (depending on concentration of modifying agent. Maximum increase of fiber diameter observed in case of BTAB has been explained by molecular modeling. Molecular modeling also revealed the stability of composites by calculating interaction energy between nanofibers and molecules of modifying substance. The best antibacterial efficiency was achieved for DTAB and CHX modification.

Keywords: electrospinning, Nanospider, antibacterial activity, functionalization

Acknowledgments: The authors acknowledge the assistance provided by the Research Infrastructure NanoEnviCz, supported by the Ministry of Education, Youth and Sports of the Czech Republic under the project No.: LM2015073. Student grant project of Internal Grant Agency SGS UJEP: Nanofiber Membranes for Specific Functions, No: UJEP-SGS-2019-53-006-3 is also acknowledged.

The influence of thin aryl layers on the surface of fillers on the properties of composites

M. Sandomierski, B. Strzemieska, A. Voelkel

¹Poznan University of Technology, Institute of Chemical Technology and Engineering, Poznań, Poland

mariuszsandomierski@wp.pl

ABSTRACT

Composite interfaces are critical regions that dictate the filler-polymer adhesion with an important output in terms of mechanical properties of the composites. Changing the type of interactions on these surfaces has a significant effect on improving the properties of the composites. In this work, we prepared active fillers (zeolite, silica, carbon) with hydroxymethyl groups on the surface and

characterized them by complementary analytical tools. The obtained materials were used as a filler in novolac composites and abrasive tools. Introducing active hydroxymethyl groups onto the surface of the filler allows for covalent bonds between the resin and the modified filler. The mechanical properties of the materials were investigated. Flexural strength increased both for novolac composite and abrasive tools. Therefore, it can be concluded that the use of a modified filler improves the properties of novolac composites and model abrasive tools.

Keywords: Filler, thin layer, diazonium, phenol-formaldehyde resin

INTRODUCTION

Phenol-formaldehyde resins are the most commonly used organic binder in the abrasive industry due to good thermal and chemical stability, low price, high hardness and the ability to bind abrasive grains and fillers together.^{1,2} The two main types of resins are novolacs and resoles.³ Resole can be crosslinked under the influence of heat. Novolacs are cured by urotropine which is an effective cross-linking agent, however its decomposition products have a negative effect to skin and mucous membranes and they can cause cancer.^{4,5} This problem occurs in abrasives, which is related to the high operating temperatures of these materials. Decreasing the amount of urotropine by using an active filler that will have the properties of a crosslinking agent will reduce the amount of emitted toxic compounds. The hydroxymethyl groups are responsible for the cross-linking process of phenol-formaldehyde resins. Therefore it is justified to introduce hydroxymethyl groups onto the surface of the fillers. It might be achieved by using diazonium salts.⁶ Already, fillers modified with diazonium salts have been used in composites such as: graphene / polyurethanes (98% increase of shape fixity), graphene / epoxy resin (47% increase of interfacial shear strength), carbon nanotubes / epoxidized natural rubber (50% increase of tensile modulus).⁷⁻⁹

In our work, we focus on an important group of fillers with potential applications in phenol-formaldehyde resins: silica, zeolite and carbon black. The aim of this work was to improve mechanical properties of abrasive tools by covalent reaction of functionalized fillers with phenol-formaldehyde resin.

EXPERIMENTAL/THEORETICAL STUDY

In this work, we prepared active fillers (zeolite, silica, carbon) with hydroxymethyl groups during the in situ reaction with 4-hydroxymethylbenzenediazonium salt. The following techniques were used to evaluate the effectiveness of filler modifications: infrared spectroscopy, Raman spectroscopy, nitrogen adsorption/desorption measurements. The following techniques were used to evaluate the effect of filler modification on the properties of novolac composites and abrasive tools: flow distance, flexural strength, dynamic thermo-mechanical analysis.

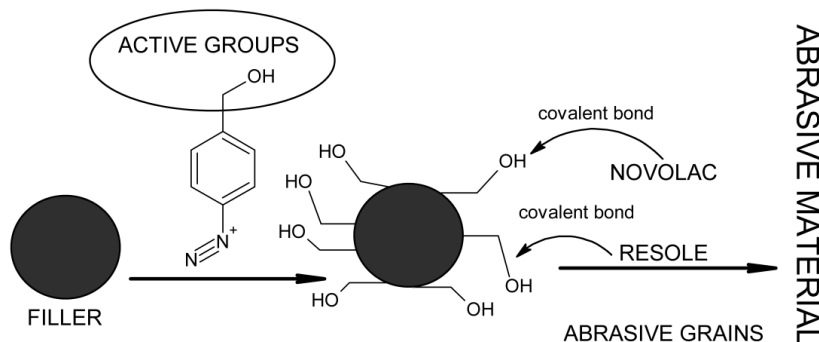


Fig. 1. Scheme of preparation of abrasive tools.

RESULTS AND DISCUSSION

The effectiveness of the filler modification confirms the presence of bands in the range 1300-1800 cm^{-1} on the FTIR. The bands at 1510 and 1600 cm^{-1} in FTIR spectra are assigned to ring breathing mode in aromatic ring of aryl group and appears only in the spectra of modified material. The results of Raman mapping indicate the effectiveness of modification of the entire filler surface. The results show that the organic layer is not present in unmodified silica. Moreover, there are no visible the places with higher amount of aromatic groups. Even distribution of the aryl layer and therefore of the hydroxyl groups is very important due to the uniform effect of the filler on the properties of the composite at its entire volume. The surface area and pore volume decrease after filler modification. This is related with the coverage of surface by the organic layer. During the modification, the pores are filled by the aryl layer, which results in a reduction of their volume. This phenomenon is particularly evident in the case of micropores. This is due to the presence of the aryl layer at the entrance to the micropores, which causes their closure. The results obtained by three-point flexural test indicate an increase in flexural strength for a novolac composites and abrasive tools with modified filler compared to an composite with unmodified filler. The increase in flexural strength is related to the resulting covalent bonds between the resin and the modified filler.

CONCLUSION

Modification by diazonium salt allow to successful introduction of active hydroxymethyl groups on the surface of fillers. The organic layer is evenly distributed. The modified fillers have a smaller surface area and pore surface than unmodified. The results obtained by three-point flexural test indicate an increase in flexural strength both for a novolac composites and abrasive tools. Therefore, it can be stated that application of active filler with thin aryl layer improves the mechanical properties of novolac composites and model abrasive tools.

Acknowledgments: This work was conducted with the financial support from the Polish National Science Centre (grant no. UMO-2015/17/B/ST8/02388).

REFERENCES

1. L.A. Pilato, Phenolic, Resins: A Century of Progress, Springer-Verlag, Berlin, 2000.
2. Gardziella, L.A. Pilato, A.Knop, Phenolic Resins Chemistry, Applications, Standarization, Safety and Ecology 2nd completely revised edition. Springer-Verlag, Berlin, 2000.
3. L.A. Pilato, React. Funct. Polym. 73 (2013) 270-277.
4. M. Wang, Z. Yuan, S. Cheng, M. Leitch, C.C. Xu, J. Appl. Polym. Sci. 118 (2010) 1191-1197.
5. Hexamethylenetetramine [MAK Value Documentation, 1993]. The MAK Collection for Occupational Health and Safety; Wiley-VCH Verlag GmbH & Co. KGaA., 2012; pp 356-372
6. M. Sandomierski, T. Buchwald, B. Strzemiecka, A. Voelkel, Spectrochim. Acta A-M. 191 (2018) 27-35.
7. S. Han, B. C. Chun, Compos. Part A-Appl. S. 58 (2014) 65-72.
8. K.M. Beggs, L. Servinis, T.R. Gengenbach, M.G. Huson, B.L. Fox, L.C. Henderson, Compos. Sci. Technol. 118 (2015) 31-38.
9. M. Qiu, S. Wu, Z. Tang, B. Guo, Compos. Sci. Technol. 165 (2018) 24-30.

Poster presentations (PP):

Pillared montmorillonites as carbon dioxide nanosorbents

K. Bahranowski¹, A. Klimek¹, A. Gaweł¹, A. Tomczyk¹, E. M. Serwicka²

¹Faculty of Geology, Geophysics and Environmental Protection, AGH University of Science and Technology, Poland; ²Jerzy Haber Institute of Catalysis and Surface Chemistry, Polish Academy of Sciences, Poland

bahr@agh.edu.pl

ABSTRACT

The study aimed at the assessment of CO₂ sorption capacity by montmorillonites modified by insertion of titania, zirconia or mixed titania-zirconia pillars between the clay layers. Sorption of carbon dioxide at 0°C was related to the textural parameters of these materials, determined from the nitrogen adsorption/desorption isotherms at -196°C. Pillaring enhanced the amount of sorbed CO₂, whose uptake did not correlate with the specific surface area but increased with the decrease of the average pore diameter of the samples. Best sorption properties were observed for the sample containing mixed Ti-Zr pillars, which was characterized by the highest share of microporosity and the lowest average pore diameter.

Keywords: Montmorillonite, clay, pillaring, CO₂ sorption

INTRODUCTION

Montmorillonite (Mt), which is the main mineral component of bentonite rocks, belongs to the family of layered silicates known as smectites. The interlayer spaces in Mt are occupied by hydrated alkali and alkali earth cations, which are easily exchangeable, and may be replaced with large inorganic oligocationic species, in the process known as pillaring. The oligocation pillars prop open the clay structure and make the interlayer space accessible to gases and vapours. After calcination the pillars bind permanently the Mt layers, yielding thermally stable porous materials, so-called pillared interlayered clays (PILCs), attractive for their sorptive and catalytic properties. In particular, PILCs containing Ti-, Zr-, or mixed Ti-Zr-pillars showed excellent properties in catalytic purification of air from chlorinated volatile organic compounds¹. In this work, the potential of such materials for CO₂ sorption is evaluated.

EXPERIMENTAL

The starting material used in this study was the Kopernica-3 bentonite (Slovakia)², containing ca. 70% of montmorillonite. Pillaring was carried out according to the previously described procedure³. Textural studies by means of nitrogen adsorption/desorption at -196°C were performed with aid of ASAP 2020 apparatus, after 3 h of sample outgassing at 200°C. The same equipment was used for investigation of CO₂ sorption at 0°C.

RESULTS AND DISCUSSION

Textural data gathered in Table 1 show that in all cases pillaring causes a substantial increase of specific surface area and porosity with respect to the starting Kopernica-3 material. The total effect depends on the nature of pillars and is related chiefly to their size. The average pillar height increases in the order: Zr-pillar (~7 Å) < Ti-Zr-pillar (~11 Å) < Ti-pillar (~14 Å), and so does the specific surface area ($S_{\text{BET}}^{\text{Ti-PILC}} > S_{\text{BET}}^{\text{[Ti,Zr]-PILC}} > S_{\text{BET}}^{\text{Zr-PILC}} > S_{\text{BET}}^{\text{Kopernica-3}}$). This shows that it is the accessibility of internal surface of clay interlayer and of intercalated pillars that controls the

magnitude of specific surface. Noteworthy, the [Ti,Zr]-PILC sample is characterized by the highest share of micropores in the total pore volume. In general, the higher the contribution of microporous character, the lower the average pore diameter (APD) of PILCs: $APD^{Kopernica-3} > APD^{Zr-PILC} > APD^{Ti-PILC} > APD^{[Ti,Zr]-PILC}$. Analysis of the amount of sorbed CO₂ shows that pillaring enhances ca. 4× the CO₂ sorption capacity of the parent Kopernica-3 material. Interestingly, there is no simple correlation between the materials specific surface areas or total pore volumes and the ability to sorb CO₂. The CO₂ uptake appears to be directly related to the average pore dimension of the sample, with materials exhibiting narrower pores and higher share of microporosity being more efficient in CO₂ entrapment.

Table 1. Textural parameters and CO₂ sorption capacity of Kopernica-3 bentonite and its pillared derivatives

Parameter	Sample			
	Kopernica-3	Zr-PILC	Ti-PILC	[Ti,Zr]-PILC
S_{BET} [m ² /g]	52	132	310	258
V_{tot} [cm ³ /g]	0.17	0.21	0.36	0.23
V_{micro}^{DR} [cm ³ /g]	0.02	0.06	0.12	0.12
$V_{micro}^{DR} / V_{tot}^{0.99}$	0.12	0.26	0.33	0.50
V_{meso}^{BJH} [cm ³ /g]	0.11	0.09	0.17	0.09
$V_{meso}^{BJH} / V_{tot}^{0.99}$	0.62	0.45	0.47	0.37
$V_{macro} = V_{tot}^{0.99} - (V_{micro}^{DR} + V_{meso}^{BJH})$ [cm ³ /g]	0.04	0.06	0.07	0.03
$V_{macro}^{BJH} / V_{tot}^{0.99}$	0.26	0.29	0.20	0.12
Average pore diameter [Å]	132	63	47	36
CO ₂ sorbed [mmol/g]	0.16	0.53	0.57	0.67

CONCLUSION

Modification by pillaring significantly increases the capacity of Kopernica-3 bentonite for sorption of CO₂. The CO₂ uptake increases with the decrease of the average pore diameter and growing share of microporosity. The CO₂ sorption capacity of the investigated samples follows the order: [Ti,Zr]-PILC > Ti-PILC > Zr-PILC > Kopernica-3.

Acknowledgments: This work was supported by the Polish National Science Center (NCN), grant OPUS 2017/25/B/ST10/00768.

REFERENCES

1. A. Michalik-Zym, R. Dula, D. Duraczyńska, J. Kryściak-Czerwenka, T. Machej, R.P. Socha, W. Włodarczyk, A. Gaweł, J. Matusik, K. Bahrnowski, E. Wisła-Walsh, L. Litńska-Dobrzyńska, E.M. Serwicka, Appl. Catal. B: Environ. 174 (2015) 293-307.
2. K. Górniak, T. Szydlak, A. Gaweł, A. Klimek, A. Tomczyk, B. Sulikowski, Z. Olejniczak, J. Motyka, E.M. Serwicka, K. Bahrnowski, Clay Minerals 51 (2016) 97-122.
3. K. Bahrnowski, W. Włodarczyk, E. Wisła-Walsh, A. Gaweł, J. Matusik, A. Klimek, B. Gil, A. Michalik-Zym, R. Dula, R.P. Socha, E.M. Serwicka, Micropor. Mesopor. Mater. 202 (2015) 155-164.

Functionalization and stability testing of nanofibrous PA6/DTAB membranes for air filtration

P. Čapková¹, P. Ryšánek¹, J. Štojdl², J. Trögl², O. Benada^{1,3}, M. Kormunda¹, Z. Kolská¹, M. Munzarová⁴

¹Faculty of Science, J. E. Purkyně University, České mládeže 8, 400 96 Ústí nad Labem, Czech Republic;

²Faculty of Environment, J. E. Purkyně University, Králova výšina 3132/7, 400 96 Ústí nad Labem, Czech Republic; ³Institute of Microbiology of the Czech Academy of Sciences, Vídeňská 1083, 14, 220 Prague 4, Czech Republic; ⁴Nanovia, s. r. o., Litvínov, Podkrušnohorská 271, 436 03 Litvínov – Chudeřín, Czech Republic

Republic

petr.rysanek@ujep.cz

ABSTRACT

Although antimicrobial activity is a hot topic in the development of new filter media, the stability of the antimicrobial effect is still neglected. Water and air filters, which operate in dark conditions, are constantly exposed to attacks from environmental microorganisms. The microorganisms captured by the filters grow rapidly, resulting in the formation of biofilms. Membrane bio-fouling is the main problem during an operation of membrane elements for water/air treatment as biofilm formation reduces the flux of water through the membrane. Thus, the filters of nanofibrous membranes with antimicrobial functionality have attracted growing attention. The aim of this work is to investigate the stability of antimicrobial effect of nanofibrous PA6/DTAB membrane.

The morphology and the changes in structure of the membranes were determined by HRSEM and XRD analysis. XPS analysis and electrokinetic measurement were used for investigation of surface chemistry and charge. Membranes were also tested on their antibacterial activity. For the antibacterial stability test, the special air-blowing device was used.

XPS spectroscopy proved the presence of modifying agent on the membrane surface before and after air filtration tests. Electrokinetic measurement also proved the presence of additive on the surface. XRD analysis confirmed smaller crystalline domains in modified membrane in comparison with pristine one. HRSEM showed the effect of additive on membrane morphology. Antibacterial tests showed very good antibacterial activity before and also after three weeks of air-blowing.

Keywords: electrospinning, Nanospider, air filtration, stability

Acknowledgments: The authors acknowledge the assistance provided by the Research Infrastructure NanoEnviCz, supported by the Ministry of Education, Youth and Sports of the Czech Republic under the project No.: LM2015073. Student grant project of Internal Grant Agency SGS UJEP: Nanofiber Membranes for Specific Functions, No: UJEP-SGS-2019-53-006-3 is also acknowledged.

PVDF/vermiculite nanocomposite films

K. Čech Barabaszová, S. Holešová, K. Švábová, L. Chlebíková

Nanotechnology Centre, VŠB - TU Ostrava, Czech Republic

Karla.cech.barabaszova@vsb.cz

ABSTRACT

Polyvinylidene fluoride (PVDF)/vermiculite nanocomposite films were prepared by both solution casting and co-precipitation methods. The ultrasound was used for homogenous distribution of Mg-vermiculite particles in PVDF matrices. The effect of isothermal crystallization conditions (temperature and time) and the presence of vermiculite particles on the PVDF films structure were studied. The structure and morphology of the nanocomposite were investigated by X-ray diffraction (XRD), polarized light microscopy (OM) and scanning electron microscopy (SEM) techniques. Fourier transform infrared spectroscopy (FTIR), and differential scanning calorimetry (DSC) were used to investigate the crystalline phases of PVDF samples. It was observed that the morphological behaviour of the nanocomposite critically depends upon the sample preparation methods. Both well orientated vermiculite sheets and completely exfoliated morphologies were successfully achieved and the detailed structure analyses were conducted. The crystallisation of PVDF at temperatures above 160 °C presents a multiform morphology composed of ringed, non-ringed and mixed spherulites.

Acknowledgments: This work was supported by the project No: SP2019/24 "Hybrid and biodegradable clay nanocomposite materials".

Towards Clay Nanoreactors: Modified Clays as Catalysts for Baeyer-Villiger Reaction

P. Grussmann¹, I. Martausová¹, Z. Lacný¹, A. Martaus², D. Cvejn³

¹Nanotechnology Centre, VSB-Technical University of Ostrava, Czech Republic; ²Institute of Environmental Technology, VSB-Technical University of Ostrava, Czech Republic; ³ENET Centre, VSB-Technical University of Ostrava, Czech Republic

iveta.martausova@vsb.cz

ABSTRACT

Baeyer-Villiger reaction is one of the most well established selective oxidation reactions in the organic synthesis. Tin(IV)-based compounds have been proven to have a good activity towards this reaction. Moreover, clay materials, layered silicates containing the exchangeable cations in the interlayer space, are considered to be a potent nanoreactor-like structure, where the unique chemical conditions of interlayer space provide a specific chemical environment capable to enhance the courses of chemical reactions. Upon these long and generally known facts, our group has decided to investigate the properties of Sn(IV)-impregnated vermiculite (Sn^{IV}-VMT) in Baeyer-Villiger reaction of adamantanone with hydrogen peroxide. Furthermore, the reactions on similar catalyst between adamantanone and hydroxylamine and hydrazine were also investigated. The reaction appears to be strongly dependent on the concentration of Sn(IV) in the interlayer space, as well as on the adamantanone/reagent ratio. Under optimal conditions Baeyer-Villiger conversions were up to 43 %. Reaction with the hydrazine lead to bis(adamant-2-ylidene)hydrazine (**3**) in conversions up

to 99 %. Reaction with the hydroxylamine lead to adamantanone-oxime (**4**) in conversions up to 98 %.

Keywords: Clays, vermiculite, Baeyer-Villiger reaction, catalysis.

INTRODUCTION

The Baeyer-Villiger reaction (B.-V. reaction) of adamantanone (Fig. 1) is one of the most commonly used reactions to screen a potential of reaction conditions and/or catalytic system towards B.-V. reaction. Tin-based reagent and catalysts¹ as well as peroxyacid-based reagents² are usually successful in the reaction. Clay materials, especially ion-exchanged vermiculites have been used in various reactions.^{3,4} The B.-V. reaction on Sn-ion exchanged vermiculites, though have never been tested.

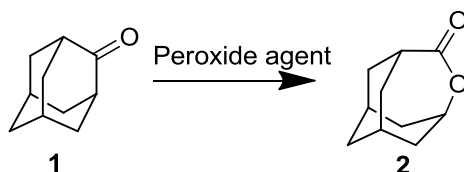


Fig. 1 Baeyer-Villiger reaction of adamantanone (**1**) to adamantane-lactone (**2**). General scheme.

EXPERIMENTAL/THEORETICAL STUDY

Sn-VMT was prepared by thermal treatment of wild-type vermiculite with the saturated solution of commercial SnCl_4 . For the experimental setups, commercial adamantanone have been mixed in various reactant/reagent ratios with hydrogen peroxide, hydrazine and hydroxylamine. The distribution of products has been observed by GC/FID and GC/MS analyses.

RESULTS AND DISCUSSION

Conversions of adamantanone in sence of B.-V. reaction are summed in Table 1.

Table 1 Conversions of adamantanone in various varieties of adamantanone/ H_2O_2 ratio for various vermiculite catalysts

Catalyst	Adamantanone/ H_2O_2 ratio	Conversions [%]
Blank	1 : 1	1
10% Sn-VMT	1 : 0,5	8
	1 : 0,75	11
	1 : 1	24
	1 : 2,5	43
	1 : 5	5
5% Sn-VMT	1 : 0,5	5
	1 : 0,75	7
	1 : 1	17
Wild type-VMT	1 : 1	3

Reactions with hydrazine and hydroxylamine (Fig. 2 and Fig. 3, respectively) have shown 99% and 98% conversion towards their products shown in respective figures.

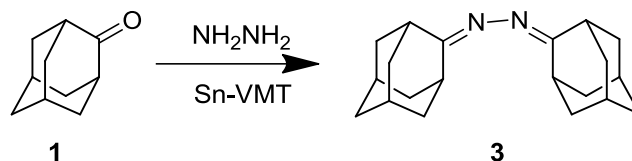


Fig. 2 Reaction of adamantanone with hydrazine in presence of Sn-VMT catalyst.

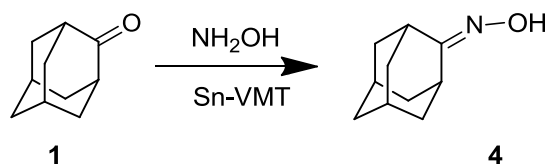


Fig. 3 Reaction of adamantanone and hydroxylamine in presence of Sn-VMT catalyst.

Acknowledgments: This research has been funded by the Ministry of Education, Youth and Sports of the Czech Republic (projects no. LO1203, SP2018/91 and SP2019/30).

REFERENCES

1. Markiton, A. M.; Szelwicka, A.; Jurczyk, S.; Chrobok, A. Superactive Tin(II) Triflate/Carbon Nanotube Catalyst for the Baeyer-Villiger Oxidation. *Appl. Catal. A, Gen.* **2018**, *556*, 81–91. <https://doi.org/10.1016/j.apcata.2018.02.033>.
2. Yvette, O. M.; Malan, S. F.; Taylor, D.; Kapp, E.; Joubert, J. Adamantane Amine-Linked Chloroquinoline Derivatives as Chloroquine Resistance Modulating Agents in Plasmodium Falciparum. *Bioorganic Med. Chem. Lett.* **2018**, *28* (8), 1287–1291. <https://doi.org/10.1016/j.bmcl.2018.03.026>.
3. (Ravichandran, J.; Sivasankar, B. Properties and Catalytic Activity of Acid-Modified Montmorillonite and Vermiculite. *Clays Clay Miner.* **1997**, *45* (6), 854–858. <https://doi.org/10.1346/CCMN.1997.0450609>.
4. Silva, F. C.; De Souza, M. C. B. V.; Ferreira, V. F.; Sabino, S. J.; Antunes, O. A. C. Natural Clays as Efficient Catalysts for Obtaining Chiral β -Enamino Esters. *Catal. Commun.* **2004**, *5* (3), 151–155. <https://doi.org/10.1016/j.catcom.2003.12.008>.

Photoactive mesoporous nanoparticles as photochemical reactors

D. Kędra¹, A. Baliś¹, Sz. Zapotoczny¹

¹Faculty of Chemistry, Jagiellonian University, Krakow, Poland;

dominika.kedra@student.uj.edu.pl

ABSTRACT

Mesoporous silica nanoparticles, characterized by the pores with diameters between 2 and 50 nm are examples of materials with large specific surface area that can be also dispersed in an aqueous medium. Possibilities of modifying their internal structure and surface chemistry already at the stage of the synthesis gave an opportunity to create materials with unique properties and wide applications as e.g., adsorbents, catalyst supports, drug delivery systems, nanoreactors or photoreactors. In this study, we developed mesoporous core-shell silica nanoparticles with

immobilized anthracene chromophores that could serve as photoreactors to conduct photosensitized reactions within the confined mesoporous environment. First, trialkoxyorganosilane, TEOS-A, was successfully synthesized, purified and its structure was confirmed by NMR and MS spectroscopy. Silica nanoparticles with solid cores and mesoporous shells with anthracene chromophores were synthesized using the sol-gel method via co-condensation of tetraethoxysilane (TEOS) and TEOS-A. The nanoparticles were characterized using UV-VIS and fluorescence spectroscopy. Förster Resonance Energy Transfer (FRET) was shown to proceed very efficiently in a model donor-acceptor system with anthracene (donors) immobilized in the nanoparticles and perylene (acceptor) solubilized in the mesopores. Similarly, efficient FRET was observed for fluorescein (acceptor) adsorbed on the surface of the nanoparticles.

Keywords: Mesoporous nanoparticles, Co-condensation, Förster Resonance Energy Transfer, photoreactors

INTRODUCTION

Mesoporous silica nanoparticles, characterized by the pores with diameters between 2 and 50 nm are examples of materials with large specific surface area that can be also dispersed in an aqueous medium. Possibilities of modifying their internal structure and surface chemistry already at the stage of the synthesis gave an opportunity to create materials with unique properties and wide application as e.g., adsorbents, catalyst supports, drug delivery systems, nanoreactors or photoreactors. These materials can be obtained in three different ways: by successive addition of organic groups to the silica matrix (grafting), simultaneous synthesis of inorganic silica parts condensing with organic silyl groups (co-condensation) or by synthesis with two organic silyl precursors, which leads to mesoporous formation periodic organosilica.¹

EXPERIMENTAL STUDY

The trialkoxyorganosilane containing anthracene chromophore (TEOS-A) was synthesized as shown in Fig.1.

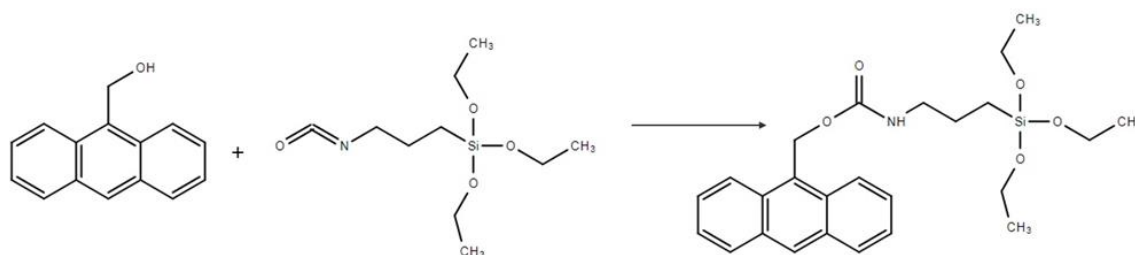


Fig. 1. Reaction scheme for synthesis of trialkoxyorganosilane with attached anthracene (TEOS-A)

Silica nanoparticles with solid cores and mesoporous shells containing the chromophores were synthesized using the sol-gel method by co-condensation of tetraethoxysilane(TEOS) with TEOS-A

RESULTS AND DISCUSSION

The synthesized nanoparticles containing incorporated anthracene groups were characterized using UV-VIS and fluorescence spectroscopy. Efficient solubilization of perylene in the pores of the particles dispersed in water could be noticed by following its fluorescence intensity (peryene does not fluoresce in water). The Förster Resonance Energy Transfer (FRET) was observed between the

excited donor molecules (anthracene) and the acceptor molecules solubilized in the pores (perylene) or present in the vicinity of the nanoparticles surface (fluorescein). Importantly, no FRET could be observed for the solutions of TEOS-A and perylene at the same total concentrations of the donor and acceptor molecules because they are not close enough in the homogenous solution. The incorporation of TEOS-A into silica microparticles (SCAMS) by co-condensation enables the creation of an microenvironment in which the acceptor (perylene) introduced by solubilization is sufficiently close to the donor and it is possible to transfer the excitation energy via FRET.

CONCLUSION

Trialkoxyorganosilane TEOS-A was successfully synthesized, purified and its structure was confirmed by NMR and MS spectroscopy. Silica nanoparticles with solid cores and mesoporous shells with anthracene chromophores were synthesized using the sol-gel method via co-condensation of TEOS and TEOS-A. The formed nanophotoreactors can be used to perform photosensitized reactions with the hydrophobic reactants solubilized in the mesopores or with hydrophilic reactants that can adsorb on the surface of the nanoparticles. Thanks to the core-shell structures the nanoparticle-based photoreactors may be easily isolated from the aqueous dispersion and reused.

Acknowledgments: The authors would like to thank Foundation for Polish Science (FNP) for financial support - Grant no. TEAM/2016-1/9

REFERENCES

1. F. Hoffmann, M. Cornelius, J. Morell, M. Fröba, *Angew. Chemie - Int. Ed.* 2006, 45, 3216–3251.

Layered double hydroxides: synthesis, exfoliation and dispersion in polymer systems

K. Kopecká^{1,2,3}, L. Beneš², K. Melánová^{2,4}, P. Knotek³, V. Zima^{1,4}, K. Zetková¹

¹SYNPO, akciová společnost, Czech Republic; ²Joint Laboratory of Solid State Chemistry, Faculty of Chemical Technology, University of Pardubice, Czech Republic; ³Department of General and Inorganic Chemistry, Faculty of Chemical Technology, University of Pardubice, Czech Republic; ⁴Institute of Macromolecular Chemistry of the Czech Academy of Sciences, Czech Republic

katerina.kopecka@synpo.cz

ABSTRACT

This work reacts to strong demand for production of novel materials with enhanced properties. An addition of special fillers to polymer matrices can strongly influence behavior of the whole system. Layered double hydroxides (LDH), as a counterpart to traditional clays, can be useful for improving mechanical durability or even reducing the flammability of polymers. To benefit from filler properties, it is necessary to disperse it homogeneously inside the polymer matrix. In this contribution, we report on preparation of LDH based on Zn and Al with three different charge compensating anions and their ability to be dispersed in epoxy resin systems. The exfoliation of these compounds was also studied and it was found to be beneficial for improving the incorporation of the filler inside the polymer matrix.

Keywords: Exfoliation; Polymer composite; Layered double hydroxides

INTRODUCTION

Layered double hydroxides represents a large group of layered solids. Their structure consists of positively charged metal hydroxide sheets, which charge is compensated by anions accommodated between these sheets (see Fig. 1). Owing to their structural similarity to clays they are nicknamed "anionic clays". Their incorporation into a polymer matrix can improve the polymer durability and resistance. Thanks to their layered nature it is possible to increase incorporation of the filler by using nanosheets prepared by exfoliation of the bulk particles. A suitable method for the exfoliation of this kind of material is the so-called liquid-based exfoliation², which is, basically explained, lowering the number of layers, from which the individual particles consist, in a solvent using mechanical forces.

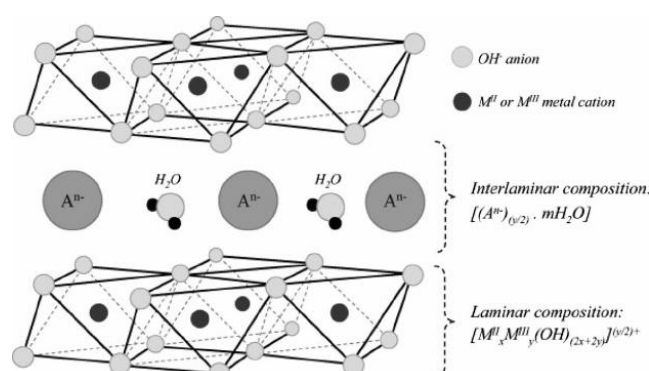


Fig. 1 Illustration of LDH structure¹.

EXPERIMENTAL

Synthesis of LDH

The LDHs were prepared by coprecipitation from aqueous solutions of soluble metal precursors in basic media in the presence of a charge compensating anion. The approach is based on a slight modification of the published procedure³.

Exfoliation

Samples were exfoliated in isopropyl alcohol using a high shear disperser. The selection of the solvent and characterisation of the nanosheets followed the procedure described in the previous work⁴.

Composites

Synthesized LDHs were dispersed in a polymer epoxy system using an ordinary mixing, three-roll milling and special dispersive stirrer. The quality of the dispersion was evaluated on free-standing films by optical and scanning electron microscopy.

RESULTS AND DISCUSSION

Three types of ZnAl-LDH were synthesized using dodecyl sulphate (ZnAl-DDS), lactate (ZnAl-LAC) and carbonate (ZnAl-CO₃) as charge compensating anions. The type of the anion strongly influenced the morphology of the particles. However, for all of them their layered structure was preserved. It is possible to exfoliate these particles by means of the liquid-based exfoliation using a high shear force. The sample with lactate was the least compatible with the epoxy system. However,

pre-exfoliation of the particles prior to mixing with the polymer lead to an improvement of the quality of the dispersion.

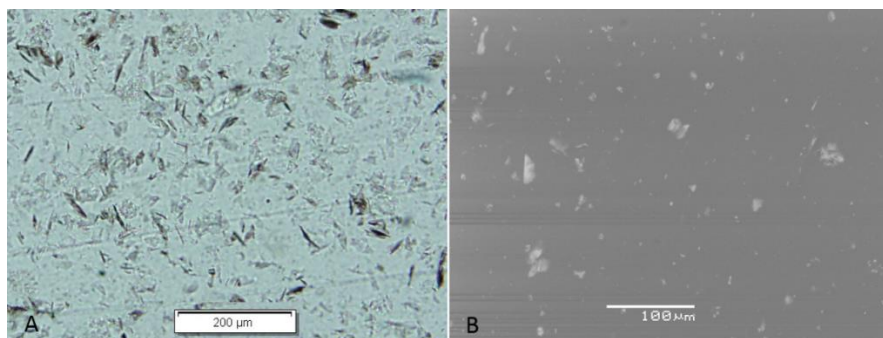


Fig. 2 Well dispersed particles of ZnAl-DDS in free-standing polymer film. A) Picture from optical microscope, B) picture from scanning electron microscope

CONCLUSION

It is possible to prepare LDH based on Zn and Al with dodecylsulphate and lactate as a charge compensating anions. It is possible to exfoliate these particles by means of liquid-based exfoliation using a high shear force. It is possible to incorporate exfoliated LDHs based on Zn and Al into an epoxy polymer matrix.

Acknowledgments: This work was supported by Technology Agency of the Czech Republic (TH02020201)

REFERENCES

1. Salomão, Rafael & Milena, L.M. & Wakamatsu, M.H. & Pandolfelli, Victor., Ceram Int, 37, 8 (2011) 3063 - 3070
2. V. Nicolosi, M. Chhowalla, M. G. Kanatzidis, M. S. Strano, J. N. Coleman. Science 340, 6139 (2013)
3. K. Melánová, L. Beneš, V. Zima, M. Vlček, Sci. Pap. Univ. Pardubice Ser. A **8** (2002) 103-110
4. K. Kopecká, L. Beneš, K. Melánová, V. Zima, P. Knotek, K. Zetková Beilstein J. Nanotechnol. 9, (2018), 2906–2915

Nanocomposite systems based on polymer brushes and superparamagnetic iron oxide nanoparticles

T. Kuciel¹, P. Nalepa¹, W. Górka², M. Szuwarzyński³, S. Zapotoczny¹

¹Faculty of Chemistry, Jagiellonian University, Poland, ²Faculty of Physics, Jagiellonian University, Poland,

³Academic Centre for Materials and Nanotechnology, AGH University of Science and Technology, Poland

kuciel@chemia.uj.edu.pl

ABSTRACT

Polymer brushes are polymer chains that are grafted to a suitable surface. If density of chains is high enough, interaction between chains cause them to straighten, developing structure similar to brush, hence the name. They are characterized by their well defined structure as well as wide range of possible modifications. However pure polymer brushes, composed solely of polymer chains have their own set of limitations. For instance, it is difficult to obtain brushes exhibiting strong magnetic properties.

To overcome this issue, nanocomposite systems were proposed. In such systems, polymer chains composing brushes would act as matrix for Iron Oxide nanoparticles of certain sizes exhibiting superparamagnetic properties (SPION) and thus very strong paramagnetic response. Due to strong electrostatic interactions, cationic polymer brushes obtained via ATRP were chosen as model. Several approaches to coupling nanoparticles and brushes were tried and evaluated. Obtained cationic nanocomposites could find their place as intelligent substrates for cell growth. Later, focus shifted to system based on conductive polymer brushes as interactions between their conjugated side chains and nanoparticles could be a key in enhancing their conductivity, which could play a role in development new generation of sensors, LEDs and light harvesting systems.

Keywords: Polymer brushes, nanocomposites, ATRP, SPION

INTRODUCTION

There are many types of coatings and films to enhance and modify surface properties, however among them polymer brushes offer unique combination of well defined structure, relative ease of synthesis and wide range of possible modifications. They can be synthesized using grafting to strategy, where pre-made chains are linked with surface or grafting from strategy, which involves coating a surface with monolayer of initiator, from which polymer chains grow. Usually, to obtain well defined structures with specified length controlled polymerization reactions are chosen. Some properties, like magnetic response or thermal conductivity is troublesome to obtain in pure carbon based polymer. To solve this, nanocomposite systems have been proposed, combining superparamagnetic iron oxide nanoparticles with polymer brushes. In first step, various synthesis strategies were tested using strongly interacting cationic polymer. These systems possess interesting structure and have been proposed as intelligent, magnetoresponsive substrate for cell growth. Later, research was focused on obtaining conductive polymer brushes based on polyTPM filled with SPIONs, hoping to enhance conductivity of the system by filling gaps in conjugated side chains and facilitating electron transport. Such layers could find use in sensors, LEDs and new generation light harvesting systems.

EXPERIMENTAL/THEORETICAL STUDY

Cationic polymer brushes were based on poly-(3-acrylamidopropyl)trimethylammonium chloride (polyAPTAC) and synthesized using copper based Atom Transfer Radical Polymerisation (ATRP), using silicon wafers as surfaces¹ Conductive polymer brushes were based on poly-3-trimethylsilyl-2 propynyl methacrylate (polyTMP), using surface initiated photoiniferter mediated polymerisation with ITO as surface². Superparamagnetic iron oxide nanoparticles were obtained using precipitation synthesis, and characterised via transmission electron microscopy (TEM) and dynamic light scattering (DLS). Obtained systems were characterised using atomic force microscopy (AFM) to determine their topography as well as mechanical and magnetic properties. Interactions between nanoparticles and brushes were determined using X-ray photoelectron spectroscopy (XPS) and secondary ion mass spectroscopy (SIMS)

RESULTS AND DISCUSSION

Images obtained using atomic force microscopy show distinct change in topography and magnetic properties as measured using MFM mode between pure polyAPTAC brushes and brushes obtained with SPIONs present in situ during polymerisation.

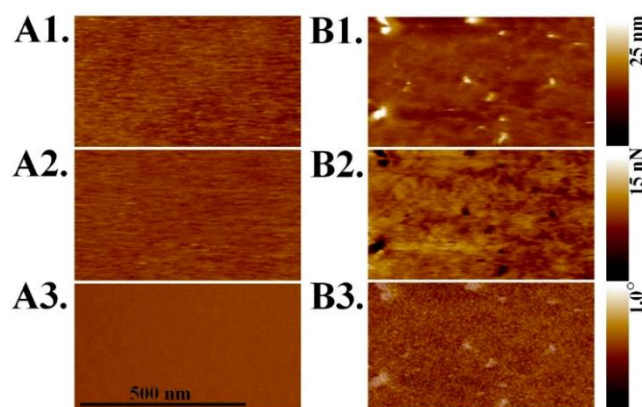


Fig. 1. PF-MFM images of poly(APTAC) brushes (A1–A3) and poly(APTAC)+SPIONs brushes (B1–B3): 1. topography, 2. adhesion, 3. magnetic phase.¹

This change seems to indicate formation of nanocomposite material further evidenced by secondary ion mass spectroscopy, showing presence of iron atoms in the system.

CONCLUSION

Results seem to suggest that polymerization of cationic monomers via ATRP with nanoparticles present in situ result in stable nanocomposite systems exhibiting magnetic properties. These systems, while interesting on their own acted as model system, which is being further developed using conductive polymer brushes to research effect of nanoparticles on electrical properties of brushes.

Acknowledgments: The authors would like to acknowledge TEAM project (2016-1/9, financed by the Foundation for Polish Science (Smart Growth Operational Program 2014-2020)) for the financial support.

REFERENCES

1. Górka, W.; Kuciel, T.; Nalepa, P.; Lachowicz, D.; Zapotoczny, S.; Szuwarzyński, M. *Nanomaterials* 2019, 9, 456.
2. Szuwarzyński, M.; Wolski, K.; Zapotoczny, S.. *Polym. Chem.* 2016, 7, 5664–5670

Comparison of TiO₂ and g-C₃N₄-based materials modified with Ag NPs utilized as a photocatalyst for degradation of model dye acid orange 7

M. Michalska¹, V. Matejka¹, J. Pavlovsky¹, P. Praus¹, G. S. Martynkova²

¹Department of Chemistry, VŠB-Technical University of Ostrava, 17. listopadu 15/2172, Ostrava-Poruba, Czech Republic; ²Nanotechnology Centre, VŠB-Technical University of Ostrava, 17. listopadu 15/2172, Ostrava-Poruba, Czech Republic

michalska.monika83@gmail.com

ABSTRACT

A new low temperature chemical synthesis of silver nanoparticles was proposed to modify the surface grains of titanium dioxide (TiO₂) and graphitic carbon nitride based material (g-C₃N₄). The comparison of two different materials modified with Ag nanoparticles and utilized as a photocatalyst for degradation of model dye acid orange 7 will be presented during the conference. The structure and morphology of the prepared composites pristine and silver modified was

characterized using X-ray diffraction (XRD) and scanning electron microscopy (SEM). Optical properties were determined using DRS (UV-vis) and photoluminescence (PL) spectroscopy. The photodegradation process using model dye acid orange 7 was performed to characterize all the materials as a photocatalyst. The best performances were obtained for both materials modified with very small content of silver – 0.5% wt. The photodegradation activity in excess 95% and 94% were achieved after 1 h under dark, and then 3 h with UV lamp processes for samples with 0.5% wt. Ag: TiO₂ and g-C₃N₄-based material, respectively.

Keywords: Ag nanoparticles, photocatalyst, TiO₂, g-C₃N₄

Acknowledgments: This work was supported by the ESF in „Science without borders“ project, reg. nr. CZ.02.2.69/0.0./0.0./16_027/0008463 within the Operational Programme Research, Development and Education and by the student projects SP2019/142 of VŠB - Technical University of Ostrava.

Magnetically-responsive polymeric scaffolds for cell cultures

P. Nalepa¹, W. Górka^{1,2}, T. Kuciel¹, M. Szuwarzyński³, S. Zapotoczny¹

¹Faculty of Chemistry, Jagiellonian University, Poland; ²Faculty of Physics, Astronomy and Applied Computer Science, Jagiellonian University, Poland; ³Academic Centre for Materials and Nanotechnology, AGH University of Science and Technology, Poland

paula.nalepa@student.uj.edu.pl

ABSTRACT

For the last two decades a huge efforts have been made to understand and control chemical, physical and biological properties of scaffolds for cell cultures. A great attention has been devoted to hybrid inorganic–polymer systems grafted or adsorbed to/from the surfaces¹, which allow controlled adsorption and desorption of biological materials. Moreover, such nanocomposites can find other potential applications as photovoltaic devices, field effect transistors and sensors². The crucial process of cell culture affecting the physiological activity of cells, including migration, orientation or proliferation is an adhesion to the substrate. In this report, we present a novel cell culturing scaffold based on organic polymer brushes and inorganic magnetic nanoparticles. The usage of a magnetic field allows good control of adhesive properties of substrates. The nanocomposites were obtained by the simultaneous introduction of super-magnetic magnetic oxide nanoparticles (SPIONs) with diameters of 8-10 nm into the matrix of macromolecules in surface-initiated atom transfer radical polymerization (SI-ATRP) in an ultrasonic bath. The obtained coatings were characterized by atomic force microscopy (AFM) operating in magnetic mode, secondary ion mass spectrometry (SIMS), X-ray photoelectron spectroscopy (XPS) and optical microscopy.

Keywords: polymer brushes, SPION, hybrid polymer/inorganic composites, cancer cells

INTRODUCTION

A rapid development in the design of materials with interfaces allowing for adsorption and desorption of biological structures is caused by a number of applications where is a need of attract a cell or protein, followed by detachment from the surface at a desirable time point. Unfortunately the sensitizing for a smart responses for external stimuli, precise tailoring of surface chemistry and

physical modification, keeping biocompatible properties and high cultures efficiency makes those materials more complicated in production. Of them all, the most promising materials seem to be all obtained with a surface-assembled polyelectrolyte films, hydrogels³, self-assembled monolayers⁴ and polymer brushes. Polymer brushes provide important for cell culture scaffold properties and moreover easy preparation, easy modification depending on the current needs during and after the synthesis. Mixed with magnetic nanoparticles, they create magnetically-responsible systems that can be used as scaffolds for cell cultures.

EXPERIMENTAL/THEORETICAL STUDY

Superparamagnetic iron oxide nanoparticles (SPIONs) with a well-defined diameter of 8-10 nm and strong magnetic properties were obtained by co-precipitation of iron salts in an aqueous environment⁵. The iron concentration in the samples was calculated on 0.871 mg/ml and zeta potential on -47.6 ± 0.4 mV. Hybrid polymer brushes-based scaffolds were obtained by simultaneous incorporation of SPIONs into a polycationic macromolecular matrix during the surface initiated atom transfer radical polymerization (SI-ATRP)⁶ reaction in an ultrasonic reactor. Scaffolds were covered with a thin layer of poly-L-lysine as a substrate for murine neuroblastoma cells. Here we present two different types of scaffolds – one based on bare polymer (poly(3-acrylamidopropyl)trimethylammonium chloride) poly(APTAC) and the second based on poly(APTAC) with incorporated SPIONs. Such prepared magnetic substrate was successfully used to neuroblastoma cells culture and to test the magnetic-triggered detachment of the cells.

RESULTS AND DISCUSSION

We managed to obtain hybrid scaffolds of various thickness from 20 to 100 nm with a facile and efficient homogeneous incorporation of well-separated magnetic nanoparticles in the whole volume of polymer matrix. Obtained magnetically-responsive systems show very strong magnetic properties which were used to controlled modifications of surface topography and adhesive properties. We have studied the influence of external magnetic field on murine neuroblastoma cells. It was observed that for systems after applying the magnetic field the cells rapidly shrank or completely detached from the substrate (see Fig. 1).

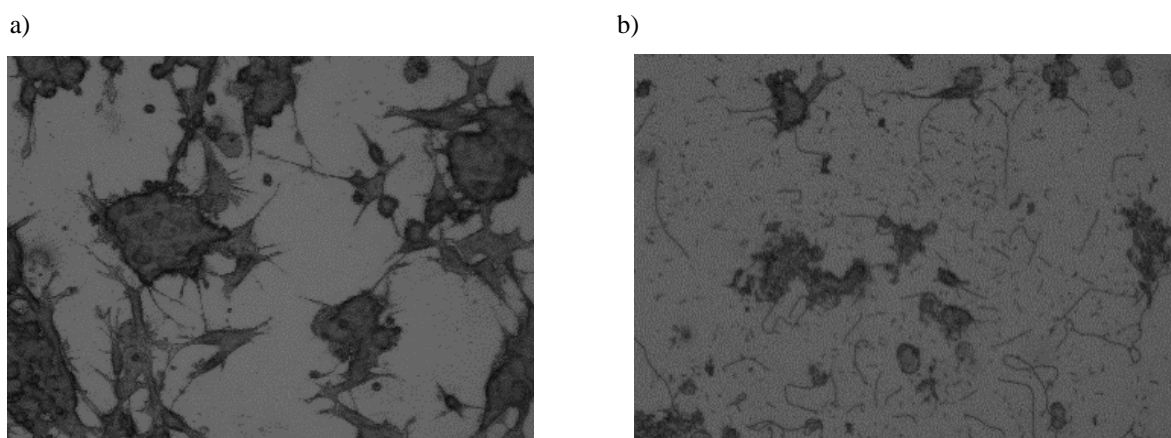


Fig. 1. Cells on poly(APTAC) with SPIONs scaffolds before (a) and after (b) applying the magnetic field.

CONCLUSION

In this report we present a novel method of synthesis a hybrid scaffolds composed of polyelectrolyte brushes and superparamagnetic iron oxide nanoparticles (SPIONs) for cancer cells culturing. Presented method prevents unwanted aggregation of nanoparticles and keeps SPIONs

homogeneously incorporated in the whole volume of polymer matrix. Moreover our scaffold was successfully studied as potential magnetically-responsive platform to stress and controlled detachment of cultured neuroblastoma cancer cells.

Acknowledgments: The authors would like to acknowledge TEAM project (2016-1/9, financed by the Foundation for Polish Science (Smart Growth Operational Program 2014-2020)) for the financial support.

REFERENCES

1. M. Al-Hussein, M. Koenig, M. Stamm and P. Uhlmann, *Macromol. Chem. Phys.*, 2014, 215, 1679.
2. C. Sanchez, B. Julián, P. Belleville and M. Popall, *J. Mater. Chem.*, 2005, 15, 3559.
3. S.-M. Ong, C. Zhang, Y.-C. Toh, S.H. Kim, H.L. Foo, C.H. Tan, D. van Noort, S. Park, H. Yu. *Biomaterials*. 29 (2008) 3237–3244.
4. Cantini E, Wang X, Koelsch P, Preece JA, Ma J, Mendes PM. *Acc Chem Res*. 2016;49(6):1223–1231.
5. Szpak, A., Kania, G., Skórka, T. et al. *J Nanopart Res* (2013) 15: 1372.
6. Górka, W.; Kuciel, T.; Nalepa, P.; Lachowicz, D.; Zapotoczny, S.; Szuwarzyński, M. *Nanomaterials* 2019, 9, 456.

Shape dependent model of EMA for nanostructured anisotropic materials

P. Otipka¹, J. Viček^{1,2}

¹Department of Mathematics and Descriptive Geometry, Faculty of Mechanical Engineering,

²Nanotechnology Centre, VŠB - Technical University of Ostrava, Czech Republic

petr.otipka@vsb.cz

ABSTRACT

A use of metal-dielectric mixtures composed as metal dielectric nanocomposites offer interesting ways to obtain materials with tailored dielectric function. An extension of effective medium approximation of anisotropic nanostructure composed from the Fe or Au nanodots in polyacrylate is presented. The proposed model is based on “strong-couple-dipole” (SCD) method including volume-integral correction term in Green tensor that enables to obtain more accurate representation of polarizability tensor.

Keywords: Effective medium; nanoparticles; polarizability; SCD method, Green tensor.

INTRODUCTION

The applicability of effective medium approximation (EMA) is restricted by the size of the structures composing the mixture: sufficiently large to preserve locally their own electromagnetic behavior and small enough for the composite to appear homogeneous compared to the wavelength of the interacting radiation. The size and/or shape of the particles may be explicitly incorporated within homogenization procedure via depolarization tensor. If the nanoparticles are not vanishingly small, then the spatial extent of associated Green tensor should not be neglected¹.

THEORETICAL STUDY

If the electrostatic interaction between nanoparticles is not negligible, it should be taken into account by generalized Maxwell-Garnett approach. It estimates the macroscopic response of the composite as average effect of the dipole field induced in the host medium by different inclusions. This can be done by the Bragg-Pippard model² of EMA with the modification for bi-anisotropic

case^{3,4}: Assuming the volume fraction f of the metallic nanoparticles in a host medium, the effective permittivity tensor $\boldsymbol{\varepsilon}_{ef}$ can be written as

$$\boldsymbol{\varepsilon}_{ef} = \boldsymbol{\varepsilon}_h + f(\boldsymbol{\varepsilon} - \boldsymbol{\varepsilon}_h) \left[f\mathbf{I} + (1-f)v\boldsymbol{\alpha}^{-1}(\boldsymbol{\varepsilon} - \boldsymbol{\varepsilon}_h) \right]^{-1} \quad (1)$$

Here $\boldsymbol{\varepsilon}$, $\boldsymbol{\varepsilon}_h = \varepsilon_h \mathbf{I}$ denote the relative permittivity tensors of particles and isotropic host medium, respectively. Further, we write \mathbf{I} for the identity matrix and $\boldsymbol{\alpha}$ for the polarizability tensor of metallic inclusion of the volume v . In cases when the inclusions aligned with principal axes, the polarizability tensor can be expressed in the form⁵

$$\boldsymbol{\alpha} = v(\boldsymbol{\varepsilon} - \varepsilon_h \mathbf{I}) \left[\mathbf{I} - k_0^2 v \langle \mathbf{G} \rangle (\boldsymbol{\varepsilon} - \varepsilon_h \mathbf{I}) \right]^{-1}, \quad (2)$$

where $k_0 = 2\pi/\lambda$. Denoting the wavenumber $k = k_0 \sqrt{\varepsilon_h}$, the Green tensor \mathbf{G} is defined as

$$\mathbf{G}(\mathbf{r}, \mathbf{r}_0) = \left(\mathbf{I} + \frac{1}{k^2} \nabla \times \nabla \right) g(\mathbf{r}, \mathbf{r}_0), \quad g(\mathbf{r}, \mathbf{r}_0) = \frac{1}{4\pi} \frac{e^{ik\|\mathbf{r}-\mathbf{r}_0\|}}{\|\mathbf{r}-\mathbf{r}_0\|}, \quad (3)$$

where g is the free space Green function of Helmholtz operator. Assuming electrically small characteristic nanoparticle dimension, the tensor $\langle \mathbf{G} \rangle$ averaged over a volume v with the unit outward normal vector \mathbf{n} of its surface S can be written in the split form⁶

$$v \langle \mathbf{G} \rangle = \int_v \mathbf{G}(\mathbf{r}, \mathbf{r}_0) dv = \int_v (\mathbf{G} - \mathbf{G}_s) dv - \frac{1}{4\pi k^2} \int_s \frac{\mathbf{n} \otimes (\mathbf{r} - \mathbf{r}_0)}{\|\mathbf{r} - \mathbf{r}_0\|^3} dS \quad (4)$$

with

$$\mathbf{G}_s = \frac{1}{4\pi k^2} \nabla \otimes \nabla \left(\frac{1}{\|\mathbf{r} - \mathbf{r}_0\|} \right). \quad (5)$$

RESULTS AND DISCUSSION

The properties of Green tensor related to various shape of nanoparticles have important influence to the effective permittivity defined by (2). We discuss this effect for typical axially symmetric nanoparticles (cylinders, spheroids etc.). The Fig. 1 demonstrates shape dependent effective permittivity of heterogeneous nanostructures containing inclusions of several forms. Moreover, the correction role of Green tensor volume part is analysed – see (4).

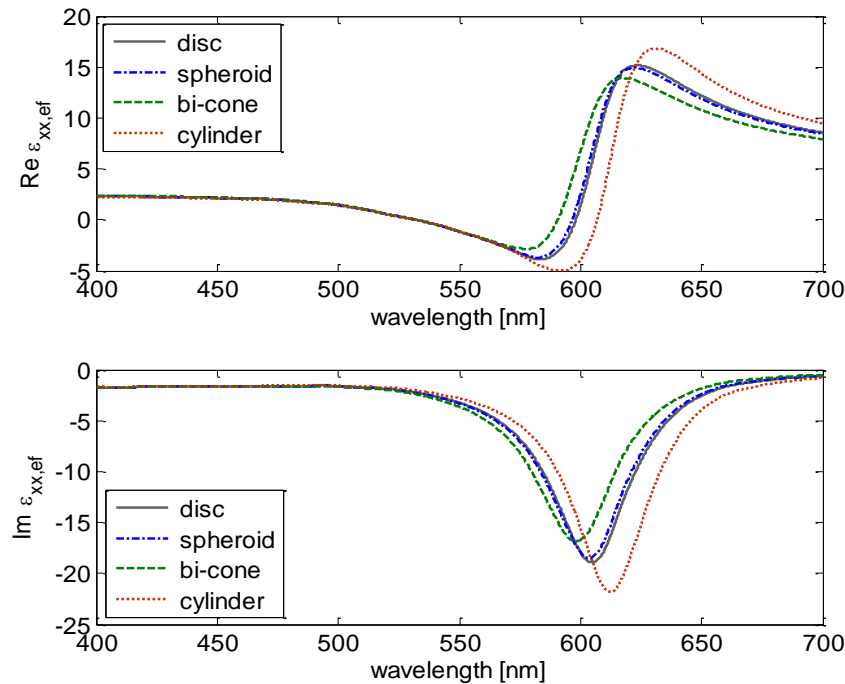


Fig. 1. Effective permittivity dependence on the geometric shape of nanoparticles of the heterogeneous system Au/polyacrylate (diameter 5 nm, height 10 nm, fill factor 0.2).

CONCLUSION

The introduced extension of EMA via SCD model for anisotropic nanoparticles offers possible tool to analyze anisotropic nanostructured heterogeneous media in various applications, where the natural or artificial composites (metamaterials) act as significant component of studied optical system. As a novel aspect an extension of the Green tensor about volume-integral term is presented.

REFERENCES

1. J. Cui and T. G. Mackay, Waves in Random and Complex Media 17, 209, (2007).
2. M. Abe, Phys. Rev. B53, 7065 (1996).
3. O. Levy and E. Cherkhev, J. Appl. Phys. 114, 164102 (2013).
4. J. Vlček et al., Proc. SPIE 9502, 950217 (2015).
5. S. Albaladejo et al., Opt. Express 18, 3556 (2010).
6. D. Yaghjian, Proc. of the IEEE 68, 248 (1980).

Tuning the properties of nanogel surface coatings by grafting weak cationic polyelectrolyte brushes

Z. Posel^{1,2}, P. Posocco²

¹Department of Informatics, Faculty of Science, Jan Evangelista Purkyně University in Ústí nad Labem, Czech Republic; ²Department of Engineering and Architecture, University of Trieste, Italy

zbysek.posel@ujep.cz

ABSTRACT

Nanogels are chemically crosslinked polymeric networks called as next generation of drug delivery systems due to their relatively high drug encapsulation capacity, uniformity, tunable size, ease of preparation, limited toxicity, stability in the presence of serum, and responsiveness to external stimuli. In particular, the presence of specific functional groups on crosslinked nanogels provides an opportunity to easily tune their surface properties and direct their biological behavior.

In this work, we used mesoscale modeling to describe the behavior of nanogel surface formed by crosslinked polyethylene glycol and linear polyethyleneimine, grafted by alkyl amines of different length n (C_n-NH_2). Simulations show that both number of chains per area and chain length have significant impact on the ability of the functionalized surface to interact with surrounding media. Localization of the partially charged amine end-groups near the surface promotes the adsorption of free ions from solution and this ability decreases when the chain length is increased. More, high density of grafted chains screens nanogel surface from surroundings, limiting their ability to respond to the external environment.

Keywords: Nanogel, Drug-delivery, Coarse-graining, Polyelectrolyte brushes, Dissipative particle dynamics

INTRODUCTION

Hydrogel-based nanoparticles (nanogels) represent a pivotal class of biomaterials in the intracellular treatment of many diseases, including for instance those involving the hard-to-treat central nervous system¹. The key ability of nanogels is to provide a biocompatible nano-environment able to encapsulate drugs and release them under specific stimuli. Nanogels can be tailored to be responsive to a variety of stimuli (pH, temperature, chemical and biological species) by integration of functional oligomers into their structure or onto their surface. Indeed, it is well known that cells sense biomaterial topography and respond by regulating a variety of cellular processes such as intracellular signaling, differentiation, adhesion, and migration. The broad variety of polymers then allow designing and tuning the properties of nanogels with respect to surrounding environment and desired biological outcome². For instance, studies about amine functionalization were proposed to tune cell adhesion on self-assembled monolayers, using cancer and endothelial cells preserving their availability.

In this work, we used dissipative particle dynamics (DPD) technique to describe the interfacial behavior of nanogel's surface made by crosslinked polyethylene glycol (PEG) and linear polyethyleneimine (PEI), grafted by alkyl amines of different length n (C_n-NH_2) (Figure 1). These systems were designed to target microglia cells, which are considered as possible therapeutic targets to treat diseases involving the central nervous system.

Specific attention was devoted to investigate the influence of the number of grafted chains (e.g. grafting density) and length of the alkyl chain ($n = 4-40$) on the ability of surface to interact with

surroundings. Distribution of water, ions and polymer chains at the interface were analyzed. Moreover, the molecular behavior of the grafted chains was characterized in terms of radius of gyration, end-to-end distance and the brush height.

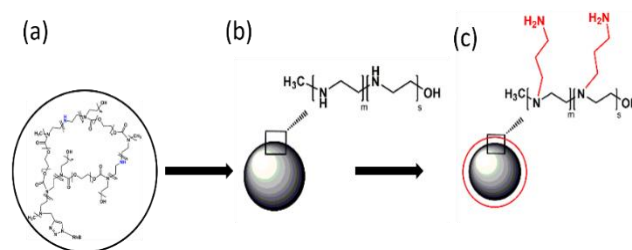


Figure 2: Panel (a) and (b) shows schematic representation of nanogel structure, where blue elements refer to residual amine groups available for grafting. (c) Nanogel structure after surface modification by propylene amine chains.

RESULTS AND DISCUSSION

Results from DPD simulations show that both grafting density and chain length have significant influence on the interfacial characteristics of the nanogel surface and control its ability to interact with the surrounding polyelectrolyte. Figure 2 illustrates the equilibrium configuration of two PEG-PEI surfaces modified with C_4-NH_2 chains at different grafting densities (1.25 and 6.25 chains/ nm^2). Localization of the partially charged amine end-groups near the surface promotes the adsorption of free ions from solution and this ability decreases when the chain length is increased. More, high density of grafted chains screens nanogel particles from surroundings, limiting their ability to respond to the external environment.

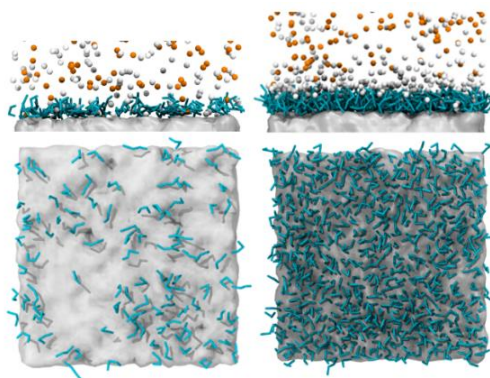


Figure 3: Front and top view snapshots from DPD simulations of PEG-PEI surfaces (white surface) grafted by C_4-NH_2 (blue) at different grafting densities (left panels, $\sigma = 1.25$ chains/ nm^2 ; right panels, $\sigma = 6.25$ chains/ nm^2). Sodium and chlorine ions are depicted as white and orange sphere, respectively. Water is not shown for clarity.

CONCLUSION

In this work we demonstrated that surface functionalization by alkyl amine chains is an effective way to tune the interfacial properties of PEG-PEI based nanogel particles. Further studies focusing on how changes of environmental factors like pH affect the behavior of these coatings are in progress.

Acknowledgments: ZP acknowledges the support from IGA UJEP (grant no. UJEP-IGA-TC-2019-53-02-2) and from ERDF/ESF project "UniQSurf -Centre of biointerfaces and hybrid functional materials "(No. CZ.02.1.01/0.0/17_048/0007411). PP is grateful to MIUR through the project "Structure and FunctiOn at the Nanoparticle bioInterfAce" (grant RBSI14PBC6). This work is part of an on-going collaboration with prof. Filippo Rossi (Politecnico di Milano, Italy), who designed the nanogel scaffolds.

REFERENCES

1. E. Mauri, G. Perale, F. Rossi, ACS Applied Nano Materials, 1 (2018) 6525-6541.

Starch as template for synthesis of nanocrystalline hydrotalcites

A. Michalik, B. D. Napruszewska, A. Walczyk, J. Kryściak-Czerwenka, D. Duraczyńska, R. Dula, R. Karcz, E. M. Serwicka

Jerzy Haber Institute of Surface Chemistry, Polish Academy of Sciences, Poland

ncserwic@cyf-kr.edu.pl

ABSTRACT

The study probes applicability of biopolymers, such a starches, in the capacity of templates enabling control over structure and texture of hydrotalcite-like materials. Hydrotalcites (Ht) of Mg/Al=3 were obtained by co-precipitation at pH=10, from aqueous solution of Mg and Al nitrates, using $\text{NH}_3\text{aq} + (\text{NH}_4)_2\text{CO}_3$, as precipitants. The investigated synthesis parameters included the type of starch (potato, corn, manioc), starch concentration, addition of starch to the selected reagent (nitrates, base, and/or carbonate solution), and temperature of the Ht product washing. The samples were characterized with XRD, SEM, FTIR, TG/DSC. Results indicate that starch template facilitates formation of nanocrystalline Ht. The effect is most pronounced when all reagents used for the synthesis contain starch additive. In the presence of starch, the formation of nitrate rather than carbonate forms of Ht is observed. FTIR analysis suggests that starch gel becomes more ordered at the Ht/biopolymer interface. Ht obtained in the presence of starch is less stable thermally than the reference Ht obtained in a conventional manner.

Keywords: Hydrotalcite, nanocrystallinity, template, starch.

INTRODUCTION

Synthetic Ht-like materials find numerous applications as catalysts, adsorbents, medicins and medicin carriers, polymer fillers etc. Of particular importance are nanostructural forms of Ht, characterized with a high surface to volume ratio and well developed porosity. The present study shows the potential of easily available and environmentally friendly biopolymers, such a starches, as soft, removable templates, enabling control over structure and texture of Ht-like materials.

EXPERIMENTAL STUDY

Synthesis of Ht with Mg/Al=3 was carried out by co-precipitation at pH=10, using aqueous solution of Mg and Al nitrates as the source of structure-forming cations, and 25% $\text{NH}_3\text{aq} + (\text{NH}_4)_2\text{CO}_3$ as precipitating agents. The materials are further referred to as Ht^{NH_3} . The investigated synthesis parameters included the type of starch (potato, corn, manioc), starch concentration (0.2 or 2 wt.%),

addition of starch to the selected reagent (nitrates, base, and/or carbonate solution), and temperature of the Ht product washing. The samples were characterized with XRD, SEM, FTIR, TG/DSC.

RESULTS AND DISCUSSION

SEM and XRD analyses reveal that the use of a starch template facilitates formation of nanocrystalline Ht materials with small particle size and (Fig. 1 and 2). The effect is most pronounced when all reagents used for the synthesis contain starch additive. Interplanar d_{003} distance increases from 7.65 Å found in the reference sample obtained by the standard co-precipitation to 8.25 Å observed in the presence of starch. The result points to the formation of nitrate rather than carbonate forms of Ht in starch-containing reaction medium. Removal of biotemplate by washing causes partial recrystallization of the precipitate. The effect can be minimized by washing the Ht product with ice-cold water. FTIR analysis (Fig. 3) suggests that starch gel becomes more ordered at the Ht/biopolymer interface. According to TG/DSC, Ht obtained in the presence of starch is less stable thermally than the standard reference.

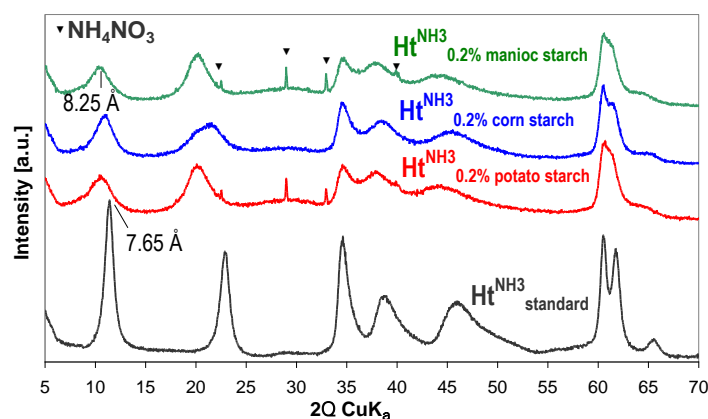


Fig. 1. XRD patterns of Ht materials synthesized in the presence of various starches (added to all reactants) and $\text{Ht}^{\text{NH}_3}_{\text{standard}}$ reference prepared in the absence of starch.

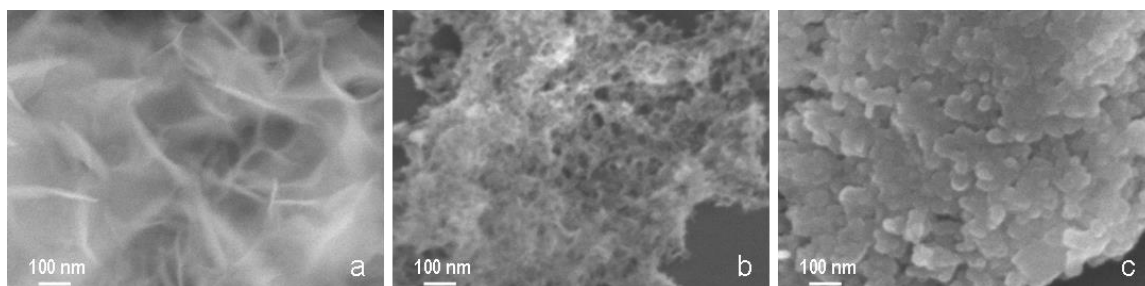


Fig. 2. SEM images of (a) $\text{Ht}^{\text{NH}_3}_{\text{standard}}$; (b) Ht^{NH_3} 0.2% potato starch; (c) Ht^{NH_3} 0.2% corn starch. Uncoated samples deposited on Cu grid.

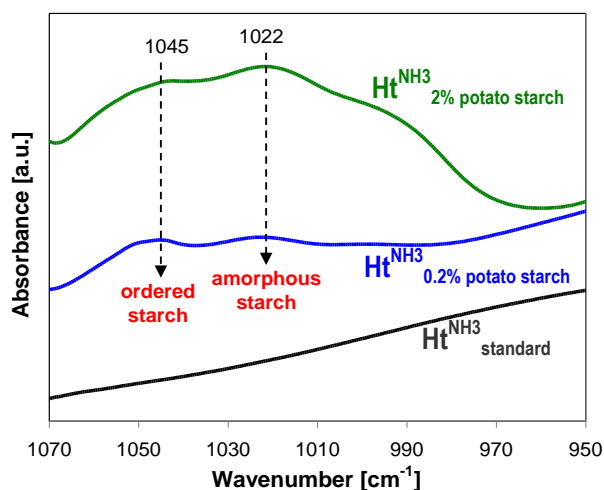


Fig. 3. FTIR spectra of $\text{Ht}^{\text{NH}_3}_{0.2\% \text{ potato starch}}$ and $\text{Ht}^{\text{NH}_3}_{2\% \text{ potato starch}}$ in the region indicative of the degree of starch ordering. $\text{Ht}^{\text{NH}_3}_{\text{standard}}$ prepared without starch is shown as a reference.

CONCLUSION

The synthesis of Ht materials in the presence of starch enables preparation of nanocrystalline precipitates with very fine ($< 50 \text{ nm}$) particle size, comparable with those obtained by means of the inverse micellar route¹, but at much lower cost and with significantly less effort.

Acknowledgments: Financial support from the National Science Center Poland, project OPUS 2017/27/B/ST5/01834, is gratefully acknowledged.

REFERENCES

1. B. D. Napruszewska, A. Michalik-Zym, R. Dula, E. Bielańska, W. Rojek, T. Machej, R.P. Socha, L. Lityńska-Dobrzyńska, K. Bahranowski, E.M. Serwicka, Appl. Catal. B 211 (2017) 46-56.

$\alpha\text{-Fe}_2\text{O}_3$ nanoparticles/vermiculite for catalytic decomposition of polystyrene

M. Valášková¹, P. Leštinský¹

¹Institute of Environmental Technology, VŠB-Technical University of Ostrava, CZ-708 00, Ostrava-Poruba, Czech Republic

marta.valaskova@vsb.cz

ABSTRACT

The chemical recycling waste plastics have expected polystyrene (PS) to be recycled into styrene monomer. The expandable layers of clay minerals provide useful two-dimensional hosts, which facilitate introduction of catalytically active metal oxide nanoparticles docked on the 2:1 layers of vermiculite. Iron oxides are used as effective acid/base catalysts to provide styrene monomers. Therefore, hematite ($\alpha\text{-Fe}_2\text{O}_3$) was selected for the synthesis of clay-based nanoparticles catalysts. Preparation conditions in particular reaction temperature, calcination and pH value play roles in determining the shape, the particle size, the size distribution, the agglomeration, the interlayer space of clay mineral and the surface properties. The precipitation method is simple, efficient and

economical. $\text{FeCl}_3 \cdot 6\text{H}_2\text{O}$ aqueous solution was the precursor of $\alpha\text{-Fe}_2\text{O}_3$ nanoparticles and NaOH precipitating agent to maintain pH value of 11. Nanoparticles of hematite in the $\alpha\text{-Fe}_2\text{O}_3$ nanoparticles/vermiculite catalysts were calcined at 500 and 700°C and characterized using X-ray powder diffraction (XRD). Morphology of nanoparticles $\alpha\text{-Fe}_2\text{O}_3$ was observed through scanning electron microscope. The mean crystallites size was at all samples about 30 nm obtained from XRD peaks using Scherrer equation in agreement with the particle size observed by SEM. The X-ray fluorescence analysis determined Fe_2O_3 about 28 mass% in $\alpha\text{-Fe}_2\text{O}_3$ nanoparticles/vermiculite catalysts.

Keywords: Iron oxide based catalyst, vermiculite carrier, polystyrene depolymerization, X-ray diffraction.

Acknowledgments: The work was supported from ERDF "Institute of Environmental Technology – Excellent Research (No. CZ.02.1.01/0.0/0.0/16_019/0000853).

TOPIC 2

Nanomaterials Characterizations and Devices

Chair: Jan Neuman

Advanced techniques for characterization in nanotechnology

Advanced testing methods for nanomaterials

Molecular modeling and simulations

Advances in computational methods for nanotechnology



Invited lecture (IL):**Friction and fracture of 2D materials**B.-C. Tran Khac¹, K.-H. Chung¹, F. W. DelRio²¹School of Mechanical Engineering, University of Ulsan, Republic of Korea;²Material Measurement Laboratory, National Institute of Standards and Technology, USAfrank.delrio@nist.gov**ABSTRACT**

Interfacial strength and surface damage of single- and multi-layer hexagonal boron nitride (h-BN), molybdenum disulfide (MoS₂), and graphene films were studied via atomic force microscopy-based progressive-force and constant-force scratch tests and Raman spectroscopy. The results showed that single-layer h-BN, MoS₂, and graphene strongly adhere to the SiO₂ substrate, which significantly improves its tribological performance. Moreover, defect formation from scratch testing was found to affect the topography and friction force differently prior to the failure, which points to distinct surface damage characteristics. Interestingly, the residual strains at scratched areas suggest the scratch test-induced in-plane compressive strains were dominant over tensile strains, thereby leading to buckling in front of the scratching tip and eventually failure. As the number of layers increased, the tribological performance of atomically-thin h-BN, MoS₂, and graphene were found to significantly improve due to an increase in the interfacial strengths and a decrease in the surface damage and friction force.

Keywords: Interfacial strength, surface damage, two-dimensional materials, atomic force microscopy

INTRODUCTION

Two-dimensional (2D) materials such as single- and multi-layer h-BN, MoS₂, and graphene have attracted intensive interest due to their remarkable frictional properties, with coefficients of friction from 0.001 to 0.1.¹⁻³ Although initial studies have demonstrated the potential of these materials in greatly reducing friction and wear in mechanical systems,^{1,2} the surface damage characteristics of atomically-thin h-BN, MoS₂, and graphene specimens have not been fully investigated. In this study, the film-to-substrate interfacial strengths and surface damage of atomically-thin h-BN, MoS₂, and graphene were studied using atomic force microscopy (AFM) progressive-force and constant-force scratch tests. Based on the progressive-force scratch tests, interfacial strengths for single-layer h-BN, MoS₂, and graphene were evaluated from critical forces, which demonstrated that these atomically-thin materials strongly adhere to SiO₂. The constant-force tests showed the evolution of damage as a function of normal force and revealed distinctive surface damage characteristics. The residual in-plane compressive strains at scratched areas suggested a general failure mechanism in 2D materials.³

EXPERIMENTAL/THEORETICAL STUDY

Single- and multi-layer h-BN, MoS₂, and graphene specimens were produced from high-quality single-crystal h-BN, MoS₂, and graphite via micro-mechanical exfoliation. The exfoliated materials were gently pressed against and transferred to an Si wafer capped with a 300-nm thick SiO₂ layer. A nanocrystalline diamond AFM tip with a tip radius of 40 nm was used in both the progressive-force and constant-force tests. In the progressive-force tests, specimens were scratched under a

progressive normal force for one scratch line with the distance of 2 μm ; the normal force increased from 400 nN to 4000 nN to find the critical force. In the constant-force tests, specimens were scratched in a defined area of 1 $\mu\text{m} \times 1 \mu\text{m}$ under constant normal force; the normal forces ranged from 500 nN to 5000 nN to observe surface damage evolution. After the scratch tests, topography and frictional behaviors of the scratched areas were studied via intermittent-contact mode and contact mode AFM and Raman.

RESULTS AND DISCUSSION

The friction force variation with respect to normal force during the progressive-force scratch tests was monitored as shown in Figure 1(a), and the critical force was characterized by the normal load at which there was an abrupt increase in friction force. Scratch tracks were observed in the subsequent topographic and friction force microscopy (FFM) images as shown in Figures 1(b) and 1(c). Based on these observations, the critical forces for single-layer h-BN, MoS₂, and graphene were 900 ± 200 nN, 1300 ± 150 nN, and $3300 \text{ nN} \pm 200$ nN, respectively. From the topographic images, single-layer h-BN and MoS₂ were found to tear off and expose the substrate, shortly after scratch tracks were observed. The scratch tracks exhibited an increase in friction just prior to the failure, which indicates that defects were likely formed. Interestingly, in the case of single-layer graphene, a height decrease was observed prior to failure. However, FFM showed that the scratch tracks maintained their low frictional behavior. This suggests that the substrate was plastically deformed, but given the superior mechanical strength of graphene, the film remained intact to failure.³

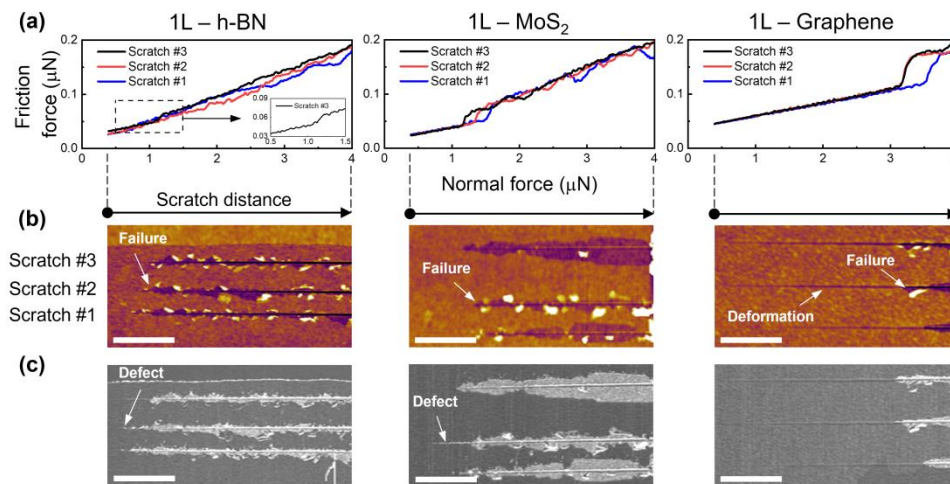


Fig. 1. Progressive-force scratch tests for single-layer h-BN, MoS₂, and graphene. (a) Friction force variation with normal force. (b) Topographic and (c) FFM images of scratch tracks. In (b) and (c), the scale bars are 500 nm.³

In the constant-force scratch tests, single-layer h-BN failed at 1500 nN normal force. Shortly before failure, a height decrease of about 0.3 nm was observed, while its friction force was constant. Raman spectra showed the E_{2g} frequency at scratched areas increased by 0.3 cm^{-1} to 0.8 cm^{-1} as compared to as-exfoliated specimens, which suggests in-plane compressive strain. As normal force increased, the blueshift of the E_{2g} peak was constant, which implied that the amount of compressive strain was also constant. For single-layer MoS₂, complete failure was observed at 2000 nN normal force, with the removal of the film from the substrate. Raman spectra showed decreases in intensity and increases in frequency for the E_{2g}^1 and A_{1g} peaks at 2000 nN, which was attributed to in-plane and out-of-plane compressive strains (smaller normal forces did not exhibit these changes). For

single-layer graphene, a height decrease of 1.6 nm was observed prior to failure at 5000 nN. No changes in friction behavior were observed at scratched areas. Raman spectra exhibited changes to the 2D and D intensities and G frequency, which were accredited to defect formation and in-plane compressive strain.³

CONCLUSION

The results suggest three stages in the evolution of surface damage. At low normal force, no change in topography and friction force was observed, which points to elastic deformation in the scratched area. As normal force increased, the formation of defects in the film and plastic deformation in the substrate were noted. At the critical force, delamination of the film occurred. The compressive strain-induced buckling in front of the tip was the primary source of mechanical instability in 2D materials.

Acknowledgments: K.-H. Chung acknowledges financial support from University of Ulsan by the 2016 research fund. F.W. DelRio recognizes support from the National Institute of Standards and Technology.

REFERENCES

1. C. Lee, Q. Li, W. Kalb, X.-Z. Liu, H. Berger, R.W. Carpick, J. Hone, *Science* 328 (2010) 76-80.
2. B. Vasic, A. Matkovic, U. Ralevic, M. Belic, R. Gajic, *Carbon* 120 (2017) 137-144.
3. B.-C. Tran Khac, F.W. DelRio, K.-H. Chung, *ACS Appl. Mater. Interfaces* 10 (2018) 9164-9177.

Oral presentations (OP):**Phenomenological and experimental investigation of exciton dissociation mechanism in organic semiconductor blends**

A. Babusenar¹, S. Mondal¹, S. Ramaswamy², S. Dutta², M. Gopalakrishnan, J. Bhattacharyya¹

¹Department of Physics, Indian Institute of Technology Madras, Chennai, 600036, India; ²Department of Physics, Indian Institute of Technology Madras, Chennai, 600036, India

anoos.kgr@gmail.com

ABSTRACT

Organic semiconductor thin films have found immense applications in photovoltaics. However, the materials have high exciton binding energies resulting in low quantum efficiencies of the devices, compared to their inorganic counterpart. Organic semiconductor blends have shown enhanced exciton dissociation leading to high free carrier densities. Though the detailed understanding of the mechanisms involved in formation of free carriers from excitons, and the influence of the composition and interfaces of blends are topics still being explored. Here, we propose a mean field based phenomenological approach to model the role of fullerene derivatives, which act as acceptors on the exciton recombination in an organic blend. We performed experiments on the widely used P3HT-PCBM [Poly(3-hexylthiophene) and phenyl-C61-butyric acid methyl ester] blend, to verify our model. We performed photoluminescence quenching measurements on blended thin films with different acceptor (PCBM) concentrations and observed a saturation of exciton dissociation for PCBM concentration of around 10%. This value is much lower than the 50% concentration of PCBM which gives highest power conversion efficiency, as reported earlier. We suggest that the enhancement of quantum efficiency beyond 10% PCBM concentration is not an outcome for higher exciton dissociation, but probably due to increase in carrier mobility due to PCBM. We also show that with higher photo-excitation intensities, the exciton dissociation attains saturation at lesser acceptor concentration, which is in agreement with our proposed model.

REFERENCES

1. G. Li, V. Shrotriya, J. Huang, Y. Yao, T. Moriarty, K. Emery, and Y. Yang, *Nat. Mater.* 2005, 4, 864-2
2. F. Laquai, D. Andrienko, R. Mauer, and P.W.M. Blom, *Macromol. Rapid Commun.* 2015, 36, 1001.
3. H. Wang, H. Wang, B. Gao, L. Wang, Z. Yang, X. Du, and Q. Chen, *Nanoscale* 2011, 3, 2280.
4. D. Chirvase, J. Parisi, J.C. Hummelen, and V. Dyakonov, *Nanotechnology* 2004, 15, 1317-1323
5. L.M. Chen, Z. Hong, G. Li and Y. Yang, *Adv. Mater.*, 2009, 21, 1434.
6. W. Ma, C. Yang, X. Gong, K. Lee and A. J. Heeger, *Adv. Funct. Mater.*, 2005, 15, 1617
7. Y. Tamai, H. Ohkita, H. Benten, and S. Ito, *J. Phys. Chem. Lett.* 2015, 6, 3417-3428. [8] M. T. Dang, L. Hirsch and G. Wantz, *Adv. Mater.* 2011, 23, 3597-3602

Interaction of electromagnetic waves with plasmonic structures in the terrestrial atmosphere

G. Jandieri, J. Pistora, M. Lesnak

Nanotechnology Centre, VSB – Technical University of Ostrava, Ostrava-Poruba, Czech Republic

georgejandieri7@gmail.com

ABSTRACT

Propagation and scattering of electromagnetic waves in the anisotropic plasmonic medium are investigated using the smooth perturbation method. In the first approximation interaction of waves with homogeneous structures of the gyrotropic plasmonic medium is considered. It was shown that two type waves are excited having opposite side circular polarization causing rotation of the polarization plane. Faraday angle depends on the distance covering by wave. Statistical characteristics of scattered electromagnetic waves on randomly inhomogeneous plasmonic structures of the upper terrestrial atmosphere are considered in the second order approximation. Plasmonic irregularities in the anisotropic gyrotropic medium have different characteristic spatial scales and ellipsoidal form generating due to different chemical and dynamical processes. Second order statistical moments of the phase fluctuations and the variance of the Faraday angle are calculated for arbitrary spectral function of irregular plasmonic structures in the upper terrestrial atmosphere. Normalized variance of the Faraday angle nonlinearly depends on the inclination angle of elongated irregularities increasing in proportion to the anisotropy factor and frequency of an incident wave; for metric electromagnetic waves it was equal to 7^0 , in agreement with experiment. It was shown that using the Stokes parameters depolarization coefficient is proportional to $6 \cdot 10^{-3}$.

Keywords: Plasmonic nanostructures, electromagnetic waves, depolarization.

INTRODUCTION

At the present time the features of light propagation in random media have been well studied [1]. Interaction of electromagnetic (EM) waves with different scale plasmonic irregularities of the terrestrial atmosphere has a significant influence on the key parameters of the wave. Depolarization aspects in thin regular anisotropic layer using the dynamic matrix theory were considered in [2]. Statistical characteristics of scattered EM waves on natural and/or artificial plasmonic structures having ellipsoidal forms and different characteristic spatial scales are considered in [3]. Analytical calculations are based on the modify smooth perturbation method considering both the boundary conditions and diffraction effects.

EXPERIMENTAL/THEORETICAL STUDY

Theoretical and numerical study is based on the interaction of metric EM wavelength waves with anisotropic plasmonic structures in the upper terrestrial atmosphere. It was shown that in the gyrotropic homogeneous medium two circularly polarized waves lead to the rotation of polarization plane. Using the experimental data Faraday angle is equal to $\theta_F = -0.01 z \text{ m}^{-1}$ (z is the distance traveling by wave). In the upper terrestrial atmosphere plasmonic structures are characterized by anisotropy factor $\chi = l_{\parallel} / l_{\perp}$ (the ratio of longitudinal and transverse linear scales of plasmonic irregularities) and inclination angle γ_0 of elongated plasmonic structures with respect to the ambient magnetic field.

RESULTS AND DISCUSSION

Fluctuations of the Faraday angle are caused by scattering of an incident linearly-polarized wave on randomly distributed plasmonic irregularities in the upper terrestrial atmosphere. Pronounced fluctuations of the angle θ_F were registered by radio beacons of the low-altitude satellites at the frequencies of 20-50 MHz [4]. Numerical analyses for an incident 3 MHz EM wave show that the Faraday angle increases in proportion of the frequency of an incident wave and for metric EM waves it is equal to 7° coinciding with experimental data. Calculating Stokes parameters it is shown that at $\chi=5$ depolarization coefficient Ξ is equal to 0.2 and 0.7 for 3 MHz and 40 MHz frequency incident wave, respectively. Figures 1 depicts the dependence of the normalized statistical moments of scattered EM waves versus a distance between receiving antennas at the frequency 3 MHz, thickness of a slab is 100 km, plasmonic irregularities are field aligned. Analysis show that correlation between scattered waves decreases in proportion to the anisotropic factor χ . Isolines of the normalized Faraday angle $\langle \theta_F^2 \rangle$ nonlinearly depends on the angle γ_0 , Figure 2. Analysis and observations show that the moderate fluctuations of the Faraday angle $\langle \theta_F^2 \rangle^{1/2} \approx 0.05$ radian can be caused by both small-scale (< 200 m) and larger $l \approx 1$ km plasmonic irregular structures.

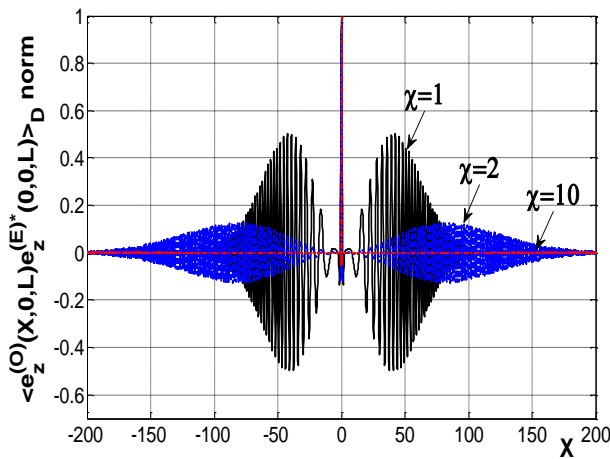


Figure 1. Normalized correlation function of scattered waves versus distance between receiving antennas.

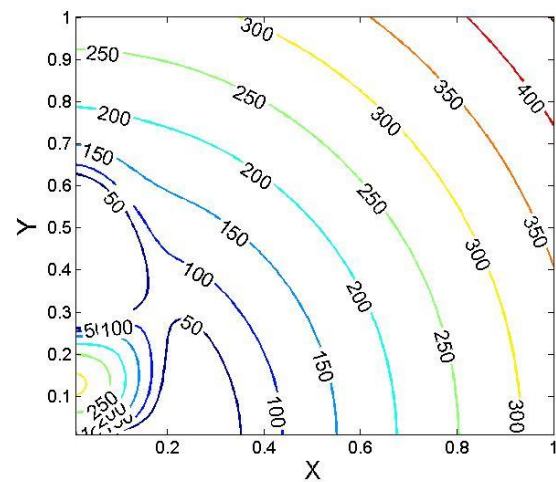


Figure 2. The root-mean square deviation of the Faraday angle versus distance between observation points.

CONCLUSION

Second order statistical characteristics of scattered EM waves by turbulent plasmonic structures are considered using the modify perturbation method. It was shown that for metric incident wave polarization plane rotates anticlockwise. Numerical calculations are carried out for anisotropic plasmonic irregularities. Application of Stokes parameters allows to define polarization characteristics of scattered waves with a big accuracy in inhomogeneous plasmonic anisotropic medium. Polarization characteristics of scattered radio signals provide important information about physical conditions in the area of localization of the sources and about the medium parameters on the path of wave propagation.

Acknowledgment: Prof. G. Jandieri acknowledges to Prof. J. Pistora for invitation to Nanotechnology Centre of the USB to become collaboration more successful (cz.02.269/0.0/0.0/16_027/000 8463).

REFERENCES

1. A. Ishimaru, "Wave Propagation and Scattering in Random Media, Vol. 2, Multiple Scattering, Turbulence," Rough Surfaces and Remote Sensing, IEEE Press, Piscataway, New Jersey, 1997.
2. J. Pistora, J. Vlcek, M. Lesnak, Optical Approaches for Nanotechnologies, Brno, 2018.
3. G.V. Jandieri, A. Ishimaru, V.G. Jandieri, A.G. Khantadze, Zh.M. Diasamidze, "Model Computations of Angular Power Spectra for Anisotropic Absorptive Turbulent Magnetized Plasma," PIER, 70 (2007) 307–328.
4. M. Kolosov, N. Armand, O. Yakovlev, "Propagation of Radio Waves at Cosmic Communication," Sviaz', Moscow, 1969 (in Russian).

Measurement of THz gain in optically pumped ammonia gas

M. Mičica^{1,2,3}, S. Eliet², M. Vanwolleghe^{2,3}, R. Motiyenko⁴, A. Pienkina⁴, L. Margulès⁴, K. Postava^{1,3}, J. Pištora^{1,3}, J.-F. Lampin²

¹Nanotechnology Centre, VŠB – Technical university of Ostrava, Czech Republic; ²Institut d'Électronique de Microélectronique et de Nanotechnologie, Lille University, France; ³IT4Innovations, VŠB - Technical University of Ostrava, Czech Republic, ⁴Physique des Lasers, Atomes et Molécules, Lille University, France

martin.micica@vsb.cz

ABSTRACT

Our contribution is aimed at the evaluation of THz gain properties in an optically pumped NH₃ gas. NH₃ molecules undergo roto-vibrational excitation by mid-infrared (MIR) optical pumping provided by a MIR quantum cascade laser (QCL) which enables precise tuning to the NH₃ infrared transition around 10.3 μm. Pure inversion transitions, (J = 3, K = 3) at 1.073 THz and (J = 4, K = 4) at 1.083 THz were selected. The THz measurements were performed using a THz frequency multiplier chain. The results show line transmission with and without optical pumping at different NH₃ pressures, and with different MIR tuning. The highest gain at room temperature under the best conditions obtained during single pass on the (3,3) line was 10.1 dB.m⁻¹ at 26 μbar with a pumping power of 40 mW. The (4,4) line showed lower gain of 6.4 dB.m⁻¹ at 34 μbar with a pumping power of 62 mW. To our knowledge these THz gains are the highest measured in a continuous-wave MIR pumped gas.

Keywords: terahertz lasers, ammonia, optical pumping, gas spectroscopy

INTRODUCTION

A terahertz molecular laser optically pumped by a MIR QCL based on ammonia (NH₃) was demonstrated recently¹ and offers many new possibilities. It is essential to know the most important parameters and the behavior of the lasing lines if one wants to optimize the design of a laser. Here we present a study of the THz gain properties of two selected optically-pumped NH₃ lasing lines near 1 THz at room temperature. Important information about the gain, the line-shape and the pressure dependence are obtained^{2,3}. For the experiment we selected two lines: (1) pumping at 967.3463 cm⁻¹ (saQ(3,3) transition) and probing around 1073049.6 MHz (ν₂ = 1 asQ(3,3)), (2) pumping at 966.8147 cm⁻¹ (saQ(4,4) transition) and probing around 1082592.4 MHz (ν₂ = 1 asQ(4,4)).

EXPERIMENTAL STUDY

The THz probe beam was generated by a frequency multiplier chain (Virginia Diodes, Inc.) and the input signal was synthesized by a high precision microwave generator (Agilent) with an amplitude modulation used for a lock-in detection. An InSb hot electron bolometer (QMC Instruments Ltd.) cooled to 4 K was employed for the detection of the THz radiation. The NH_3 gas flowed through a gas cell made from a 50 cm long copper tube with 10 mm inner diameter. The gas cell was terminated by THz and MIR transparent high resistivity Si window inclined at the Brewster angle in order to avoid any reflection in the cell. MIR optical pumping was provided by a distributed feedback MIR quantum cascade laser (QCL) with a central wavelength around $10.3 \mu\text{m}$ (AdTech) and a power up to 100 mW.

RESULTS AND DISCUSSION

Figure 1 (a) shows the transmittance as a function of the MIR pumping power². The transparency when the stimulated emission is equal to the absorption is about 1 mW for both lines. The gain dependence on the pump power is linear up to approximately 13 mW where probably depletion of the ground states starts, probably due to the slow vibrational relaxation of $v_2 = 1(s)$ states after stimulated emission. The slope of the linear part of the gain for the (3,3) line is 0.08 mW^{-1} and 0.05 mW^{-1} for the (4,4) line.

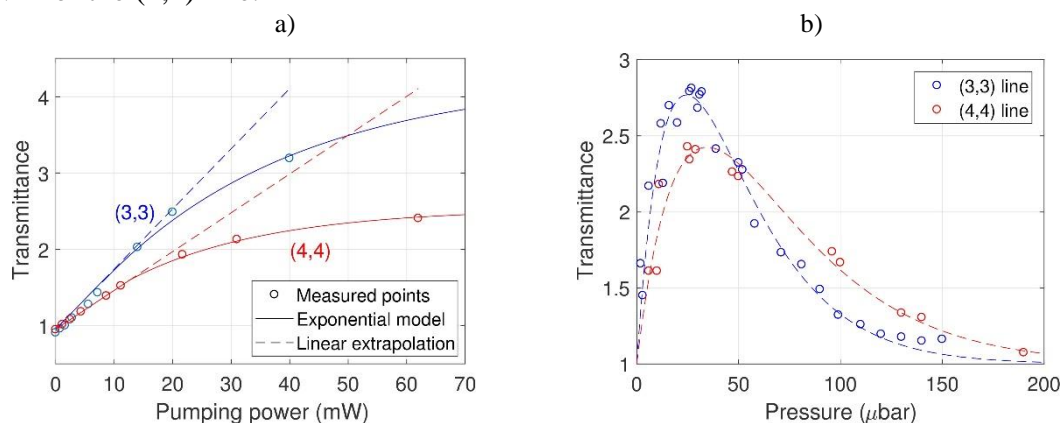


Fig. 1. Transmittance through optically pumped ammonia as a function of pumping power² (a) and as a function of ammonia pressure² (b).

Figure 1 (b) shows the THz gain as a function of the pressure². The gain increases linearly with the pressure due to the higher number of molecules in the volume up to a certain point where collisions between molecules and/or cavity walls cause increased nonradiative relaxation and exponentially decrease of population inversion. The optimal pressure is between 20 – 30 μbar and 25 – 45 μbar for (3,3) and (4,4) line respectively.

CONCLUSION

In this contribution we presented measurements of important parameters of optically pumped NH_3 . Two lines were selected at 1.073 and 1.083 THz. Measurements were performed at different pumping power, frequency and pressure values. Measured gains up to 10.1 dB.m^{-1} and up to 6.4 dB.m^{-1} were obtained during one-way copropagation for the (3,3) and (4,4) lines respectively². We attribute the high gain measured to the strong inversion transition chosen and to the fact that the QCL allows perfect resonant pumping. It is possible to achieve even higher gain by improving conditions, e. g. matching the THz probing beam with a preferred waveguiding mode of the cell.

Obtained parameters will help a better understanding of the lasing gas behaviour and may serve as an information for improving performance of the existing NH₃ THz optically pumped molecular gas lasers¹.

Acknowledgments: This work was supported by Ministry of Education, Youth and Sports of Czech Republic (SP2019/92, LQ1602), Agence Nationale de la Recherche (ANR-16-CE30-0020 HEROES), Czech Science Foundation (18-22102S) and European Regional Development Fund (CZ.02.1.01/0.0/0.0/16_013/0001791).

REFERENCES

1. A. Pagies, G. Ducournau, J.-F Lampin, APL Photonics 1 (2016).
2. M. Mičica, S. Eliet, M. Vanwolleghem, R. Motiyenko, A. Pienkina, L. Margulès, K. Postava, J. Pištora, J.-F. Lampin, Optics Express 26 (2018) 21242-21248.
3. M. Mičica, M. Vanwolleghem, K. Postava, J. Pištora, J.-F. Lampin, Spectroscopy of optically pumped ammonia and deuterium oxide near 1 THz, 42nd International Conference on Infrared, Millimeter, and Terahertz Waves, Cancun, 2017.

Structural study of thin films of graphene oxide with biosilver nanoparticles

G. Simha Martynková^{1,3}, G. Kratošová¹, R. Škuta¹, S. Sathish¹, K. Lafdi²

¹Nanotechnology Centre, VSB-Technical University, Czech Republic; ²University of Dayton, USA;

³IT4Innovations, VSB-Technical University, Czech Republic

grazyna.simha@vsb.cz

ABSTRACT

The study of carbon nanostructures is very extensive due to their unmatched properties and numerous applications. Among the various species of carbon, graphene is one of the most talked about in the present era due to its remarkably excellent properties. We used the method to prepare graphene oxide (GO) dispersion and stopping the process at pH around 4. Simple casted thin layer film we prepared out of basic GO and GO enriched with Ag nanoparticles. Silver particles are prepared via biosynthesis using linden phyto-stabilizers and metal salt precursor. The amount of additive silver was maintained at dispersion concentration of mmols. The comparison of both was performed in sense of structural characterization and microbial and conductivity testing. The study of films morphology revealed different roughness of the surface which is connected to chemistry and apparently to microbial activity as well. Test on *Staphylococcus aureus* and *Escherichia coli* were positive for both films on exposition at 48h. Film with biosilver was active even after 72h of exposition. Both films are stable at room temperature and moisture, but are highly hydrophilic. Morphology of films shown by scanning electron microscopy and transmission electron microscopy image of silver particles, and XRD patterns of both films.

Keywords: Graphene oxide, nanosilver, thin films, structure, morphology.

Acknowledgments: The National Programme of Sustainability (NPU II) project „IT4Innovations excellence in science - LQ1602“ and Ministry of Education, Youth and Sport of the Czech Republic SP2019/50 partially supported the research.

The importance of adhesion between fillers and polymer matrix on the utility macro-properties of the composites materials

B. Strzemiecka¹, A. Jamrozik¹, Ł. Kłapiszewski¹, P. Jakubowska¹, D. Matykiewicz², M. Sandomierski¹, T. Jesionowski¹, A. Voelkel¹

¹Institute of Chemical Technology and Engineering, Poznan University of Technology, Poland

²Poznań University of Technology, Faculty of Mechanical Engineering and Management,
Department of Polymer Processing, Institute of Materials Technology, Poland

Beata.Strzemiecka@put.poznan.pl

ABSTRACT

In this paper the way of the estimation of the filler-polymer adhesion as well as filler-filler cohesion was described. Inverse Gas Chromatography technique was used to determine the aforementioned adhesion and cohesion. The thermodynamic values of adhesion and cohesion forces in composites were correlated with the storage modulus (G') determined by dynamic thermo-mechanical analysis. The data obtained by Inverse Gas Chromatography enable to estimate the ratio of adhesion to cohesion forces what makes possible to assess dispersion of the filler in polymer matrix. Adhesion to cohesion ratio was in agreement with SEM images showing dispersion of filler particles in polymer matrix. Moreover, the influence of fillers on the thermo-mechanical behavior of composite may be explained in relation to the adhesion/polymer force.

Keywords: adhesion, cohesion, thermomechanical properties of composites, polymer composites

INTRODUCTION

The mechanical properties of the nano/microcomposites depend on the dispersion and set of the nanoparticles in the polymer matrix. Only well-dispersed fillers in such polymer system as abrasive materials can transfer mechanical forces and be effective as heat collector protecting the polymer against melting and degradation during the grinding processes. The interface filler-polymer is critical region. The estimation of the strength of the filler-polymer as well as filler-filler interactions is difficult, especially for nanomaterials. Adhesive forces are described by a variety of theories which are often limited to certain phenomena. Thus, physical and chemical processes comprising adhesion are extremely diverse. For this reason, the study of adhesion is multidisciplinary, and interpretations of adhesion phenomenon must be a synthesis of achievements in many fields of science. Nowadays, there are several techniques for studying the adhesion.¹ In this paper Inverse Gas Chromatography (IGC) was applied to predict the thermodynamic, relative value of the adhesion and cohesion strength. The ratio of adhesion to cohesion (W_{coh}/W_{adh}) was correlated with SEM micrographs and the storage modulus (G') determined by the thermo-mechanical analysis (DMTA). The aim of the performed research was to check if the adhesion and cohesion values determined by IGC influence further macro-behaviour of final, model resin-bonded abrasive materials (here represented by parameters determined by DMTA). Authors described the IGC procedure of the adhesion and cohesion determination in several papers.²⁻⁴

EXPERIMENTAL STUDY

The different fillers such as aluminosilicates, lignin-derived were used for preparation of the model composites consisting of abrasive grains covered by resole and bounded together by novolak, hardened according to special temperature program (heating from 50°C until 180°C; heating rate

0.2 deg/min and then heated at 180°C for 10h). IGC measurements were carried out by using Surface Energy Analyser produced by Surface Measurement System Ltd., London. The tested materials were placed into the chromatographic columns by the tap-and-fill method. The measurements were carried out at 30 °C. The temperature of injector as well as FID detector was 180 °C. Helium was a carrier gas with flow rate 15 ml/min. The dynamic-mechanical properties of the cured samples were investigated by DMTA in a torsion mode by means of Anton Paar MCR 301 apparatus, operating at frequency $f=1$ Hz at the temperature range between 25°C and 350°C (heating rate 2°C/ min).

RESULTS AND DISCUSSION

SEM micrographs (Fig. 1.) present composites consist of: novolak, resole, abrasive grains and different fillers: standard filler used in industry PAF - $K_3AlF_6+KAlF_4$ (a), kraft lignin (b), synthetic zeolite (c) and natural zeolite (d). Less homogenous is the composite with synthetic zeolite. It may be explained by the highest value of W_{coh}/W_{adh} that suggests stronger cohesion between synthetic zeolite particles than adhesion of this filler with novolak and resole resins. Thus, the final composite is not homogenous, the filler particles agglomerate, and it is reflected in the lower value of G' than for composites with standard filler PAF and natural zeolite characterized by W_{coh}/W_{adh} equal approx. 1 which means adhesion and cohesion forces are in equilibrium which should result in composites homogeneity. The composite with lignin is a special case. Lignin has stronger adhesion to resins than cohesion between its particles that results the plastizizing effect of lignin in this particular composition (G' much lower than for other tested composites).

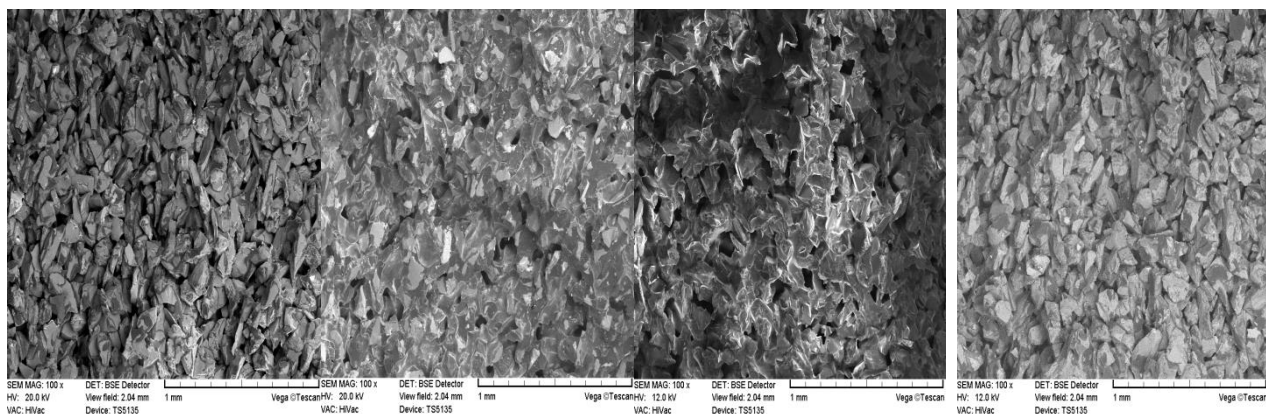


Fig. 1. SEM micrographs and W_{coh}/W_{adh} , G' values for studied composites differing in the used filler: a) system with $K_3AlF_6+KAlF_4$ b) system with kraft lignin c) system with synthetic zeolite d) system with natural zeolite $W_{coh}/W_{adh} = 1.0$ $G' = 7.1$ GPa $W_{coh}/W_{adh} = 0.6$ $G' = 1.5$ GPa $W_{coh}/W_{adh} = 1.7$ $G' = 5.9$ GPa $W_{coh}/W_{adh} = 1.3$ $G' = 6.9$ GPa

CONCLUSION

The application of IGC method supported by DMTA analyses makes it possible to practical and cost-effective assessment of filler/resin interfacial bonding. The results of IGC technique help to explain the observed macro-behaviour of the model composites using for abrasive articles production. Thanks to obtained results it was possible to predict which filler gives the homogenous composite that should reflect in the higher value of storage modulus, G' , of the final product. However, the thermo-mechanical properties depends also on the type of the filler and for example lignin reflects strong adhesion to phenolic resins but its structure makes the final composites characterized by the relatively low value of G' . It can be sum up that using IGC and DMTA

together make possible to predict and design the applications of the abrasive article with the given filler.

Acknowledgments: This work was supported by the National Science Centre. Poland. under research project No. UMO- 2015/17/B/ST8/02388.

REFERENCES

1. S. Abbott, Adhesion Science: Principles and Practice, DEStech Publication, Inc., 2015.
2. B. Strzemiescka, A. Voelkel, Int. J. Adhes. Adhes. 38 (2012) 84-88.
3. B. Strzemiescka, A. Voelkel, J. Donate-Robles, J. M. Martin-Martinez, Appl. Surf. Sci. 316 (2014) 315–323.
4. B. Strzemiescka, A. Voelkel, D. Chmielewska, T. Sterzyński, Int. J. Adhes. Adhes. 51 (2014) 81-86.

Magnetically modified montmorillonite - characterization, sorption properties and stability

M. Tokarčíková¹, L. Bardoňová¹, J. Seidlerová¹, K. Drobíková^{1,2}, O. Motyka¹

¹Nanotechnology Centre/VŠB-Technical University of Ostrava, 17. listopadu 15/2172, 708 00 Ostrava-Poruba, Czech Republic; ²IT4Innovations Centre of Excellence, VŠB-Technical University of Ostrava, 17. listopadu 15/2172, 708 33 Ostrava-Poruba, Czech Republic

Michaela.tokarcikova@vsb.cz

ABSTRACT

Clay mineral montmorillonite (Mt) magnetised by Fe_xO_y nanoparticles (NPs) was prepared by precipitation in two steps. Magnetically modified montmorillonite (MMt) was tested as a sorbent for the elimination of heavy metals ions from aqueous solutions. Zn(II), Cd(II), Pb(II) ions and their combination were successfully sorbed by magnetic composite (MMt). The equilibrium was achieved after 30 minutes of interaction of the liquid phase with MMt. The influence of solid-to-liquid ratio on the MMt sorption properties was studied as well. The amounts of ions removed by Mt and MMt were comparable. Therefore, magnetisation of Mt did not influence its sorption capacity. The composite can be easily removed by a magnetic field from the solution after sorption.

Keywords: magnetically modified montmorillonite; Fe_xO_y nanoparticles; sorption; heavy metals

INTRODUCTION

The main sources of heavy metal contamination are (e.g.) alloy industries, metal plating, mining operation, pesticides, agricultural activities, smelting or batteries manufacture^{1,2}. Lead, cadmium and zinc are one of the most toxic and carcinogenic heavy metals that could cause serious environmental and health problems even at low concentrations^{2,3}.

There are several technics to treat metal polluted wastewaters, e.g. chemical precipitation, ion exchange, reverse osmosis, membrane separation or electrolysis^{4,5}. However, adsorption is fast, low-cost and relatively easy to realisation. The magnetisation of the adsorbent can lead to other beneficial properties of the material. Mainly, the adsorbent with adsorbed pollutants can be easily removed from the solution after sorption using a magnetic field.

EXPERIMENTAL/THEORETICAL STUDY

The MMt was prepared using a two-step method. In the first step, the suspension containing Fe_xO_y NPs was prepared. In the second step, the suspension of 1:4 Fe_xO_y :water ratio was mixed with deionised water and an appropriate amount of montmorillonite under stirring. The mixture was filtered the following day^{6,7}.

Batch sorption experiments were carried out in plastic flasks at laboratory temperature. 0.1 ± 0.01 g and of MMt sample with 100 ml or 25 ml of solution containing Cd(II), Pb(II) or Zn(II) ions (the initial concentrations of 10 mg/L) were shaken at a constant speed (4.5 rpm) in different time intervals to determine the optimal contact time. After shaking, the mixture was filtered through a $0.23 \mu\text{m}$ pore filter (PRAGOPOR). Concentrations of Cd(II), Pb(II) and Zn(II) ions in the filtrate were determined by flame atomization of atomic absorption spectrometer (ContrAA 800, Analytik Jena).

RESULTS AND DISCUSSION

The percentage of heavy metals ions combination (10 mg/L) eliminated by MMt from solution is presented in Fig. 1. The amounts of Pb(II) removed by MMt achieved almost to 100 % for 0.1 g/25 ml solid-to-liquid ratio. The efficiency of Zn(II) and Cd(II) removed from solution was higher than 80 % for 0.1 g/25 ml solid-to-liquid ratio. The maximum amount of Pb(II), Zn(II) and Cd(II) adsorbed to MMt was achieved after 30 minutes of contact time for 0.1 g/25 ml solid-to-liquid ratio. The percentage of removed Pb(II) was higher than 90 %, and for Zn(II), Cd(II), it was higher than 50 % for 0.1 g/100 ml solid-to-liquid ratio. The maximum amount of Zn(II) and Cd(II) adsorbed to MMt was achieved after 6 hours of contact time for 0.1 g/100 ml solid-to-liquid ratio.

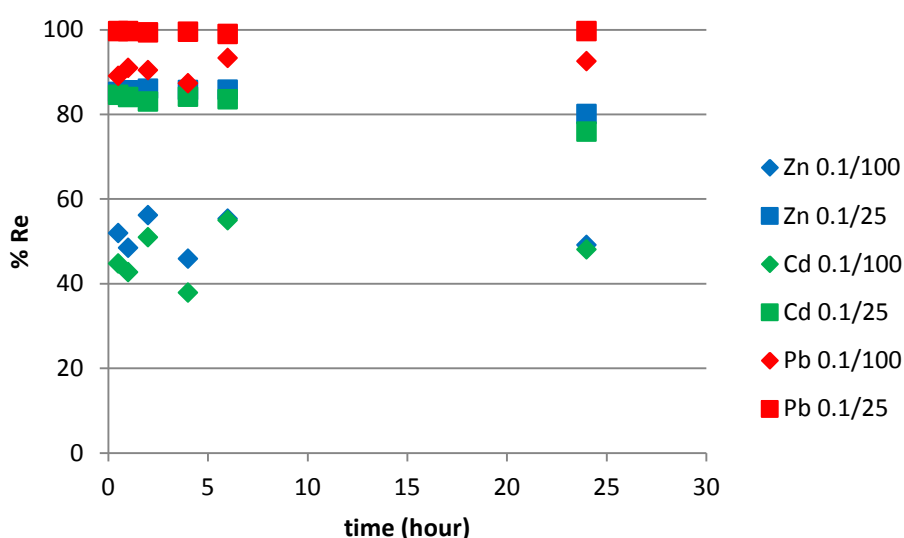


Fig. 1. The percentage of Cd(II), Pb(II) and Zn(II) removed (% Re) from solution.

CONCLUSION

Magnetically modified montmorillonite was tested as the sorbent for heavy metals ions from aqueous solution. The solid-to-liquid ratio influenced the percentage of removed Cd(II), Pb(II) and Zn(II) ions. Better sorption properties were achieved for 0.1 g/25 ml solid-to-liquid ratio - higher than 80 %. The equilibrium between MMt and adsorbed ions was achieved after 30 minutes of

interaction for 0.1 g/25 ml solid-to-liquid ratio. The composite is efficient sorbent for Zn(II), Pb(II) and Cd(II) ions and can be easily removed by magnet following the sorption.

Acknowledgments: This work was supported by ERDF/ESF New Composite Materials for Environmental Applications (No. CZ.02.1.01/0.0/0.0/17_048/0007399).

REFERENCES

1. K. Kadirvelu, K. Thamaraiselvi, C. Namasivayam, *Bioresour. Technol.* 76 (2001) 63–65.
2. S.K. Yadav, D.K. Singh, S. Sinha, *J. Environ. Chem. Eng.* 2 (2014) 9–19.
3. M. Inyang, B. Gao, Y. Yao, Y. Xue, A.R. Zimmerman, P. Pullammanappallil, X. Cao, *Bioresour. Technol.* 110 (2012) 50–56.
4. Ch.O. Ijagbemi, M.-H. Baek, D.-S. Kim, *J. Hazard. Mater.* 166 (2009) 538–546.
5. A.K. Bhattacharya, S.N. Mandal, S.K. Das, *Chem. Eng. J.* 123 (2006) 43–51.
6. Safarik, M. Safarikova, *Int. J. Mat. Res.* 105 (2014) 104–107.
7. K. Pospiskova, I. Safarik, *Mater. Lett.* 142 (2015) 184–188.

Resonance states in plasmonic-waveguiding structures

J. Vlček^{1,3}, J. Pištora^{1,2}, M. Lesňák¹

¹Nanotechnology Centre; ²IT4Innovations; ³Department of Mathematics and Descriptive Geometry, Faculty of Mechanical Engineering; VŠB – Technical University of Ostrava, Czech Republic

jaroslav.vlcek@vsb.cz

ABSTRACT

The model study is made for planar layered structure consisting from coupling prism, Au film and high-index interlayer for SPP's generation and dielectric waveguide composed from ferromagnetic garnet on sGGG substrate separated by air gap. The mutual coupling of surface plasmon polariton (SPP) with an optical mode excited in planar waveguide is discussed. The dependence of coupling conditions on the multilayer parameters is analyzed to obtain optimal field intensity enhancement for design of plasmonic sensing elements.

Keywords: Plasmon polariton, planar waveguide, coupling conditions.

INTRODUCTION

The coupling of resonance states in various optical nanostructures offers many promising ways for the development of new photonic devices. This expectation follows the recent results obtained for plasmonic coupled modes occurring in plasmonic metal-dielectric nanostructures¹. The coupling between surface plasmon polariton and waveguide mode belongs to intensively investigated effects^{2,3}.

THEORETICAL STUDY

We analyze the dependence of coupling conditions on the multilayer structure described on Fig. 1a. The attention pays to the number and location of Au films as well as to the role of dielectric interlayer relating to coupling forces. The water is considered as the analyte.

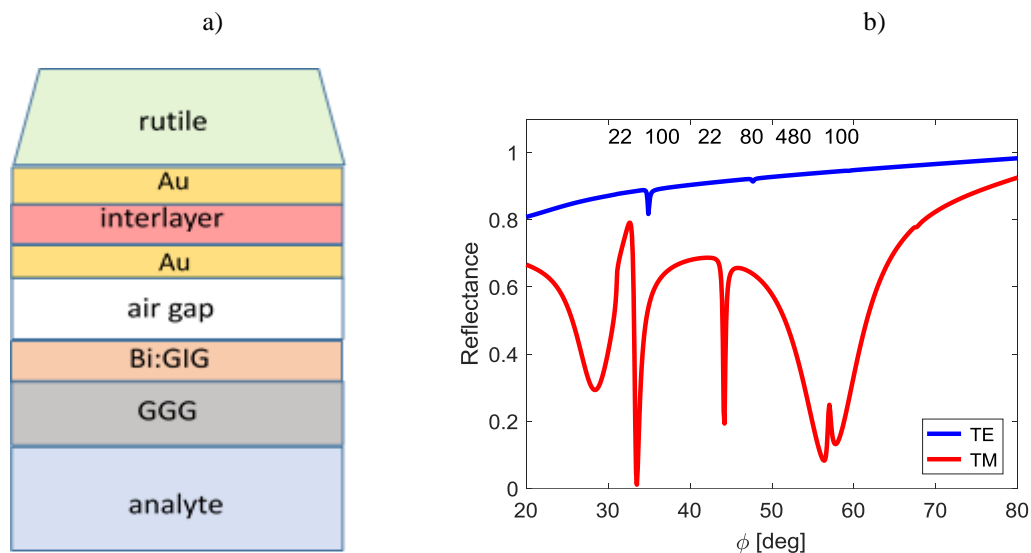


Fig. 1. (a) Geometrical configuration; (b) Reflection response with the sequence of finite layer thicknesses in nm scale (Au/interlayer/Au/air gap/Bi:GGG/GGG).

The analysis is executed for reflectance interrogation at the wavelength 632.8 nm using rigorous coupled wave algorithm (RCWA) implemented as the Matlab code.

RESULTS AND DISCUSSION

In the reflection response the resonance dips of two kinds are observed as the waveguide resonance modes and/or the plasmonic ones. The mutual influence of resonance states is discussed from the point of view of coupling strength represented by minima location and their deepness and width. Among other, the combinations of multilayer parameters leading to optical Fano effect are demonstrated.

CONCLUSION

Presented results offer extending view on the optical systems with coexistent plasmonic and waveguide modes.

Acknowledgments: This work was partially supported by the Ministry of Education, Youth and Sports: by the National Program of Sustainability (NPU II) project „IT4Innovations excellence in science - LQ1602“.

REFERENCES

1. Z. Sekkat et al., Plasmonic coupled modes in metal-dielectric multilayer structures: Fano resonance and giant field enhancement, *Opt. Express* 24 (2016) 20080.
2. S. Hayashi et al., Waveguide-coupled surface plasmon resonance sensor structures: Fano lineshape engineering for ultrahigh-resolution sensing, *J. Phys. D: Appl. Phys.* 48 (2015) 325303.
3. J. Pištora et al., Plasmonic nanostructures with waveguiding effect, *PNFA* 31 (2018) 22-26.

Poster presentations (PP):**Synthesis and structural, thermal and magnetic properties of Mn-doped CuCr_2Se_4 nanoparticles**

I. Jendrzejska¹, Z. Barsova¹, T. Goryczka², E. Pietrasik¹, J. Goraus³, J. Czerniewski³, J. Jampilek^{4,5}

¹University of Silesia, Institute of Chemistry, Katowice, Poland; ²University of Silesia, Institute of Materials Science, Katowice, Poland; ³University of Silesia, Institute of Physics, Katowice, Poland; ⁴Department of Analytical Chemistry, Faculty of Natural Sciences, Comenius University, 842 15 Bratislava, Slovakia;

⁵Regional Centre of Advanced Technologies and Materials, Faculty of Science, Palacky University, 783 71 Olomouc, Czech Republic

izabela.jendrzejska@us.edu.pl

ABSTRACT

Nanocrystalline samples with general formula $\text{CuCr}_{2-x}\text{Mn}_x\text{Se}_4$ ($x = 0.1, 0.2$) were obtained by applying two different techniques: sintering in 1073K and high-energy ball-milling of the obtained polycrystalline samples. The average crystallite size and lattice strain were calculated from X-ray line broadening, using Williamson-Hall method. The size of crystallite is about 10nm. DSC/TG analysis confirmed thermal stability of obtained samples. Magnetic measurements confirmed the ferromagnetic properties of polycrystalline $\text{CuCr}_{1.9}\text{Mn}_{0.1}\text{Se}_4$.

Keywords: Nanoparticles, Spinel Compounds, X-ray Diffraction, Thermal Analysis, Magnetic Properties.

INTRODUCTION

The spinels with general formula ACr_2Se_4 have attracted for their potential application [1].

A parent CuCr_2Se_4 -compound is a normal spinel with lattice parameter 10,321-10,337Å. This compound shows ferromagnetic and *p*-type semiconducting properties ($T_C = 414,5 - 460\text{K}$,

$\theta = 452 - 465\text{K}$ and possesses the magnetization saturation of 4.76 B.M./f.u. at 4.2 K and the effective magnetic moment of 4.65 B.M./f.u. [2-4]. Mn-ions, which locate in octahedral sites of the spinel structure, have strong impact on properties of the CuCr_2Se_4 spinel.

EXPERIMENTAL STUDY

Nanocrystalline samples with general formula $\text{CuCr}_{2-x}\text{Mn}_x\text{Se}_4$ ($x = 0.1, 0.2$) were obtained by applying two different techniques: 1) sintering in 1073K from the binary selenides (MnSe , CuSe and Cr_2Se_3 , and 2) high-energy ball-milling of the obtained polycrystalline samples. After sintering and ball-milling, the sample were investigated using XRD – method. Chemical composition was determined using SEM method. TG – DSC analyses of $\text{CuCr}_{2-x}\text{Mn}_x\text{Se}_4$ ($x = 0.1, 0.2$) compounds were carried out using a Labsys Evo system. The samples with a mass of 10.9mg for $\text{CuCr}_{1.9}\text{Mn}_{0.1}\text{Se}_4$ and 54.8mg for $\text{CuCr}_{1.8}\text{Mn}_{0.2}\text{Se}_4$ were placed in small crucibles and heated in a flowing Ar – atmosphere (high purity) with the heating rate of $10^\circ\text{C}/\text{min}$. Magnetic properties were investigated using a SQUID superconducting magnetometer.

RESULTS AND DISCUSSION

In Fig. 1, there are visible diffraction lines of the cubic $\text{Cu}_{0.77}\text{Cr}_{1.40}\text{Mn}_{0.10}\text{Se}_4$ phase (SG Fd-3m, blue line) after sintering and the $\text{Cu}_{0.77}\text{Cr}_{1.40}\text{Mn}_{0.10}\text{Se}_4$ monoclinic phase (SG I2/m, red line), type- Cr_2Se_3 with the basic lattice parameters: $a = 6,227 \text{ Å}$, $b = 3,582 \text{ Å}$, $c = 11,528 \text{ Å}$ and $\beta = 90,77^\circ$

[5]. These phases were identified after sintering and after 30h of milling (Fig. 1). The average crystallite size and lattice strain were calculated from X-ray line broadening, using Williamson-Hall method. The results are presented in Table 1. In Fig.2, the high – magnification SEM microphotographs of obtained samples are presented.

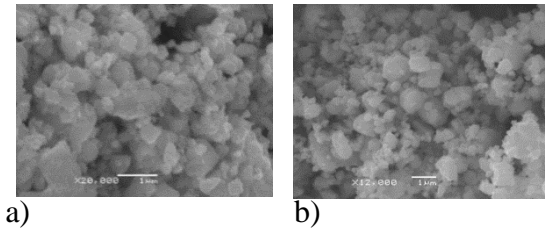
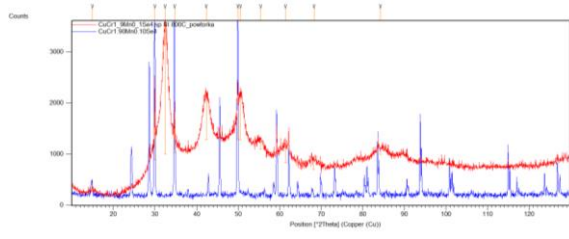


Fig.1. XRD pattern of the $\text{Cu}_{0.77}\text{Cr}_{1.40}\text{Mn}_{0.10}\text{Se}_4$ compound after sintering (blue line) and after 30h of milling (red line).

Fig.2. A fracture surface by SEI for:

- a) $\text{Cu}_{0.77}\text{Cr}_{1.40}\text{Mn}_{0.10}\text{Se}_4$, scale bar = $1\mu\text{m}$,
b) $\text{Cu}_{0.84}\text{Cr}_{1.28}\text{Mn}_{0.19}\text{Se}_4$, scale bar = $1\mu\text{m}$.

Table 1. The values of crystallite size(d) and lattice strain (η) for $\text{CuCr}_{2-x}\text{Mn}_x\text{Se}_4$ – compounds

Nominal compound	Real compound	d (nm)	η
$\text{CuCr}_{1.9}\text{Mn}_{0.1}\text{Se}_{4.0}$	$\text{Cu}_{0.77}\text{Cr}_{1.40}\text{Mn}_{0.10}\text{Se}_{4.0}$	11.2 ± 1.4	0.96 ± 0.12
$\text{CuCr}_{1.8}\text{Mn}_{0.2}\text{Se}_{4.0}$	$\text{Cu}_{0.84}\text{Cr}_{1.28}\text{Mn}_{0.19}\text{Se}_{4.0}$	7.2 ± 1.6	1.52 ± 0.23

Thermal analysis, showed in Fig. 3, confirmed, that obtained samples are stable and resistant to high temperature up to 800°C and the presence of manganese further increases their thermal stability. Magnetic measurements showed ferromagnetic properties of polycrystalline $\text{CuCr}_{1.90}\text{Mn}_{0.10}\text{Se}_{4.0}$. The Curie temperature has a value of 360K. Magnetic properties of $\text{Cu}_{0.77}\text{Cr}_{1.40}\text{Mn}_{0.10}\text{Se}_4$ and $\text{Cu}_{0.84}\text{Cr}_{1.28}\text{Mn}_{0.19}\text{Se}_4$ will be presented during the conference.

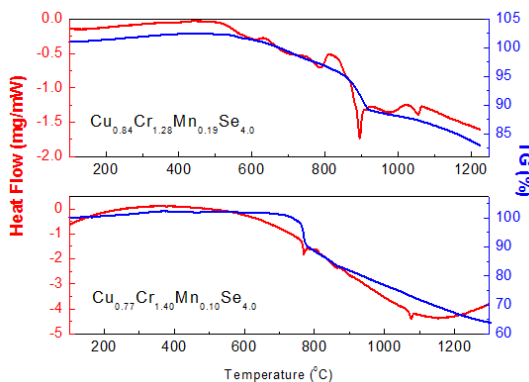


Fig. 3. DSC/TG curves for $\text{CuCr}_{2-x}\text{Mn}_x\text{Se}_4$ – samples.

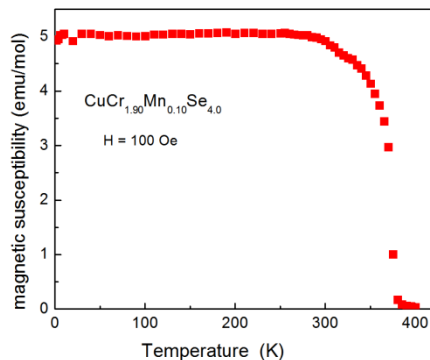


Fig.4. The magnetic susceptibility vs. temperature for $\text{CuCr}_{1.9}\text{Mn}_{0.1}\text{Se}_{4.0}$.

CONCLUSIONS

The results of $\text{Cu}_{0.77}\text{Cr}_{1.40}\text{Mn}_{0.10}\text{Se}_4$ and $\text{Cu}_{0.84}\text{Cr}_{1.28}\text{Mn}_{0.19}\text{Se}_4$ nanoparticles mentioned above suggest that the decrease of the size of grains causes a change from cubic to monoclinic phase. The obtained nano-samples possess thermal stability until 800°C . The value of Curie temperature was calculated to 360K and is lower than for pure CuCr_2Se_4 (460K).

Acknowledgement: This study was supported by the Slovak Research and Development Agency (Grant No. APVV-17-0373) and by the Ministry of Education of the Czech Republic (LO1305).

REFERENCES

1. J. Hemberger, H.-A.K. v.Nidda, V. Tsurkan, A. Loidl, Phys. Rev. Lett. 98 (2007) 147203.
2. J. Krok, J. Spálek, S. Juszczuk, J. Warczewski, Phys. Rev. B 28, 6499 (1983).
3. F.K. Lotgering, in: Proc. 1964 Int. Conf. on Magnetism, Nottingham, Ed. L.F. Bates, Institute of Physics, London 1965, p. 533.
4. F.K. Lotgering, R.P. Van Staple, Solid State Commun. 5, 143 (1967).
5. E. Maciążek, J. Panek, M. Kubisztal, M. Karolus, T. Groń, H. Duda, Acta Phys. Pol. 126 (2014) 1137.

Surface polaritons at periodic interface – near field analysis

J. Krček

Department of Mathematics and Descriptive Geometry, Faculty of Mechanical Engineering;
VŠB – Technical University of Ostrava, Czech Republic

jiri.krcek@vsb.cz

ABSTRACT

The optical diffraction on a periodical interface belongs to relatively fewer exploited applications of the boundary integral equations method. This contribution presents a less frequent formulation of the diffraction problem based on vector tangential fields. There are discussed properties of obtained boundary operators with singular kernel and the numerical implementation is described. The mathematical model is applied to the diffraction problem on the smooth sine boundary between two dielectrics as well as between a dielectric and a metal.

Keywords: Optical diffraction, polaritons, tangential fields, boundary elements method.

INTRODUCTION

The diffraction of an optical wave on a periodical interface between two media belongs to frequently solved problems, especially, when the grating period Λ is comparable with the wavelength λ of the incident beam. One of the relatively new approaches is based on the Boundary Integral Equations (BIE)¹. Unlike the usually used rigorous coupled waves algorithm (RCWA) advantageous in the far fields analysis, the BIE models enable effective modelling of near fields in the spatially modulated region.

THEORETICAL STUDY

The optical diffraction problem on periodical interface is formulated on the basis of vector tangential fields, for which the system of boundary integral equations is established^{2,3}. Obtained mathematical model is numerically solved using boundary element method and applied to sine interface profile.

RESULTS AND DISCUSSION

We attend to the optical diffraction problem on the periodical boundary between two semi-infinite homogeneous domains (Fig. 1a). We solve the problem for the TM polarised monochromatic plane

wave that is incoming from the domain $\Omega^{(1)}$ under the angle of incidence θ measured from the x_3 direction.

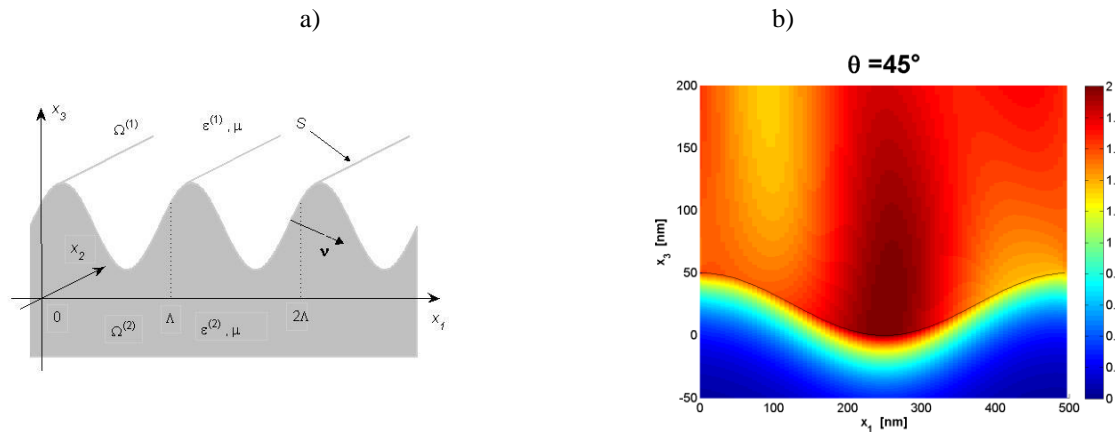


Fig. 1. (a) Scheme of the domains; (b) Tangential component $|H_2|$, $\lambda = 632.8$ nm, glass/gold interface.

We seek for the space-dependent amplitudes \mathbf{E} and \mathbf{H} of the electromagnetic intensity vectors and formulate the problem as the boundary integral equations for their tangential fields. The properties of obtained boundary operators with singular kernel are discussed and the numerical implementation is described.

RESULTS AND DISCUSSION

We successfully tested proposed mathematical model for diffraction problem on the periodical sine interface between two dielectrics (air/glass) or dielectric-metal interface (glass/gold – Fig. 1b).

CONCLUSION

The mathematical model of the optical diffraction based on the tangential fields was verified to be applicable to practical calculations. An extension to multilayer model is supposed as the future goal.

REFERENCES

1. X. Chen, A. Friedman, Maxwell's equations in a periodic structure. Trans. Am.Math. Soc., Vol. 323 (1991), No. 2, 465-507.
2. J. Krček, J. Vlček, Tangential fields in optical diffraction problems, Programms and Algorithms of Numerical Mathematics 16, Institute of Mathematics AS CR, Prague 2013, 124-129.
3. J. Krček, J. Vlček, Tangential fields in mathematical model of optical diffraction, Programms and Algorithms of Numerical Mathematics 17, Institute of Mathematics AS CR, Prague 2015, 112-117.

Thermal behaviour of organically modified smectites

E. Plevova^{1,2}, L. Vaculikova^{1,2}, V. Valovicova¹, G. Simha Martynkova³

¹Institute of Geonics of the AS CR, Studentska 1768, 708 00 Ostrava – Poruba, Czech Republic; ²Institute of Clean Technologies for Mining and Utilization of Raw Materials for Energy Use – Sustainability Programme, Studentska 1768, 708 00 Ostrava – Poruba, Czech Republic; ³VŠB - Technical University of Ostrava, 17. listopadu 15, 708 33 Ostrava – Poruba, Czech Republic

eva.plevova@ugn.cas.cz

ABSTRACT

The smectites were modified with different types of alkylammonium cations. The X-ray powder diffraction was used to calculate the values of the basal space of the modified smectites to confirm the intercalation of cations into the structure. The montmorillonites were also characterized by means of FTIR spectroscopy, which proved sorption or intercalation of the alkylammonium cations too. Thermal behaviour of the smectites was investigated by simultaneous thermogravimetry and differential thermal analysis. The temperatures of dehydration and dehydroxylation and the temperatures related to total melting and recrystallization generally changed for organically modified samples. Study of temperatures changes together with determination of kinetic parameters helped to obtain a comprehensive assessment of smectite thermal stability.

Keywords: Smectites, intercalation, thermal analysis

INTRODUCTION

The hydrophobic, organophilic materials with good sorption properties can be formed from clay minerals by their organic modification. Quaternary alkylammonium cations are the most commonly used organic compounds for the preparation of organo-clays¹. Such clay composites can be used in various applications (environment protection - immobilization of contaminants, pharmacy, electrochemistry, packaging storage, ceramics etc.).² Interactions between organic compound and clay mineral leads to a formation of component with properties different from those of the original, e.g. the better sorption properties, the lower flammability, the lower weight, the easier biodegradability of polymers etc.^{3,4} In addition to the improved above mentioned properties the organically modified clay minerals exhibit thermal stability different from the origin clays.

EXPERIMENTAL

Two samples of montmorillonite and two of bentonite were treated by sedimentation and subsequent centrifugation to prepare fraction with the particle size below 5 µm. The smectites were modified with alkylammonium cations (hexadecyltrimethylammonium, benzyldimethylhexadecylammonium and hexadecylpyridinium) by sorption procedure. The X-ray powder diffraction was used to calculate the values of the basal spacing of the modified smectites. The found basal spacing of the prepared organo-smectites were compared with that of the unmodified. The original and the modified smectites were characterized by means of FTIR spectroscopy, too. The detailed interpretation of the corresponding absorption bands were performed. Thermal behaviour were determined by simultaneous thermogravimetry and differential thermal analysis. For smectites and structurally related minerals, the reactions occurring during heating can be divided into endothermic (desorption of surface water, removal of interlayer water, removal of constitutionally bound water) and exothermic (recrystallization and other structural transformations).

RESULTS AND DISCUSSION

The enhancement of the basal spacing obtained by X-ray diffraction confirmed the intercalation process of cations into bentonite samples. Also the IR spectra provided evidence of sorption and intercalation of the organic cations. Thermal analysis also confirmed the presence of all three alkylammonium cations in both types of modified montmorillonites and bentonites. The temperatures of the first peak of dehydration / desorption in both montmorillonites and bentonites has shifted to lower temperatures due to an improvement in hydrophobic character over the original minerals. The decomposition of the cations adsorbed on the smectite surface occurs and then the cations present in the interlayer are decomposed. In case of dehydroxylation process at the temperature interval 600-700 °C, the values of temperature peaks related to dehydroxylation decreased with addition of alkylammonium cations. However the peak of total dehydroxylation/melting increased with the concentration of the added and the same trend was possible to find for the exotherm effect connected to recrystallization and transformation above 1000 °C.

CONCLUSION

Thermal behaviour of the modified smectites was investigated, the temperatures of dehydration and dehydroxylation decreased with concentration of alkylammonium cations contrariwise the temperatures related to the total melting and recrystallization increased with the concentration. It is evident, that surfactants caused the improvement of total thermal stability of modified smectites, but each type of smectite reported different affinity for the sorption of alkylammonium cations as well as slightly different kinetic parameters.

Acknowledgments: The research has been done in connection with Project “Institute of Clean Technologies for Mining and Utilization of Raw Materials for Energy Use”- Sustainability program. Identification code: LO1406. The project is supported by National Programme for Sustainability I (2015-2019) and financed by the means of state budget of the Czech Republic.

REFERENCES

1. Borisover M, Bukhanovsky N, Lapidés I. Applied surface science. 256 (2010) 1-6.
2. Mousavi SM, Alemzadeh I, Vossoughi M. Iranian Journal of Science & Technology. 30 (2006) 613-619.
3. Zhou W, Wang X, Chen C, Zhu L. Chemical Engineering Journal. 233 (2013) 251-257.
4. Li, Y et al. Journal of the Taiwan Institute of Chemical Engineers. 62 (2016) 104-111.

Gyromixer of nanostructured systems and method of mixing thereof

A. Slíva¹, R. Brázda¹, K. Čech Barabaszová², G. Simha Martynková²

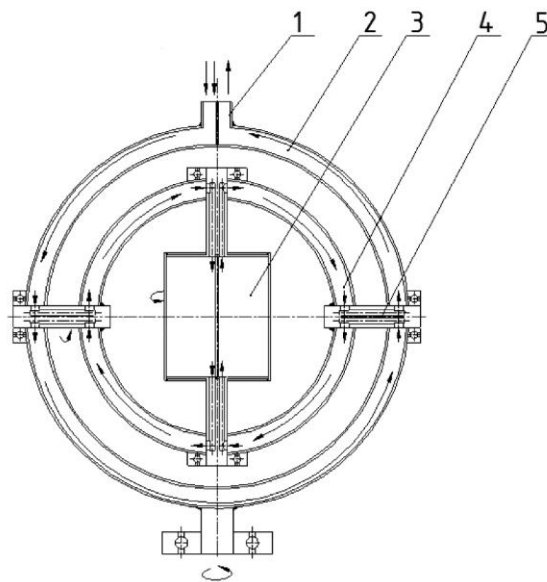
¹Institute of Transport, Faculty of Mechanical Engineering, VSB-Technical University of Ostrava, Czech Republic; ²Nanotechnology Centre, VSB-Technical University of Ostrava, Czech Republic

ales.sliva@vsb.cz

ABSTRACT

The paper deals with a design and a method of mixing of the invention called “Gyromixer of nanostructured systems”. The invention is disclosed as a gyromixer of nanostructured materials comprising an outer ring (2) that is provided inside and all over its periphery with a channel. In upper portion thereof, there is situated a split hopper (1) serving for both supply of material and carrying medium and for discharge thereof. In inner ring (4), being inserted in the outer ring (2), is

provided with pins (5) ensuring, along with the aid of bored channels, a correct distribution of material. The inner ring (4) accommodates a rotary hollow cylinder (3), in the internal portion of which there is a partition enabling motion of material in two directions. This member serves at the same time as a starter, which manages to rotate due a gyroscopic effect, both the rings. Material is supplied through the split hopper (1) into the inner portion of the external ring (2). With the aid of a carrying medium and by the action of a gyroscopic effect, the material is agitated and fed via a guide pin (5) into the internal ring (4). Here, owing to the gravity force and stream of the carrying medium, the material passes over through internal channels into the rotary cylinder (3) with the partition (9), wherefrom the material flows again back into the internal ring (4) and through the guide pin (5) into the external ring (2). From the external ring (2), the material is guided due to the action of air stream and gravity force again through the guide pin (5) back into the internal ring (4) and from it into the rotary cylinder (3). Further, the material is fed in the internal ring (4) through the guide pin (5) into the external ring (2) wherefrom the mixed material is discharged along with the carrying medium via the split hopper (1) out of the apparatus.



Keywords: Gyromixer; Nanostructured systems; Invention

Acknowledgements: The work has been done in connection with project Innovative and additive manufacturing technology - new technological solutions for 3D printing of metals and composite materials, reg. no. CZ.02.1.01/0.0/0.0/17_049/0008407 financed by Structural Funds of Europe Union and project SP2019/101 - Research, Science and Development in a Transport - Traffic Simulations, Adhesion Models, Storage Processes.

Structural characterization of ladder-like conjugated polymer brushes

M. Słowikowska, A. Wójcik, K. Wolski, S. Zapotoczny

Faculty of Chemistry, Jagiellonian University, Kraków, Poland

slowikowska@chemia.uj.edu.pl

ABSTRACT

Conjugated polymers because of their attractive electrical properties have been used in electronic devices like field effect transistors, organic photovoltaic solar cells, LEDs. However classical polymer films are not well organized and do not provide directional transport of charge carriers. Polymer brushes possess these desirable features as conjugated polymer chains are perpendicularly oriented with respect to the substrate. In these studies we have synthesized poly(3-trimethylsilyl-2-propynyl methacrylate) brushes (PTPM) with conjugated polyacetylene chains in ladder-like architecture.

Surface-initiated photoiniferter-mediated polymerization (SI-PIMP) was used to synthesize parent polymer brushes. In the second step conjugated chains were introduced by self-templating polymerization of pendant acetylene groups using rhodium based catalyst. Mechanical properties of parent and ladder-like conjugated brushes were tested by means AFM tribological and nanoindentation measurements. The obtained results revealed substantial changes in stiffness and in tribological properties after self-templating polymerization.

Keywords: Conjugated polymer brushes, Mechanical properties, Surface-Initiated Polymerization, Self-templating Polymerization

Acknowledgments: The authors would like to thank Bratniak foundation for the financial support.

Preparation and characterization of fly ash based membranes for microfiltration and ultrafiltration

B. Thomasová¹, J. Thomas², L. Gembalová², V. Tomášek¹

¹Nanotechnology Centre, VŠB-TU Ostrava, Czech Republic ²Institute of Clean Technologies for Mining and Utilization of Raw materials for Energy Use/ Faculty of Mining and Geology, VŠB-TU Ostrava, Czech Republic

barbora.thomasova@vsb.cz

ABSTRACT

The main objective of this work is the preparation of fly ash based ceramic support and membranes for micro and ultrafiltration applications. The choice of this material is based primarily on its low cost and its beneficial properties. The tubular supports were prepared by alkali activated modification of non-grinded fly ash and additives. Material produced by geopolymerization has shown great potential for wastewater treatment by filtration due to its porous structure formed after sintering at 1000°C. Porosity of the support was 39%, with average pore size of 2,3 µm. The support such prepared was effective for removal of colloidal particles and was successfully used for pretreatment of mine waters. For ultra and nanofiltration applications where high and low molecular weight substances need to be removed, preparation of a membrane layer with smaller pores is necessary. For this purpose, the average particle size of fly ash was decreased by intensive grinding.

The elaboration of the layer based on milled fly ash powder was performed by slip-casting method. Water glass and polyvinylalcohol (PVA) were used to form the casting suspension. The effect of slip concentration, casting time and withdrawal speed of sintered membranes was investigated by scanning electron microscopy (SEM). SEM images have shown that optimization of all parameters is necessary to avoid cracks formation in the coating and to prepare a homogenous thin layer of appropriate width and porosity.

Keywords: Fly ash, Support, Ceramic membranes, Microfiltration

Characterization of fine-grained montmorillonite fractions suitable for composite preparation

V. Valovičová¹, L. Vaculíková^{1,2}, E. Plevová^{1,2}, S. Dolinská³, I. Znamenáčková³, Z. Danková³

¹Institute of Geonics of the Czech Academy Sciences, Studentská 1768, 708 00 Ostrava – Poruba, Czech Republic; ²Institute of Clean Technologies for Mining and Utilization of Raw Materials for Energy Use – Sustainability Programme, Studentská 1768, 708 00 Ostrava – Poruba, Czech Republic ; ³Institute of Geotechnics of Slovak Academy of Sciences, Watsonova 45, 040 01 Košice, Slovak Republic

vera.valovicova@ugn.cas.cz

ABSTRACT

The aim of this experimental study was to characterize a fine-grained fraction of montmorillonites (SAz-2, STx-1, SWy-2 and Kunipia-F). It was investigated in order to provide more precise information of used montmorillonites than could be obtained by analysis of the unfractionated montmorillonites. At first, the fine fraction of montmorillonites were prepared by sedimentation and activation by means of Na₂CO₃. The prepared clay materials were characterized by the X-ray diffraction analysis and FTIR spectroscopy. The thermal behaviour of the studied samples was determined according to the characteristic temperatures obtained from TG/DTA curves. The temperatures of dehydration and dehydroxylation were evaluated and kinetic parameters were also calculated. The porosity and surface properties of the studied samples were gained by the nitrogen adsorption measurements. The obtained results confirmed that the fine fraction of montmorillonites could be a suitable material for subsequent preparation of composites with enhanced sorption properties, especially montmorillonite /MnO₂ composite.

Keywords: montmorillonite, activation, characterization, composites

INTRODUCTION

Clays may be composed of mixtures of fine grained clay minerals and clay-sized crystals of other minerals such as quartz, carbonate and metal oxides.¹ This study is focused on characterization of fine-grained montmorillonite fractions suitable for composite preparation. Clays and their modified derivatives play an important role in the environment by acting as a natural scavenger of pollutants by taking up cations and anions through adsorption or ion exchange. The montmorillonite, key component of bentonite, belongs to the universal natural adsorbents, able to accept substances with quite a wide range of ionic or molecular size.² Using clays and clay-based composites as adsorbent materials received wide attention because of their easy availability and comparatively less cost.¹⁻⁴

EXPERIMENTAL/THEORETICAL STUDY

At first, the natural montmorillonites (SAz-2, STx-1, SWy-2 and Kunipia-F) were purified by sedimentation to eliminate inorganic mineral impurities. The time of sedimentation was derived from the chosen particle size (5 μm). The fine fractions were collected according to Stokes law. Then the monoionic chemical activation of the fine montmorillonite fractions with the aim to improve their sorption properties were carried. These fractions of investigated montmorillonites with the calcium cations in the interlayer space was modified by the saturation with sodium salt: SAz-2, STx-1, SWy-2 fine fractions were carefully dispersed in 0.5 M Na_2CO_3 solution by shaking for about 24 h, and separated by centrifugation. The sediment of the Na^+ -exchanged clay mineral was washed with distilled water. This procedure was repeated 3 times. The obtained samples were characterized by X-ray diffraction, FTIR spectroscopy, thermogravimetry and surface and porosity distribution analysis.

RESULTS AND DISCUSSION

The structural changes of fine-grained montmorillonite fractions before and after natrification were studied. The XRD analysis of the sodium montmorillonite forms obtained by Na_2CO_3 activation suggests that the Na^+ ions were replaced by Ca^{2+} ions in the montmorillonite interlayer. Activated sodium forms has a lower d(001) spacing than the original calcium montmorillonite forms. The natrification process was also evaluated by FTIR spectroscopy. The traces of carbonates were occurred in IR spectra measured after natrification of montmorillonite fractions. The simultaneous thermogravimetry and differential thermal analysis was used to evaluate thermal stability of natrified samples. The shape of DTA curve as well as peak temperatures for modified minerals were slightly different compared to nature minerals. The surface parameters of original and activated fine montmorillonite fractions were determined by low temperature nitrogen adsorption measurements.

CONCLUSION

Purified Na^+ -fine montmorillonite fractions were prepared by sedimentation and Na_2CO_3 chemical activation. The X-ray diffraction analysis demonstrated the structural changes of the purified activated samples. Thermal stability was determined for both nature mineral and modified mineral. The changes of surface properties after the modification of fine montmorillonite fractions were observed, natrification causes an increase of the surface area and changes in adsorption properties. The study showed that prepared natrified fine-grained montmorillonite fractions are suitable for composite preparation. They will be used for subsequent modification with manganese oxides, in order to prepare composites with enhanced sorption properties. The synthesis of montmorillonite/ MnO_2 composites offer to obtain materials used as sorbents of heavy metals from aqueous solutions.

Acknowledgments: The research has been done in connection with Project "Institute of Clean Technologies for Mining and Utilization of Raw Materials for Energy Use"- Sustainability program. Identification code: LO1406. The project is supported by National Programme for Sustainability I (2015-2019) and financed by the means of state budget of the Czech Republic. This work was also supported by the Slovak Grant Agency for Science VEGA grant No. 2/0055/17 and 2/0029/19.

REFERENCES

1. F. Bergaya, B.K.G. Theng, G. Lagaly, Handbook of Clay Science, first edition, Elsevier, Oxford, 2006.
2. K.G. Bhattacharyya, S.S. Gupta Advances in Colloid and Interface Science. 140 (2008) 114 – 131.
3. V. B. Yadav, R. Gadi, S. Kalra, Journal of Environmental Management, 232 (2019) 803 – 817.
4. T.Schütz, S. Dolinská, P. Hudec, A. Mockovčiaková, I. Znamenáčková, International Journal of Mineral Processing. 150 (2016) 32 – 38.

Ag-AgCl Nanoparticles Fixation on Electrospun PVA Fibers: Technological Concept and Progress

Z. Vilamová¹, Z. Konvičková^{1,2}, P. Mikeš³, V. Holířová¹, P. Mančík⁴, E. Dobročka⁵, G. Kratošová¹, J. Seidlerová¹

¹Nanotechnology Centre, VŠB – Technical University of Ostrava, Czech Republic; ²ENET Centre, VŠB – Technical University of Ostrava, Czech Republic; ³Department of Chemistry, Faculty of Science, Humanities and Education, Technical University of Liberec, Czech Republic; ⁴IT4 Innovations, VŠB – Technical University of Ostrava, Czech Republic; ⁵Institute of Electrical Engineering, Slovak Academy of Sciences, Slovak Republic

Zuzana.Vilamova.st@vsb.cz

ABSTRACT

Polymer-metal based material with unique 3D structure was prepared through: (1) preparation of silver nanoparticles (Ag NPs) by phytosynthesis and (2) incorporation of these NPs in a fibrous membrane prepared by electrospinning. The NPs biosynthesis was performed in a pure environmental-friendly, easy, static, bottom-up regime using *Tilia* sp leachate. TEM and XRD depict the formation, stabilization and encapsulation of crystalline Ag NPs (14 ± 9 nm) in one simple step with low tendency to aggregate. We achieved successful incorporation in the uniform electrospun polyvinyl alcohol (PVA) fibers, and this confirms the possibility of its use in the biomedical field. Both SEM with EDX and TEM analysis determined fiber uniformity with the presence of Ag NPs.

Keywords: Biosynthesis, silver nanoparticles, nanofiber, electrospinning

INTRODUCTION

Biosynthesis of Ag NPs by bacteria, live plants, waste biomass and/or different plant extract types has been confirmed by many scientific teams. The most significant benefit of biosynthesis is synthesis and stabilization of NPs in the same time by organic compounds present in the biomass. Those NPs play a role in degradation of contaminants or can be used as antibacterial agents. Scientists have also focused on artificial dressings with active agents prepared by electrospinning. The electrospinning is a technique using a high voltage electrostatic field to charge the surface of liquid (e.g. polymer) solutions and this process leads to creation of solid fibrous web. These medicinal artificial dressings should meet the special criteria such as: (1) mechanically stable; (2) biodegradable and (3) provide an appropriate environment for tissue repair. They should fulfill the antibacterial properties. Those antibacterial electrospun nanofibers are usually produced by incorporating antibiotics, described silver NPs or other metallic and metal oxide NPs. In this study we have focused on the preparation of phytosynthesized Ag-AgCl NPs and their fixation into the PVA fibrous web¹.

EXPERIMENTAL STUDY

Ag-AgCl NPs were synthesized using leachate of flower-clusters from the *Tilia* sp. deciduous tree and initial AgNO_3 ($C = 0.01 \text{ mol.dm}^{-3}$) were chosen to obtain the colloid of Ag-AgCl NPs. Two 10 wt. % polymer solutions were prepared: (1) in DEMI water and (2) in Ag-AgCl colloid to obtain homogeneous liquid solution. Fiber samples were prepared by 4SPIN (Contipro, Czech Republic) using $\varnothing=0.8$ mm needle, static continual collector, 18 cm collector-emitter distance and

20 $\mu\text{l}/\text{min}$ fixed flow rate. Each solution was electrospun by different applying voltage and final fibrous samples were compared by different techniques.

RESULTS AND DISCUSSION

TEM and XRD analysis confirmed bi-phased Ag-AgCl NPs presence and these had spherical shape mostly. The image analysis determined average NP size at approximately 14 ± 9 nm. The Ag-AgCl NPs in the colloid formed “clusters” from the presence of organic components in the *Tilia* sp. leachate which formed stabilizing coating, but aggregation/agglomeration was not visible. Fibers from the pure PVA solution had the smallest diameters at 40 kV and 15 kV, while the blended PVA-Ag NP fibers were the largest. Herein, we chose two representative samples with 25 kV applied voltage. The PVA fiber web has 242 ± 33 nm average diameter and lacks a significant number of beads, and also was more heterogeneous than the PVA-Ag web with fiber average 221 ± 24 nm diameter.

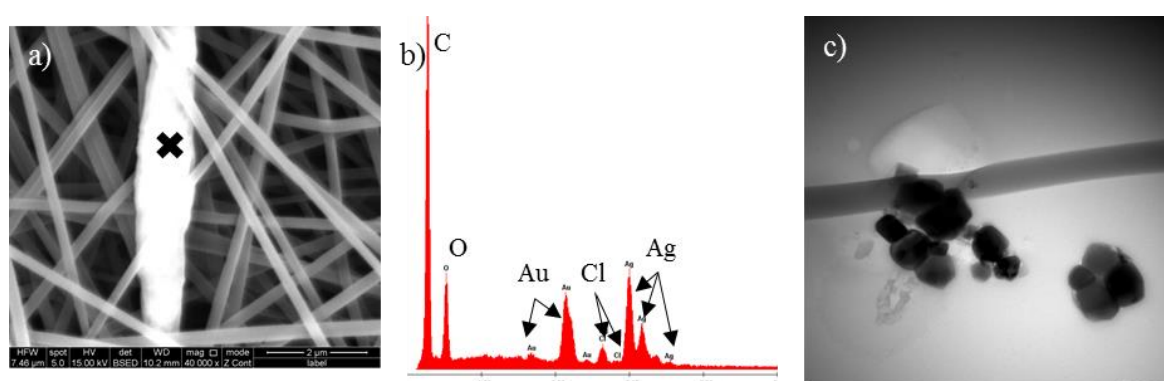


Fig. 1. Images of PVA-Ag fibrous web: a) SEM image of fibrous PVA web; b) EDX analysis confirmed a presence of Ag-AgCl compounds in fiber; c) TEM image of Ag-AgCl NPs and PVA fiber, scale bar 200 nm.

SEM and EDX analysis (Fig. 1) confirmed Ag-AgCl NPs presence in PVA nanofibers. The creation of random localized clusters was most likely due to application of the entire electrospinning process, and the location and amount of Ag-AgCl in the sample clusters was easier to identify when lower voltage was applied. TEM analysis a presence of NPs has confirmed too.

CONCLUSIONS

Bi-phased Ag-AgCl NPs have been successfully synthesized with average size 14 ± 9 nm. Both prepared polymers PVA and mixture of PVA-Ag were homogenous and spun with reproducible results. The average diameter of the PVA and mixture PVA-Ag fibers was repeatedly in the range 200 – 300 nm and Ag-AgCl NPs obviously influenced the ability of electrospinning process leading to homogenous webs without a large number of defects. We have found that NPs did not significantly disrupt the structure of PVA fibers, however Ag-AgCl NPs slightly aggregated during the electrospinning process and/or polymer solution preparation, which was mostly observed by SEM analysis.

Acknowledgement: Our work has been supported by the by the Ministry of Education, Youth and Sports of the Czech Republic under the Students' Grant Competition Project Nos. SP2018/50, SP2019/75. We especially appreciate the kindness of the PrimeCell Advanced Therapy Company for the use of its laboratory equipment in our nanofiber material preparation.

REFERENCES

1. Vilamová Z, Konvičková Z, Mikeš P, et al (2019) Ag-AgCl Nanoparticles Fixation on Electrospun PVA Fibers: Technological Concept and Progress - under review. Appl Nanosci

TOPIC 3

Nanotech for Energy

Chair: Tezel Oguz

Nanomaterials for energy storage

Nanotechnology for renewable energy harvesting and conversion

Hydrogen storage

Sustainability of materials recycling for energy



Invited lectures (IL):**Nanocomposite Ceramic Based Negative Electrodes for Li-ion Batteries**

H. Akbulut^{1,2}, M. Tokur^{1,2}, T. Çetinkaya^{1,2}

¹Sakarya University, Engineering Faculty, Department of Metallurgical & Materials Engineering, Esentepe Campus, 54187, Sakarya/Turkey; ²Sakarya University Research, Development and Application Center (SARGEM), Sakarya/Turkey

akbulut@sakarya.edu.tr

ABSTRACT

Ceramic based anodes (SiO_x, GeO, SnO₂, ZnO, Fe₂O₃ or more complex stoichiometry, etc.) have much higher Li storage capacity than the intercalation-type graphite anode that is currently used in Li-ion batteries (LIBs). However, the practical implementation of metal (M) and metal oxide (MO) anodes is still blocked due to three major problems [1]: poor cycle-life results from pulverization during the huge volumetric fluctuations (>300 %), drastic irreversible capacity loss and low coulombic efficiency, the solid electrolyte interphase (SEI) breaks as the nanostructure shrinks during delithiation [2]. The critical issue of fabricating high specific capacity, high rate capability, and long cycle life LIB device is the advanced nano architected design and flexible electrode materials with good mechanical deformations [3]. In order to prevent these challenges, most common and effective strategy to adopt nanoscale materials with various morphologies, including nanoparticles and, nanowires, nanotubes and hollow spheres. Compared to bulk active materials, such nanostructured ceramic based oxides, nitrides and carbides are able to accommodate elevated mechanical stress, resulting in prolonged cycling stability. Optimization of ceramic based electrodes can be achieved by incorporating nano structures with various conductive matrixes, such as graphene and, carbon nanotubes, and carbon and to form core-shell and yolk-shell nanocomposites. The introduction of such a carbon architectures with ceramic phases play a key role in alleviating the agglomeration of nano structured active materials [4]. In this review, we summarized the recent progresses on developments of ceramic based nanocarbon supported (CNT, CNF, Graphene etc.) negative electrodes for high performance Li-ion batteries. The synthesis techniques of the 1-D, 2-D and 3-D electrodes has been discussed for special hierarchical structures and free standing electrodes. The main research activities of Sakarya University electrochemical energy storage group has also summarized. The electrochemical performances of the ceramic based active materials and their nanocomposite structures were reviewed.

Keywords: Li-ion batteries, ceramic nanocomposite electrodes, nanocarbon, metal oxide

REFERENCES

1. Kang, Meng, Breger, Grey and Ceder, Science 311, 977 (2006).
2. Wu and Cui, Nano Today 7, 414 (2012).
3. Tokur, Algul, Ozcan, Cetinkaya, Uysal, Akbulut, Electrochimica Acta 216, 312 (2016).
4. Li, Tang, Kang, Zhang, Yang, Zhu, Zhang and Lee, Small 11, 1345 (2014)

One dimensional anodic nanostructures for energy applications

J. M. Macak^{1,2}

¹Center of Materials and Nanotechnologies, Faculty of Chemical Technology, University of Pardubice, Nam. Cs. Legii 565, 530 02 Pardubice, Czech Republic; ²Central European Institute of Technology, Brno University of Technology, Purkynova 123, 61200 Brno, Czech Republic

jan.macak@upce.cz

ABSTRACT

The self-organized 1D TiO₂ nanotubular layers have attracted considerable scientific and technological interest over the past two decades, all motivated by a great performance in the range of applications including photo-catalysis, solar cells, hydrogen generation and biomedical uses.^{1,2} The synthesis of these nanotubular layers has been carried out by a conventional electrochemical anodization of Ti sheet. Except the 1D character, these nanotubes possess unique features such as tunable dimensionality, structural flexibility, unidirectional electron transport through nanotube walls, chemical and mechanical stability and biocompatibility. One of the major application targets of TiO₂ nanotubes has been their utilization as scaffolds or templates for deposition of secondary materials towards new applications. For instance, tailoring the TiO₂ anode chromophore interface can increase the efficiency of the cells, such as DSSC³ and perovskite-based solar cells⁴. The enhancement can be achieved by increasing the interfacial surface area between the chromophore and the TiO₂ oxide in order to facilitate charge separation. Unlike randomly ordered mesoporous TiO₂ support, ordered nanostructures, such as self-organized TiO₂ nanotubes with high aspect ratio, offer the advantage of directed charge transport and controlled phase separation between donor and acceptor materials and thus they seem to be one of the most promising nanoscale solar hybrid technologies.⁵ Numerous techniques were utilized for this purpose, such as for example wet chemical and electrochemical routes or physical deposition techniques.⁶ However, recently it has been shown that the utilization of Atomic Layer Deposition (ALD) can extend the functional range of TiO₂ nanotubes by homogenous coatings or decoration of tube interiors by a secondary materials.⁶⁻¹⁴ ALD is the only technique of choice to coat in particular high-aspect ratio nanotube layers. Overall, the deposited coatings influence strongly photo-electrochemical properties of nanotube layers. The presentation will be focused in detail on TiO₂ nanotube layers of various aspect ratios coated by CdS and other chalcogenides using ALD. Experimental details and some very recent photo-electrochemical and structural characterization of a new type of heterostructured photo-chemical cells^{11,13,14} will be presented and discussed.

REFERENCES

1. J. M. Macak et al., *Curr. Opin. Solid State Mater. Sci.*, 1-2 (2007) 3-17.
2. K. Lee, A. Mazare, P. Schmuki, *Chem. Rev.*, 114 (2014) 9385-9454.
3. P. Roy et al., *Nanoscale*, 2 (2010) 45-59.
4. X. Gao et al., *Chem. Commun.*, 50 (2014) 6368-6371.
5. B. O'Regan and M. Grätzel, *Nature* 353 (1991) 737.
6. J. M. Macak, Chapter 3 in: D. Losic and A. Santos, *Electrochemically Engineered Nanoporous Structures*, Springer International Publishing, Switzerland, 2015.
7. H. Sopha et al., *Appl. Mater. Today*, 9 (2017) 104-110.
8. Q. Gui et al., *ACS Appl. Mater. Interfaces*, 6 (2014) 17053-17058.
9. Ghobadi et al., *Sci. Rep.*, 6 (2016) 30587.
10. S. Ng et al., *Adv. Eng. Mater.*, DOI: 10.1002/adem.201700589
11. M. Krbal et al., *Nanoscale*, 9 (2017) 7755-7759.
12. L. Assaud, et al., *ACS Appl. Mater. Interfaces*, 7 (2015) 24533-24542.
13. R. Zazpe et al., *Nanoscale*, 10 (2018) 16601-16612.
14. F. Dvorak et al., *Appl. Mater. Today*, 14 (2019) 1-20.

Oral presentations (OP):**Flexible anode materials and their protection**

D. Legut¹, H. Tian², Z. W. Seh³, K. Yan⁴, Z. Fu², P. Tang², Y. Lu⁵, R. F. Zhang², Y. Cui⁴, and Q. Zhang²

¹IT4Innovations & Nanotechnology Centre, VSB-Technical University, Czech Republic; ²School of Material Science and Engineering, Beihang University, Beijing, China; ³Institute of Materials Research and Engineering, Agency for Science, Technology and Research, Singapore; ⁴Department of Materials Science and Engineering, Stanford University, Stanford, California, USA; ⁵College of Chemical and Biological Engineering, Zhejiang University, Hangzhou, China

dominik.legut@vsb.cz

ABSTRACT

MXenes exhibit outstanding properties and therefore been considered as promising electrode material candidates. Taking 2D transition metal carbides (TMCs) as representatives, we systematically explored several influencing factors, including transition metal species, layer thickness, functional group, and strain on their mechanical properties (e.g., stiffness) and their electrochemical properties (e.g., ionic mobility). Considering potential charge-transfer polarization, we employed a charged electrode model to simulate ionic mobility and found that ionic mobility has a unique dependence on the surface atomic configuration influenced by bond length, valence electron number, functional groups, and strain. Under multiaxial loadings, electrical conductivity, high ionic mobility, low equilibrium voltage with good stability, excellent flexibility, and high theoretical capacity indicate that the bare 2D TMCs have potential to be ideal flexible anode materials, whereas the surface functionalization degrades the transport mobility and increases the voltage due to bonding between the nonmetals and Li.[1] In order to protect the rechargeable batteries based on lithium (sodium) metal anodes that are currently under increasing attention due to their high capacity and energy density, but exhibit drawbacks, such as low Coulombic efficiency and dendrites growth we investigate layered materials as protective films (PFs). Here we use first-principles calculations to determine the properties and feasibility of various 2D layered PFs. It is found that the introduction of defect, the increase in bond length, and the proximity effect by metal can accelerate the transfer of Li^+ (Na^+) ion and improve the ionic conductivity, but all of them make negative influences on the stiffness of materials [2].

Keywords: 2D materials, graphene, silicene, strength, strain, CI-NEB, diffusion, adsorption, Li-anode

Acknowledgments: This work was supported by CSF grant No. 17-27790S and Path to Exascale project No.CZ.02.1.01 /0.0/0.0 /16_013/0001791 and SGS grant No. SP2019/110.

REFERENCES

1. H. Zhang, Z. Fu, R. Zhang, Q. Zhang, H. Tian, D. Legut, T. C. Germann, Y. Guoa, S. Due, and J. S. Francisco Designing flexible 2D transition metal carbides with strain-controllable lithium storage, *Proc. Nat. Acad. USA* **114**, E11082-E11091 (2017).
2. H. Tian, Z. W. Seh, K. Yan, Z. Fu, P. Tang, Y. Lu, R. Zhang, D. Legut, Y. Cui, Q. Zhang, Theoretical Investigation of Two-Dimensional Layered Materials as Protective Films for Lithium and Sodium Metal Anodes, *Advan. Ene. Mat.* **7**, 1602528 (2017).

Li₄Ti₅O₁₂ spinel modified with carbon or oxide coatings as an advanced anode material for high-rate lithium-ion batteries

M. Michalska¹, J.-Y. Lin²

¹Łukasiewicz Research Network - Institute of Electronic Materials Technology, Wólczyńska 133, 01-919 Warsaw, Poland; ² Department of Chemical Engineering, Tatung University, No. 40, 3rd Section, Zhongshan North Road, Taipei 104, Taiwan

michalska.monika83@gmail.com

ABSTRACT

Lithium titanium oxide (Li₄Ti₅O₁₂, LTO) of spinel structure is recognized as a promising anode material for commercial high-rate lithium ion batteries as well as supercapacitors because of some unique characteristics in the comparison with carbon (graphitic) anode materials [1-3]. It shows excellent cyclability due to negligible volume change during intercalation/deintercalation reactions (so called “zero-strain” electrode material) [1-3]. Moreover, it has higher equilibrium potential, showing a voltage plateau at 1.55 V vs. Li/Li⁺. Nevertheless, the low electronic and ionic conductivity, which lead to poor rate capability, still limit its practical usage [1-3].

In our work we focus on the surface modification of LTO using carbon or titanium dioxide coatings. The structure, morphology and chemical compositions of the synthesized pristine and surface modified spinel LTO powders were characterized by several complementary techniques: X-ray powder diffraction (XRD), Raman spectroscopy, scanning, and transmission electron microscopy techniques. The electrochemical charge-discharge tests were investigated. The results of these measurements will be presented at the conference.

Keywords: Lithium titanium oxide, Li₄Ti₅O₁₂, anode material, lithium ion battery

Acknowledgments: This work is financially supported by The National Centre for Research and Development through the research project cooperation between National Centre for Research and Development (NCBR) and the Ministry of Science and Technology of Taiwan (MOST), contract no. PL-TW/IV/6/2017.

REFERENCES

1. M. Michalska, M. Krajewski, D. Ziolkowska, B. Hamankiewicz, M. Andrzejczuk, L. Lipinska, K. Korona, A. Czerwinski, Influence of milling time in solid-state synthesis on structure, morphology and electrochemical properties of Li₄Ti₅O₁₂ of spinel structure, *Powder Technology* 266 (2014) 372-377.
2. M. Michalska, D. A. Ziolkowska, M. Andrzejczuk, A. Krawczyńska, A. Roguska, A. Sikora, New synthesis route to decorate Li₄Ti₅O₁₂ grains with GO flakes, *Journal of Alloys and Compounds* 719 (2017) 210-217.
3. P. Dhaiveegan, H.-T. Peng, M. Michalska, Y. Xiao, J.-Y. Lin, C.-K. Hsieh, Investigation of carbon coating approach on electrochemical performance of Li₄Ti₅O₁₂/C composite anodes for high-rate lithium-ion batteries, *Journal of Solid State Electrochemistry* 22 (2018) 1851-1861.

Nanocatalysts for hydrolysis of Al and H₂O reaction: Efficient synthesis of graphite-derived thin layer with Al(OH)₃ based nanoparticles

S. Prabu, H.-W. Wang*

Department of Chemistry, Chung-Yuan Christian University, Zhongli, 320, Taiwan, R.O.C.

hongwen@cycu.edu.tw

ABSTRACT

Hydrogen generation is one of the best skills for understanding hydrogen expensive. In this current work, we recognized the high catalytic performance for hydrogen generation system using the G-Al(OH)₃ and its compounds (different amount of graphite doped Al(OH)₃) for catalyzing the hydrolysis of Al and H₂O system. These Al-based mixtures for hydrolysis process were synthesized through a simple solvothermal procedure. Synthesized catalysts characterization by using powder X-ray diffraction, field emission scanning electron microscopy (FESEM), and Brunauer–Emmett–Teller (BET) adsorption analysis showed G-Al(OH)₃ nanoparticles attached to the aluminum hydroxide surface. The results exhibit that small amounts of G-Al(OH)₃ added could significantly accelerate and enhance the hydrolysis reaction of Al and H₂O, releases 1360 mL g⁻¹ hydrogen in 20 mins (about 100% of the theoretical hydrogen generation yield) and the synthesized catalysts exhibit great cycle stability, which is a greatest significant achievement in this current work. Besides, different amount of with graphite doped Al(OH)₃ and without graphite are moreover demonstrated to show the different improvement on the hydrolysis reaction of Al and H₂O reaction.

Study of Clay-PEO system as application as solid electrolyte in Li-ion batteries

S. K. Sathish¹, B. Novosad², K. Chrobáček¹, G. Simha Martynková^{1,3}

¹Nanotechnology Centre, VSB-Technical University, Czech Republic; ²Faculty of Electrical Engineering and Computer Science, VŠB - Technical University of Ostrava, Czech Republic; ³IT4Innovations, VSB-Technical University, Czech Republic

sajjan.sathish.st@vsb.cz

ABSTRACT

The solid electrolytes are an eco-friendly and safer alternative to conventional organic electrolytes, that cannot be used in batteries over 60 °C, due to their low boiling temperature; the vapors that form beyond 80 °C can lead to an explosion. Composite polymer electrolyte a mixture of ceramic nanofiller and polymer electrolyte are known to be able to enhance mechanical or thermal stability as well as ionic conductivity of polymer electrolyte. In our work, we selected clays montmorillonite (MMT) and vermiculite (VMT) for solid electrolyte study. The clays were mixed with polyethylene oxide (PEO) using ball mill and temperature treatment for intercalation. The graphene oxide (GO) was added to improve mixture conductivity¹. Both the natural forms of the clay and the lithiated forms (Li-MMT/Li-VMT) with PEO/GO mixture were studied. X-ray diffraction analysis was used to confirm the intercalation of the materials after heat treatment. The high crystallinity of PEO provides low ionic conductivity by limiting the lithium ion transport; Fourier Transform Infrared Spectroscopy was used to identify the influence of the clay mixture on crystallinity of polymer. The electrical conductivity of nanocomposite was measured RLC meter. The structure, crystallinity and electrical conductivity of clay/polymer nanocomposites were investigated.

Keywords: Clay minerals, PEO, intercalation, solid electrolyte.

Acknowledgments: The National Programme of Sustainability (NPU II) project „IT4Innovations excellence in science - LQ1602“ and Ministry of Education, Youth and Sport of the Czech Republic SP2019/50 partially supported the research.

Towards high capacity rGO/MWCNT/ yolk-shell structured silicon composite anodes for li-ion batteries

U. Toçoğlu*, H. Akbulut

Sakarya University, Dept. of Metallurgy and Materials Engineering, Sakarya/TURKEY

utocoglu@sakarya.edu.tr

ABSTRACT

Currently, in commercial lithium ion batteries graphite is utilized as anode material with theoretical specific capacity of 372mAhg^{-1} . Graphite is widely used for secondary lithium ion batteries since it has stable capacity and chemical characteristics with reasonable production costs. However, besides being stable and cheap, low energy storage capacity makes graphite incompatible for next generation advanced battery system. Since the capacity of graphite is low for high energy density lithium ion battery system there are significant efforts for developing new anode materials capable of storing energy more efficiently. Silicon is the most promising one among the other candidate anode material since it has highest know theoretical capacity value of 4200mAhg^{-1} at elevated temperatures. In fact, at room temperature silicon is able to deliver 3570mAhg^{-1} specific capacity by formation of $\text{Li}_{15}\text{Si}_4$ amorphous phase. Despite of delivering remarkable capacity values, volume variations during electrochemical reactions with lithium, causes pulverization and quick capacity fading. Volume expansions leads strain induced fracture of silicon particles and eventually complete anode failures. In order to solve these problems we have developed free-standing binder free electrode architecture that consist yolk-shell silicon particles embedded between layers of graphene/MWCNT framework. Since graphene, MWCNT and silicon ratios are important factor for determining the performance enhancement in this composite anode structures we have carried out a comprehensive study for determining the effect of anode constituents on performance. There different MWCNT: graphene ratios were employed as 1:1, 1:2, 2:1 and for each MWCNT: graphene ratios, anodes were fabricated with three different silicon loading of 10, 20 and 30 %. In total nine different composite anodes were fabricated in order to determine the optimal silicon, MWCNT and graphene amounts. The morphological and phase characterization of electrodes were performed via X-Ray Diffraction analysis, RAMAN spectroscopy and scanning electron microscopy techniques. In the stage of electrochemical performance analysis galvanostatic charge/discharge, cyclic voltammetry and electrochemical impedance spectroscopy analyses were carried out.

Keywords: Silicon, Yolk-shell, Graphene, Lithium.

Poster presentations (PP):**Synthesis and electrochemical properties of $\text{LiNi}_{0.5}\text{Mn}_{1.5}\text{O}_4$ surface modified with NiO coating as a cathode material for lithium-ion batteries**

M. Michalska¹, J.-Y. Lin²

¹Lukasiewicz Research Network - Institute of Electronic Materials Technology, Wólczyńska 133, 01-919 Warsaw, Poland; ² Department of Chemical Engineering, Tatung University, No. 40, 3rd Section, Zhongshan North Road, Taipei 104, Taiwan

michalska.monika83@gmail.com

ABSTRACT

Lithium-ion batteries (LiBs) technology have drawn a lot of attention as a feasible solution for versatile energy storage devices with wide range of applications including consumer electronic, transportation, space applications and power generation where they are often combined with renewable energy generation systems. While exploring new anode and cathode materials, transition metal oxides (TMOs) nanomaterials with spinel structure have been seriously considered due to their several advantages: relatively high theoretical capacity, low cost, safety, environmental friendliness, and natural abundance. Lithium nickel manganese oxide ($\text{LiNi}_{0.5}\text{Mn}_{1.5}\text{O}_4$, LNMO) is one the promising candidates for next-generation cathode materials dedicated to lithium ion batteries used for electric vehicles and other high-energy density applications due to its high operating voltage ~ 4.7 V potential (vs. Li/Li^+), its good cycling performances (without Jahn-Teller effect related to the presence of Mn^{3+}), good thermal stability, low cost, and environmental friendliness. Nevertheless, the LNMO material still suffers from unsatisfied cycle life due to severe electrolyte decomposition at high voltage and metal dissolution in HF-contained LiPF_6 -based electrolytes. In order to resolve this complicated problem many approaches including metal doping, surface coating with metal, ceramic oxides to minimize the surface area of $\text{LiNi}_{0.5}\text{Mn}_{1.5}\text{O}_4$ contacting with the electrolyte have been proposed. Finally, it should to improve the electrochemical properties. During conference, we will present the modified sol-gel method to obtain lithium nickel manganese (LNMO) oxide modified with NiO coating. The crystal structure and morphology were characterized by X-ray powder diffraction (XRD), and scanning electron microscopy (SEM). The electrochemical performances were investigated with CR2032 coin-type cells with Li counter and working electrode made of LNMO with NiO coating. The electrochemical charge-discharge tests were also performed.

Keywords: Lithium nickel manganese oxide, $\text{LiNi}_{0.5}\text{Mn}_{1.5}\text{O}_4$, cathode material, lithium ion battery

Acknowledgments: This work is financially supported by The National Centre for Research and Development through the research project cooperation between National Centre for Research and Development (NCBR) and the Ministry of Science and Technology of Taiwan (MOST), contract no. PL-TW/IV/6/2017.

Nanocatalysts for hydrolysis of Al and H₂O reaction: Efficient synthesis of graphite-derived thin layer with Al(OH)₃ based nanoparticles

S. Prabu, H.-W. Wang*

Department of Chemistry, Chung-Yuan Christian University, Zhongli, 320, Taiwan, R.O.C.

hongwen@cycu.edu.tw

ABSTRACT

Hydrogen generation is one of the best skills for understanding hydrogen expensive. In this current work, we recognized the high catalytic performance for hydrogen generation system using the G-Al(OH)₃ and its compounds (different amount of graphite doped Al(OH)₃) for catalyzing the hydrolysis of Al and H₂O system. These Al-based mixtures for hydrolysis process were synthesized through a simple solvothermal procedure. Synthesized catalysts characterization by using powder X-ray diffraction, field emission scanning electron microscopy (FESEM), and Brunauer–Emmett–Teller (BET) adsorption analysis showed G-Al(OH)₃ nanoparticles attached to the aluminum hydroxide surface. The results exhibit that small amounts of G-Al(OH)₃ added could significantly accelerate and enhance the hydrolysis reaction of Al and H₂O, releases 1360 mL g⁻¹ hydrogen in 20 mins (about 100% of the theoretical hydrogen generation yield) and the synthesized catalysts exhibit great cycle stability, which is a greatest significant achievement in this current work. Besides, different amount of with graphite doped Al(OH)₃ and without graphite are moreover demonstrated to show the different improvement on the hydrolysis reaction of Al and H₂O reaction.

Fe(III) source-dependent properties of mechano/thermally synthesized LiFeSi₂O₆

O. Skurikhina¹, R. Tarasenko², V. Tkáč², M. Orendáč², M. Fabián¹, M. Senna³, V. Šepelák^{1,4}, E. Tóthová¹

¹Institute of Geotechnics, Slovak Academy of Sciences, Slovakia; ²Institute of Physics, Faculty of Science, P.J. Šafárik University, Slovakia; ³Department of Applied Chemistry, Faculty of Science and Technology, Keio University, Japan; ⁴Institute of Nanotechnology, Karlsruhe Institute of Technology, Germany

skurikhina@saske.sk

ABSTRACT

The combination of mechanochemical activation and subsequent thermal treatment was used for synthesis of lithium iron methasilicate (LiFeSi₂O₆), a material with potential application as cathode for Li-ion batteries. Different sources of Fe(III) were used for synthesis, namely α -Fe₂O₃ (hematite) or α -FeO(OH) (goethite). Although these two products have different colors, the formation of pure phase was confirmed by X-ray diffractometry. A SQUID magnetometer was used for study of magnetic properties of both products. Differences in magnetic properties of these materials have been found. It can be concluded that α -Fe₂O₃ used as precursor leads to formation of LiFeSi₂O₆ with better magnetic properties.

Keywords: mechanochemistry, pyroxene, SQUID

INTRODUCTION

Pyroxene family, which lithium iron methasilicate belongs to, has been drawn scientists' attention because of its various combinations of electric and magnetic properties.^{1, 2} There are studies that show possibility of using carbon composites based on $\text{LiFeSi}_2\text{O}_6$ as cathode for Li-ion batteries.^{3, 4} However the process of synthesis is too long and energy consuming. Combination of mechanochemical activation and thermal process can decrease the time and energy consumption. There was a study that stated that despite the same chemical composition and way of synthesis the nature of reactant can influence the final magnetic properties of a product.⁵ The suggested non-conventional method of preparing lithium iron methasilicate is a promising alternative for creating material with multiferroic properties.

EXPERIMENTAL/THEORETICAL STUDY

Mechanochemical activation of stoichiometric mixture of precursors Li_2O and SiO_2 with $\alpha\text{-Fe}_2\text{O}_3$ or $\alpha\text{-FeO(OH)}$ was held in a planetary ball mill Pulverisette 7 premium line (Fritsch, Germany) at 600 rpm in air atmosphere using WC balls (18 pcs, diameter 10 mm) and 80 cm³ chamber. The total amount of powdered mixture was 4 g, ball to powder ratio was 33:1. Subsequent thermal treatment has been performed in a Muffle furnace which was heated from room temperature up to 1273 K and then cooled back to room temperature in air atmosphere. XRD data were collected over an angular range from 10° to 80° with step of 0.030° using a Bruker D8 Advance diffractometer. Study of temperature dependence of magnetic susceptibility was performed in two modes: Zero-field cooling (ZFC) and field cooling (FC) using a commercial Quantum Design SQUID magnetometer.

RESULTS AND DISCUSSION

The XRD patterns (not shown) of mechano/thermally synthesised materials starting with different iron sources consist of the same phase which correspond to the pattern of pyroxene $\text{LiFeSi}_2\text{O}_6$ (JCPDS PDF 71- 1064). Figure 1 shows the data obtained from the SQUID magnetometer for both materials. As it can be seen from Fig. 1(a), the material which has been synthesized using $\alpha\text{-Fe}_2\text{O}_3$ as iron source has higher magnetic susceptibility. Both products that have been synthesized have the T_N (Neel temperature) at around 20 K.

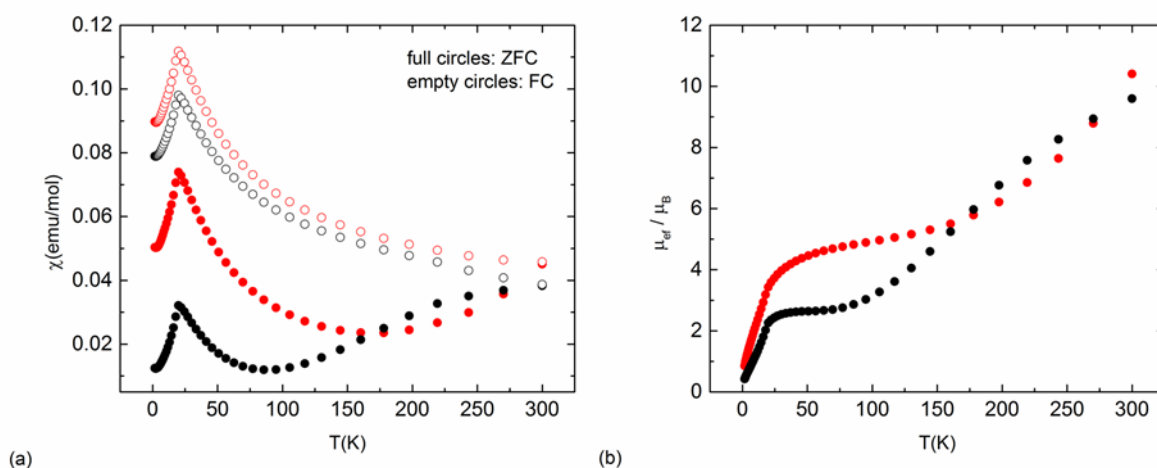


Fig. 1 (a) temperature dependence of magnetic susceptibility and (b) temperature dependence of effective magnetic moment for mechano/thermally synthesized $\text{LiFeSi}_2\text{O}_6$ using $\alpha\text{-Fe}_2\text{O}_3$ (red) or $\alpha\text{-FeO(OH)}$ (black) as Fe(III) source.

Fig. 1(b) shows temperature dependence of effective magnetic moment and there is a notable difference between them.

CONCLUSION

The mechano/thermal synthesis is the more effective way of preparing $\text{LiFeSi}_2\text{O}_6$ in terms of saving time and energy. Using different sources of Fe(III) brings out differences in magnetic properties of the final product. These results drive us to conclusion about possible existence of differences in electrochemical properties of lithium iron methasilicate materials which is expected to be verified in the future.

Acknowledgments: The present work is supported by the project of Slovak Grant Agency VEGA (2/0175/17, 1/0255/19). V.Šepelak acknowledges the support by the Deutsche Forschungsgemeinschaft (project SE 1407/4).

REFERENCES

1. Jodlauk, S., Becker, P., Mydosh, J., Khomskii, D., Lorenz, T., Streltsov, S., Hezel, D. and Bohatý, L. (2007). Pyroxenes: a new class of multiferroics. *Journal of Physics: Condensed Matter*, 19 (43), p.432201.
2. Redhammer, G., Roth, G., Treutmann, W., Hoelzel, M., Paulus, W., André, G., Pietzonka, C. and Amthauer, G. (2009). The magnetic structure of clinopyroxene-type $\text{LiFeGe}_2\text{O}_6$ and revised data on multiferroic $\text{LiFeSi}_2\text{O}_6$. *Journal of Solid State Chemistry*, 182(9), pp.2374-2384.
3. Ishida, N., Sakatsume, K., Kitamura, N., Idemoto Y. (2017). Improvement of electrochemical property of pyroxene type $\text{LiFeSi}_2\text{O}_6$ and crystal-structure analysis. *Journal of the Ceramic Society of Japan*, 125 (4), pp.281-286.
4. Zhou, S., King, G., Scanlon, D., Sougrati, M. and Melot, B. (2014). Low Temperature Preparation and Electrochemical Properties of $\text{LiFeSi}_2\text{O}_6$. *Journal of The Electrochemical Society*, 161(10), pp.A1642-A1647.
5. Tóthová, E., Senna, M., Yermakov, A., Kováč, J., Dutková, E., Hegedüs, M., Kaňuchová, M., Baláž, M., Bujňáková, Z., Briančin, J. and Makreski, P. (2019). Zn source-dependent magnetic properties of undoped ZnO nanoparticles from mechanochemically derived hydrozincite. *Journal of Alloys and Compounds*, 787, pp.1249-1259.

New acetylene and pyridine derivatives as monomers for conductive polymer brushes fabrication

A. J. Wójcik¹, M. Słowikowska¹, K. Wolski¹, S. Zapotoczny¹

¹Faculty of Chemistry, Jagiellonian University in Kraków, Poland

artur.wojcik@doctoral.uj.edu.pl

ABSTRACT

Taking an advantage of renewable energy sources, like e.g. sun, would play a key role in the development of present and future human civilizations. The construction of efficient, inexpensive and eco-friendly photovoltaic solar cells remains a subject of interest of many scientists around the world. In order to assure an effective, directional and fully-controlled transport of electrons or ions inside the above-mentioned systems, materials composed of conductive polymer nanobrushes, especially with a ladder-like structure, could be successfully used. However, their fabrication, the structure and the synthetics procedures of monomers serving as building blocks for their production have to be optimized.

In response to these challenges, we present here the synthetic routes to bifunctional pyridine- and acetylene-based monomers designed for production of conductive polymer nanobrushes.

The developed and/or optimized procedures enable formation of pure compounds with satisfying yields.

Furthermore, we present here preliminary results concerning fabrication of nanobrushes from the synthesized monomers. The chemical structure and topography of the obtained materials were characterized by means of atomic force microscopy (AFM), IR and UV-VIS-NIR spectroscopy.

Keywords: Conductive polymer brushes, pyridine- and acetylene-based monomers, ST-SIP polymerization.

INTRODUCTION

Renewable sources, like sun, wind and thermal spring, play an important role in an energy mix of many countries from around the world. An acquisition of sun energy, especially by individual households, companies or “things”, becomes more and more popular. However, the construction of efficient, inexpensive and eco-friendly solar cells remains a demanding task which has to be solved in context of commercial applications. In order to assure an effective and fully-controlled transport of charge carriers inside the mentioned systems, polymer materials, like e.g. conductive polymer nanobrushes with a ladder-like architecture, could be successfully used.¹ Unfortunately, their fabrication procedure, as well as the structure and the syntheses of monomers serving as building blocks for their construction should be still optimized.

In response to these challenges we present here the synthetic routes to bifunctional pyridine- and acetylene-based monomers, designed for production of conductive polymer nanobrushes. The developed and/or optimized procedures enabled formation of pure compounds with satisfying yields.

Apart from that, we present here preliminary results concerning fabrication of nanobrushes by means of self-templating surface-initiated polymerization (ST-SIP) of the obtained monomers.

EXPERIMENTAL STUDY

In order to obtain the desired structures we carried out the following types of reactions: nucleophilic substitution, Sonogashira coupling etc. Our products were fully characterized by means of IR spectroscopy, ¹H and ¹³C NMR spectroscopy, UV-Vis spectroscopy, elemental analysis.

Polymer nanobrushes were fabricated by ST-SIP method and characterized by means of IR-spectroscopy, atomic force microscopy etc.

RESULTS AND DISCUSSION

We have obtained and characterized among others compounds: 2-[2-(trimethylsilyl)ethynyl]pyridin-5-yl methacrylate, 5-[2-(trimethylsilyl)ethynyl]pyridin-2-yl methacrylate, 3-(trimethylsilyl)prop-2-ynyl methacrylate, 5-(trimethylsilyl)pent-4-ynyl methacrylate. These substances were synthesized with satisfying yields as really pure compounds and used as building blocks for fabrication of polymer nanobrushes.

CONCLUSION

Two new acetylene- and pyridine-based monomers were successfully synthesized with satisfying yields and purities. To the best of our knowledge such syntheses have not been described before in the literature. We also have optimized synthetic procedure of other known monomers. Apart from that, we have proved that our new compound – 2-[2-(trimethylsilyl)ethynyl]pyridin-5-yl methacrylate – could be successfully used to obtain polymer nanobrushes.

Acknowledgments: The authors would like to acknowledge TEAM project (2016-1/9) financed by the Foundation for Polish Science (Smart Growth Operational Programme 2014-2020) for the financial support.

REFERENCES

1. K. Wolski, M. Szuwarzyński, S. Zapotoczny, Chem. Sci. 6 (2015) 1754–1760.

TOPIC 4

Nanotech for Medicine and Pharmacy

Chair: Josef Jampílek

Nanopharmacology and targeted drug delivery
Biocompatible and biodegradable nanomaterials
Nanotoxicology



Invited lecture (IL):

Amphiphilic hyper-branched co-polymer nanoparticles for the controlled delivery of novel anti-tumor agents

Q. Miao^{1,2}, D. Xu^{1,2}, Z. Wang², L. Xu², T. Wang¹, Y. Wu¹, D. B. Lovejoy³, D. S. Kalinowski³, G. Nie¹, Y. Zhao^{1,4}, D. R. Richardson³

¹CAS Key Laboratory for Biological Effects of Nanomaterials & Nanosafety, National Center for Nanoscience and Technology of China, Beijing, China; ²Key Laboratory for Molecular Enzymology and Engineering, The Ministry of Education, Jilin University, Changchun, China; ³Department of Pathology and Bosch Institute, University of Sydney, Sydney, New South Wales 2006, Australia; ⁴CAS Key Laboratory for Biological Effects of Nanomaterials & Nanosafety, Institute of High Energy Physics, Chinese Academy of Sciences, Beijing, China

d.richardson@med.usyd.edu.au

INTRODUCTION

In this investigation, we have designed and synthesized an amphiphilic co-polymer with hyper-branched poly(amine-ester) and polylactide (HPAE-co-PLA) to generate nanoparticles (NPs).¹

Keywords: nanoparticles, anti-tumor agents, Bp4eT, lysosomes.

EXPERIMENTAL

These NPs have been used to encapsulate a highly active hydrophobic anti-tumor agent, 2-benzoylpyridine 4-ethyl-3-thiosemicarbazone (Bp4eT). Encapsulation in NPs was done in an effort to increase the anti-tumor activity of this agent by facilitating its delivery to tumor cells. We have also examined and optimized the formulation parameters of the NPs that alter their drug-loading capacity and their physical, chemical and biological properties.

RESULTS AND DISCUSSION

The resulting NPs exhibited high Bp4eT-loading capacity and substantial stability in aqueous solution. In vitro drug release studies demonstrated a controlled drug release profile with increased release at acidic pH. Anti-tumor proliferation assays showed that both free drug and drug-encapsulated NPs markedly inhibited tumor cell proliferation in a time- and concentration-dependent manner. Direct microscopic observation revealed that the fluorescent NPs were taken up by cells and localized, in part, in organelles consistent with lysosomes.

CONCLUSION

These results demonstrate a feasible application of the amphiphilic hyper-branched co-polymer, HPAE-co-PLA, as nanocarriers for intracellular delivery of potent anti-tumor agents.

Acknowledgements: D.R.R. thanks the National Health and Medical Research Council of Australia (NHMRC) for Project Grants and a Senior Principal Research Fellowship.

REFERENCES

1. Q. Miao, D. Xu, Z. Wang, L. Xu, T. Wang, Y. Wu, D.B. Lovejoy, D.S. Kalinowski, D.R. Richardson, G. Nie and Y. Zhao, *Biomaterials* 31:7 (2010) 364-7375.

Oral presentations (OP):**Antimicrobial Silicate Nanomaterial with High Specific Surface Area**

J. Bednář^{1,2}, P. Mančík¹, L. Svoboda¹, V. Foldyna^{2,3}, R. Dvorský^{1,2}

¹IT4-Innovations, VŠB-Technical University of Ostrava; ²Nanotechnology Centre, VŠB-Technical University of Ostrava; ³Institute of Geonics of the Czech Academy of Science, Department of Material Disintegration, Czech Republic

jiri.bednar@vsb.cz

ABSTRACT

In this work, we present nanocomposite with antimicrobial properties, based on silver nanoparticles nucleated in the general silicate nanostructure $\text{Si}_x\text{O}_y\text{Zn}_z$ with high specific surface area. The silicate nanostructure was prepared by gelation of sodium water glass that was very quickly added to vigorously stirred water solution of zinc acetate and homogenized by sonification. In following precipitation reaction, a fine silicate net nanostructure $\text{Si}_x\text{O}_y\text{Zn}_z$ with zinc content up to 30 wt% is created. Its morphology is similar to silicagel and the specific surface area of this material reaches values about $250 \text{ m}^2/\text{g}$. The resulting silicate net nanostructure was then four-times washed by demineralized water, rapidly frozen and subjected to vacuum-freeze drying. The dried material was then put into the aqueous solution of AgNO_3 ($c = 0.5 \text{ mol/dm}^3$) and homogenized by stirring for 20 minutes, so the molecules of AgNO_3 could sufficiently fill pores of nanostructure. After that, the vigorously stirred dispersion was exposed to 200 nm UV light irradiation for 100 minutes. The photolysis of AgNO_3 in limited volumes within the silicate net caused nucleation and growth of Ag nanoparticles that have high surface curvature, which increases the effectiveness of dissociation of silver ions into water environment. For this reason and due to the additional presence of zinc in the nanocomposite, the prepared material exhibits antimicrobial activity, that was successfully tested on *Escherichia coli* CCM3988, *Pseudomonas aeruginosa*, *Streptococcus salivarius* CCM4046, *Staphylococcus aureus* CCM4223 and *Candida albicans* CCM8186. The minimal inhibition concentration was found for all strains in the range of $2.81 \text{ mg/cm}^3 - 22.5 \text{ mg/cm}^3$.

Keywords: antimicrobial, zinc silicate, silver nanoparticles, nanomaterial

Nanomaterials for management of toxigenic fungi

J. Jampilek^{1,2}

¹Division of Biologically Active Complexes and Molecular Magnets, Regional Centre of Advanced Technologies and Materials, Faculty of Science, Palacky University Olomouc, Czech Republic; ²Department of Analytical Chemistry, Faculty of Natural Sciences, Comenius University, Bratislava, Slovakia

josef.jampilek@gmail.com

ABSTRACT

Toxigenic fungi capable of producing mycotoxins (e.g., aflatoxins, zearalenone, ochratoxin, patulin, etc.), which attack cereals, legumes, fruits, vegetables, etc., represent a significant problem worldwide due to notable yield losses and possible contamination of food and feed by mycotoxins. This contribution summarizes recent findings related to the effects of nanoscale fungicides on the growth and mycotoxin production of toxigenic fungi, with the main focus on *Aspergillus* sp.,

Fusarium sp., *Alternaria* sp. and *Penicillium* sp. Attention is devoted to effective fungicidal nanoformulations of encapsulated essential oils, metal-based (Ag, Au, Cu, Zn, Ni, Fe, TiO₂) and carbon-based nanoparticles as well as to nanoformulations of encapsulated organic fungicides and their mechanism of action towards toxigenic fungi. The benefits of the application of nanoscale fungicides in the field at preventing yield losses and in postharvest management are discussed.

Keywords: fungi, mycotoxins, nanoparticles, nanomaterials

INTRODUCTION

Mycotoxins represent a significant health risk for both humans and animals.¹ They are produced by some fungi and belong to very serious food and feed contaminants. Mycotoxin-producing fungi can grow in fruits, vegetables, cereals, legumes, nuts, etc., and the occurrence of these fungi is increasingly widespread due to changing environmental conditions; thus, they cause notable yield losses.² Mycotoxins, such as aflatoxins, deoxynivalenol, fumonisin B1, ochratoxin, patulin, zearalenone and candidalysin, are dangerous to health causing fatal damage of the body after prolonged exposure. Mycotoxins enter the dietary system by direct contamination, when the food or feed becomes infected with a toxigenic fungus with subsequent toxin formation, or by indirect contamination, when an ingredient of a process has previously become contaminated with a toxin-producing fungus, the fungus was not killed/removed during processing and thus mycotoxins that are generally quite resistant to most forms of food and feed processing remain in the final product.³

RESULTS AND DISCUSSION

A wide spectrum of chemical compounds is used as antifungals/fungicides.^{4,5} As potent antifungal agents, various nanoformulations started being used more and more frequently;^{6,7} thus, the main objective of this contribution is to summarize findings related to nanosystems based on organic polymeric and inorganic matrices or hybrid materials as effective antifungal agents. Attention is devoted to fungicidal nanocomposites effective especially against *Aspergillus* sp., *Fusarium* sp., *Alternaria* sp., *Penicillium* sp. and *Candida albicans*.

CONCLUSION

The benefits of the application of fungicide nanomaterials, such as essential oils or metal nanoparticles, in the field for the prevention of yield loss and in postharvest management are indisputable. It is very important to apply proper fungicides combating fungi already in the field, because the mycotoxins are on average more than 200-fold more toxic than such fungicides having short half-life.

Acknowledgments: This study was supported by the Slovak Research and Development Agency (Grant No. APVV-17-0373) and by the Ministry of Education of the Czech Republic (LO1305).

REFERENCES

1. A. Alshannaq, J.H. Yu, Int. J. Environ. Res. Public Health 14 (2017) E632.
2. H.J. Van der Fels-Klerx, C. Liu, P. Battilani, World Mycotoxin J. 9 (2016) 717–726.
3. D. Milicevic, I. Nastasijevic, Z. Petrovic, J. Environ. Sci. Health C 34 (2016) 293–319.
4. J. Jampilek, Expert Opin. Drug Dis. 11 (2016) 1–9.
5. FRAC Code List[©] 2019: Fungal control agents sorted by cross resistance pattern and mode of action, Croplife International. Brussels, 2019.
6. J. Jampilek, K. Kralova, in: A. Fica, A.M. Grumezescu (Eds.), Nanostructures for Antimicrobial Therapy, Elsevier, Amsterdam, 2017, pp. 23–54.

7. J. Jampilek, K. Kralova, in: K. Abd-Elsalam, R. Prasad (Eds.), *Nanobiotechnology Applications in Plant Protection*, Springer, Cham, 2018, 189–246.

Polymeric nanocomposites as a prevention of biofilm formation

D. Lazecká¹, S. Holešová¹, G. S. Martynková^{1,2}

¹Nanotechnology Centre, VSB-Technical University, Czech Republic; ²IT4Innovations, VSB-Technical University, Czech Republic

diana.klushina.st@vsb.cz

ABSTRACT

Polymeric stents for patients with a weak health must be improved due to the stent life-time inside the body - up to three months - then it is replaced within the repeated surgery. Such short life-time often occurs because of biofilm formation on the stent, which therefore complicates the flow of fluids through the stent. We develop new polymeric nanocomposite coatings, which can prevent the biofilm formation and prolong the life-time of the stent.

The focus of the research was on biofilm formation on polymeric nanocomposites and their properties in simulated inside-the-body conditions (in our case - gastric fluid). Three polymeric matrix were selected - polyvinyl acetate, polyvinyl alcohol, polyethylene oxide - with five different antimicrobial compounds and three types of clay. Prepared samples were tested on three main bacterial cultures - E.coli, S.aureus, S47 (enterococcus). The obtained results show the combinations in the nanocomposite which are more likely to survive the human body conditions.

Keywords: stent, polymeric nanocomposite, biofilm, antimicrobials.

Acknowledgments: The National Programme of Sustainability (NPU II) project IT4Innovations excellence in science - LQ1602 and Ministry of Education, Youth and Sport of the Czech Republic SP2019/50 partially supported the research.

The influence of technical procedure on the hydrodynamic diameter of conjugates of lamivudine with biodegradable poly-ε-caprolactone microspheres for controlled drug delivery via cellular uptake

W. Musiał¹, T. Urbaniak¹

¹Department of Physical Chemistry, Faculty of Pharmacy with Division of Laboratory Diagnostics, Wrocław Medical University, Poland

witold.musial@umed.wroc.pl

ABSTRACT

One of the critical features of submicron drug delivery systems is particle size - parameter determining efficiency of cellular uptake, membrane crossing and tissue penetration. The main path of parenterally administered particle clearance is size-dependent phagocytosis by monocyte-derived cells. Recent findings confirmed their contribution in fibrotic diseases and obesity development. Capacity for phagocytosis exhibited by macrophages may be exploited as drug delivery strategy in macrophage-linked diseases. Properly designed polymeric microparticles with drug fixed to carrier may serve as targeted drug delivery system. The aim of presented study was to investigate influence

of preparation parameters on particle size in solvent evaporation method. In order to ensure drug release after cellular uptake, model drug lamivudine was covalently conjugated to polymeric chains. Conjugate was utilized as material for multiple particle preparations via solvent evaporation technique. Following important parameters of emulsification process were investigated: homogenization speed, homogenization time, phase ratio, conjugate concentration, surfactant type and concentration. Particle diameter and polydispersity index were measured via dynamic light scattering, morphology of selected particle batches was investigated with scanning electron microscopy. Homogenization speed, time and surfactant concentration were identified as crucial parameters enabling control of particle diameter.

Keywords: phagocytosis, targeted drug delivery, particle size control, solvent evaporation method

INTRODUCTION

In recent decade, number of research groups focused their attention on contribution of monocyte derived immune cells to various diseases including obesity, fibrosis and microbial infections¹. Their exceptional capacity to phagocyte foreign bodies is usually considered as unwanted particle clearance path. Nonetheless, it can be exploited as drug delivery strategy. Cellular uptake, membrane crossing, tissue penetration are size-dependent phenomena², therefore particle diameter is crucial parameter considered during submicron drug delivery system design. In case of drug delivery to phagocytic cells, drug release should be possibly delayed up to the moment of particle internalization. Covalent bonding of drug molecule to the polymer matrix is one of approaches ensuring drug release after cellular uptake. Drug tagged polymers may preserve physical properties of non-modified polymers, and can be formulated as particle-based drug delivery systems. Presented approach ensures uniform drug distribution and drug loading depending slightly on particle preparation procedure. In context of macrophage targeted drug delivery, particle diameter should be in a range preferred by phagocytes, determined i.a. by cell membrane curvature³. Employed targeting strategy varies according to aimed macrophage subpopulation, and may require different diameter allowing blood-brain barrier crossing, possibility of deep alveolar inhalation or accumulation in particular tissue. Consequently, control of particle size during preparation procedure is a factor of crucial importance. In presented study, influence of preparation parameters on lamivudine and poly- ϵ -caprolactone conjugate (LV-PCL) particle diameter obtained via solvent evaporation technique (SET) was investigated. Evaluated particles may be a potential targeted drug delivery system aiming HIV infected macrophages.

EXPERIMENTAL STUDY

Drug tagged polymer was prepared via bulk ring opening polymerization of ϵ -caprolactone initiated by model drug lamivudine, catalyzed by tin 2-ethylhexanoate. Reaction was conducted in 130°C in dry nitrogen atmosphere for 5 hours. Polymer – drug covalent bonding was confirmed with ESI-ToF mass spectrometry, polymeric structure and molecular weight were evaluated with HNMR and GPC methods. Conjugate was utilized in o/w SET in order to prepare submicron particles. Emulsion was obtained by homogenization of conjugate solution in dichloromethane with aqueous surfactant solution. Different homogenization parameters, surfactant types, concentrations and oil/water phase ratios were employed in order to obtain various size of particles. Further the intermediates were stirred in room temperature to evaporate oil phase. Particle hydrodynamic diameter was investigated via DLS measurements, morphology of selected batches was investigated using SEM.

RESULTS AND DISCUSSION

Mass spectra of obtained product exhibited distributions of peaks with peak sets separated from each other by 114 Da which is equal to molecular weight of PCL monomer unit. Isotopic distribution of peaks in the set with highest intensities matched to distribution simulated by software for positively charged formula of LV-PCL conjugate with sodium adduct. Number average molar mass of product obtained with GPC, corrected with Mark-Houwink equation parameter was equal 3997 Da, which is close to values derived from HNMR spectra and calculated from reactant ratio. Particles obtained via SET had diameters ranging from 0.2 to 2.3 μm with varying polydispersity index. SEM micrographs confirmed formation of spherical structures with smooth surface. Among investigated surfactants, preparation with polyvinyl alcohol (PVA) resulted in smallest particles with most narrow polydispersity index. Exponential decrease in hydrodynamic diameter was observed with increasing homogenization speed and PVA concentration. In line with expectations, higher amount of stabilizer was able to orient on larger interphase surface, and hence form stable structures with lower hydrodynamic diameters. Smaller particles were obtained with higher homogenization speeds supposedly due to increased shear stress at faster rotation speeds, which led to a larger tangential stress, and finally resulted in formation of smaller emulsion droplets⁴. Linear decrease of diameter with increasing homogenization time up to 7 minutes was observed, however further homogenization time extension did not result in diameter decrease. In employed homogenizer type, droplet breakup takes place mostly in region close to stator. Presumably, oil phase needs sufficient number of flow cycles in the region between the rotor and stator, to achieve minimal diameter dictated by other homogenization parameters⁵.

CONCLUSION

Preparation of particles with diameters in range from 0.2 to 2.3 μm from poly- ϵ -caprolactone conjugated with lamivudine is hereby reported. Among evaluated preparation parameters, the homogenization speed, the time and the surfactant concentration were identified as crucial factors influencing hydrodynamic diameter of particle. Obtained results may be helpful during design of size-dependent sub-micron drug delivery systems.

Acknowledgments: Research was funded by Wroclaw Medical University Young Scientist Project, STM.D060.16.032.

REFERENCES

1. S. Bashir, Y. Sharma, A. Elahi, F. Khan, *Inflamm. Res.*, 65 (2016) 1–11.
2. S. E. Langille, *PDA J. Pharm. Sci. Technol.* 67 (2013) 186–200.
3. J. Champion, A. Walker, S. Mitragotri, *Pharm. Res.* 25 (2008) 1815–1821.
4. V. Cristini, Y. Renardy, *Copyr. c Tech Sci. Press FDMP 2* (2006) 77–93.
5. A. Utomo, M. Baker, A. W. Pacek, *Chem. Eng. Res. Des.* 87 (2009) 533–542.

Graphenic materials for biomedical applications

D. Plachá

Nanotechnology Centre, VSB-Technical University of Ostrava, Czech Republic

daniela.placha@vsb.cz

ABSTRACT

Graphene family nanomaterials are based on planar sheets of sp^2 hybridized carbons. The most widely studied representatives are graphene, graphene oxide, and reduced graphene oxide together with many functionalized graphenic materials. Due to their excellent physicochemical properties many applications have been explored so far among them biomedical technologies such as drug/gene/protein delivery, tissue engineering bio-imaging and biosensing, phototherapy, cellular growth and differentiation, cancer or disease detection and therapeutics. Interesting results were achieved also in preparations of nanocomposite materials with antimicrobial properties. This presentation is focused on summarizing temporary research in the field of biomedical applications of graphenic materials including their biocompatibility and toxicity. The future directions and perspectives will be also presented.

Keywords: Graphene, graphene oxide, functionalized graphenic material, biomedicine

Acknowledgments: This work is supported by projects SP2019/23 and CZ.02.1.01/0.0/0.0/17_049/0008441.

The water-soluble [60]fullerene derivatives for anti-cancer studies

M. Serda^{1,4}, M. J. Ware², J. M. Newton², M. Krzykawska-Serda³, K. Malarz¹, A. Mrozek-Wilczkiewicz¹, R. Musioł¹, S. J. Corr², S. A. Curley², Lon J. Wilson⁴

¹University of Silesia in Katowice, Poland; ²Baylor College of Medicine, USA; ³Jagiellonian University, Poland; ⁴Rice University, USA

maciej.serda@us.edu.pl

ABSTRACT

Glycoconjugated C_{60} derivatives are of particular interest as potential cancer targeting agents, due to an upregulated metabolic glucose demand, especially in the case of pancreatic adenocarcinoma and its dense stroma, which is known to be driven by a subset of pancreatic stellate cells. Herein, we have described the synthesis and biological characterization of a glucosamine C_{60} derivatives GF1 and GF2. Synthesized fullerene derivatives predominantly accumulate in the nucleus of pancreatic stellate cells; they are inherently nontoxic up to concentrations of 1 mg/ml; and photoactive when illuminated with blue and green light, allowing its use as a photodynamic therapy agents. Moreover, we have identified buckyballs as a novel class of non-receptor Src kinases inhibitors, interesting targets for the pancreatic cancer treatment.

Keywords: nanomedicine; [60]fullerene; cancer nanotechnology; pancreatic cancer

INTRODUCTION

We have previously shown that C_{60} derivatives can be used as convenient scaffolds for anticancer therapeutic drug delivery, and that such agents preferentially localize in both the intracellular nuclear pore complex and tumor vasculature¹. Nanomedical strategies which include metallofullerenol-based ($Gd@C_{82}(OH)_{22}$) inhibitors of matrix metalloproteinases (MMPs), photothermally active nanoparticles, and several nanodelivery systems are also being presented in attempts to improve survival in pancreatic cancer patients. In addition, glycoconjugated [60]fullerenes have been investigated for enhanced cancer-targeting properties. This is because cancer cells have an increased demand for glucose, which is then metabolized at a higher rate in order to generate the energy that is necessary for many features of cancer cell proliferation and tumorigenesis. Additionally, the family of glucose transporter membrane proteins (GLUTs) are overexpressed in several cancers including pancreatic cancer, making them an attractive molecular target for novel nanotherapeutics.

RESULTS AND DISCUSSION

We optimized and applied nucleophilic cyclopropanation reactions (Bingel reactions) as an efficient method for obtaining the glycofullerenes in moderate yields². Acetate protecting groups were used to block all glucosamine hydroxyl groups during the cyclopropanation reactions. Interestingly, we have investigated whether [60]fullerene derivatives can have a cytotoxic effect upon PSCs when illuminated with LED blue and green light the cytotoxic mechanism of which is hypothesized to be from ROS generation. The phototoxicity studies of glycofullerenes exhibit a strong photodynamic cytotoxic effect for PSCs after blue (Em 470 nm) and green (Em 530 nm) LED treatment. A similar but slight reduced effect was also observed for PANC-1 cells. This could be due PANC-1 cells having elevated heat shock protein (HSP) and enzymes to deal with ROS (e.g. due to different redox potentials in tumors and cancer cells).

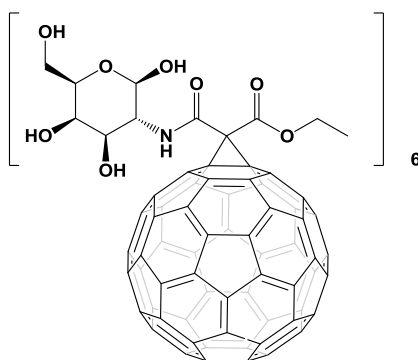


Fig. 1 The chemical structure of glycofullerene **GF2**

CONCLUSION

The PSCs are a subset of cells involved with the establishment of dense stroma regions in cases of advanced pancreatic adenocarcinoma. As such, new methods to target and treat PSCs are needed. Our results show predominant cellular nuclear internalization of the [60]fullerene derivatives. In addition, the glycofullerenes are inherently nontoxic up to concentrations of 1 mg/ml, and displays strong photodynamic cytotoxic behavior, when illuminated with both blue and green light.

Acknowledgments: Dr Maciej Serda and Dr Katarzyna Malarz thank National Science Center (Poland) for the support (SONATA UMO-2016/23/D/NZ7/00912 and PRELUDIUM 2016/23/N/NZ7/00351 grants).

REFERENCES

1. Lapin, N. A.; Krzykawska-Serda, M.; Dilliard, S.; Mackeyev, Y.; Serda, M.; Wilson, L. J.; Curley, S. A.; Corr, S. J. *Journal of Controlled Release* **2017**, 260, 92-99.
2. Serda, M.; Ware, M. J.; Newton, J. M.; Sachdeva, S.; Krzykawska-Serda, M.; Nguyen, L.; Law, J.; Anderson, A. O.; Curley, S. A.; Wilson, L. J.; Corr, S. J. *Nanomedicine (Lond)* **2018**, 13, (23), 2981-2993.

Identification of biomolecules – a frustrating nano-business

J. Silberring, A. Drabik, J. Ner-Kluza, A. Bodzoń-Kułakowska, P. Suder

Department of Biochemistry and Neurobiology, AGH University of Science and Technology, Mickiewiczza Ave. 30, 30-059 Kraków, Poland

jerzy.silberring@agh.edu.pl

ABSTRACT

The lecture will discuss the most important methodological aspects of analytical tasks dealing with identification of molecules, which may lead to the vague results, to show significance of sample handling, experimental set-up and detailed identification at micro/nano level. Proper sampling is also a challenge during affinity chromatography, commonly used for selective and efficient separation, as nonspecific interactions are quite frequent, and their elimination may be sometimes more troublesome than development of a new and better technique. Not only particular separation steps are important but also a vast diversity of "homogenous" tissues. A good example might be the entire population of neurons in the brain where diversity of each nerve cell ("to each his own") has recently been discovered. This also shreds a brighter light on a single-cell analysis, as bearing analytical error and, though attractive, provides a very limited amount of information, which cannot be related to the overall function. Such analytical challenges are performed at molecular level, leading to a discovery and design of potential drugs, in particular involving theranostics.

Keywords: nanoseparations, sample preparation, proteomics, identification

Acknowledgements: This work was supported by the Polish-Taiwanese grant HEMO (PL-TW/V/2017/17).

Applications of Inverse Gas Chromatography and Dynamic Vapor Sorption for the physicochemical characterization of nanomaterials

A. Voelkel¹, B. Strzemieska¹, M. Sandomierski¹

¹Institute of Chemical Technology and Engineering, Poznan University of Technology, Poland

Adam.Voelkel@put.poznan.pl

ABSTRACT

In all applications of nanomaterials control over their surface properties are crucial for the interface aspects. Indeed, the strong interfaces are critical regions that ensure not only the long term use of

the polymer composites but contribute also to the performances of the end products. For this reason, they must be controlled at the molecular level with appropriate chemistry strategies in order to ensure their long term stability.

In this paper the usefulness of Inverse Gas Chromatography technique in the nanomaterials characterization is presented. It is shown that this technique is sensitive and accurate to notice changes in monolayer on the surface after e.g. its modification, influence of storage, synthesis conditions. Moreover, it enables to study nanomaterials in the real conditions, which means no special pretreatment is needed before measurements e.g. degassing, heating. The measurements are performed for materials just as received.

Dynamic Vapor Sorption enables to test adsorption properties by using different adsorbates (such as water, alcohols, alkanes) the same as Inverse Gas Chromatography without special pretreatment of the investigated materials under real conditions.

Both techniques can be easily applied for quick and accurate surface characterization of wide range of nanomaterials such as fillers for polymers, biomaterials.

Keywords: inverse Gas Chromatography, Dynamic Vapour Sorption, surface characterization, fillers.

INTRODUCTION

Nowadays, there are many techniques for studying the surface chemistry, adsorption properties, surface activity and energy.¹ Nitrogen adsorption is most often used technique for assessment adsorption properties of the solid surface. However, it does not reflect the surface properties fully. Wettability and contact angle methods are also very popular as it is simple and relatively cheap. The limits of the wettability and contact angle methods were discussed in². Inverse Gas Chromatography (IGC) is perfect complement of the aforementioned techniques. IGC does not require condensing the powders and other processing that changes the surface: the studied material is put into the chromatographic column and on the basis of retention parameters for known test compounds the physicochemical parameters describing the surface properties of solid are calculated. In accordance with the literature information³, there is a good correlation between the results obtained by using contact angle and IGC methods.

Furthermore, the water vapour or moisture sorption properties of nanomaterials are critical factors in determining their storage, stability, processing and application performance. The Dynamic Vapour Sorption (DVS) methodology makes possible the rapid quantitative analysis of the water sorption. DVS rapidly measures uptake and loss of moisture by flowing a carrier gas at a specified relative humidity over a sample suspended from the weighing mechanism of an ultra-sensitive recording microbalance.

IGC, DVS, nitrogen adsorption and contact angle techniques were used to characterize the different, new obtained aluminosilicates with potential used in polymer composites. Using of all these techniques for studying such broad range of the aluminosilicates and description of the dependences between the results obtained from them has not been done yet.

EXPERIMENTAL STUDY

The different aluminosilicates such as natural zeolite, synthesized with the different ratio of Si to Al, were characterized by IGC, DVS, nitrogen sorption and contact angle techniques. IGC measurements were carried out by using Surface Energy Analyser produced by Surface Measurement System Ltd. From London. The tested materials were placed into the chromatographic columns by the tap-and-fill method. The measurements were carried out at 30 °C.

The temperature of injector as well as FID detector was 180 °C. Helium was a carrier gas with flow rate 15 ml/min. Dispersive component of the free surface energy, γ_s^d that express dispersive properties of the surface was estimated according to Schultz-Lavielle procedure⁴. The specific components of the free surface energy was estimated using polar compounds according to procedure described in¹. DVS measurements were performed by using Dynamic Vapour Sorption Advanced produced by Surface Measurement System Ltd., London. The sorption isotherms of water were estimated. Nitrogen Adsorption/Desorption Measurements were carried out using a conventional volumetric technique on an ASAP 2420 sorptometer (Micromeritics). Before experiments the samples were outgassed at 200 °C in a vacuum chamber. The estimation of contact angle for water were performed using optical tensiometer Theta Lite produced by Attension Biolin Scientific, Finland.

RESULTS AND DISCUSSION

It was found that the increase of aluminium content (decrease of Si/Al ratio in final aluminosilicate) lead to increase of the value of γ_s^d parameter. The new synthesized aluminosilicates were characterized by more active surface than the natural zeolite and substrates used for synthesis of them: SiO₂ and NaAlO₂. All synthesized materials have a Type IVa isotherm what indicates that they are mesoporous ones. The materials with the highest content of silicon have two characteristic narrow ranges of pore size distribution between 2-5 nm. DVS showed clearly the differences of the water sorption between the studied materials. Generally, the sorption of water was the largest for aluminosilicates with the highest silica content.

CONCLUSION

The properties of the aluminosilicates with the different Si/Al ratio are closely related to the amount of aluminum and silicon in the tested materials. The surface properties of the synthesized aluminosilicate does not depend on the source of alumina and silica used as substrate. The particle size of the material agglomerates visibly increases with the increase of the amount of aluminum. The water sorption increased with the increase of the silica amount.

Acknowledgments: This work was supported by the National Science Centre. Poland. under research project No. UMO- 2015/17/B/ST8/02388.

REFERENCES

1. B. Strzemieska, A. Voelkel, J. Donate-Robles, J. M. Martin-Martinez, Appl. Surf. Sci. 316 (2014) 315–323.
2. M. Rojewska, A. Bartkowiak, B. Strzemieska, A. Jamrozik, A. Voelkel, K. Prochaska, Carbohydr. Polym. 171 (2017) 152–162.
3. J. W. Dove, G. Buckton, C. Doherty, Int. J. Pharm., 138 (2) (1996) 199–206.
4. J. Schultz, L. Lavielle, C. Martin, J. Chim. Phys. 84 (1987) 231-237.

Poster presentations (PP):**Nanoparticles as effective delivery systems for steroidal drugs**

M. Dołowy¹, P. Perez Martinez², A. Pyka-Pająk¹, J. Jampilek^{3,4}

¹Department of Analytical Chemistry, School of Pharmacy with the Division of Laboratory Medicine in Sosnowiec, Medical University of Silesia in Katowice, Poland; ²Erasmus+Participant Universidad CEU San Pablo, Madrid, Spain; ³Department of Analytical Chemistry, Faculty of Natural Sciences, Comenius University, Bratislava, Slovakia; ⁴Division of Biologically Active Complexes and Molecular Magnets, Regional Centre of Advanced Technologies and Materials, Faculty of Science, Palacky University Olomouc, Czech Republic

mdolowy@sum.edu.pl

ABSTRACT

Steroids is a large group of organic compounds that are widely used as drugs. Low aqueous solubility of these compounds is the major problem that has impact on their administration and bioavailability. Due to this fact, finding of innovative delivery system that can improve the efficacy of steroidal drugs delivery is very important.

This contribution is focused on describing of new delivery nanosystems used for the steroidal drugs.

Keywords: nanoparticles, steroids, drug delivery systems

INTRODUCTION

The current literature review (2011-2017) reveals that many different types of nanoparticles (NPs) have been successfully used as drug delivery systems [1]. In the case of steroidal drugs a special attention is paid to finding an affective topical delivery systems for corticosteroids [2,3].

RESULTS AND DISCUSSION

Recently, the steroid-loaded nanoparticles have been used in *in vitro* as well *in vivo* studies. The relatively new one described the applicability of dexamethasone as well as prednisolone acetate loaded biodegradable nanoparticles (PA, PLC, PLGA) for prevention of corneal allograft rejection in rats [2,3]. Another one showed the efficacy of dexamethasone loaded hemostatic nanoparticles (hDNP) in the treatment of lung injury after blast trauma [4]. The newly published articles highlighted the applicability of fructose chitosan (FC) and lecithin/chitosan based nanoparticles in overcoming the poor solubility of vitamins and steroids [5,6].

CONCLUSION

Overview the results demonstrated in current literature confirmed the successful application of steroids-loaded nanoparticles as efficient drug delivery systems. The newly published scientific papers showed the utility of fructose chitosan based nanoparticles for sustained release of steroids and vitamins.

Acknowledgments: This research was supported by the research grants from Medical University of Silesia in Katowice, Poland, KNW-1-057/K/8/O.

REFERENCES

1. S. Rao B, K. Bhushanam, U. N Das, T.N.V.K.V. Prasad, K. Subbarao. J Med Sci Res 1 (2013) 95-102.
2. Y. Ch. Liu, Y. Pang, N. Ch. Lwin, S. S. Venkatraman, T. T.Wong. Plos One, 8 (2013) 1-12.
3. Q. Pan, Q. B. Xu, N.J. Boylan, N.W. Lamb, D.G. Emmert, J.C. Yang, L.Tang, T. Heflin, S. Alwadani, C.G. Eberhart, W.J. Stark, J. Hanes. J Control Release, 201 (2015) 32-40.
4. W. B. Hubbard, M. M. Lashof-Sullivan, E. B. Lavik, P. J. V. Vord. ACS Macro Lett. 4 (2015) 387–391.
5. J. P. Quiñones, O. Brüggemann, C. P. Covas. JSM Nanotechnol Nanomed 5(3): 1056-1064.
6. Eroğlu, E. Azizoğlu, M. Özyazıcı, M. Nenni, H. Güler Orhan, S. Özbal, I. Tekmen, I. Ertam, I. Ünal, O. Özer. Drug Deliv, 23 (2016) 1502-1513.

Variability of electrokinetic potential of N-isopropylacrylamide derivatives in function of particles composition

M. Gasztych¹, W. Musiał¹

¹Department of Physical Chemistry, Pharmaceutical Faculty, Wrocław Medical University, Borowska 211, Wrocław 50-556

monika.gasztych@umed.wroc.pl, witold.musial@umed.wroc.pl

ABSTRACT

The interest in medical and pharmaceutical nanoscience is significant. Nanospheres and microspheres as a potential drug forms are investigated and evaluated. The aim of the study was to synthesize and characterize particles, which are sensitive to external stimuli. The poly-N-isopropylacrylamide (pNIPA) core was chosen, as it is thermosensitive polymer with volume phase transition temperature (VPTT) around 32 – 33 °C [1]. N-isopropylacrylamide (NIPA) derivatives were obtained via surfactant free precipitation polymerization (SFPP). The hydrodynamic diameter (D_H) of the obtained nanoparticles was evaluated by using dynamic light scattering (DLS) method. Measurements of the zeta potential (ZP) were carried out in the same DLS device. The particles in solutions have a surface charge, and respective ZP is measured to determine electrostatic interactions between microspheres. This value affects the degree of aggregation. Usually particles with low ZP absolute values are less stable, comparing to those with high values of ZP. VPTT of the synthesized microspheres may be evaluated using the UV-Vis absorbance measured as a function of temperature range.

Keywords: poly-N-isopropylacrylamide, thermosensitivity, zeta potential, volume phase transition temperature

INTRODUCTION

Scientific team of Physical Chemistry Department at Wrocław Medical University since several years is engaged in the synthesis and physicochemical evaluation of the polymers sensitive to external factors. Very interesting topic includes thermosensitive polymers, especially those that exhibit characteristic properties close to the human body temperature. NIPA monomer enables synthesis of numerous thermosensitive pNIPA derivatives with its VPTT around 32 – 33 °C. Utilization of various initiators and co-monomers leads usually to diversification of properties, including the values of VPTT [2].

EXPERIMENTAL/THEORETICAL STUDY

Fourteen batches of different particles were synthesized by SFPP. The D_H of the obtained particles was measured by DLS (Zeta Sizer Malvern Instruments) at a wavelength of 678 nm, and at the temperature range between 18 and 42 °C. Zeta potential ZP of all synthesized particles was measured as a function of temperature range 18 – 42 °C in water solution. The UV-Vis method (Agilent 8453 Spectrophotometer) was applied to measure VPTT of the obtained particles.

RESULTS AND DISCUSSION

In all samples, the increase of turbidity of the particles dispersion was observed with the increase of temperature, what was reflected by the characteristic increase of the absorbance. In some cases, specific point was observed, which manifests the value of the VPTT [3]. It was observed that among the polymers crosslinked with N,N'-methylene bisacrylamide, the VPTT values were diversified and less characteristic, whereas particles crosslinked with poly(ethylene glycol) chains presented more specific VPTT results. Selected examples are presented on the Figure 1. The results of ZP measured at 18 °C for polymers synthesized with anionic initiator ranged between -21,40 mV and -4,97 mV, whereas in the case of cationic initiator, the results covered the range -3,06 mV and 27,40 mV. Considering the absolute values, the highest potential was demonstrated by the S2 particle. From the group synthesized with cationic initiator, the highest absolute potential was noted for the S8 example. The size and the ZP results are presented in the table 1. It was found that the initiator affect the ZP values whereas not affect the particle D_H .

Type of initiator	Type of polymer	18 °C		42 °C	
		D_H [nm]	ZP [mV]	D_H [nm]	ZP [mV]
Anionic initiator	S 1	517,00	- 6,41	256,60	- 25,63
	S 2	514,46	- 21,40	361,24	- 29,38
	S 3	574,08	- 20,33	276,74	- 28,87
	S 4	121,50	- 14,87	185,33	- 28,97
	S 5	868,10	- 4,97	87,70	- 26,10
	S 6	915,30	- 8,26	245,20	- 17,57
	S 7	483,20	- 13,27	115,90	- 21,1
Cationic initiator	S 8	798,48	27,40	413,20	47,97
	S 9	896,58	22,70	344,20	31,50
	S 10	332,48	3,70	100,70	35,73
	S 11	155,46	9,07	163,60	23,00
	S 12	1064,00	- 3,06	178,90	30,4
	S 13	-	-	-	-
	S 14	1618,10	1,68	141,80	26,23

Tab. 1. Hydrodynamic diameter (D_H) and zeta potential (ZP) values of the aqueous dispersions of synthesized polymers.

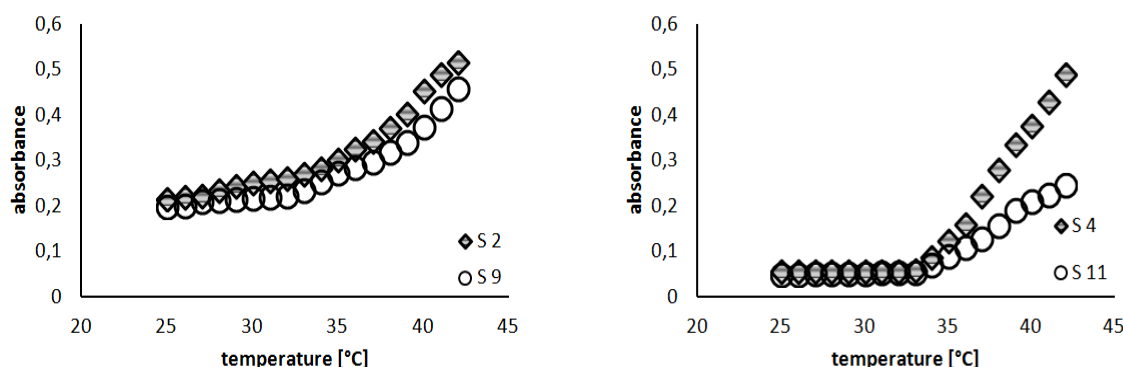


Fig. 1. Volume phase transition temperature (VPTT) values of the obtained polymers observed in aqueous dispersions via UV-Vis evaluations; S2 and S4 synthesized with anionic initiator, S9 and S11 synthesized with cationic initiator.

CONCLUSION

Polymers synthesized with the application of anionic initiator were characterized by negative value of the ZP, confirming the negative charge on the particle surface, whereas the D_H of these particles did not exceed the value of 915,30 nm. Consequently the use of a cationic initiator resulted in a positive superficial charge. The initiator slightly influenced the D_H of the NIPA derivatives, however it significantly determined the ZP. Modification of the various cross-linkers and comonomers may substantially modify the VPTT, ZP and D_H in assessed systems.

REFERENCES

1. M. Gasztych, K. Komsa, W. Musiał, J. Nanosci.Nanotechnol, 2019 vol.19, 5, p. 2514-2521.
2. M. Gasztych, A. Kotowska, W. Musiał, Materials 2018 vol.11, 2, p. 261-274.
3. M. Gasztych, A. Gola, J. Kobryn, W. Musiał, Molecules 2016 vol.21, 11, p. 1473-1484.

The influence of initiator concentration on physico-chemical properties on n-vinylcaprolactam derivatives

A. Gola, A. Niżniowska, W. Musiał

Department of Physical Chemistry, Pharmaceutical Faculty, Wrocław Medical University, Poland

agnieszka.gola@umed.wroc.pl witold.musial@umed.wroc.pl

ABSTRACT

The aim of the project was to synthesize, analyse and characterize poly-N-vinylcaprolactam (PNVCL) and study the effect of different concentration of cationic initiator 2,2'-Azobis(2-methylpropionamidine) dihydrochloride (AMPA) on the physicochemical properties of obtained products. Polymeric particles P1 and P2 were produced via the surfactant free precipitation polymerization (SFPP) at 70°C in the presence of AMPA system in water solution. The course of reactions were monitored by measuring the conductivity of reacting mixtures. Chemical composition of investigated samples were evaluated using ATR-FTIR and ^1H NMR spectroscopy. Hydrodynamic diameter (HD), zeta potential (ZP) and polydispersity index (PDI) were measured in aqueous dispersions of the synthesized polymers by dynamic light scattering (DLS) in temperature

range 18°C-45°C and were found to be for P-1: 37,56 nm (PDI = 0,85) and 10,47 mV, for P-2: 64,06 nm (PDI = 0,60) and 18,93 mV, at 18°C, respectively. This study revealed that the concentration of initiator affect the size of polymeric spheres and the volume phase transition temperature (VPTT) of the obtained polymeric spheres P1 and P2.

Keywords: Nanospheres, N-vinylcaprolactam, cationic initiator, electrical conductivity

INTRODUCTION

Thermosensitive polymers are “intelligent” materials that have the ability to react reversibly to environmental temperature changes. N-vinylcaprolactam (NVCL) polymeric derivative, are sensitive to temperature, amphiphilic, biodegradable biocompatible, indicate a sharp lower critical solution temperature (LCST) in the body physiological temperature range 32-34°C [1]. These characteristics lead to variety of applications for these particles in different biomedical applications e.g. as drug delivery system [2,3], entrapment of enzymes and cells [4,5] and in tissue engineering [6]. Obtaining (PNVCL) with specific and desirable physicochemical characteristics, i.a. size, shape or charge, increases its chances of being used in individualized and targeted pharmacotherapy. The synthesis of PNVCL has been performed in different media and to the best of our knowledge there are only few studies performed in water as solvent via SFPP.

EXPERIMENTAL/THEORETICAL STUDY

The polymeric nanoparticles (P1, P2) were prepared via free radical precipitation polymerization without emulsifier at 70°C in water solution, during 6 h, with respective mixing (250 rpm) under nitrogen atmosphere. In each synthesis, the same amount of monomer (ca. 3,00 g) and the variable amounts of cationic initiator (ca. 3,00 g for P1 and ca. 4,40 g for P2) was used. The polymer solutions were purified by dialysis. To confirm the composition the pure and lyophilized products were subjected to measurements of ATR-FTIR and ¹H NMR. The measurements of HD, PDI and ZP of synthesised polymers in water solution were performed by DLS (HD, PDI) and by electrophoretic measurements (ZP).

RESULTS AND DISCUSSION

The conductivity measurements of reaction mixtures, during the synthesis, were carried out at 30-second intervals (Figure 1 A-B). The value of the conductivity has changed from ca. 2450 $\mu\text{S}\cdot\text{cm}^{-1}$ to ca.1800 $\mu\text{S}\cdot\text{cm}^{-1}$ and from ca. 3550 $\mu\text{S}\cdot\text{cm}^{-1}$ to ca. 2550 $\mu\text{S}\cdot\text{cm}^{-1}$ respectively for P1 and P2 polymers. The highest, rapid and most significant changes in conductivity occurred after adding the monomer solution to the reactor containing the initiator solution.

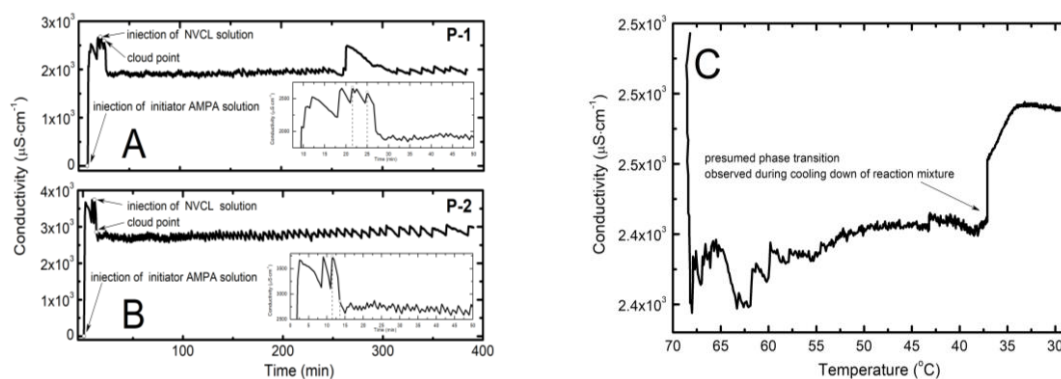


Figure 1. Changes in the conductivity in the course of the polymerization reaction of P1 (Figure 1A) and P2 (Figure 1B) and during cooling down of P2 (Figure 1C) in reaction mixtures.

The influence of the temperature in the range 18–45°C on hydrodynamic diameter (HD), polydispersity index (PDI) and zeta potential (ZP) of synthesized polymer particles in aqueous suspension has been investigated (Figure 2 A-B).

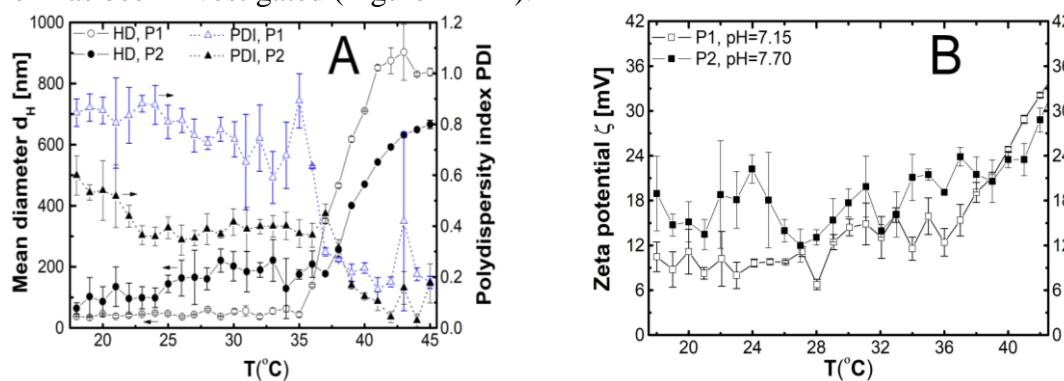


Figure 2A-B The effect of temperature on the HD, PDI (Figure 2A) and on the ZP (Figure 2B) of synthesized polymers P1, P2.

Due to the data in Figure 2A-B the values of HD, PDI, ZP for both P1 and P2 polymeric particles change distinctively in the temperature range 35–42°C.

CONCLUSION

ATR-FTIR and ¹H NMR spectra proved that PNVCL was obtained as a result of the carried out polymerization reaction. According to the conductometric studies the individual polymerization stages during synthesis course may be estimated. The results of HD measurements confirm synthesis of nano- and thermosensitive particles with tendency to aggregate. The sharp changes in the values of HD, PDI, ZP in function of temperature may indicate the VPTT of the tested polymers. Due to the PDI and ZP data obtained nanoparticles reveal enhanced stability over the VPTT value. Based on the obtained results can be concluded that the initiator concentration affects the HD of the particles. The obtained series of data will be supplemented with subsequent syntheses with varied amounts of initiator and the results will be successively developed and interpreted in the further stages of the research. Additionally thermal characteristic of all products will be carried out by thermogravimetry.

REFERENCES

1. J. Li, et al. Int. J. Pharm. 2, (2006), 513-519.
2. R.C. Mundargi et al. J. Microencapsulation 28, (2011), 384-94.
3. N.S. Rejinold et al. J Colloid Interface Sci. 360, (2011), 39-51.
4. M.V. Donova et al. Biotechnol. Tech. 7, (1993), 415-22.
5. E. A. Markvicheva et al. Appl. Biochem. Biotechnol. 88, (2000), 145-57.
6. B. Lee et al. Acta Biomater. 9, (2013), 7691-8.

Synthesis and antimicrobial activity of ciclopiroxolamine/ZnO/vermiculite nanocomposites

S. Holešová, K. Čech Barabaszová, M. Hundáková, M. Ščuková

Nanotechnology Centre, VŠB – Technical University of Ostrava, Czech Republic

sylva.holesova@vsb.cz

ABSTRACT

The current topics of material research focused on medical use deal with development of hybrid organic-inorganic nanocomposites with antimicrobial activity based on layered materials. The clay minerals are commonly used materials in pharmaceutical field both as inorganic excipients or active agents, because they may undergo ion exchange reaction with functional antimicrobial molecules via intercalation process. Some of the antifungal drugs have limitation due to its low dissolution rate in the aqueous media resulting in low bioavailability. Therefore, it is required to develop a drug delivery system that can minimize side effects and increase drug bioavailability. Ciclopiroxolamine is a hydroxypyridone antifungal agent that is structurally unrelated to the common imidazole derivatives or other antifungals. It is broad-spectrum antifungal agent with additional antibacterial and anti-inflammatory activities. Inorganic metal oxides, such as ZnO, may serve as effective disinfectants, due to their strong antibacterial effect, good chemical stability and relatively non toxic profile. ZnO demonstrates significant growth inhibition of broad spectrum of bacteria. The aim of this study is to anchor antifungal drug ciclopiroxolamine on ZnO/vermiculite prepared via ultrasound method and evaluate its antimicrobial activity against common bacterial strains and especially against yeast *Candida albicans*.

Keywords: vermiculite, ciclopiroxolamine, ZnO, antimicrobial activity.

Acknowledgments: This work was supported by project No. SP2018/112 (Ministry of Education, Youth and a Sports of Czech Republic).

Determination and characterization of metronidazole/imidazole/clay interaction

S. Holešová¹, Y. Tarasiuk¹, M. Hundáková¹, E. Pazdziora²

¹Nanotechnology Centre, VŠB – Technical University of Ostrava, Czech Republic; ²Institute of Public Health Ostrava, Centre of Clinical Laboratories, Ostrava, Czech Republic

sylva.holesova@vsb.cz

ABSTRACT

Within the challenging issue of the targeted drug delivery, to specific areas of the body, several systems have been proposed with the major purpose of achieving a controlled and low release rate of the drug in order to ensure a constant in vivo drug concentration for a longer period of time while preventing harmful side-effects and drawbacks. These systems allow to both efficiently control the site and the rate of delivery and obtain more advantages in the administration of bioactive molecules. Particular attention has been paid to the drug delivery systems, which are composed of inorganic clay minerals and organic drug. The reason of the considerable interest on the clay minerals intercalated by drug molecules can be attributed to the novel physical and chemical properties exhibited by these hybrids. This study is focused on the preparation and characterization of organoclay (vermiculite and/or bentonite) nanocomposite materials based on imidazole (IM) and its derivative metronidazole (ME), which is antibiotic drug used predominantly for treatment of intestinal and periodontal diseases. The structure of prepared samples was characterized by the X-ray diffractometry (XRD) and infrared spectroscopy (IR). Furthermore, the content of organic carbon was determined in the nanocomposite samples by multiphase carbon and hydrogen/moisture analyzer. Antimicrobial activity of nanocomposites was tested against bacterial strains *S. aureus*, *E. faecalis*, *P. aeruginosa* and *E. coli*, and it was evaluated by finding minimum inhibitory concentration (MIC).

Keywords: vermiculite, bentonite, imidazole, metronidazole, clay nanocomposite, antimicrobial effect, minimum inhibitory concentration.

CdTe QDs-based electrochemical assay for sensitive detection of African swine fever virus

M. Gargulák^{1,2}, N. Štrofová^{1,2}, M. Kepinska³, H. Milnerowicz³, A. E. Ofomaja⁴, B. Hosnedlová², C. Fernandez⁵, P. Vašíčková⁶, R. Kizek^{1,2,3,6}

¹Department of Human Pharmacology and Toxicology, Faculty of Pharmacy, University of Veterinary and Pharmaceutical Sciences Brno, Czech Republic, ²Department of Research and Development, Prevention Medicals, Studénka-Butovice, Czech Republic, ³Department of Biomedical and Environmental Analyses, Faculty of Pharmacy with Division of Laboratory Medicine, Wrocław Medical University, Poland; ⁴Department of Chemistry, Faculty of Applied and Computer Sciences, Vaal University of Technology, South Africa, ⁵School of Pharmacy and Life Sciences, Robert Gordon University, Aberdeen, United Kingdom, ⁶Department of Food and Feed Safety, Veterinary Research Institute Brno, Czech Republic

michaelgargulak@seznam.cz

ABSTRACT

Rapid and effective diagnostic approaches to the detection of dangerous viral diseases such as influenza, Ebola or African swine fever are increasingly being sought. Quantum dots (QDs) are nanocrystals that due to their high stability, ease of preparation and biocompatibility are suitable for

labelling biomolecules. The modified biomolecules of QDs are applicable to the labelling of nucleic acids or antibodies. QDs were prepared in a wide range of colors. Their long-term stability, including their application onto paper, was tested. CdTe QDs exhibit very good electrochemical detection with LOD in nanomolar concentration. African swine fever virus (ASFV) was detected with QDs-labelled antibody.

Keywords: QDs, green synthesis, viral infection, CdTe, sensors, electrochemistry, antibody

INTRODUCTION

African Swine Fever Virus (ASFV) is a DNA virus of the *Asfivirus* genus of the *Asfarviridae* family that is found in blood, body fluids, internal organs and all secretions and excretions and can be secreted 1–2 days before clinical symptoms^{1,2}. ASFV was described more than 40 years ago^{3,4}. This virus spreads pandemically among members of the *Suidae* family, and the mortality rate of the virus-related disease ranges from 90 to 100 %^{5,6}. The design and construction of sensors/biosensors require very sensitive detection and recognition parts. Very sensitive tools for analyte identification are fluorescence methods. QDs (nanoparticles of a size of 2–10 nm) are used for such purposes. In addition to their fluorescence properties, their electrochemical behavior can be used. CdTe detection limits may be in nM. The aim of this work was to propose a procedure for QDs antibody modification and their sensitive electrochemical detection.

EXPERIMENTAL PART

The preparation of CdTe quantum dots (QDs) was performed as follows: Cd(CH₃COO)₂ (20 mM), MSA solution (0.4 M) or plant extract, Na₂TeO₃ (20 mM), and NaBH₄ were stirred. The vial containing the mixture was placed in a microwave, which was set to a power of 300 W. Coat protein polyclonal antibody (Merck, USA) was diluted at 1 : 1,500. The absorbance spectra of nanoparticles were recorded within the range of 400 to 800 nm using a UV-3100PC UV–VIS spectrophotometer. Determination of Cd²⁺ by DPV was performed at 663 VA Stand (Metrohm, Switzerland). Acetate buffer (0.2 M sodium acetate and 0.2 M acetic acid, pH = 5) was used as a supporting electrolyte. The parameters of the measurement were as follows: initial potential -1.2 V, end potential 0 V, deoxygenating with argon 120 s, accumulation time 120 s, step potential 5 mV, modulation amplitude 25 mV, the volume of injected sample: 50 µL.

RESULTS AND DISCUSSION

ASFV is given attention because of its lethal ability and is being studied in detail⁷. CdTe QDs were prepared using a green synthesis approach⁸ with typical green, yellow, orange, and red fluorescence under UV light. In addition to the usual methods of analysis, QDs were also studied electrochemically^{9,10}. Linear dependencies were obtained by conventional DPV analysis as follows: green QDs: $y = 345.1x - 1243$, RSD 4.1 %, LOD 2.0, LOQ 8.0 nM; yellow QDs: $y = 444.1x - 545$, RSD 5.4 %, LOD 1.8, LOQ 8.5 nM; orange QDs: $y = 578.6x - 423$, RSD 7.1 %, LOD 2.4, LOQ 6.5 nM; red QDs: $y = 844.6x - 296$, RSD 10.3 %, LOD 1.4, LOQ 4.5 nM. Fig. 1 shows a schematic representation of the detection part of a prepared biosensor for detecting viral particles. In the experiment, the antibody was anchored to the membrane after binding of the virus to this antibody; in the system, a second antibody was used which was labelled with CdTe QDs. CdTe QDs was subsequently determined electrochemically.

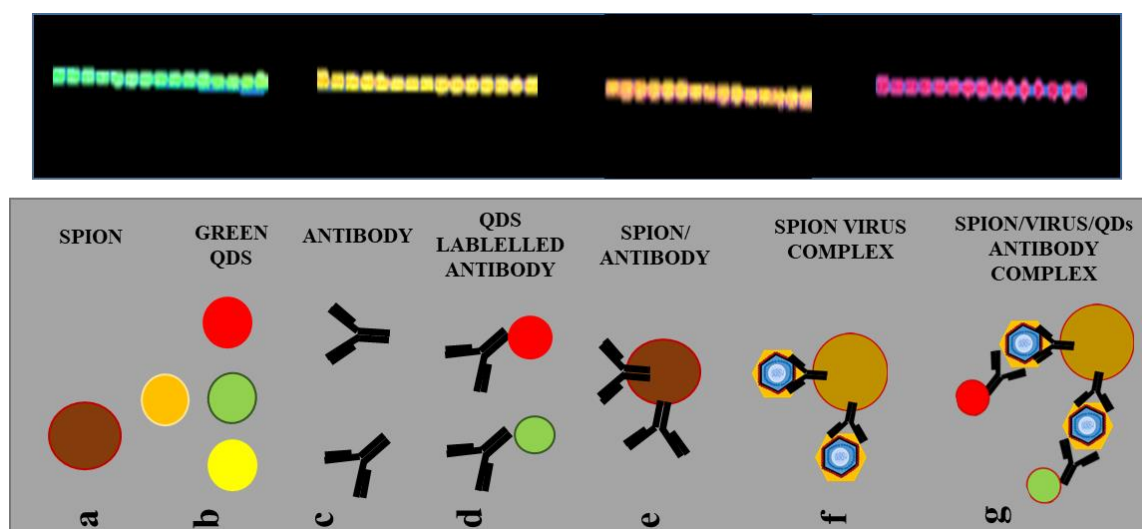


Fig. 1. QDs deposited on paper and visualized at 260 nm. The proposed method for virus detection, the use of SPION particles for easy purification of viral nanoparticles (a) green QDs are used to label antibodies, (b) suitable antibodies for capturing viral particle, (c) antibodies modified by suitable QDs, (d) SPION particles are modified by an antibody with a high affinity to the viral capsid, (e) SPION/VIRUS complex, (f) SPION/VIRUS/QDS/ANTIBODY complex (g). The complex formed was analyzed electrochemically.

CONCLUSION

Rapid detection of viral pathogens is essential for the introduction of appropriate anti-epidemic measures. Viruses with high infectivity and mortality rate of virus-related disease pose serious threats to both humans and animals. A sensitive electrochemical detection method of ASFV has been proposed.

Acknowledgments: The work was realized thanks to the project QK1920113.

REFERENCES

1. Freitas, T. R. P.; de Paula Lyra, T. M.: *Arq. Inst. Biol.* 85, 1 (2018).
2. Callaway, E.: *Nature*. 488, 565 (2012).
3. Parker, J.; Plowright, W.: *Nature*. 219, 524 (1968).
4. Plowright, W.; Parker, J.; Peirce, M. A.: *Nature*. 221, 1071 (1969).
5. Dixon, L. K.; Sun, H.; Roberts, H.: *Antiviral research.* (2019).
6. Capua, I.; Monti, M.: *Nature*. 566, 326 (2019).
7. Chen, Y. Q.; Liu, H. H.; Yang, C.; Gao, Y. Q.; Yu, X.; Chen, X.; Cui, R. X.; Zheng, L. N.; Li, S. H.; Li, X. H.; Ma, J. B.; Huang, Z.; Li, J. X.; Gan, J. H.: *Nature Communications*. 10, 13 (2019).
8. Leitner, W.: *Science*. 284, 1780 (1999).
9. Galland, C.; Ghosh, Y.; Steinbruck, A.; Sykora, M.; Hollingsworth, J. A.; Klimov, V. I.; Htoon, H.: *Nature*. 479, 203 (2011).
10. Rubin, H. D.; Humphrey, B. D.; Bocarsly, A. B.: *Nature*. 308, 339 (1984).

Effect of silver nanoparticles (AgNPs) prepared by green synthesis from sage leaves (*Salvia officinalis*) on maize plants

N. Štrofová¹, M. Gargulák¹, K. Sehnal², M. Kepinska³, H. Milnerowicz³, C. Fernandez⁴, J. Sochor², B. Hosnedlová², R. Kizek^{1,2,3}

¹Department of Human Pharmacology and Toxicology, Faculty of Pharmacy, University of Veterinary and Pharmaceutical Sciences Brno, Czech Republic; ²Department of Viticulture and Enology, Faculty of Horticulture, Czech Republic; ³Department of Biomedical and Environmental Analyses, Faculty of Pharmacy with Division of Laboratory Medicine, Wrocław Medical University, Poland; ⁴School of Pharmacy and Life Sciences, Robert Gordon University, United Kingdom

Nikola.Strofova@seznam.cz

ABSTRACT

The AgNPs have considerable industrial potential and are intensively studied with regard to their antibacterial properties. Using green synthesis, the nanoparticle surface can be coated with molecules that exhibit biologically significant properties. Increased use of nanoparticles enhances the risk of their release into the environment. However, there is still little known about the behaviour of AgNPs in the eco-environment. In this study, the effect of AgNPs prepared by green synthesis on germinated plants of maize was investigated. The effects on germination, basic growth and physiological parameters of the plant were monitored. We found that the growth inhibition of the above-ground parts of plants was about 40 % and AgNPs had a significant effect on photosynthetic pigments.

Keywords: green synthesis, electrochemistry, phytotoxicity, phyto-nanotechnology

INTRODUCTION

Nanoparticle research is one of the rapidly developing areas of nanotechnology. The subject of interest is gold (37 %), silver (24 %), and zinc (10 %) nanoparticles (according to WOS). Silver nanoparticles (AgNPs) are the most studied because of their antibacterial properties. In case of their industrial use, however, their possible release into the environment can be expected¹. To date, little is known about the effect of AgNPs on plants, although silver ions are commonly used to stimulate growth in explant cultures. It is necessary to study the effects of AgNPs on morphological and physiological changes in plants^{2,3}. These effects may vary depending on the size, shape and concentration of the nanoparticles and the age and species of the plant. AgNPs are known to induce oxidative stress in eukaryotic cells, disrupt the organelle membranes, cause nucleic acid damage, affect photosystem I (PSI) and mitochondrial metabolism, including the respiratory chain (**Fig. 1A**). The aim of this work was to study the effect of different concentrations of AgNPs on germinated plants of maize (*Zea mays*).

EXPERIMENTAL PART

Dried sage leaves (*Salvia officinalis*) were purchased (Valdemar Grešík – Natura s.r.o., Czech Republic). The mixture was homogenized by milling to 1–2 mm particles, then it was extracted and subsequently stirred in ultrapure water (80 °C, 60 min) at a ratio of 5 DW g/100 mL, v/w. The leachate was further centrifuged (30 min, 4000 g) and then mixed with 0.1 M AgNO₃ (1 : 1). The solution was stirred on a magnetic stirrer (80 °C, 24 h). The particles were washed with methanol

(1 : 1) and left on a magnetic stirrer (60 min); (**Fig. 1B**). After purification, the supernatant was removed and the particles were allowed to dry (24 h, 60 °C, VWR dryer, USA). *Zea mays* seeds of the Silen variety were watered with tap water (250 mL, conductivity 485 $\mu\text{S}/\text{cm}$, pH 6.6, 25 °C) and germinated. For the experiment, 7-day-old maize seedlings were selected. The seedlings were then placed into a hydroponic system with 3 litres of cultivation solution. Distilled water was chosen as a negative control. Silver nitrate and AgNPs were applied at concentrations of 1, 50, and 150 mg/L.

RESULTS AND DISCUSSION

Fig. 1C,D shows a typical appearance and UV/VIS spectra of solvent, AgNO_3 (1 mg/mL) and AgNPs (1 mg/mL). AgNPs formation was monitored photometrically at 452 nm. AgNPs (1, 50, and 150 mg/mL) were applied to germinated plants of maize (on day 7 of cultivation). **Fig. 1E** shows a typical appearance of plants on day 6 of the experiment. Plants were analyzed on days 4, 5 and 6 after administration of AgNO_3 and AgNPs. After administration of AgNPs, plants showed a gradual leaf tip drying and a slight change in leaf and root colour. A significant change in plant growth parameters (growth reduction of about 40 %) was observed. There was a change in root biomass, but their number remained unchanged. **Fig. 1F** shows the expected effect on a number of photosynthetic dyes. The amount of chlorophyll a, chlorophyll b, carotenes, and xanthophylls increased [control 600 $\mu\text{g}/\text{g}$ fresh weight (FW); AgNO_3 830 $\mu\text{g}/\text{g}$ FW; AgNPs 1300 $\mu\text{g}/\text{g}$ FW]. In the case of using AgNPs, the increase in photosynthetic dyes by more than 50 % is likely caused by a plant defence response due to increased oxidative stress. However, this link should be further studied. A statistically significant difference compared to control was found in all studied variants at the 95 % significance level.

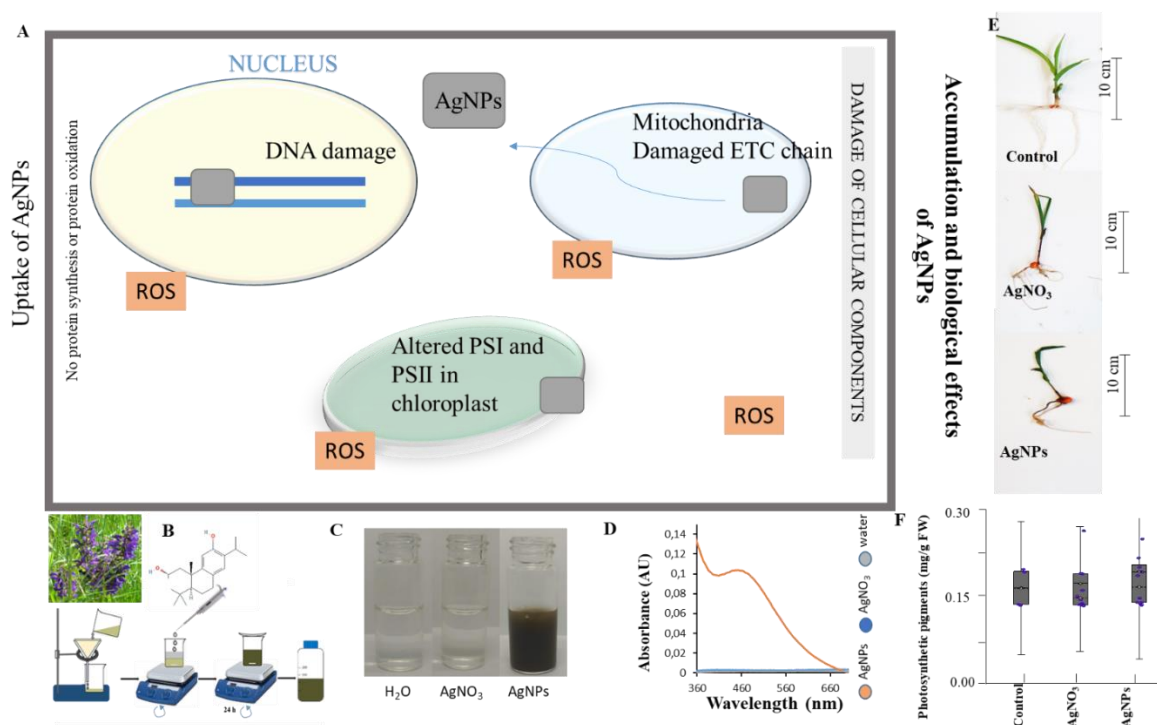


Fig. 1. The expected biological effects of AgNPs on plants. A) Effect of AgNPs on eukaryotic cell; B) Green synthesis of AgNPs; C) Photos of the individual solutions used (water, AgNO_3 , AgNPs); D) Typical UV/VIS spectra of water, AgNO_3 , and AgNPs; E) A typical plant appearance after 6 days of cultivation; F) Changes in photosynthetic pigments.

CONCLUSION

Silver nanoparticles were synthesized from the sage leaves using green synthesis. AgNPs were biophysically characterized and their phytotoxicity was tested in germinated plants of maize. AgNPs were chemically stable over the course of the experiment and showed the effect on the germinated plants in most of the analyzed morphological parameters. These findings should be further investigated.

Acknowledgments: The work was carried out with the support of the H2020 CA COST Action CA15114, INTER-COST LTC18002.

REFERENCES

1. Pokhrel, L. R.; Dubey, B.: *Science of the Total Environment*. 452, 321 (2013).
2. Jafari, S.; Davoodi, D.; Jonoubi, P.; Majd, A.; Alizadeh, H.; Shobbar, Z. S.: *Applied Ecology and Environmental Research*. 16, 2391 (2018).
3. Zheng, Y. L.; Hou, L. J.; Liu, M.; Newell, S. E.; Yin, G. Y.; Yu, C. D.; Zhang, H. L.; Li, X. F.; Gao, D. Z.; Gao, J.; Wang, R.; Liu, C.: *Science Advances*. 3, 11 (2017).

Potential Anticancer Drug Nanocarriers

V. Kozik¹, A. Bąk¹, A. Świetlicka¹, A. Środa¹, J. Jampilek^{2,3}, W. Priebe⁴, J. Jazowiecka-Rakus⁵, A. Sochanik⁵

¹Institute of Chemistry, University of Silesia in Katowice, Poland; ²Division of Biologically Active Complexes and Molecular Magnets, Regional Centre of Advanced Technologies and Materials, Faculty of Science, Palacky University Olomouc, Czech Republic; ³Department of Analytical Chemistry, Faculty of Natural Sciences, Comenius University, Bratislava, Slovakia; ⁴Department of Experimental Therapeutics, University of Texas MD Anderson Cancer Center, Houston, TX, USA; ⁵Center for Translational Research and Molecular Biology of Cancer, Maria Skłodowska-Curie Institute - Cancer Center, Gliwice, Poland

violetta.kozik@interia.eu

ABSTRACT

Chemical functionalization of graphene oxide (GO) conferring novel physical and chemical properties involves either covalent alterations of GO, leading to surface changes *via* formation of chemical bonding whereas alterations of non-covalent kind involve van der Waals forces, hydrogen bonding and π - π stacking interactions. Covalent modifications appear to be superior as they yield compounds with defined properties whereas carriers prepared by non-covalent methods are less stable. This study has been focused on synthesis and assessment of biologically active novel derivatives of GO, potential anticancer drug nanocarriers. Therefore, novel GO-based nanocarriers were synthesized using covalent approach involving nucleophilic substitution of GO nanoparticles with iminodiacetic acid (IDA) or glycine (Gly). As the first step, iminodiacetic acid or glycine were transformed into iminodiacetic acid or glycine methyl ester hydrochlorides, respectively, for C-terminus protection. The obtained products were then activated *in situ*, and used to form amide bonds between GO and iminodiacetic acid, or glycine, respectively. Ease of functionalization and ability to transport biologically active substances made it possible to investigate usefulness of both GO-IDA and GO-Gly as carriers of an advanced antimelanoma chemotherapeutic. As numerous studies have suggested that chemotherapeutics useful for melanoma treatment require customization, we tested in here GO-derived nanocarriers with WP760, one of the first melanoma-specific chemotherapeutic candidates with previously demonstrated antimelanoma activity *in vitro*.

It is a bis-anthracycline exploiting daunomycinone and adriamycinone as intercalating moieties, two minor groove-binding sugars related to daunosamine and 4-amino-2,3,6-trideoxy- α -L-lyxohexopyranose, as well as equipped with selected linkers ('click' chemistry). Doxorubicin was used as a reference.

Keywords: graphene oxide, melanoma, anticancer, drug nanocarriers

Acknowledgments: This study was supported by the Slovak Research and Development Agency (projects APVV-17-0373 and APVV-17-0318) and by the Ministry of Education of the Czech Republic (LO1305).

REFERENCES

1. A. Alshannaq, J.H. Yu, *Int. J. Environ. Res. Public Health* 14 (2017) E632.
2. H.J. Van der Fels-Klerx, C. Liu, P. Battilani, *World Mycotoxin J.* 9 (2016) 717–726.
3. D. Milicevic, I. Nastasijevic, Z. Petrovic, *J. Environ. Sci. Health C* 34 (2016) 293–319.
4. J. Jampilek, *Expert Opin. Drug Dis.* 11 (2016) 1–9.
5. FRAC Code List[®] 2019: Fungal control agents sorted by cross resistance pattern and mode of action, Croplife International. Brussels, 2019.

Adsorption of pharmaceuticals from aqueous solutions onto clay minerals

S. Vallová^{1,2}, B. Sokolová², V. Valovičová³, E. Plevová³

¹Department of Chemistry, VŠB-Technical University Ostrava, Czech Republic; ²Institute of Environmental Technology, VŠB-Technical University Ostrava, Czech Republic; ³Institute of Geonics of the CAS, Czech Republic

silvie.vallova@vsb.cz

ABSTRACT

The objective of this work was to investigate to possibility of clay minerals for the removal of drugs from aqueous solutions. Natural minerals such as montmorillonite, vermiculite, kaolinite and modified montmorillonites KSF and K10 (intercalated by Fe^{3+}) were used as potential sorbents for three analgetics: paracetamol, ibuprofen and diclofenac from aqueous solutions. This research demonstrated that adsorption of all three pharmaceuticals onto natural untreated clay minerals, except paracetamol sorption on Na-MMT, is negligible. On the other hand, the chemically modified montmorillonites demonstrated significant sorption ability in the order diclofenac>ibuprofen>paracetamol.

Keywords: Adsorption, clay minerals, montmorillonite, paracetamol, ibuprofen, diclofenac

INTRODUCTION

Pharmaceutical wastewaters are very hazardous and toxic not only for the human but also for environmental life. Therefore, various physicochemical and biological methods have been testified to remove organic and inorganic contaminants from wastewater and adsorption is one of the most extensively employed technique¹.

Natural materials, especially clay minerals based on MMT and their modified derivatives, are good sorbents for many contaminants such as organic contaminants, cationic/anionic dyes, heavy metal

cations, radioactive nuclides, due to their availability, low cost, environmental stability and ion exchange properties².

Common treatment of clay minerals for adsorption are acid washing, thermal treatment, intercalation of surfactant molecules such as quaternary ammonium salts and loading hydroxymetals³.

EXPERIMENTAL/THEORETICAL STUDY

Four natural minerals: Na-montmorillonite (Na-MMT), Ca-montmorillonite (Ca-MMT), vermiculite (Ver), kaolinite (Ka) and two commercial montmorillonites: KSF and K10 were used as a potential sorbent for the uptake of paracetamol (PAR), ibuprofen (IBU) and diclofenac (DC) from aqueous solutions. The clay minerals were characterized by thermogravimetry (TGA), X-ray diffraction (XRD), X-ray Fluorescence (XRF), specific surface area (SSA) were determined using the BET equation. Adsorption experiments were carried out in a batch mode, mass of sorbents were 100, 300 and 500 mg, initial concentration and volume of PAR, IBU and DC solutions were 10 mg l⁻¹ and 20 ml. The equilibrium concentrations of the organic pollutants in aqueous solutions after adsorption were measured using HPLC analysis.

RESULTS AND DISCUSSION

The results of the present study for the adsorption of PAR, IBU, DC onto 300 mg of clay minerals (shown in Table 1) indicate that commercial MMT KSF and K10, which are modified by acid leaching and loading with Fe³⁺, proved a good affinity for drug sorption.

Table 1. Adsorbed amount of PAR, IBU, DC onto 300 mg of clay minerals.

Clay mineral/ 300 mg	PAR-adsorbed amount (%)	IBU-adsorbed amount (%)	DC-adsorbed amount (%)
MMT KSF	50.5	58.5	90.8
MMT K10	19.3	31.9	75.1
Na-MMT	46.2	-	-
Ca-MMT	-	-	-
Ver	-	-	-
Ka	-	-	-

CONCLUSION

From the present study, it can be concluded that:

Only the modified clay minerals with acid treatment and intercalation of Fe³⁺ can be effectively applied for the removal of PAR, IBU and DC from aqueous solutions.

The adsorption of the pharmaceuticals from aqueous solutions follows the order DC>IBU>PAR for both KSF and K10.

The SSA of K10 is around ten times higher than that of KSF while the adsorption capacity is lower. This means that SSA is not a limiting factor and the interlayer space of the clay minerals plays a vital role in increasing PAR, IBU and DC uptake.

On the contrary, natural clay minerals: Ca-MMT, Na-MMT, Ver and Ka do not adsorb any drugs (PAR, IBU, DC) from aqueous solutions. Only Na-MMT had higher adsorption capacity to PAR.

Acknowledgments: The authors would like to thank The Ministry of Education, Youth and Sports Czech Republic for supporting this study (grant number CZ.02.1.01/0.0/0.0/16_019/0000853).

REFERENCES

1. G. Z. Kyzas, J. Fu, N. K. Lazaridis, D. N. Bikiaris, K. A. Matis, *Journal of Molecular Liquids*. 209 (2015) 87–93.
2. M. Nafees, A. Waseem, *Clean-Soil, Air, Water*. 42 (2014) 1500–1508.
3. R. Zhu, J. Fu, Q. Chen, Q. Zhou, Y. Xi, J. Zhu, H. He, *Applied Clay Science*. 123 (2016) 239–258.

Micro- and mesoporous zeolites with high ion exchange capacity as materials with potential biomedical applications

M. Sandomierski, Z. Buchwald, M. Zielińska, A. Voelkel

¹Poznan University of Technology, Institute of Chemical Technology and Engineering,

Poznań, Poland;

mariuszsandomierski@wp.pl

ABSTRACT

The purpose of this work was to receive micro- and mesoporous type A and X zeolites with high ion exchange capacity and to apply these materials as an active fillers in the dental composites with the remineralizing potential and potential material for drug release. Six different synthesis pathways were applied to receive A and X type zeolites. All zeolites were subjected to the ion exchange process. As a result a calcium form of these materials were prepared. The effectiveness of synthesis was confirmed by infrared spectroscopy, X-ray Diffractometry, scanning electron microscopy, energy dispersive spectroscopy and nitrogen adsorption/desorption measurements. The remineralizing potential was specified as an ability to release calcium ions during the incubation in saline with the use of inductively coupled plasma-mass spectrometry. Composites containing calcium form of zeolites proved to have the ability to release calcium ions. The ability to release calcium ions and good mechanical properties indicates potential of prepared composites in dental applications. The second type of application was the release of drugs. Zeolite properties as a carrier of drugs and the possibility of their release were tested using UV-VIS spectroscopy.

Keywords: Filler, dental materials, drug release, bisphosphonates

INTRODUCTION

Zeolites are crystalline aluminosilicates with a porous structure which is crucial for many industrial applications.^{1,2} Zeolites are promising for detoxication, controlled drug delivery and tissue engineering.³ They are also used as a fillers for many polymers.^{4,5} Composites based on methacrylate resins and zeolites show high mechanical strength.⁶ There are several different types of zeolites in the environment which are non-toxic to living beings what affects their potential application in the drug release process.^{7,8} One of the zeolite types used in this process is type A.⁹ Type A zeolites are flavorless, odorless, harmless and have high cation exchange capacity.^{10,11} Ability of zeolites to ion exchange allows for incorporation of some amount of the calcium cations in their structure. Ca^{2+} ions are considered to be a confirmed anticaries agents. Calcium ions delivered from the external sources to the human mouth environment are able to rebuild the hydroxyapatite.¹²

In this work the synthesis of zeolites was conducted. Several methods were applied to describe the structure and the properties of obtained materials. Moreover, the obtained materials were used as fillers in the methacrylate resins. The prediction was that the composite with such filler will release calcium ions. Their second application was to use them as drug carriers. That properties were tested using UV-VIS spectroscopy.

EXPERIMENTAL/THEORETICAL STUDY

In this work, we prepared A and X type zeolites. They were synthesized by the methods proposed by Gomez et al. and Hasan et al.^{13,14} The following techniques were used to evaluate the effectiveness of synthesis: infrared spectroscopy, X-ray Diffractometry, scanning electron microscopy, energy dispersive spectroscopy and nitrogen adsorption/desorption measurements. The following techniques were used to evaluate the effect of filler on the properties of composites: flexural strength, compressive strength, inductively coupled plasma – mass spectrometry. The amount of drug retained and released from the zeolites was tested using UV-VIS spectroscopy.

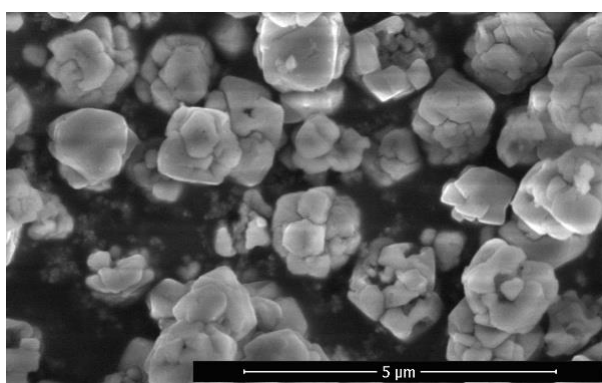


Fig. 1. SEM image of zeolite X.

RESULTS AND DISCUSSION

Bands occurring in the IR spectra of all obtained zeolites in the range of $1200\text{--}600\text{ cm}^{-1}$ are connected with the vibrations of the zeolite framework. XRD patterns of all examined materials are typical for the highly crystalline A and X zeolites. The surface area and pore volume depends on the type of zeolite A and X synthesis. Prepared zeolites differ in the crystals size. Analysis of the energy dispersive spectroscopy results indicates the distribution of calcium cations on the entire analyzed fillers surface. All prepared zeolite composites are able to release some amount of calcium ions. Flexural strength of the composites depends on the type of zeolite A and X synthesis. These zeolites have the ability to retain a large amount of risedronate. The drug is then released gradually under the influence of simulated body fluid. The effectiveness of the retention and release depends on the type of zeolite synthesis.

CONCLUSION

The results confirm effectiveness of the zeolite synthesis and ion exchange. Composites containing calcium zeolites proved to show the ability to release calcium ions. Flexural strength of the composites depends on the type of zeolite synthesis. Our results proved that calcium zeolites composites have good mechanical properties and the high remineralization potential. The effectiveness of the bisphosphonate retention and release depends on the type of zeolite synthesis.

Acknowledgments: This work was conducted with the financial support from the Polish National Science Centre (grant no. UMO-2015/17/B/ST8/02388).

REFERENCES

1. V. Van Speybroeck, K. Hemelsoet, L. Joos, M. Waroquier, R. G. Bell, C. Richard, A. Catlow, *Chem. Soc. Rev.*, 44 (2015) 7044–7111.
2. D. Bastani, N. Esmaeili, M. Asadollahi, *J. Ind. Eng. Chem.*, 19 (2013) 375–393.
3. L. Bacakova, M. Vandrovicova, I. Kopova, I. Jirka, *Biomater. Sci.* 6 (2018) 974.
4. A. C. Lopes, C. Ribeiro, V. Sencadas, G. Botelho, S. Lanceros-Mendez, *J. Mater. Sci.*, 49 (2014) 3361–3370.
5. B. Strzemiecka, A. Voelkel, M. Kasperkowiak, *Colloid. Surface. A*, 372 (2010) 80–85.
6. A. U. Metin, *Polym. Compos.*, 37 (2016) 2313–2322.
7. R. Szostak, *Handbooks of Molecular Sieves*, Van Nostrand Reinhold, New York (1992).
8. M. Spanakis, N. Bouropoulos, D. Theodoropoulos, L. Sygellou, S. Ewart, A. M. Moschovi, A. Siokou, I. Niopas, K. Kachrimanis, V. Nikolakis, P. A. Cox, I. S. Vizirianakis, D. G. Fatouros, *Nanomed-Nanotechnol.*, 10 (2014) 197–205.
9. R. Amorim, N. Vilaça, O. Martinho, R. M. Reis, M. Sardo, J. Rocha, A. M. Fonseca, F. Baltazar, I. C. Neves, *J. Phys. Chem. C*, 116 (2012) 25642–25650.
10. H. F. Youssef, W. H. Hegazy, H. H. Abo-Elmaged, G. T. El-Bassouni, *Bioinorg. Chem. Appl.*, 2015 (2015) 1–12.
11. Y. Watanabe, T. Ikoma, Y. Suetsugu, H. Yamada, K. Tamura, Y. Komatsu, J. Tanaka, Y. Moriyoshi, *J. Eur. Ceram. Soc.*, 26 (2006) 469–474.
12. S. V. Dorozhkin, *Biomaterials*, 31 (2010) 1335–1363.
13. J. M. Gómez, E. Díez, A. Rodríguez, M. Calvo, *Micropor. Mesopor. Mat.* 270 (2018) 220–226.
14. F. Hasan, R. Singh, G. Li, D. Zhao, P. A. Webley, *J. Colloid Inter. Sci.* 382 (2012) 1–12.

The novel inhibitor of cysteine proteases

K. Piechura¹, P. Mielczarek^{1,2}, J. Silberring^{1,3}

¹Department of Biochemistry and Neurobiology, AGH University of Science and Technology, Cracow, Poland; ²Institute of Pharmacology, Polish Academy of Science, Cracow; ³Centre of Polymer and Carbon Materials, Polish Academy of Sciences, Zabrze, Poland

jerzy.silberring@agh.edu.pl

ABSTRACT

Years of research proved the importance of enzyme inhibitors. Such compounds may serve as potential drugs, by controlling the activity of enzymes, which seems to be disrupted in various pathophysiological states. Moreover, besides acting as therapeutic agents, these compounds may also play significant role in biological and clinical studies. Namely, immobilized or labeled inhibitors can be applied to localize and identify a given class of enzymes, and thus, they may comprise useful of biological probes. In the present work, the novel inhibitor of cysteine proteases and its potential use in identifying this class of enzymes, have been described.

Keywords: enzymes, inhibitors, peptides, analysis

METHODOLOGY

To obtain inhibitor, the standard Fmoc solid-phase synthesis has been used. The structure of a synthesized compound was confirmed by MALDI-TOF/TOF mass spectrometry. To purify the obtained peptide, reversed phase HPLC has been applied. The enzymatic reactions were performed using the model enzyme – Staphopain C.

CONCLUSIONS

The novel inhibitor of cysteine proteases has been synthesized. Using mass spectrometry, it was performed that obtained compound act by binding to the active site of enzyme. It was demonstrated that inhibitor binds to cysteine of Staphopain C (confirmed by MS/MS spectra). Owing to interest of our group in enzymes that convert neuropeptides, this research is a part of our long-term studies aimed at identifying and isolating the enzymes that convert dynorphins to shorter, bioactive fragments.

Acknowledgements: Authors are grateful to the The National Centre for Research and Development under the project No. POWR.03.02.00-00-I004/16. and to the Polish-Taiwanese collaborative grant HEMO (PL-TW/V/2017/17).

Biocompatible polymer materials with antimicrobial properties for preparation of stents

K. Škrlová¹, Z. Rybková², K. Malachová², D. Plachá¹

¹VŠB - Technical University of Ostrava, Czech Republic; ²University of Ostrava, Czech Republic

katerina.skrlova@vsb.cz

ABSTRACT

In this study were prepared antibacterial and antimicrobial materials, which may be suitable as materials for biodegradable stents. In the first phase were prepared fillers, which were tested for their antibacterial and antimicrobial properties. Tests using disc methods or minimal inhibition concentration determination confirmed their antibacterial and antimicrobial character and consequently polymer composites using these antibacterial fillers were prepared. However, resulting polymer samples do not show antibacterial and antimicrobial character.

Keywords: Polylactide; stents; antibacterial; antimicrobial; biodegradable

INTRODUCTION

Diseases of blood vessels and other body ducts are an extensive problem of current medicine. Severe illnesses cause narrowing and clogging of body ducts and a patient suffers from severe pain. Stents are one of solutions of this problem. The stents are small tubes made of plastic or metal which are used to restore the body fluids flows and strengthen the walls of ducts. In this study biodegradable polymeric materials were prepared which were modified by antibacterial fillers. These materials can be used in the future as material for stents.

EXPERIMENTAL/THEORETICAL STUDY

In first phase were prepared antibacterial fillers which were created by combination of graphene oxide, vermiculite, silver, hexadecylpyridinium bromide and hexadecyltrimethylammonium bromide.

The fillers were tested for antibacterial properties and characterization properties.

In second phase were prepared biodegradable polymeric materials which were modified by antibacterial fillers. For every samples polylactide granules were used, which were provided by company Plasty Mladeč. Six samples were prepared in three concentrations. Four samples were

modified by antibacterial fillers and then the samples were tested for antibacterial properties and selected methods were used for characterization.

RESULTS AND DISCUSSION

Fillers were tested for their antibacterial and antimicrobial properties. Some samples showed antibacterial and antimicrobial properties. Therefore, were prepared modified polymeric samples which were also tested for their effects. However, polymer samples do not show distinctive antibacterial and antimicrobial character. Polylactide is biodegradable polymer which has a long degradation time. Likely, fillers are enclosed within the polymer and are not released within a short (24 hours) time interval. Our new approach was to prepare a long-time degradation tests throughout them antimicrobial and antibacterial properties were tested continuously.

CONCLUSION

We prepared five fillers with antimicrobial and antibacterial properties which were confirmed using disc method and minimal inhibition concentration. Then six polymeric samples with antibacterial and antimicrobial fillers were made without no antimicrobial activity. It was due to polymer composite structure which does not release antimicrobial fillers. New approach is prepared to study process of fillers release.

Acknowledgments: This paper was created by the project No. CZ.02.1.01/0.0/0.0/17_049/0008441 „Innovative therapeutic methods of musculoskeletal system in accident surgery“ within the Operational Programme Research, Development and Education financed by the European Union and from the state budget of the Czech Republic, and by project Development of biocompatible nanocomposite materials with antimicrobial effects (SP2019/23).

Application of silver nanoparticles for analysis of pharmaceutical samples by microchip isotachophoresis with Raman spectroscopy

M. Masár¹, P. Troška¹, J. Hradski¹, I. Talian²

¹Department of Analytical Chemistry, Faculty of Natural Sciences, Comenius University in Bratislava, Slovakia; ²Department of Medical and Clinical Biophysics, Faculty of Medicine, Pavol Jozef Šafárik University in Košice, Slovakia

peter.troska@uniba.sk

ABSTRACT

Surface enhanced Raman spectroscopy (SERS) based on the use of silver nanoparticles (Ag-NPs) was investigated as a new detection technique for microchip isotachophoresis (μ ITP). A polymer microchip with coupled separation channels was preferred for μ ITP separations of four synthetic dyes. Sample was injected into the microchip in the presence of discrete spacers, which provided spatial separation of the analytes. A 532 nm Raman laser was focused at the beginning of the second separation channel of the microchip containing mixture of Ag-NPs and leading electrolyte. This approach led to reliable identification of Raman-active dyes present in model sample as low as 0.2 μ mol/L. The proposed μ ITP-SERS method was applied to the qualitative analysis of pharmaceutical preparations.

Keywords: Silver nanoparticles, microchip isotachopheresis, surface enhanced Raman spectroscopy, synthetic dyes

INTRODUCTION

Microchip isotachopheresis (μ ITP) is a miniaturized electrophoretic separation technique characterized by low sample and reagents consumption and reduced waste production. Various detection techniques, such as laser-induced fluorescence,¹ conductivity detection² and Raman spectroscopy³ have been combined with μ ITP. Surface enhanced Raman spectroscopy (SERS) provides greatly enhanced Raman signal for Raman-active molecules that have been adsorbed onto specially prepared metal surfaces, e.g. silver nanoparticles. Combination of zone electrophoresis performed on a glass microchip and SERS using silver nanoparticles (Ag-NPs) was applied to detection of riboflavin in a barbecue sauce.⁴ So far, this detection technique has not been coupled to μ ITP having huge preconcentration power.

This work was focused on the use of Ag-NPs for development of new μ ITP-SERS coupling for the identification of the dyes in pharmaceutical preparations.

EXPERIMENTAL

ITP separations were carried out on a microchip with coupled separation channels (CC) and integrated conductivity detection. Raman spectra were obtained using a Raman Spectrometer B&W Tek Model BWS 415-532H. Ag-NPs were synthesized according to the Lee-Meisel protocol.⁵ Stock solutions of the analytes (Ponceau 4R, Brilliant Black, Sunset Yellow and Azorubine), discrete spacers (glutaric acid, acetic acid, butyric acid, valeric acid and pantothenic acid) and leading (LE) and terminating electrolyte (TE) solutions were prepared from p.a. chemicals. Samples of pharmaceutical preparations (Coldrex and Strepsils) were purchased in local pharmacy. Prior to the analysis, samples were dissolved, centrifuged for 2 min and diluted appropriately.

RESULTS AND DISCUSSION

Electrolyte solutions with pH 6.0 (LE) and pH 6.1 (TE) were used for the μ ITP separations of the dyes. The spatial separation of the dyes was achieved by addition of discrete spacers to the injected sample. An isotachopherograms from the separation of the dyes obtained from conductivity detector implemented in the first separation channel of the CC microchip are shown in Fig. 1 A, B. The second channel of CC microchip was filled with a mixture of Ag-NPs and LE (1:1). Raman spectra of the separated compounds were acquired in timeline of 50 ms at the beginning of the second separation channel. This approach allowed reliable identification of the dyes present in the model samples at 0.2 μ mol/L concentration (Fig. 1 B1-B4).

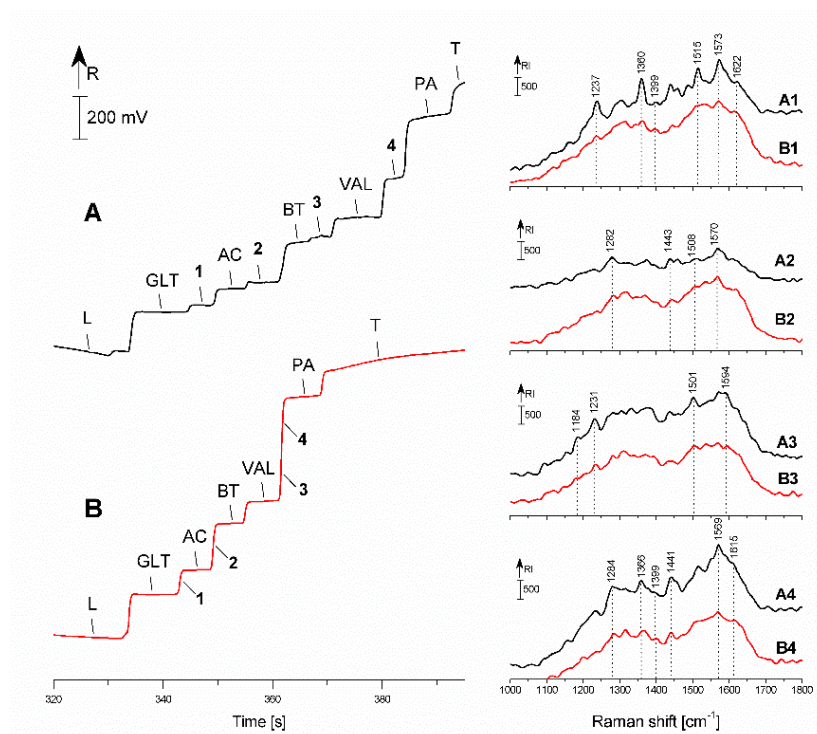


Fig. 1. μ ITP-SERS analyses of the dyes (1 - Ponceau 4R, 2 - Brilliant Black; 3 - Sunset Yellow; 4 -Azorubine). ITP separations of the dyes at (A) 0.2 mmol/L and (B) 0.2 μ mol/L concentration with addition of discrete spacers (GLT - glutarate; AC - acetate; BT - butyrate; VAL - valerate; PA - pantothenate) at 0.5 mmol/L concentration. SERS spectra of (A1, B1) Ponceau 4R, (A2, B2) Brilliant Black, (A3, B3) Sunset Yellow and (A4, B4) Azorubine acquired under the given ITP separation conditions. L - leading ion; T - terminating ion; R - resistance; RI - Raman intensity.

The proposed μ ITP-SERS approach was applied for qualitative analysis of synthetic dyes in pharmaceutical preparations (Coldrex and Strepsils). Samples pretreated only by centrifugation were injected together with discrete spacers to the microchip. Ag-NPs which were added to the second separation channel of the CC microchip allowed reliable identification of Ponceau 4R and Brilliant Black in Coldrex sample, and Ponceau 4R and Sunset Yellow in Strepsils sample.

CONCLUSION

This work has shown analytical potential of newly developed μ ITP-SERS combination using Ag-NPs for the identification of synthetics dyes in pharmaceutical preparations.

Acknowledgments: This research was supported by the Slovak Research and Development Agency (APVV-0259-12 and APVV-17-0318) and by the Slovak Grant Agency for Science (VEGA 1/0787/18).

REFERENCES

1. G.V. Kaigala, M. Bercovici, M. Behnam, D. Elliott, J.G. Santiago, C.J. Backhouse, Lab on a chip 10 (2010) 2242-2250.
2. M. Masár, J. Hradski, in: D. Dutta (Eds.) Microfluidic Electrophoresis. Methods in Molecular Biology, Humana Press, New York, 2019, pp. 99-111.
3. P.A. Walker, M.D. Morris, M.A. Burns, B.N. Johnson, Anal. Chem. 70 (1998) 3766-3769.
4. A. Tycova, R.F. Gerhardt, D. Belder, J. Chromatogr. A 1541 (2018) 39-46.
5. P.C. Lee, D. Meisel, J. Phys. Chem. 86 (1982) 3391-3395.

Molecular modeling study of antibacterial molecules on nylon 6,6 surface

A. Verner¹, J. Tokarský^{1,2}

¹Nanotechnology Centre, VŠB-Technical University of Ostrava, Czech Republic; ²IT4Innovations, VŠB-Technical University of Ostrava, Czech Republic

adam.verner.st@vsb.cz

ABSTRACT

Present study is focused on the molecular modeling of various compounds serving as antibacterial agents – nystatin (NYS), chlorhexidine (CH), and dodecyltrimethylammonium bromide (DTAB) – on ideal and imperfect, i.e. containing surface defects, (100) and (010) surfaces of nylon 6,6 nanofibers. The study was performed in the Materials Studio/Forcite modeling environment using COMPASS force field. After successful validation of modeling strategy, interactions between the molecule and the surface were monitored. Also the movement of the molecules over the surface was simulated under normal conditions (atmospheric pressure and temperature 25 °C). NYS exhibits the strongest attractive interaction with nylon 6,6 while the weakest interaction was observed in the case of nylon 6,6 - DTAB models. The study revealed importance of size and shape of antibacterial molecules on the interaction. Stronger interaction between DTAB or CH and the imperfect nylon 6,6 surface were observed in comparison with NYS-containing models. The diffusion coefficients of single antibacterial molecules were determined on each surface and compared with diffusion coefficients obtained from the models containing higher number of molecules. The results can be used for further experimental research on nonwoven textile prepared from the surface-modified nylon 6,6 nanofibers in various applications where the antibacterial properties are needed.

Keywords: molecular modeling, nanofiber, antibacterial agent, interaction

INTRODUCTION

Nanofibers are currently being studied primarily as drug carriers^{1,2} and antibacterial layers^{3,4}. However, interactions between molecules on nanofibers are still poorly described and explained. Along with increasing computing power, molecular modeling can be used to explore nanostructures more closely. In this work, interactions between antibacterial agents (NYS, CH, DTAB) and polymeric surface (nylon 6,6) were studied for the first time using molecular modeling. Two planes of nylon 6,6 structure and their ideal and imperfect versions have been studied to describe the surface structure of the fibers. In particular, interaction energies and diffusion coefficients were determined. Deeper understanding of these interactions could lead to new applications and modifications to existing structures.

EXPERIMENTAL / THEORETICAL STUDY

Models containing NYS, CH, and DTAB molecules on (100) and (010) surfaces of nylon 6,6 structure (denoted as NYL66_100 and NYL66_010) were studied under periodic boundary conditions using geometry optimization and molecular dynamics calculations performed in Materials Studio / Forcite module. Antibacterial molecules / NYL66 interaction energies were calculated from optimized models. Means square displacement of the molecules on NYL66_100 and NYL66_010 were determined from the molecular dynamics trajectories.

RESULTS AND DISCUSSION

Accuracy of the modeling strategy used was confirmed via comparison of CH / nylon 6 model with previously published data⁵. A good match found proved the suitability of the modeling strategy used for the intended purpose. The surface of NYL66_100 appears to be a more suitable variant for anchoring antibacterial molecules than NYL66_010 because of stronger interactions between the molecule and the surface. This is due to better availability of functional groups of polymer chains. The most suitable orientation of the NYS molecule on NYL66_100 is the angle of 90° of its longest axis to NYL66 chains, while for DTAB the position parallel to the NYL66 chains is preferred. The CH molecule tends to lie flat on the surface. Stronger interactions with CH and DTAB molecules have been observed in the case of imperfect surfaces with missing chains (denoted as NYL66_100_I and NYL66_010_I). A significant change in orientation was observed for CH on NYL66_010_I where the CH molecule was angled with its edge to the imperfect surface. This position was found to be the most stable, i.e., the most energy-efficient (Fig. 1).

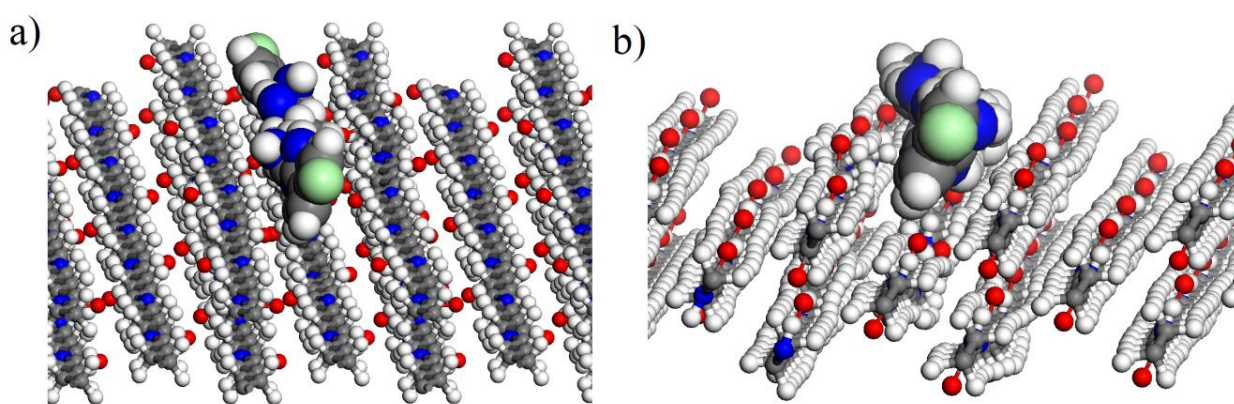


Fig. 1. The most energy-efficient orientation of the NYS molecule on the imperfect surface of (a) NYL66_010_I, and (b) NYL66_100_I. Color legend: C – grey, H – white, O – red, N – blue, Cl – green

Using molecular dynamics, it was found that the diffusion coefficient of single smaller molecules (DTAB, CH) on NYL66_010 and NYL66_100 surfaces is greater than the diffusion coefficient found in models containing higher amount of molecules on NYL66 surfaces. The reason is the formation of molecular clusters, and the associated decrease in potential energy. Only for diffusion coefficient of the heaviest and least movable NYS, no significant difference between the single molecule on NYL66_010 and the multi-molecule systems was found.

CONCLUSION

This work showed differences in the behavior of antibacterial molecules on the NYL66 surface. The results of this work and the modeling strategy used may be helpful in designing new antibacterial nanomaterials, or to understand the interactions in already existing nanofiber-based nanostructures containing antibacterial agents.

Acknowledgements: This work was supported by the Ministry of Education, Youth and Sports of the Czech Republic, project SP2019/31, and LQ1602 (National Programme of Sustainability II “IT4Innovation of Science Excellence”).

REFERENCES

1. P. Jaituronga, B. Sirithunyaluga, S. Eitsayeamb, C. Asawahamec, P. Tipduangtaa, J. Sirithunyalug, *Asian J. Pharm. Sci.* 13 (2018) 239 – 247
2. S.W. Tsai, W.X. Yu, P.A. Hwang, S.S. Huang, H.M. Lin, Y.W. Hsu, F.Y. Hsu, *Pharm.* 10 (2018) 179
- A. Celebioglu, F. Topuz, Z.I. Yildiz, T. Uyar, *Carbohydr. Polym.* 207 (2019) 471 – 479
3. W.Y. Cheah, P.L. Show, I.S. Ng, G.Y. Lin, C.Y. Chiu, Y.K. Chang, *Int. J. Biol. Macromol.* 126 (2019) 569 – 577
4. P. Ryšánek, M. Malý, P. Čapková, M. Kormunda, Z. Kolská, M. Gryndler, O. Novák, L. Hocelíková, L. Bystrianský, M. Munzarová, *J. Polym. Res.* 24 (2017) 208

TOPIC 5

Nanotech for Environmental Solution

Chair: Ivo Šafařík

Green chemistry for nanomaterials

Environmental chemistry

Ecotoxicology and Environmental Safety



Invited lecture (IL):**Neutron Activation Analysis and Related Analytical Techniques in the Assessment of Nanoparticle Uptake in Organisms**

I. Zinicovskaia^{1,2,3}

¹Department of Nuclear Physics, Joint Institute of Nuclear Research, Dubna, Russian Federation;

²Department of Nuclear Physics /Horia Hulubei National Institute for R&D in Physics and Nuclear Engineering, Romania; ³The Laboratory of Quantum Chemistry, Chemical Kinetics and Magnetic

Resonance, The Institute of Chemistry, Moldova

zinikovskaia@mail.ru

ABSTRACT

Nanomaterials, including metal nanoparticles, are widely used today in industry as well as ordinary life. Despite the rapid development of nanotechnology, information about the exposure of humans and the environment to nanoparticles is very scanty. To understand the effect of metal nanoparticles on living organisms it is important to estimate the amount of nanoparticles accumulated by living organisms and to depict their localization. Present work focuses on application of neutron activation analysis and electron microscopy techniques in the investigation of metal nanoparticles uptake by living organisms.

Oral presentations (OP):**Mechanochemistry as a versatile tool for nanomaterials synthesis**

M. Baláž

Institute of Geotechnics, Slovak Academy of Sciences, Slovakia

balazm@saske.sk

ABSTRACT

Mechanochemistry represents an environmentally friendly approach for the nanomaterials synthesis. On the contrary to traditional methods, there is no need to utilize toxic organic solvents and precursors, as the synthesis is realized in solid state and at ambient conditions. Our research group has a large experience in this field. In this presentation, examples of application of this method for the synthesis of nanomaterials for various purposes will be demonstrated. Namely, the methodology of mechanochemical synthesis of nanomaterials for energy conversion (namely solar cells absorbers and thermoelectric materials), for biomedical applications (quantum dots) or with antibacterial activity (silver nanoparticles) will be briefly described. The possibility to up-scale these processes will be also mentioned.

Keywords: Mechanochemistry, nanoparticles, energy, biomedicine, antibacterial agents, up-scale

INTRODUCTION

Mechanochemistry with its ability to utilize tools of high-energy ball milling is suitable for various research fields. This method is still gaining popularity. Regarding the scope of this conference, a short review on the nanoparticles production using this method could be interesting. This particular viewpoint was exhaustively summarized in paper ¹. Our research group devotes a significant effort toward broadening the utilization scope of this method, also within the nanomaterials synthesis research field. Within this report, I would like to highlight three possible application fields of the nanomaterials prepared within our group and the up-scale possibilities.

ENERGY CONVERSION

Nanocrystalline chalcogenides are suitable materials for energy conversion applications. In couple of works, we focused on the preparation of sulfides suitable as solar cells absorbers or for thermoelectric materials. As examples binary copper sulfide CuS, ternary molybdenite Cu₂SnS₃, or quaternary kesterite Cu₂ZnSnS₄, and stannite Cu₂FeSnS₄, representing cheaper and safer alternative in comparison with CIGS solar cells, can be mentioned. The synthetic method is very straightforward, as just stoichiometric mixture of elements is co-milled and the products can be prepared until 1 hour, which is much faster than in the case of classical solution-based synthesis of NPs ²⁻⁵. However, as the production of whole solar cell is a challenge, we stayed only at the synthetic level. In order to prepare a functioning solar cell device, intensive collaboration with other research groups would be necessary to finalize the process.

The sulfide-based nanomaterials, namely those with iron in structure, are suitable also for thermoelectric applications, thus converting thermal energy into electric one. Very recently, a paper on mechanochemical synthesis and thermoelectric performance of quaternary sulfide mawsonite Cu₆Fe₂SnS₈ was published ⁶. The key here is that mechanochemistry brings about very strong reduction in particle size, defects and disharmony into the structure, which is favorable, as it

decreases the thermal conductivity of the products, which is beneficial for the final thermoelectric effect.

BIOMEDICAL APPLICATIONS

Mechanochemical approach has been successfully applied also for the preparation of quantum dots, namely based on CdS nanocrystals, exhibiting excellent fluorescent properties, which could be thus used in bioimaging applications. However, if pure elements were used for the synthesis, it was not possible to obtain nanocrystals with size small enough to serve their roles as quantum dots. If the compounds are applied as precursors (so-called acetate route), it is possible to obtain NPs of few nanometers. Due to toxic nature of cadmium, it was necessary to make a composite with another material, in order to stop its leakage and additionally boost its luminescent properties. This was achieved by introduction of zinc sulfide⁷. The final composite had the necessary properties, but in order to be applied to human body, it needs to be capped with biocompatible organics. For this purpose, L-cysteine and polyvinyl pyrrolidone were used and the capping procedure was performed in wet stirred media mill, which resulted in the formation of nanosuspension⁸. This was then applied for *in vitro* tests on cancer cell lines.

ANTIBACTERIAL APPLICATIONS

Green synthesis using biological materials (e.g. plant extracts) for the reduction of silver into its elemental form is being widely applied these days. However, it is possible to prepare silver nanoparticles with antibacterial activity also by a solid-state approach, by directly milling the plant material with silver nitrate serving as a precursor of Ag NPs⁹⁻¹⁰. The advantage of mechanochemistry in this case is the stability of the prepared products (powder form) and the possibility to obtain nanoparticles also when higher concentrations of the precursor are used.

UP-SCALE

Mechanochemistry can be up-scaled from laboratory to the hundred-gram, or even pilot plant scale. The eccentric vibratory mill can be used for larger scale production of already mentioned kesterite and mawsonite nanomaterials^{6, 11}. Twin screw extrusion is also very interesting alternative, which offers continuous production of the desired materials by applying similar forces as ball milling¹².

CONCLUSION

In this brief review, the possibilities of using mechanochemistry for nanomaterials synthesis have been outlined. As it was demonstrated, it is applicable for different fields (e.g. for solar cells or thermoelectric materials, for biomedical applications or antibacterial nanomaterials). Its environmental soundness is particularly attractive and is the key of the recent research interest into this method.

Acknowledgements: This study was supported by Slovak Agency VEGA G/0044/18, Slovak Agency for Science and Development (project no. APVV-14-0103) and COST Action CA18112: Mechanochemistry for Sustainable Industry.

REFERENCES

1. P. Baláž; M. Achimovičová; M. Baláž; P. Billík; Z. Cherkezova-Zheleva, et al., Chem. Soc. Rev. 42 (2013) 7571-7637. M. Baláž; A. Zorkovská; F. Urakaev; P. Baláž; J. Briančin, et al., RSC Adv. 6 (2016) 87836-87842.
2. P. Baláž; M. Baláž; M.J. Sayagués; I. Škorvánek; A. Zorkovská, et al., Nanoscale Research Letters 12 (2017) art. ID 256.
3. M. Baláž; N. Daneu; M. Rajňák; J. Kurimský; M. Hegedüs, et al., J. Mater. Sci. 53 (2018) 13631-13642.
4. M. Hegedüs; P. Baláž; M. Baláž; P. Šiffalovic; N. Daneu, et al., J. Mater. Sci. 53 (2018) 13617-13630.
5. P. Baláž; M. Hegedüs; M. Reece; R. Zhang; T. Su, et al., J. Electron. Mater. 48 (2019) 1846-1856.

6. P. Baláž; M. Baláž; E. Dutková; A. Zorkovská; J. Kováč, et al., *Mater. Sci. Eng., C* 58 (2016) 1016-1023.
7. Z. Bujňáková; M. Baláž; E. Dutková; P. Baláž; M. Kello, et al., *J. Colloid Interface Sci.* 486 (2017) 97-111.
8. M.J. Rak; T. Friscic; A. Moores, *RSC Adv.* 6 (2016) 58365-58370.
9. M. Baláž; N. Daneu; L. Balážová; E. Dutková; L. Tkáčiková, et al., *Adv. Powder Technol.* 28 (2017) 3307-3312.
10. P. Baláž; M. Hegedüs; M. Achimovičová; M. Baláž; M. Tešínský, et al., *ACS Sust. Chem. Eng.* 6 (2018) 2132-2141.
11. D.E. Crawford; J. Casaban, *Adv. Mater.* 28 (2016) 5747-5754.

Magnetically modified bentonite: characterization and stability

K. Drobíková^{1,2}, K. Štrbová^{1,3}, M. Tokarčíková¹, O. Motyka¹, J. Seidlerová¹

¹Nanotechnology Centre, VŠB – Technical University of Ostrava, Czechia;

²IT4Innovations Centre of Excellence, VŠB – Technical University of Ostrava, Czechia;

³ENET Centre, VŠB – Technical University of Ostrava, Czechia

klara.drobikova@vsb.cz

ABSTRACT

Bentonite – clay mineral of smectite group, with main portion of montmorillonite is a sorbent widely used in waste water treatment. The aim of the presented work was to evaluate the effect of the microwave radiation on the structure and stability of raw bentonite, which is to be applied as a sorbent of ions from water solution. Water extracts were prepared by batch method using deionized water. The leachate was prepared for 1, 6 and 24 hours in different ratios of solid and liquid phase from the samples of raw clay and the magnetically modified clay – prepared by interaction with microwave radiation. In the filtrate, pH was determined as well as concentrations of Al, Ca, Fe, K, Mg, Na and Si using Atomic emission spectrometry with inductively coupled plasma. The results imply that microwave treatment of the bentonite changes the pH of the leachates to more acidic compared to the raw bentonite in which the pH increases. Magnetically modified bentonite treated by microwaves contained 2.67 wt. % of the iron oxide which is four times more than in the raw bentonite. The microwave treatment of bentonite did not cause higher leaching of observed elements in comparison with the raw bentonite.

Keywords: Bentonite, leaching, microwave treatment, iron oxide

INTRODUCTION

Clays and clay minerals play important role as natural scavengers of toxic species in the environment via ion exchange or adsorption or both¹. One of the clays most widely used as adsorbents is bentonite – due to its large specific surface area, chemical and mechanical stability, relative high cation-exchange capacity and good adsorption capability, wide availability and low cost². Bentonite consist mainly of montmorillonite (hydrous magnesium-calcium-aluminium silicate) – clay mineral of smectite group³. Bentonite has a net negative surface charge; thus, it is efficient for removal cationic compounds. However, it has limitations in practical application in waste water treatment due to its difficulty of separating from the water, its modification is, therefore, necessary. On the other hand, magnetic materials such as Fe₃O₄ can be separated from the solution easily using external magnetic fields, therefore, combination of bentonite with Fe₃O₄ can result in a magnetic hybrid with high adsorption capacity for variety of pollutants⁴.

EXPERIMENTAL/THEORETICAL STUDY

Magnetically modified bentonite was prepared by a simple method using microwave radiation⁵. The raw bentonite and magnetically modified bentonite were studied using scanning electron microscopy and X-ray powder diffraction. Raw clay material (bentonite) was dried, milled, and sieved. Clay particles having size $\leq 40 \mu\text{m}$ were used for the experiments. Two sample types were used for the experiment – raw bentonite (RB) and magnetically modified bentonite (MB). Both RB and MB were leached in DEMI water using the batch method. The leachates were prepared for 1, 6, and 24 hours in different ratios of solid and liquid phase from RB and MB (1:10 000, 1000, 500, 100 resp.). In the filtrates, the pH value was determined as well as the concentrations of K, Na, Ca, Mg, Al, Fe and Si using Atomic emission spectrometry with inductively coupled plasma (AES-ICP).

RESULTS AND DISCUSSION

Magnetically modified bentonite treated by microwaves contained 2.67 wt. % of the iron oxide which is four times more than in the raw bentonite (0.65 wt. %). The pH values of the leachate provide important information on the two-way interaction between the solid and liquid phase. Elements present in the solid phase may dissolve into the extraction solution (DEMI water) and alter the pH, as shown in Fig. 1. Microwave treatment of the material during magnetically modified bentonite preparation led to a shift of the leachate pH towards more basic values (around 7.48), while the pH was unaffected by the particular time of the treatment. The leachate pH from the original material was 6.75–8.89 which reflects the inhomogeneity of the bentonite samples. The elements of ion exchange leached to the water mainly in the case of RB. The leaching of the magnetically modified bentonite did not affect the amount of Fe in MB.

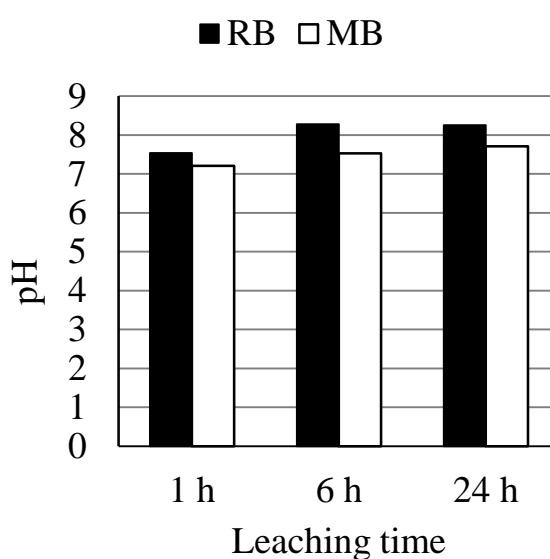


Fig. 1. pH of extract solution prepared from RB and MB.

CONCLUSION

The raw bentonite and its modified form were subjected to 1, 6 and 24 hour leaching in deionized water applying various ratios of solid and liquid phase. Magnetically modified bentonite treated by microwaves contained four times more iron oxide than raw bentonite. Hence, it was proved that the magnetic iron oxides are bound to the magnetically modified bentonite more strongly and are, most

probably, located on its surface. Microwave radiation was found not to affect the leaching of the elements of the basic structure of the bentonite (Al and Si).

Acknowledgments: The work was supported by ERDF/ESF New Composite Materials for Environmental Applications (No. CZ.02.1.01/0.0/0.0/17_048/0007399), the Ministry of Education, Youth and Sports of the Czech Republic, grant numbers SP2019/70 and LQ1602 (National Programme of Sustainability II).

REFERENCES

1. R. Srinivasan, Adv. Mater. Sci. Eng. (2011) 1-17
2. M. Toor, B. Jin, S. Dai, and V. Vimonses, J. Ind. Eng. Chem. 21 (2015) 653-661
3. F. Uddin, Montmorillonite: An Introduction to Properties and Utilization, in Current Topics in the Utilization of Clay in Industrial and Medical Applications, IntechOpen, London, 2018
4. L. Jiang, Q. Ye, J. Chen, Z. Chen, and Y. Gu, J. Colloid Interface Sci. 513 (2018) 748-759
5. Šafařík, I. and M. Šafaříková, Int. J. Mater. Res. 105 (2014) 104-107

Microwave preparation of activated carbons from residual agricultural biomass

Z. Jankovská¹, M. Vaštyl¹, G. J. F. Cruz², L. Matějová¹

¹Institute of Environmental Technology, VŠB – Technical University of Ostrava, 17. listopadu 15/2172, 708 00 Ostrava-Poruba, Czech Republic; ²Universidad Nacional de Tumbes, Facultad de Ciencias Agrarias, Laboratorio de Análisis Ambiental, Av. Universitaria s/n, Campus Universitario– Pampa Grande, Tumbes, Peru

zuzana.jankovska@vsb.cz

ABSTRACT

Activated carbons have been used as adsorbents, catalysts support and energy storage materials. Microwave heating in inert atmosphere (microwave pyrolysis) is a promising technology for the preparation of activated carbon due to its short processing time and fast, selective and volumetric heating, compared to conventional heated pyrolysis. This work deals with the microwave pyrolysis of three raw materials - coffee husk, cocoa pod husk and corn cob, with and without chemical activator (ZnCl_2 vs. K_2CO_3). The effect of raw material treated and chemical activator was evaluated with respect to the yield of microwave pyrolysis products, rate of raw material carbonization and textural properties of prepared activated carbons.

Keywords: microwave, pyrolysis, chemical activation, agricultural waste biomass, activated carbon

INTRODUCTION

Coffee (*Coffea Arabica L.*), cacao (*Theobroma cacao*) and corn (*Zea mays*) are three of the most promising agricultural products in Peru. Processing of these raw materials generates a significant amount of waste that is usually composed of organic matter with different biodegradability. Only a part of these materials is recycled as animal food, for the production of fertilizers or energy. The rest is disposed of in dumps or burnt. One of feasible alternatives to recycle such residues is to use them as precursors for the production of activated carbon (AC), a material with a large surface area and usually a large portion of micropores, suitable for adsorption and catalytic applications¹. Microwave heating in inert atmosphere (microwave pyrolysis) can be a suitable alternative to

conventional methods for the production of AC due to its fast, uniform and volumetric heating, no direct contact between microwave source and biomass, shorter processing time and saving more energy and cost, compared to conventional heating¹.

Nowadays, the number of studies focused on microwave pyrolysis of biomass is growing. On the other hand, there is limited information on the characterization of ACs from the pyrolysis of various biomass types, activators and microwave pyrolysis conditions. Thus, this work investigates the effect of different agricultural raw materials and chemical activators on the physicochemical properties of ACs prepared by microwave pyrolysis. The yield balance of individual products of microwave pyrolysis was evaluated as well.

EXPERIMENTAL PART

The pyrolysis of three raw materials - coffee husk (CH), cocoa pod husk (CPH) and corn cob (CC) - was carried out in a commercial microwave cavity oven (NNSD 271S, Panasonic). Before microwave pyrolysis, each raw material was crushed into 0.4 - 1 mm particle-size fraction and dried at 80 °C overnight. ZnCl_2 (Penta) and K_2CO_3 (Lachema) were used as chemical activators. Activator was used at a weight ratio of 1:1 (biomass:activator), via impregnation in dry conditions. Pyrolytic char was also added at a weight ratio of 1:5 (biomass: pyrolytic char) to increase microwave adsorption. Prior to the microwave treatment, a quartz flask containing sample (biomass, activator and char) was placed in the oven and purged with nitrogen gas at a flow rate of $150 \text{ ml} \cdot \text{min}^{-1}$ for 2 min to create an oxygen-free atmosphere. Time of pyrolytic microwave treatment was 20 min at power input 440 W. The volatile pyrolyzate was condensed after passing through a water-cooled column and collected in a flask (bio-oil). Not condensed gas was gurgled through three gas washing bottles filled with water and organic solvent (acetone). The amount of clean gas was measured by a gas meter. At the end of the treatment, the solid product (activated carbon, AC) and bio-oil was allowed to cool to room temperature before it was weighed. After that, the AC was washed with 0,15M HCl and distilled water. Finally, all ACs were dried at 105 °C overnight and sieved to required particle-size fraction with respect to its application.

Proximate analysis according to the Standard ASTM D7582 (LECO, TGA 701) was done for raw materials and all ACs. The iodine number of ACs was calculated according to the Standard ASTM D4607-94. Nitrogen adsorption-desorption analysis at 77 K was performed on a 3Flex (Micromeritics, USA) to reveal textural properties of ACs and raw materials. XRF analysis was performed on the Spectro Xeposto spectrometer for raw materials and prepared ACs to determine their chemical composition.

RESULTS AND DISCUSSION

All ACs produced by microwave pyrolysis of raw materials (CC, CPH, CH) were granular. Despite of the same processed initial particle-size fraction (0.4–1 mm) of CH-RM, CPH-RM and CC-RM, the particle-size of produced ACs was different depending on the type of raw material and chemical activator. Chemical activators were chosen according to previous studies^{2,3}. ZnCl_2 and K_2CO_3 were identified as the most effective chemical activators, producing ACs of better textural and adsorptive properties. XRF analysis confirmed sufficient washing of produced ACs, no K_2CO_3 and minimum ZnCl_2 were detected. Concerning the yield balance of individual products of microwave pyrolysis for individual raw materials, the effect of chemical activator addition on microwave pyrolysis of CH, CPH and CC raw materials was proved. The addition of activators increased the yield of AC at the expense of bio-oil and gas. Activators increased AC yields from 20 wt.% (in the case of CPH-AC, ZnCl_2) to 31 wt. % (in the case of CC-AC, K_2CO_3). Different composition of ACs was also confirmed by proximate analysis. The amount of fixed carbons varied from 54 % (in the case of CH-AC, K_2CO_3) to 77 % (in the case of non activated AC from CH). Iodine number measurements and nitrogen physisorption revealed different volume of micropores in individual ACs (based on

iodine number the highest for CPH-AC, K_2CO_3 and CC-AC, $ZnCl_2$). Different yields of pyrolysis products and textural properties of ACs may be explained by (i) different raw material composition; since cellulose, hemicelluloses and lignin show different volatilization, the differences in the levels of weight loss may depend on the proportion of these lignocellulosic compounds in each raw material⁴, (ii) different type of activator and (iii) different porosity of raw material.

CONCLUSION

The pyrolysis of three raw materials (coffee husk, cacao pod husk and corn cob) with the addition of activators ($ZnCl_2$ and K_2CO_3) was investigated in microwave field. In the case of $ZnCl_2$ activator the best results of AC yield, amount of fixed carbon and ash were obtained by the pyrolysis of corn cob, in the case of K_2CO_3 by the pyrolysis of cocoa pod husk.

Acknowledgements: This work was supported from ERDF “Institute of Environmental Technology – Excellent Research” (No. CZ.02.1.01/0.0/0.0/16_019/0000853). Experimental results were accomplished using Large Research Infrastructure ENREGAT supported by the Ministry of Education, Youth and Sports of the Czech Republic under project No. LM2018098.

REFERENCES

1. R. Wahi, et al. Biomass and Bioenergy 107 (2017) 411-421.
2. G. J. F. Cruz, et al. ACS Sustainable Chem. Eng. 5 (2017) 2368-2374.
3. G. Cruz, et al. Civil Environment Eng. 2 (2012) 1-6.
4. I. G. J. F. Cruz, et al. Water Air Soil Pollut. 226:214 (2015) 1-15.

Effects of Biomass Heterogeneous Composition in Silver Nanoparticles Phytosynthesis Using *Tilia* sp. Leachate

Z. Konvičková^{1,2}, V. Holíšová¹, M. Kolenčík³, K. Dědková⁴, E. Dobročka⁵, H. Otoupalíková¹, G. Kratošová¹, J. Seidlerová¹

¹Nanotechnology Centre, VŠB - Technical University of Ostrava, Czech Republic; ²ENET Centre, VŠB – Technical University of Ostrava, Czech Republic; ³Department of Soil Science and Geology, Slovak University of Agriculture in Nitra, Slovak Republic; ⁴Center of Advanced Innovation Technologies, VŠB – Technical University of Ostrava, Czech Republic; ⁵Institute of Electrical Engineering, Slovak Academy of Sciences, Slovak Republic

zuzana.konvickova@vsb.cz

ABSTRACT

The processes in nature have still inspired us to mimic and copy them to laboratory controlled conditions. We have prepared Ag-AgCl nanoparticles (NPs) via phytosynthesis – a synthesis using leachates from high plants. *Tilia* sp. (linden) biomasses from three different locations have been chosen as verified templates to synthesize Ag-AgCl NPs. However, we have found by FTIR and ion chromatography (IC) analyses a presence of organic and inorganic elements and heterogeneous composition of the biomass used.

Ag-AgCl NPs have been studied by TEM and DLS to determinate their size, by XRD to prove their bi-phase composition and we have studied their physical-chemical properties using ζ-potential. MIC method has been used for antibacterial properties against G+, G- pathogenic bacteria and methicillin-resistant *S. aureus* to prove their functionality in the medicine.

We have observed that different location of harvested linden caused different composition of the biomass and different Ag-AgCl objects have been found. All Ag-AgCl NPs have been bi-phased with different size distributions and morphologies and the most significant antibacterial effects have been found at human pathogens *E. coli* and *P. aeruginosa*.

Keywords: Biosynthesis; silver nanoparticles; interfacial phenomena, antibacterial

INTRODUCTION

Recently, nanoparticles (NPs) have been prepared via bottom-up green method called biosynthesis. Despite countless advantages such as time and financial ease, this method can find several situations negatively influencing the final result. It is the reproducibility of a method whose difficulties lie in: (i) the heterogeneous composition of organic compounds in the organism/leachate/biomass; (ii) large number of these organic compounds complicates the mechanism clarification; (iii) and the presence of inorganic elements that naturally and/or anthropogenically occur in the material. Therefore, some difficulties can be expected during the reproducibility of the metallic NPs' preparation. From the previous experiments we have verified Ag-AgCl NPs biosynthesis protocol¹ and we have prepared three leachates by the same method. We have chosen a linden flower-clusters (*Tilia* sp.) and we have harvested linden from three different locations - the mountain location in Nová Ves u Frýdlantu nad Ostravicí (linden 1), the city of Klimkovice (linden 2) and Hrabyně (linden 3). Finally, we have studied prepared Ag-AgCl NPs using TEM, XRD, ζ -potential, DLS and MIC method to prove their antibacterial properties in medicine.

EXPERIMENTAL STUDY

All three pure leachates have been analyzed prior the biosynthesis by FTIR and IC to identify the part of organic compounds occurring naturally in this biomass and inorganic anions. The resultant colloids with Ag-AgCl NPs (10 mM initial AgNO₃ precursor) have been subjected to TEM, XRD as well as colloidal properties (ζ -potential) and DLS. Final samples have been tested using MIC method for antibacterial properties against *S. aureus*, *E. faecalis*, *E. coli*, *P. aeruginosa* and MRSA.

RESULTS AND DISCUSSION

We have successfully synthesized Ag-AgCl NPs with all three linden samples. However, significant changes have occurred and different biomass composition has influenced NPs' appearance. In all monitored samples Cl⁻, SO₄²⁻ and PO₄³⁻ have been found in tens of mg/L and these can have an influence on Ag-AgCl ratio in final samples. These anions have formed substances such as AgCl and it has been proved by XRD. Further, TEM has depicted: (i) different morphologies from spherical 12 ± 3 nm Ag-AgCl NPs synthesized with linden 1 with presence of 68 ± 12 nm NPs; (ii) growth of silver macrocrystals using linden 2; and (iii) spherical and rod-like 16 ± 6 nm Ag-AgCl NPs synthesized with linden 3 with presence of 43 ± 10 nm NPs.

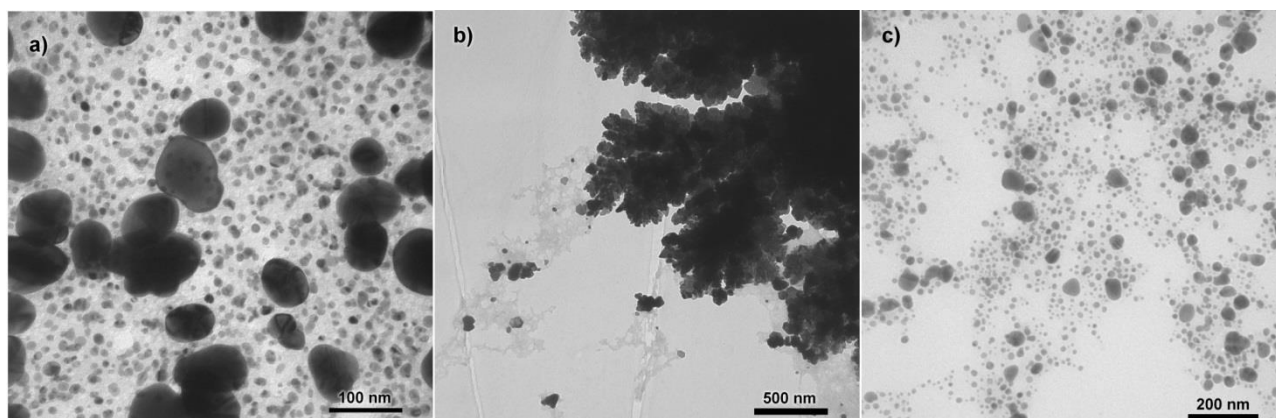


Fig. 1. TEM images of Ag-AgCl NPs phytosynthesized using different linden biomasses: (a) Ag-AgCl NPs synthesized using linden 1 with size 12 nm; (b) silver macrocrystal has grown in the presence of the linden 2 and (c) spherical and rod-like Ag-AgCl NPs synthesized using linden 3.

MIC testing successfully showed Ag-AgCl antibacterial properties among all three samples. We have not been able to confirm the NP size dependency on antibacterial effectiveness however the least sensitive bacteria were, as expected, MRSA and *E. faecalis* (MIC value 11.1 mg/mL). The most significant antibacterial effects have been found at human pathogens *E. coli* and *P. aeruginosa* (MIC value 3.7 mg/mL).

CONCLUSION

We have observed that different location of harvested linden caused different composition of the biomass and different Ag-AgCl objects have been found. All Ag-AgCl NPs have been bi-phased with different size distributions and morphologies. All observed samples have showed antibacterial properties against G- and G+ bacteria and methicillin-resistant *S. aureus*. The most significant antibacterial effects have been found against human pathogens *E. coli* and *P. aeruginosa*. Our future work will focus on synthesis with pure phenolic acids to clarify the possible synthesis mechanism of the metallic NPs.

Acknowledgments: This work supported by the Ministry of Education, Youth and Sports of the Czech Republic under the Students' Grant Competition Project No. SP2019/75 and Slovak Academy of Sciences via grants VEGA 1/0164/17, VEGA 1/0146/18 and KEGA 013SPU-4/2019.

REFERENCES

1. Konvičková, Z. *et al.* Phytosynthesis of colloidal Ag-AgCl nanoparticles mediated by *Tilia* sp. leachate, evaluation of their behaviour in liquid phase and catalytic properties. *Colloid Polym. Sci.* **296**, 677–687 (2018).

Preparation of tailored nanoparticles using flow microreactors and green synthesis

G. Kratošová¹, S. Teplická¹, J. Klusák², M. Večeř²

¹Nanotechnology Centre, VŠB – Technical University of Ostrava, Czech Republic; ²Department of Chemistry, Faculty of Material Science and Technology, VŠB – Technical University of Ostrava, Czech Republic

gabriela.kratosova@vsb.cz

ABSTRACT

Progressive microfluidic techniques could be employed in colloidal metallic nanoparticles preparation. Generally known benefits of microfluidic synthesis compared to batch synthesis are precise control of on-chip reaction, high conversion and selectivity, flexibility, safety and uniform product quality. Advantages of nanoparticle biosynthesis as green, cheap and simple method are already well known. However, the considerable disadvantage of nanoparticles biosynthesis is worse reproducibility. Our goal is to transform green synthesis from batch layout to microfluidic platform to improve both reproducibility and nanoparticles properties.

It was observed, that nanoparticles of gold and silver prepared by microfluidic phytosynthesis were more homogenous and only spherical in comparison to nanoparticles prepared out of chip. Nanoparticles prepared outside the chip had a tendency to form chains and not only spherical particles were observed, but also triangular and hexagonal ones in case of gold and nanorods in case of silver.

Parameters of on-chip synthesis can be flexibly modified and monitored to see how process conditions influence resulting nanoparticles. Moreover, if we realize the importance of green chemistry approaches, green synthesis together with microfluidics may be a current path to reproducible preparation of nanoparticles with uniform characteristics and thus high application potential.

Keywords: microfluidic, phytosynthesis, nanoparticles

Acknowledgments: Authors thank MSMT CR (project SGS No.SP2019/50) for the financial support.

Chlorophyll content in two medicinal plant species following nano-TiO₂ exposure

O. Motyka^{1,2}, K. Štrbová^{1,2,3}, I. Zinicovscaia³

¹Nanotechnology Centre, VSB – Technical University of Ostrava, Ostrava, Czechia; ²ENET Centre, VSB – Technical University of Ostrava, Ostrava, Czechia; ³Department of Power Engineering, Faculty of Mechanical Engineering, VSB – Technical University of Ostrava, Ostrava, Czechia; ⁴Frank Laboratory of Neutron Physics, Joint Institute of Nuclear Research, Dubna, Russia

oldrich.motyka@vsb.cz

ABSTRACT

Chlorophyll content on leaves is a convenient indicator of the physiological state of the plant following an exposure to a stressor. In this study, pot experiment was carried out using two medicinal plant species to establish the link between the chlorophyll content in the plant leaves following the exposure of the plants to nano-TiO₂ either through the leaves (in suspension) or

through the root system (in soil). After the termination of the experiment, the shoots were analysed for the contents of Ti, Al, Ca, K, Mg, Mn, and Na in their tissues. Significant decrease in chlorophyll content was observed in all the nano-TiO₂ treatments, the differences in the determined element content was mostly species-dependent, Ti and Al content was related to each other and the difference in the chlorophyll content.

Keywords: Medicinal plants, chlorophyll, stress, nanoparticles

INTRODUCTION

Since chlorophyll (namely chlorophyll a) is the most sensitive to photodegradation from all the other photosynthetic pigments, its content in plant shoots is a convenient indicator of the impact the exposure to nanoparticles has on the plant¹. Several studies on photosynthetic organisms proved that before any detrimental effect on post-exposure viability or growth was observed, the chlorophyll levels already decreased noticeably^{2,3}. Chlorophyll content was also found in plants when no signs of toxicity were apparent using the conventional toxicological methods⁴. In addition, non-destructive methods using a method based on radiation transmittance allow measurements *in vivo* and monitoring of the response of an individual plant over the course of the experiment⁵.

EXPERIMENTAL STUDY

Mentha X piperita L. and *Salvia officinalis* L. plants were subjected (n = 5 per treatment) either to the TiO₂ nanoparticles either by being planted in the nano-TiO₂ enriched soil (1g/kg) or by exposure of its leaves to nano-TiO₂ suspension (1g/L) for the total of 14 days. Chlorophyll content in the shoots (mmol/m²) was measured both before and following the exposure *in vivo* in set intervals using MC-100 Chlorophyll Concentration Meter (Apogee) in ten replications per measurement. Following the exposure, shoots were dried, pulverized and analysed for content of Ti, Al, Ca, K, Mg, Mn, and Na in their tissues using Neutron activation analysis (NAA).

RESULTS AND DISCUSSION

Chlorophyll content in both the species was originally approximately similar. No significant difference was found in the chlorophyll content of the control plants and suspension-exposed *S. officinalis* plants, significant decrease in chlorophyll content was observed in all the other treatments following 14 days of exposure (ANOVA, $\alpha = 0.05$). Interesting observation was also the significant increase – followed by the decrease in the next, 14 day, measurement – of the chlorophyll content of both the species exposed to NPs via soil in the seventh day of exposure.

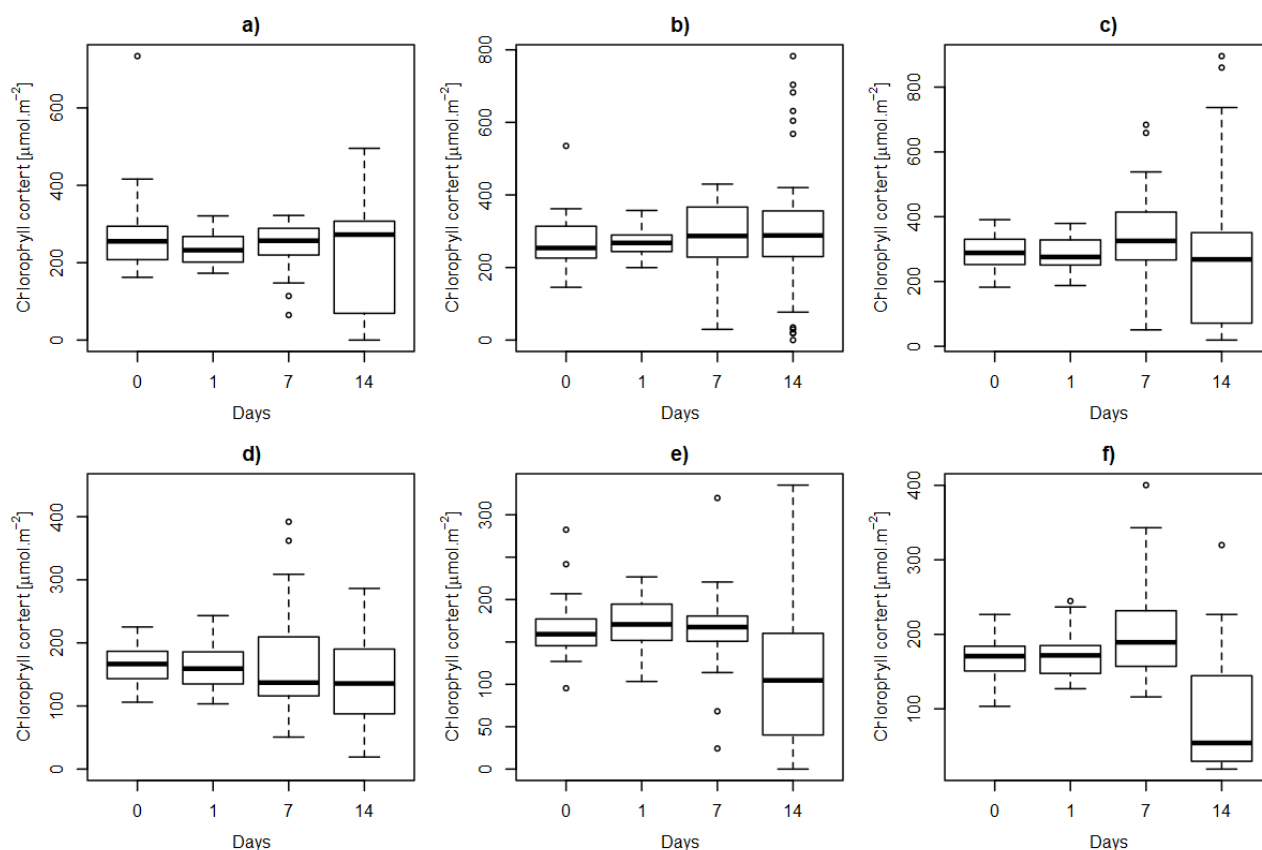


Fig. 1. (a) *S. officinalis*, control; (b) *S. officinalis*, suspension exposure; (c) *S. officinalis*, soil exposure; (d) *M. piperita*, control; (e) *M. piperita*, suspension exposure; (f) *M. piperita*, soil exposure.

The elemental content assessed by NAA reflected mainly the difference in the plant species, the difference between treatments was significant only in the content of Ti. Whereas large amounts of Ti were found in the shoots of the suspension-exposed plants, no detectable amount of Ti was found in controls and soil-exposed plants of both species.

CONCLUSION

The exposure to nano-TiO₂ lead to decrease of the chlorophyll content in most of the treatments except for the suspension-treated *S. officinalis*. This could be caused by the leaf habitus of this species – abundance of trichomes may serve as a natural barrier for the NP accumulation to the symplast. NAA results indicate that no translocation of accumulated NPs from roots to shoots took place, hence, the physiological NP-exposure-induced stress expressed as the chlorophyll content decrease originated in the roots of the soil-exposed plants.

Acknowledgments: This research was supported by the SP2019/90 grant Nanoparticle uptake by plants and their distribution in the plant organism and 3+3 project 209/28 Nuclear methods in nanoparticle phytotoxicity and uptake assessment.

REFERENCES

1. C.M. Rico, J.R. Peralta-Videa, J.L. Gardea-Torresdey, in: M.H. Siddiqui, H.M. Al-Whaibi, F. Mohammad (Eds.), Nanotechnology and plant sciences, Springer Berlin Heidelberg, New York, 2015, pp. 1-17.

2. Mingyu, S., Xiao, W., Chao, L., Chungxiang, Q., Siaoqing, L., Liang, C., Hao, H., Hong, H. Biol. Trace Elem. Res. 119 (2007) 183-192.
3. Lei, Z., Mingyu, S., Chao, L., Liang, C., Hao, H., Xiao, W., Xiaoqing, L., Fan, Y., Fengqing, G., Fashui, H. Biol. Trace Elem. Res. 119 (2007) 68-76
4. Gao, J., Xu, G., Qian, H. Liu, P., Zhao, P., Hu., Y. Environ. Pollut. 176 (2013) 63-70
5. Wei, C., Zhang, Y., Guo, J., Han, B., Yang, X., Yuan, J. Environ. Sci. 22 (2010) 155-160.

Progressive magnetically responsive materials for pollutants detection and removal

I. Safarik^{1,2}, J. Prochazkova¹, E. Baldikova¹, K. Pospiskova², K. Drobikova³, J. Seidlerova³

¹Department of Nanobiotechnology, Biology Centre, Ceske Budejovice, Czech Republic; ²Regional Centre of Advanced Technologies and Materials, Olomouc, Czech Republic; ³Nanotechnology Centre, VSB – Technical University of Ostrava, Ostrava, Czech Republic

ivosaf@yahoo.com

ABSTRACT

Magnetically responsive (bio)materials can be efficiently used both for the analysis and removal of various organic and inorganic pollutants. This presentation will focus on three progressive procedures employing magnetic materials, namely Magnetic solid phase extraction and Magnetic textile solid phase extraction for preconcentration of target analytes, use of iron oxide based peroxidase-like activity for catalytic decomposition of target pollutants, and application of new magnetic adsorbents for pollutants removal.

Keywords: Magnetically responsive materials, magnetic solid phase extraction, nanozymes, adsorption

INTRODUCTION

Magnetically responsive materials of various origin have found many interesting applications in environmental analysis and technology. Preconcentration of analytes from diluted solutions and suspensions has to be often used before the instrumentation analysis; currently especially solid phase extraction procedures are preferred. Pollutants removal can be usually performed by their adsorption to various (bio)sorbents or by (bio)catalytic degradation. All the mentioned procedures can successfully employ magnetic nano- or microparticles or other magnetic materials. New approaches in this area will be summarized.

DISCUSSION

Magnetic solid phase extraction (MSPE) is currently frequently used analytical procedure for the preconcentration, extraction and clean-up of both organic and inorganic pollutants from variety of biological and environmental samples. Recently a new type of preconcentration procedure, based on the use of magnetically modified textile (Magnetic textile solid phase extraction; MTSPE) has been developed (see Fig. 1)¹. This extremely simple procedure has already been used for the extraction of food dyes and copper ions from large volume of water. In the standard procedure, the analytes adsorbed on the textile squares modified with an appropriate affinity ligand are eluted and subsequently analyzed using a suitable analytical procedure, such as spectrophotometry or liquid chromatography. Alternatively, a new analytical approach enabling elution-free assay of colored compounds or reaction products by image analysis of the photos of dyed textile squares was developed; freely available software can be used for evaluation. Using HSB color space, the value of saturation was directly proportional to the initial dye concentration of the analyzed solutions².

Magnetic textile solid phase extraction can be easily adapted for the detection of large variety of analytes important in environmental technology. Further optimization of this procedure can involve the type of textile used, its size and the type of affinity ligand bound.

Peroxidases are catalysts able to decontaminate huge variety of toxic compounds by a free radical mechanism resulting in oxidized or polymerized products exhibiting significantly lowered toxicity. Enzymatic catalysis can offer high selectivity and superior catalytic efficiency under given reaction environment. However, enzymes can be rather expensive and sometimes not sufficiently stable. Currently various types of nanozymes are available which can substitute standard enzymes. Magnetic iron oxide nanoparticles exhibit peroxidase-like activity (see Fig. 1)³ which could be used in environmental technology applications.

Many procedures have been developed for the magnetic modification of originally diamagnetic materials (e.g., organic and inorganic adsorbents and biosorbents). Recently a very simple modification procedure based on the use of microwave synthesized nano- and microparticles has been developed.⁴ This procedure enables to prepare magnetically responsive materials at low cost and with minimum instrumentation. Typical examples of magnetically modified material will be presented.^{5,6}

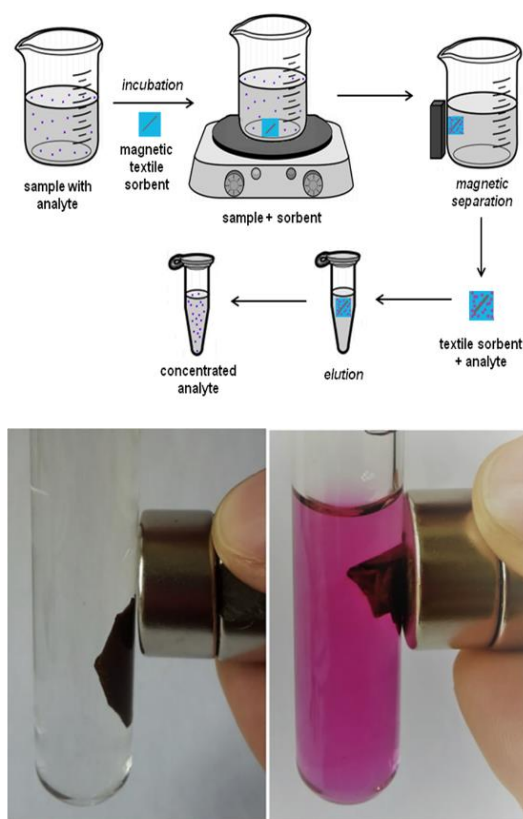


Fig. 1. (left) Scheme of magnetic textile solid phase extraction; (right) peroxidase-like activity of nanotextile modified with magnetic iron oxide nanoparticles.

CONCLUSION

Newly developed magnetically responsive materials and methods can have many interesting applications in environmental analysis and technology, especially for the processes of contaminants removal, based on sorption or catalysis, or for the preconcentration of analytes from diluted solutions (MTSPE). These approaches offer lowering of material costs or simplification of common procedures employing separation of materials by magnetic separators even from difficult environments. Our current research is also intensively focused on easily performable detection and determination methods connected with MTSPE-procedures.

Acknowledgments: The research was supported by the ERDF/ESF project “New Composite Materials for Environmental Applications” (No. CZ.02.1.01/0.0/0.0/17_048/0007399).

REFERENCES

1. Safarik, E. Baldikova, M. Safarikova, M., K. Pospiskova, J. Ind. Textiles 48 (4) (2018) 761-771.
2. Safarik, S. Mullerova, K. Pospiskova, Food Chem. 274 (2019) 215-219.
3. J. Prochazkova, K. Pospiskova, I. Safarik, J. Magn. Magn. Mater. 473 (2019) 335-340.
1. Safarik, M. Safarikova, Int. J. Mater. Res. 105 (2014) 104-107.
4. Y. Jiraskova, J. Bursik, J. Seidlerova, K.M. Kutlakova, I. Safarik, M. Safarikova, K. Pospiskova, O. Zivotsky, J. Nanomater. (2018) Article No. 3738106.
5. J. Seidlerova, O. Motyka, K. Drobikova, I. Safarik, Materials Today: Proceedings 5 (2018) S61–S70.

Several ways of Fe_xO_y /phyllosilicate composite preparation

J. Seidlerová¹, M. Tokarčíková¹, K. Mamulová Kutlákova¹, O. Životský²

¹Nanotechnology Centre, VŠB-Technical University of Ostrava, Czech Republic; ²Department of Physics, VŠB-Technical University of Ostrava, Czech Republic

jana.seidlerova@vsb.cz

ABSTRACT

Fe_xO_y /phyllosilicate composites have been successfully used as a sorbent of various pollutants from wastewater. Fe_xO_y nanoparticles were confirmed in the composites both in the form of magnetite (Fe_3O_4) and maghemite ($\gamma\text{-Fe}_2\text{O}_3$). Method of preparation affects the type of iron oxides, their size and sorption affect the properties of the final composite. Composite preparation is based on two steps: preparation of the iron oxides suspension and mixing of the suspension with the phyllosilicate. To change the magnetic and sorption properties of the composites, methods of the iron oxides preparation were modified. First, the syntheses of iron oxides were carried out under controlled conditions (amount of $\text{FeSO}_4 \cdot 7\text{H}_2\text{O}$, pH of precipitation, time of microwave activity) using a simple microwave-assisted synthesis from $\text{FeSO}_4 \cdot 7\text{H}_2\text{O}$ and, subsequently, the composites – based on bentonite, vermiculite and intercalated vermiculite – were prepared. Then, the syntheses of iron oxides were carried out in the presence of hydrogen peroxide. The prepared composites were characterised by chemical analyses. X-ray diffraction, scanning electron microscopy, and magnetic properties measurement. The results showed that the method of magnetic phyllosilicate preparation is applicable in the case of intercalated vermiculite. Hydrogen peroxide addition lead to the creation of maghemite particles only, and the properties of composites were changed.

Keywords: Phyllosilicate, composites, nano- Fe_xO_y , modification

Acknowledgments: The work was supported by ERDF/ESF New Composite Materials for Environmental Applications (No. CZ.02.1.01/0.0/0.0/17_048/0007399).

Poster presentations (PP):**Effect of titanium dioxide nanoparticles on extracellular polymeric substances under sunlight****A. Behal^{*1,2}, V. D. Rajput³**

¹Laboratory of Environmental Pollution and Bioremediation, Xinjiang Institute of Ecology and Geography, China; ²Department of Biotechnology, Goswami Ganesh Dutta Sanatan Dharma College, India; ³Academy of Biology and Biotechnology, Southern Federal University, Russia

behalbiotech@gmail.com

ABSTRACT

Extracellular polymeric substances (EPS) are an important part of an aquatic habitat. This EPS acts as an interface between microorganisms and environment, protecting microorganisms from metal and other ions at high concentration. Increasing concentration of nanoparticles is leading to contamination of environment and water bodies. Titanium dioxide nanoparticles are among the highly used nanoparticles, significant for their photocatalytic affect under UV light. Their effect on EPS was studied in presence and absence of solar light. Increasing concentration of nanoparticles was incubated for 8 days with EPS extracted from lake microbial mat. Proteins, polysaccharide, pH and TOC were the main parameters monitored. Decrease in protein (55%), polysaccharide (90%) and TOC (44%) was observed. 3D EEM fluorescence spectroscopy confirmed the quenching effect of nanoparticles on protein molecules present in EPS. Changes in molecular weight of EPS molecules were detected by HPLC-SEC and FTIR also observed shifting in wavelength pattern. Effects of solar light on EPS under the influence of nanoparticles is stated in this study, which otherwise is mostly reported in a specific wavelength of UV under lab conditions. Results demonstrate consequence of nanoparticle pollution in lakes or reservoirs.

Keywords: Extracellular Polymeric Substances, Titanium dioxide nanoparticles, Photocatalytic, Biodegradation

INTRODUCTION

Extracellular polymeric substances (EPS) comprise a conglomeration of biopolymers released by microorganisms used to embed microorganisms in a biofilm. These different biopolymers of EPS are mainly polysaccharides, a wide variety of proteins, glycoproteins, glycolipids, humic like substances and extracellular DNA.¹ Cells have EPS as their immediate environment, which act as gel-like matrix and microbial aggregates are protected by EPS from harsh external environment. Toxicity studies of metals include effect on EPS, as latter act as barrier as well as absorb or bind to metals.²

As the production and use of titanium dioxide nanoparticles (TiO₂ NPs) has been increasing, their exposure in environments has also amplified and concentration is increasing continuously. TiO₂ is a photo catalyst under UVA irradiation and is capable to produce toxic reactive oxygen species (ROS) and cause damage to internal molecules of a cell.³ Photodegradation of EPS is further influenced by irradiation wavelengths, intensities and exposure duration.

Present study was designed to study the influence of increasing concentration of NPs under natural conditions like sun light.

EXPERIMENTAL STUDY

Extracellular polymeric substances were extracted from fresh microbial mat collected from Bosten Lake, Xinjiang, China. Effect of TiO₂ NPs (0-25 ppm) on EPS was studied under exposure of sunlight for 8 days with sampling every 48 hours with control in dark conditions. Total organic content, proteins, polysaccharides, pH change, FTIR, size exclusion chromatography and 3D EEM (Excitation–emission-matrix) fluorescence spectroscopy were analysed along with quenching effect of NPs on EPS.

RESULTS AND DISCUSSION

Increasing concentration of TiO₂ NPs under sun light is able to reduce the total organic carbon, protein, polysaccharide more as compared to control. Combination of UV light and TiO₂ is used for photocatalytic reduction of organic matter.⁴ The same happened in natural light by NPs. pH and FTIR spectrum changed with changing reaction products, ions and mineralization at different time interval. HPLC data showed change in size of organic compounds and proteins. Different amino acids have different reaction under photocatalytic activity by NPs leading to degradation.⁵ 3D EEM showed quenching effects indicating that NPs could quench its intrinsic fluorescence. EPS components are highly affected by increasing concentration of TiO₂ NPs as a result of binding interaction between protein and NPs.

CONCLUSION

Study of organic content degradation of extracellular polymeric substances in the presence of titanium dioxide nanoparticles and solar light reveals the active interaction between EPS and NPs, further leading to breakdown of individual components *e.g.* total organic carbon, proteins and polysaccharides. Nanoparticles act as catalyst for the reaction by the way of first adsorbing and then decomposing or mineralizing the organic molecules with the availability of irradiation. Absence of light makes the process slow as photocatalytic TiO₂ NPs are unable to enhance the reaction under dark. This study reflects that titanium dioxide nanoparticles are able to react with EPS under natural conditions also. Furthermore, increasing concentration of these nanoparticles in environment is capable to disturb the normal microbial habitat. Hence, TiO₂ NPs at elevated concentration are ecotoxic to natural water bodies.

Acknowledgment: Arvind Behal thanks UCAS China and CAS-TWAS President's Fellowship for International PhD Students, for infrastructure and financial support.

REFERENCES

1. H.C. Flemming, T.R. Neu, D. J. Wozniak. J. Bacteriol. 189 (2007) 7945-7947.
2. C.M. Hessler, M.Y. Wu, Z. Xue, H. Choi, Y. Seo. Water Res. 46 (2012) 4687-4696.
3. M. Planchon, T. Jittawuttipoka, C. C. Chauvat, F. Guyot, A. Gelabert, M. F. Benedetti, F. Chauvat, O. Spalla. J. Colloid Interface Sci. 405 (2013) 35–43.
4. H.K. Kang, D. Kim. Bioprocess. Biosyst. Eng. 35 (2012) 43-48.
5. L. Muszkat, L. Feigelson, L. Bir, K.A. Muszkat. Pest. Manag. Sci. 58 (2002) 1143-1148.

A synthesis of composites of kaolin/g-C₃N₄ and metakaolin/g-C₃N₄

K. Foniok¹, A. Smýkalová^{1,2}, V. Matějka^{1,2}, P. Praus^{1,2}

¹Department of Chemistry, VŠB Technical University of Ostrava; Czech Republic; ²Institute of Environmental technologies, VŠB Technical University of Ostrava, Czech Republic

krystof.foniok@vsb.cz

ABSTRACT

The composites of graphitic carbon nitride with kaoline and metakaoline were prepared by the calcination of the mixtures of kaoline or metakaoline with melamine. A weight ratio of kaoline (metakaoline) and melamine was 1:1. The prepared mixtures were calcined in a muffle furnace at 500 and 550 °C. The prepared samples were characterized using selected methods of chemical and structural analysis (elemental analysis, X-ray diffraction method, infrared spectroscopy) and optical properties were characterized using photoluminescence spectroscopy and UV-VIS diffuse reflectance spectroscopy. The specific surface area was measured using BET method. A character of the composite particles was studied using scanning electron microscopy and their thermal stability was tested using TG/DTA analysis. A photodegradation activity of the composites was tested using UV light assisted photodegradation of acid Orange 7 (AO7).

Keywords: g-C₃N₄, kaolin, metakaolin, photocatalysis

INTRODUCTION

Natural clay minerals are being widely used as a support for different kind of photocatalysts and thus new photocatalytically active composites were prepared¹. A number of existing research articles dealing with this kind of composites underline the importance of research focusing on this topic. Matějka et. al.² tested vermiculite as a nanoreactor for synthesis of CdS nanoparticles. Mamulová Kutkláková et al.³ used kaolinite as a support of TiO₂ nanoparticles and proved good photocatalytical performance of this composite against the model dye AO7. Recently graphitic carbon nitride (g-C₃N₄) has attracted a great attention of scientists dealing with photocatalysis⁴. Its band gap value of 2.7 eV indicates this material is photoactive in visible part of the electromagnetic spectrum. In general, g-C₃N₄ suffers from low photodegradation activity mainly due to a fast electron-hole recombination rate and low specific surface area. To overcome these disadvantages, different approaches including doping with metal and non-metal elements, exfoliation and synthesis of composite materials were proposed. In a case of the composites, a different localization of valence and conduction bands in components causes a separation of charge carriers and improves the photodegradation activity.

In this work we focused on a preparation of the kaoline/g-C₃N₄ and metakaoline/g-C₃N₄ using a thermal polymerization of melamine in mechanical mixtures with kaoline and metakaoline. The prepared samples were characterized using selected instrumental technique of material analysis and the specific surface area was determined using BET method.

EXPERIMENTAL

Kaolinite from Dorfner GmbH, (Germany) was used in received state; melamine was purchased from Carl Roth (Germany). Both components were mixed together in weight ratio 1:1. Mechanical mixtures were calcined for 1h at 500°C and 550°C in a muffle furnace to obtain the KGCN_500(550) and MKGCN_500(550) composites. Resulting samples were characterized using

elemental analysis on a LECO CHN 628 analyzer (LECO), X-ray diffraction was performed on a SmartLab diffractometer equipped with a Co tube (Rigaku Corporation), ATR Fourier Transformed Infrared spectroscopy was performed on NEXUS iS50 (Nicolet). UV-VIS DRS spectra were recorded using an UV-2600 spectrometer equipped with an integrating sphere IRS-2600Plus (Shimadzu). Photodegradation activity tests were based on UV assisted discoloration of AO7. In a typical experiment an aqueous suspension of AO7 with a given composite was stirred 1h in dark to achieve an adsorption equilibrium, after this step a suspension was irradiated with UVA light (368nm) for 2 hours. A decrease of AO7 concentration was obtained by recalculation of the absorbances of filtered solutions obtained before and after the irradiation, the absorbance of filtered solutions was measured using the UV-VIS spectrometer UV-2600.

RESULTS AND DISCUSSION

Reflectance spectra of the prepared composites are shown in Fig. 1. The absorbance of the light by the composites calcined at 550°C is obviously red shifted in comparison to the composites calcined at 500°C and thus band gap energies decreased with the calcination temperature (2.67 – 2.74 eV). The photodegradation performance of the prepared composites is demonstrated in Fig. 2 and it is evident that the photodegradation activity of the composites decreased with the calcination temperature. Fig. 2 indicates metakaolinite as a better substrate with respect to the photodegradation activity of final composites.

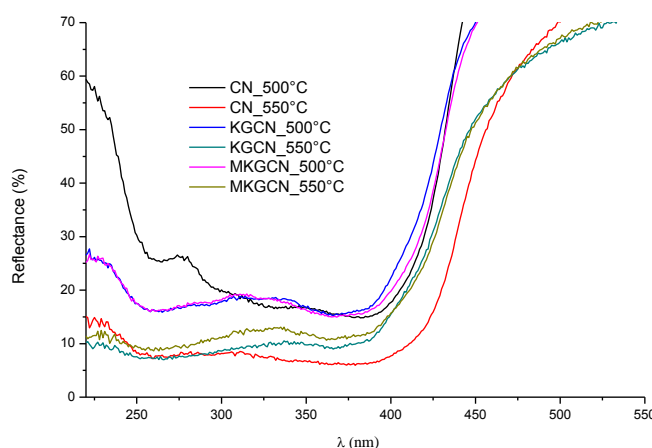


Fig. 1 UV-VIS diffuse reflectance spectra of prepared composites

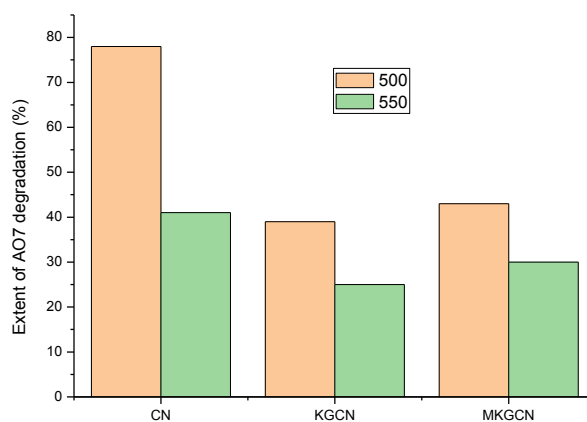


Fig. 2 Extent of a AO7 photodegradation

CONCLUSION

The composites kaoline/g-C₃N₄ and metakaoline/g-C₃N₄ were successfully prepared using the thermal polymerization the melamine. In general, the band gap energies as well as the photodegradation performance decreased with the calcination temperature. The composites containing metakaolinite showed higher photodegradation performance.

Acknowledgments: This work was financially supported by project “Institute of Environmental Technologies - Excellent Research”, project No. CZ.02.1.01/0.0/0.0/16_019/0000853 and by the student projects SP2019/142 of VŠB - Technical University of Ostrava.

REFERENCES

1. V. Matějka, J. Tokarský, J. Nanosci. Nanotechnol. 14 (2014) 1597-1616.
2. V. Matějka, M. Šupová, V. Klem, D. Rafaja, M. Valášková, J. Tokarský, J. Lešková, E. Plevová, Microporous Mesoporous Mat. 129 (2010) 118–125.
3. K. Mamulová Kutláková, J. Tokarský, P. Kovář, S. Vojtěšková, A. Kovářová, B. Smetana, J. Kukutschová, P. Čapková, V. Matějka, J. Hazard. Mater. 188 (2011) 212–220.
4. G. Dong, Y. Zhang, Q. Pan, J. Qiu, J. Photochem. Photobiol. C-Photochem. Rev. 20 (2014) 33-50.

A case study of waste scrap tyre-derived carbon blacks tested for nitrogen, carbon dioxide and cyclohexane adsorption

Z. Jankovská¹, M. Večeř¹, I. Koutník¹, L. Matějová²

¹Department of Chemistry, Faculty of Materials Science and Technology, VŠB – Technical University of Ostrava, 17.listopadu 15/2172, 708 00 Ostrava, Czech Republic; ²Institute of Environmental Technology, VŠB – Technical University of Ostrava, 17.listopadu 15/2172, 708 00 Ostrava, Czech Republic

zuzana.jankovska@vsb.cz

ABSTRACT

Carbon black was prepared by pyrolysis of waste scrap tyres at at600 °C for 3 min in inert flow of Ar. After pyrolysis, carbon black was activated by solution of KOH at 800 °C for 20 min. The sorption capacity of activated and non-activated carbon blacks was measured with high-pressure thermal analyzer (TGA – HP50) in the presence of carbon dioxide, nitrogen and cyclohexane vapour in the pressure range from 0.03 to 2 MPa or 4 MPa at the temperature 20, 30 and 40 °C. The results indicate that activation have significant effect on sorption capacity and textural properties of carbon black. Specific surface area of carbon black increased 7times after activation. For activated carbon black, the uptake of CO₂was approximately 3 times higher and the uptake of cyclohexane is ~10 time higher than for non-activated carbon black. The affinity of activated carbon black to cyclohexane vapors was higher by 3 % than to CO₂.

Keywords: adsorption, scrap tyres, activated carbon, pyrolysis

INTRODUCTION

Production, consumption and, consequently, waste of polymers increase very sharply every year because these materials have excellent properties and nowadays are irreplaceable from point of view of human life. Upgrading of polymer waste is a necessity both for environmental protection and for sustainable development, however, nowadays waste disposal and incineration of polymer-

based waste are the most widely used method. Pyrolysis of polymer waste can be a perspective way for their conversion into valuable products and for a reduction of their volume. Generally, pyrolysis is a thermal degradation (without oxygen agent) leading to solid, liquid and gas products, which have a big potential as useful end products.

For reasons mentioned above, pyrolysis of scrap tyres (ST) which leads to producing valuable solid product (carbon black) currently receiving some attention. Production of carbon black by pyrolysis offer one of the effective way of uses such waste materials and for reusing ST as new applicable material. Carbon black can be used e.g as filler, for water treatment, as a binder for coke manufacturing, a fuel source, a pigment in xerographic toners or a sorbent.

This work follows earlier works^{1,2}, where ST and its products were characterized by thermogravimetry and adsorption methods. Carbon black (called CBp) investigated in previous study¹ was prepared by pyrolysis of ST at different temperature, heating rate and time. Optimum process conditions were investigated at temperature 600 °C for 3 min with heating rate 10 °C.min⁻¹. In this study, pyrolytic carbon black was activated in order to improve its textural and surface properties (called CBa). A sorption capacity of non-activated CBp and activated CBa for two gases (inert nitrogen and carbon dioxide) at relatively high pressures and for pure vapours of cyclohexane at relatively low pressures was examined and correlated with CBs physicochemical properties.

EXPERIMENTAL

CBp was prepared from scrap tyres using TG-DTA NETZSCH STA 409 EP (dynamic inert atmosphere of Ar of 100 cm³.min⁻¹ flow, 600 °C for 3 min, heating rate of 10 °C min⁻¹).

CBp was mixed with KOH and tenside and it was keep at room temperature for 24 h. Activation took place in quartz tube at 800 °C for 30 min in nitrogen. Than sample was washed by distilled water to achieve neutral pH and dried at 105 °C. Activated CBp was denoted as CBa.

Sorption experiments were carried out in a high pressure thermogravimeter TGA-HP50 at pressure up to max 5 MPa. Primary data were the weight change, temperature, time and pressure. Experiments were performed with pure gases (CO₂, N₂) and with vapours of organic solvent (cyclohexane). The sorption experiments were carried out at the temperature of 20, 30 and 40 °C.

Experimental data were treated by the linearized model of Langmuir isotherm and textural properties (i.e. properties of porous structure) of produced CBp and CBa were determined from the nitrogen and krypton physisorption measurements.

RESULTS AND DISCUSSION

The results of the individual tests, representing the amount of adsorbed gas at maximum achieved pressure (2 MPa for CO₂ and 4 MPa for N₂), were expressed in percentage by weight. It was revealed that the gas uptake of CO₂ is more than 5 times greater than uptake of N₂ at the same temperature for CBs. Activation of CBs increased sorption capacity once so much. Sorption capacity of CBp for CO₂ is 8% and of CBa 16% at 20 °C.

From the behavior of Langmuir adsorption isotherms, a surge in the amount of adsorbed CO₂ for CBa was evident up to a relative pressure $p/p_0 = 0.05$. On the contrary, for cyclohexane, the most pronounced effect of the relative pressure up to $p/p_0 = 0.04$ was observed. A further increase in pressure of CO₂ caused an increase in the adsorbed amount by 0.04 g/g and for cyclohexane by 0.05 g/g. It was evaluated that adsorption capacity of monolayer n_m in the whole investigated pressure range follows the order: CBa for cyclohexane > CBa for CO₂ > CBp for cyclohexane > CBp for CO₂ > CBp for nitrogen. As it was expected, activated CBa had a higher adsorption capacity for both gases/vapor.

CONCLUSION

The sorption properties of two carbon blacks prepared from scrap tyres pyrolysis – non activated CBp and CBa (consequently activated CBp by KOH) - were examined. It is found out that activated carbon black CBa showed significantly enhanced sorption capacity and improved textural properties than non-activated carbon black CBp.

Acknowledgements: This work was elaborated in the framework of the projects SP 2019/43 and SP 2019/142.

REFERENCES

1. Z. Mikulová, I. Šeděnková, L. Matějová, M. Večeř, V. Dombek, Therm. Anal. Calorim. 111 (2013) 1475-1481.
2. M. Večeř, Z. Jankovská, 40 th International Conference of Slovak Society of Chemical Engineering (2013): proceedings 1-7: hotel Hutník, Tatranské Matliare, Slovakia, May 27-31.
3. M. Večeř, B. Špitová, I. Koutník, J. Therm. Anal. 121 (2015) 429-436.

Effect of different type of nanoparticles on crop production

M. Kolenčík¹, D. Ernst², M. Šebesta³, M. Urík³, G. Kratošová⁴, Z. Konvičková⁵, M. Bujdoš³, I. Černý², E. Dobročka⁶, I. Vávra⁶, H. Feng⁷, Y. Qian⁸, R. Illa⁹

¹Department of Soil Science and Geology, ²Department of Crop Production, Slovak University of Agriculture in Nitra, Slovak republic; ³Institute of Laboratory Research on Geomaterials, Comenius University in Bratislava, Slovak Republic; ⁴Nanotechnology Centre, VŠB – Technical University of Ostrava, Czech Republic; ⁵ENET Centre, VŠB – Technical University of Ostrava, Czech Republic; ⁶Institute of Electrical Engineering, Slovak Academy of Sciences, Slovak Republic; ⁷Department of Earth and Environmental Studies, Montclair State University, USA; ⁸School of Ecology and Environmental Sciences, Yunnan University, China; ⁹Department of Chemistry, Rajiv Gandhi University of Knowledge Technologies, India

marekkolencik@gmail.com

ABSTRACT

The aim of this work was to evaluate the foliar application of metal-oxide nanostimulators to real condition with plant (*Helianthus annuus* L.) and their impact on quantitative, qualitative, and physiological parameters. The development in nanoparticles also reflect the field of agriculture, especially beneficial, and positive effects on plants including more available control of agrochemicals. Our result showed that from qualitative point of view (sunflower seed yield) the most effective variant poses the titanium dioxide compared to zinc oxide variants, and control experiment. Similar trend was appeared with sunflower qualitative parameters (content of oil in sunflower seed). However, better impact of physiological indicators (chlorophyll content, photosynthetic activity, and etc.) correspond to zinc oxide variant. Our result confirmed the importance of nanoparticles as nanostimulators for progressive agriculture and agronomical development.

Keywords: Metal-oxides, Nanostimulators, Crop Production, *Helianthus annuus* L.

INTRODUCTION

Nanoparticles (NPs) are particles defined to have at least one dimension smaller than 100 nm. They usually demonstrate unique physical, chemical and biological properties compared to similar “macro-size” counterparts. Nowadays, the progressive growing field of nanotechnology is connected to all areas of life including nanomaterials’ application in electronics, human implants, bionanotechnology, etc.¹. The development of nanomaterials is also reflected in agriculture related disciplines, where NPs have beneficial effects on plants e.g. the delivery-target activity by more available control of agro-chemicals². However, there is still missing information about behavior of NPs in real (natural) matrices, involving their transport, and translocation in plants, accumulation, bioavailability or potential toxicity^{2,3}. Additionally, from consumer point of view the quality of plants (e.g. nutritional value, taste, and others) we should take into the consideration. Due to these reasons our study addresses i) using of foliar application of metal-oxide nanostimulators to real condition with plant *Helianthus annuus* L., and ii) analysis of their effects on quantitative, qualitative (content of sunflower oil), physiological (vegetative index *NDVI* - normalized difference vegetation index, and *PRI* - photochemical reflectance index), and other parameters associated with crop production.

EXPERIMENTAL STUDY

NPs were purchased from Sigma Aldrich, and for analysis of size, morphology were used the Transmission Electron Microscopy (TEM), and NPs’ crystallinity was verified using X-ray analysis (XRD). Field experiment with *Helianthus annuus* L. and foliarly applied NPs (zinc oxide, and titanium dioxide) were performed on the research field “Dolná Malanta” which is located in Nitra, Slovak Republic. Field experiments were conducted in three variants (i) control without nanostimulators, (ii) application with titanium dioxide, and (iii) zinc oxide. Continual photosynthesis indicators of sunflower were evaluated based on measurement with PlantPen 300U equipment, and acquired data were compute to *NDVI*, and *PRI* indexes. Morphological changes of leaves during experiments were observed using Scanning Electron Microscopy (SEM). At the end of experiments, the content of sunflower oil from sunflower seeds in variant’s samples were approved applying Soxhlet extraction⁴.

RESULTS AND DISCUSSION

The TEM, and XRD analysis evidenced that zinc oxide NPs have size until 70 nm, with dominant hexagonal-prisms morphology, and hexagonal symmetry. Titanium dioxide NPs correspond to size no bigger than 40 nm, mainly with prismatic crystals with confirmation of the bi-phase tetragonal symmetry. After foliar application of NPs several significant discrepancies in quantitative, qualitative, and physiological parameters on crop production were observed. From qualitative parameter of sunflower is obvious that the most abundant crop production (sunflower seed yield) corresponds to variant with titanium dioxide more than zinc oxide, and control experiment. This is confirmed even by ANOVA test with high significant influence ($\alpha = 0.05$; $P = 0.002$). Regarding the qualitative parameters data, e.g. total content of oil in sunflower seeds was the lowest in the control experiment (less than 60%), compared to samples with zinc oxide (more than 60 %). The most abundant content of oil was detected in variant with applied titanium dioxide NPs with statistically verified influence ANOVA parameters ($\alpha = 0.05$; $P = 0.012$). In the growing season, the average value of the sunflower vegetation index (*NDVI*, and *PRI*) reached an annual value of 0.0437, and -0.0199, respectively. In comparison between all three variants and based on physiological indicators we may deduce that Zn-related experiments shown the higher leaf chlorophyll content, increased photosynthetic activity, and photosynthetic radiation-use efficiency more than titanium dioxide NPs application, and control experiments without using NPs. These facts do not fully correlate with quantitative, and qualitative results (the most effective was Ti-based

experiments) which could be matter of the delivery-target activity associated with transport, and translocation of NPs^{2,3}.

CONCLUSION

From the obtained results of foliarly applied metal-oxide NPs to sunflower plant in the field experiments, it follows that there is no strong correlation between physiological parameters and the quantity and quality of final crop production. It could be caused due to various “field” factors including concentration of effective nanostimulators, time, and period of application, combination of other agrochemicals, availability of elements, and others. For future development of our work it could be really attractive the analysis of metal oxides NPs pathway e.g. translocation of NPs from soil solution to plant root system, or from leaves to other parts of plant with impact of quality to final crop production.

Acknowledgments: This work was financial support by the Slovak Academy of Sciences via grants VEGA 1/0164/17, VEGA 1/0146/18 and KEGA 013SPU-4/2019, and we also appreciate the Ministry of Education, Youth and Sports of the Czech Republic grant number SP2019/75.

REFERENCES

1. M. Kolenčík et al., J. Nanosci. Nanotechnol. 19, 5 (2019) 2983-2988.
2. R. Prasad, A. Bhattacharyya, Q. D. Nguyen, Front Microbiol. 8 (2017) 1-13.
3. L. Kořenková, Acta Agric. Scand. B. 67, 4 (2017) 285-291.

Bio-mechanochemical synthesis of silver nanoparticles using *Thymus vulgaris* L. plant

M. Kováčová¹, M. Baláž¹, E. Dutková¹

¹Institute of Geotechnics, Slovak Academy of Sciences, Slovakia

kovacovam@saske.sk

ABSTRACT

The combination of mechanochemistry and green approach (utilization of plant material, namely *Thymus vulgaris* L., TYM) was used for the synthesis of silver nanoparticles (Ag NPs). The experiments were performed at various AgNO₃-to-plant ratios (1:1, 1:10, 1:50 and 1:100), while the former one served as a silver precursor and the latter one as a reducing agent. The successful formation of Ag NPs was proven by powder X-ray diffraction in all cases, except the Ag-TYM 1:100 sample, where the amount of plant was too high to register any reflections corresponding to Ag⁰. The as-received powders were washed, which resulted in the removal of non-reacted AgNO₃ and non-stabilized Ag⁰. After washing, the Ag-TYM 1:1 sample was characterized by UV-Vis spectroscopy. The result confirmed the successful synthesis of Ag NPs by showing the peak at 454 nm in the spectrum. The concentration of silver (altogether elemental and ionic) determined in the filtrates after washing by atomic absorption spectrometry showed significant decrease with increasing plant amount, thus pointing to increased stability of the NPs when more plant was used.

Keywords: silver nanoparticles, *Thymus vulgaris* L., mechanochemistry, X-ray diffraction

INTRODUCTION

Green synthesis of silver nanoparticles (strong antibacterial agents) using plants is excessively studied these days¹. Among many others, also *Thymus vulgaris* L. plant was used for this purpose²⁻³. The completely solid-state approach using mechanochemistry represents an interesting alternative, as it can produce stable NPs at ambient conditions⁴⁻⁵.

EXPERIMENTAL/THEORETICAL STUDY

The bio-mechanochemical synthesis was realised in a Pulverisette 7 premium line planetary ball mill (Fritsch, Germany) under the following conditions: milling time 2 hours, milling speed 500 rpm, WC balls (15 pieces, diameter 10 mm) and chamber (45 mL) in air atmosphere. Various amounts of AgNO₃ and *Thymus vulgaris* L. plant (in the weight ratio 1:1, 1:10, 1:50 and 1:100) in total mass 3 g were milled. One gram of as-received powder was washed with 100 mL of distilled water in order to remove residual AgNO₃. The products were characterized using X-ray diffraction and UV-Vis spectroscopy. The filtrate after washing was analysed for Ag content using atomic absorption spectrometry.

RESULTS AND DISCUSSION

Powder X-ray diffraction was used to pursue the formation of Ag NPs for various AgNO₃-to-plant weight ratios. The XRD patterns are presented in Fig. 1a. In the sample Ag-TYM 1:1 the peaks for both silver nitrate and elemental silver are visible. The ones for silver nitrate are more abundant and intense indicating that the reaction is not fully completed. However, after washing, all diffractions corresponding to AgNO₃ are eliminated and only those corresponding to Ag are present. In the case of the sample Ag-TYM 1:10, silver nitrate peaks are no longer observed and peaks of silver become more evident. The most of the diffraction peaks could be well-indexed to cubic silver. For the samples Ag-TYM 1:50 and Ag-TYM 1:100, the mass of *Thymus vulgaris* L. is too high to identify silver peaks (in the former case only a small one at around 38° can be detected). In addition to the peaks corresponding to AgNO₃ or Ag, also the one at 26,6° can be observed in all samples, the intensity of which increases with the amount of plant. This peak is the most significant one in the XRD pattern of pure plant. Obviously the AgNO₃-to-plant ratio is important as the reaction proceeds more rapidly when more reduction agent (plant) is introduced.

In Fig. 1b, the UV-Vis spectrum of the washed Ag-TYM 1:1 is presented. Two peaks can be identified, the one at 352 nm corresponds to the plant matrix and the one at 454 nm is characteristic for silver nanoparticles, thus confirming the successful synthesis. Similarly in the paper² using the same plant the absorption peak was registered at 440 nm.

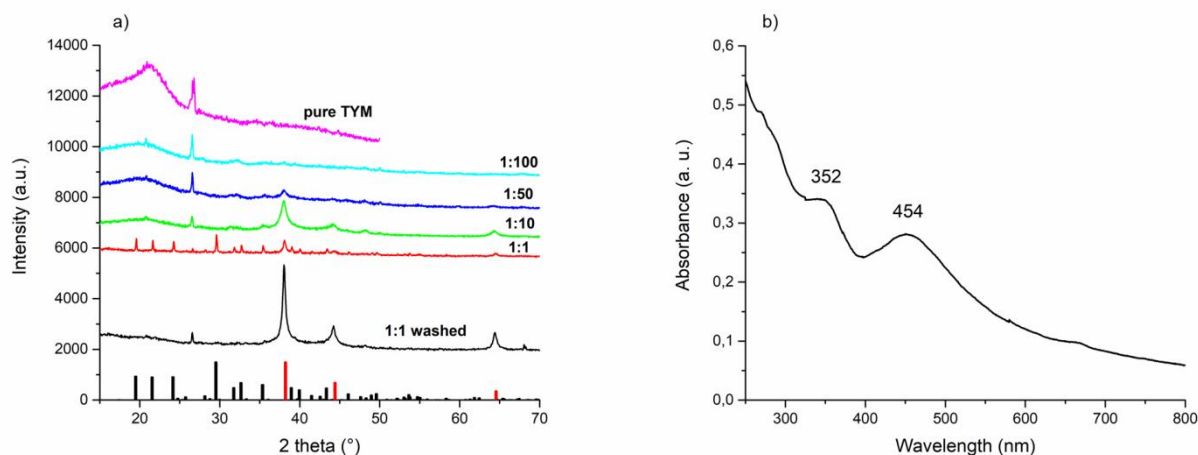


Fig. 4. (a) XRD patterns of *Thymus vulgaris* L. plant and Ag NPs synthesized by *Thymus vulgaris* L. (the presented bars at the bottom correspond to the diffractions according to JCPDS database: AgNO_3 (black, 01-074-2076) and Ag (red, 03-65-2871); (b) UV-Vis spectrum of Ag-TYM 1:1 washed sample.

The concentrations of Ag in the filtrates determined by AAS were 3225 mg/L and 11 mg/L for Ag:TYM 1:1 and 1:10 samples, respectively. These values correspond to 100 % and 1.9 % of overall silver introduced into the reaction. Very high value detected in the Ag-TYM 1:1 sample hints to the fact that in addition to non-reacted AgNO_3 , also reduced Ag^0 which could not be effectively stabilized was present in the filtrate and that most probably the plant material undergoes some decomposition during milling. The values for Ag-TYM 1:50 and 1:100 were very low (0.6 mg/L (0.48 %) and 1.23 mg/L (1.95 %), respectively), which points to very effective stabilization of Ag in the plant matrix.

CONCLUSION

The possibility to prepare Ag NPs using *Thymus vulgaris* L. plant using bio-mechanochemical synthesis was demonstrated in this study. The AgNO_3 -to-plant ratio plays very important role in the stabilization of the prepared NPs. The products are potential antibacterial agents, which will be verified in close future.

Acknowledgments: This study was supported by the Slovak Agency for Science and Development (project no. APVV-14-0103) and by the Slovak Grant Agency VEGA (project no. 2/0044/18).

REFERENCES

1. L.Y. Wei; J.R. Lu; H.Z. Xu; A. Patel; Z.S. Chen; G.F. Chen, *Drug Discov. Today* 20 (2015) 595-601.
2. Z. Heidari; A. Salehzadeh; S.A.S. Shandiz; S. Tajdoost, *3 Biotech* 8 (2018).
3. A. Jafari; L. Pourakbar; K. Farhadi; L. Mohamadgolizad; Y. Goosta, *Turk. J. Biol.* 39 (2015) 556-561.
4. M. Baláž; N. Daneu; Ľ. Balážová; E. Dutková; Ľ. Tkáčiková; J. Briančin; M. Vargová; M. Balážová; A. Zorkovská; P. Baláž, *Adv. Powder Technol.* 28 (2017) 3307-3312.
5. M.J. Rak; T. Friscic; A. Moores, *RSC Adv.* 6 (2016) 58365-58370.

Utilization of photoactive clay/TiO₂ and quartz/TiO₂ composites in cement pastes

S. Rebilasová¹, V. Matějka^{2,3}, K. Foniok², K. Mamulová Kutláková¹, J. Vlček^{3,4}

¹Nanotechnology Centre, VŠB Technical University of Ostrava; Czech Republic; ²Department of Chemistry, VŠB Technical University of Ostrava; Czech Republic; ³Institute of Environmental technologies, VŠB Technical University of Ostrava, Czech Republic, ⁴Department of Thermal Engineering, VŠB Technical University of Ostrava; Czech Republic

vlastimil.matejka@vsb.cz

ABSTRACT

The composites quartz/TiO₂, kaolinite/TiO₂, vermiculite/TiO₂ and montmorillonite/TiO₂ were prepared using hydrothermal treatment of the suspension of given support particles (quartz, kaolinite, vermiculite and montmorillonite) with titanyl sulphate. By this process the composites with 60 wt.% of TiO₂ were prepared. The samples were characterized using selected methods of chemical and structural analysis (X-ray fluorescence spectroscopy, X-ray diffraction method, infrared spectroscopy), the weight loss of the samples during the heating was studied using thermal analysis, the specific surface area was measured using BET method. The photodegradation activity of the composites was tested using UV light assisted photodegradation of acid orange 7 (AO7). Prepared composites were used for the preparation of the cement pastes. The samples of cement pastes were characterized using compression strength method, the self-cleaning properties of the surface of the cement pastes were tested by the photodegradation of Rhodamine B deposited on the surface of the hardened cement pastes.

Keywords: TiO₂, composites, cement pastes, photocatalysis

INTRODUCTION

The photocatalytic degradation of the harmful substances from air and water represents an elegant way to improve the quality of living environment and is widely discussed and studied topic. The photocatalytical process is based on the generation of electron-hole pairs during the irradiation of selected semiconductors using light of suitable wavelength. Generated electron and holes are subsequently responsible for the degradation of the harmful substances via different reaction mechanisms. Undoubtedly, the most studied photocatalyst is titanium dioxide in its anatase form with the band gap energy 3.2 eV¹. The photoactivity depends on several factors and is also closely related to the particle and crystallite size. The nanoparticles perform better than bulk materials, but on the other hand are more difficult to separate from reaction mixture after the photodegradation process. The way to overcome this issue is to capture the nanoparticles on the surface of suitable carriers. Clay minerals were proved to be the suitable substrates for capturing of photocatalytic nanoparticles², whereas new class of nanocomposites is obtained. The application of the composite kaoline/TiO₂ in cement pastes and its photodegradation activity against NO_x has been already proved³. Present research is focused on the comparison of three raw clays (kaoline - KA, vermiculite - VE and bentonite - BE) and fine quartz particles as the substrates for immobilization of TiO₂ nanoparticles. Prepared composites (KATI, VETI, BETI) were tested as the photoactive components of cement pastes by the photodegradation of RhB deposited on the surface of hardened cement pastes.

EXPERIMENTAL

The composites substrate TiO_2 (60wt.%) were prepared using thermal hydrolysis of TiOSO_4 colloid suspension according to the procedure published by Kutlakova et al.⁴. Prepared composites were calcined 2h at 500°C and used as the fillers in cement pastes. The amount of the individual filler was 10 wt.% and water to solid ratio was 0.5. The hardened cement pastes (28days) were subjected to RhB test⁵.

RESULTS AND DISCUSSION

Fig. 1 shows the compressive strength values obtained for the reference cement paste and pastes modified with given photocatalytic admixture. The lowest value of compressive strength was achieved for the sample with admixture bentonite/ TiO_2 , while the cement paste modified with VETI reached the same level of compressive strength as a reference cement paste. The extent of discoloration of originally pink colored surface of the cubes of reference cement pastes (without photoactive admixture) and cement pastes with 10wt.% of given composite due to 26h long of UVA irradiation is shown in Fig. 2. Comparing the pictures of the sample surface it is evident that in the case of the samples the samples with photoactive composites subjected to UV irradiation the intensity of originally pink color of the surface caused by the presence of RhB decreased due to the photocatalytic degradation of RhB.

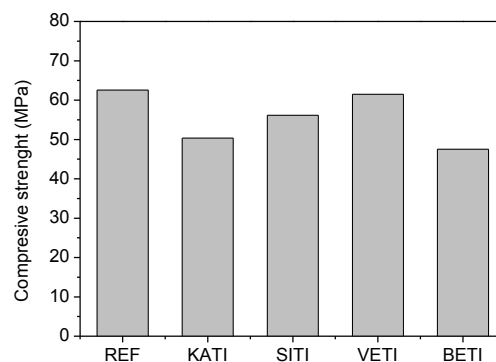


Fig. 1 Comparison of the compressive strength values of the samples after 28days of hydration

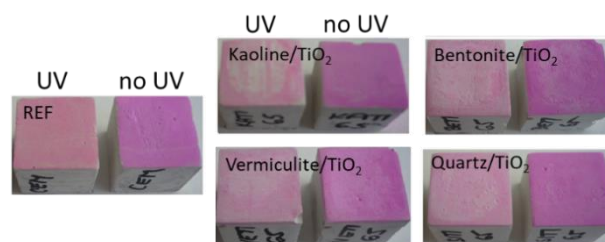


Fig. 2 Demonstration of the photodegradation activity of the pastes colored with RhB

CONCLUSION

The photocatalytic admixtures based on TiO_2 captured on the surface of three selected clays (kaoline, vermiculite and bentonite) and quartz were successfully prepared by thermal hydrolysis of titanyl sulphate. The calcined composites were used as the photocatalytic admixture of cement pastes whereas the lowest compressive strength value was measured for cement paste with composite BETI (bentonite/ TiO_2). Comparing the colored surface of cement pastes it was observed that all of the composites showed more pronounced degradation of RhB in comparison to reference cement paste.

Acknowledgments: This work was financially supported by project “Institute of Environmental Technologies - Excellent Research”, project No. CZ.02.1.01/0.0/0.0/16_019/0000853 and by the student project SP2019/142 of VŠB - Technical University of Ostrava.

REFERENCES

1. S.-Y. Lee, S.-J. Park, J. Ind. Eng. Chem. 19 (2013) 1761-1769.
2. V. Matějka, J. Tokarský, J. Nanosci. Nanotechnol. 14 (2014) 1597-1616.
3. V. Matějka, P. Matějková, P. Kovář, J. Vlček, J. Příkryl, P. Červenka, Z. Lacný, J. Kukutschová, Constr. Build. Mater. 35 (2012) 38-44.

Activation of granulated blast furnace slag using powder activator

P. Matějková¹, V. Matějka², J. Vlček³

¹CPIT, VŠB Technical University of Ostrava; Czech Republic; ²Department of Chemistry, VŠB Technical University of Ostrava; Czech Republic; ³Department of Thermal Engineering, VŠB Technical University of Ostrava, Czech Republic

petra.matejkova@vsb.cz

ABSTRACT

The suitability of powder alkali activator for activation of granulated blast furnace slag (GBFS) was evaluated. Three solid powder activators Na_2SiO_3 (NS), $\text{Na}_2\text{SiO}_3 \cdot 5\text{H}_2\text{O}$ (NSH₅) and $\text{Na}_2\text{Si}_2\text{O}_5 \cdot 3\text{H}_2\text{O}$ (NS₂H₃) were used for GBFS alkali activation without their initial dissolution in water. Mixing water, which is necessary for hydration processes at these systems, was added subsequently after the mechanical mixture of given powder alkali activator and GBFS was prepared. The effect of the type and the amount of the Na_2O carried by given activator on the compressive strength values of the prepared pastes were evaluated after 2, 7, 28 and 56 days of hydration in the moist environment (99% RH). It was observed that the activation using powder activators is possible and the highest compressive strength values after 56 days hydration reached approximately 80 MPa for the pastes activated with NS. The lowest values of compressive strength in the range 30-50 MPa were obtained for the pastes prepared with the activator NSH₅. The hardened samples of GBFS with NS were further characterized using X-ray diffraction method and Fourier transformed infrared spectroscopy. The extent of the dissolution of solid powder activator was studied using scanning electron microscopy on the fracture surface area originated after the compressive strength test.

Keywords: granulated blast furnace slag, alkali activation, compressive strength

Acknowledgments: This work was supported by the EU Regional Development Fund within the Operational Programme Research, Development and Education under the aegis of Ministry of Education, Youth and Sports of the Czech Republic; Project number CZ.02.1.01/0.0/0.0/17_049/0008426.

Non-traditional glaze from iron waste

H. Ovčáčíková¹, J. Vlček¹, M. Klarová¹, M. Topinková¹

¹Department thermal engineering, Faculty of Material Science and Technology, VŠB -Technical University of Ostrava, Czech Republic

hana.ovacikova@vsb.cz

ABSTRACT

Variability of industrial waste supports new processes for their disposal or reusing. Especially interesting is inorganic waste containing metals such as clean scale. These can be used as a pigment. Iron pigments are among the most widely used dyes for industrial applications. Changes in temperature have a direct influence on the modification of oxides Fe and colour of the final pigment. Based on the results of XRDF analyses, the tested scale contains FeO (78%) and Fe₃O₄ (16%) in cubic form and 3% of Fe₂O₃ in rhombohedral form. When exposed to temperature above 1100°C, the share of Fe₂O₃ in rhombohedral form rises to 98%. This article simply describes the preparation of a new glaze from the scale. The scale was mixed with commercial glaze at 10 wt% and applied to a fired ceramic body. 3 firing temperature regimes, 800°C, 900°C and 1060°C, were established, to obtain different colour shades.

Keywords: scale, pigment, glaze, ceramic

INTRODUCTION

In 2017, there were 234 large industrial companies in the Moravian-Silesian region. A large part of these companies produce a lot of industrial waste during their production process. Part of this waste is cleaned scale, which can be used in a number of different ways. The used scale is industrial waste, evaluated according to Czech legislation in the waste catalog under the code 1002 Industrial waste: Rolling mill scale 100210. The scale is represented by three types of oxides, wüstite FeO, magnetite Fe₃O₄ and hematite Fe₂O₃. In general, they show dynamic properties that are characterised by both the formation and reduction of higher iron oxides.¹ The word pigment means a substance consisting of small particles that is practically insoluble in the applied medium and is used for its coloring, protective, or magnetic properties. Both pigments and dyes are included in the general term “colouring materials”.² The reason for the use of iron pigments is the higher stability of oxides soluble in silica glaze. Glaze is glass coating on a ceramic body. From the technical point of view, glaze improves the appearance of the product and design, lowers the porosity of the body and increases mechanical strength of the glazed body. Glaze consists of several types pigments on oxide basis, that bring the colours and properties that are required.

EXPERIMENTAL/THEORETICAL STUDY

The glaze was prepared from 10 hm% scale as pigment + 100 hm% powder transparent glaze containing up 80% SiO₂. The glazes were homogenized in a ball mill. They were applied by spray method and dipping on the firing body. The temperature was 800, 900 and 1060°C. SEM analysis shows irregularly shaped grains, Fig. 1a and XRD record present FeO (78%) and Fe₃O₄ (16%) and 3% Fe₂O₃, Fig. 1b. Above 1000°C, the only stable phase is hematite. Hematite (α -Fe₂O₃) is the most stable iron oxide and it is traditionally used as a red pigment from ancient times.³ Thermodynamically, it is a stable product.

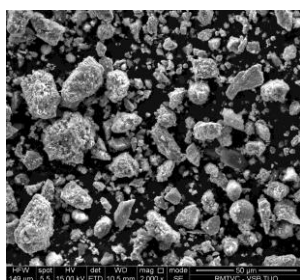
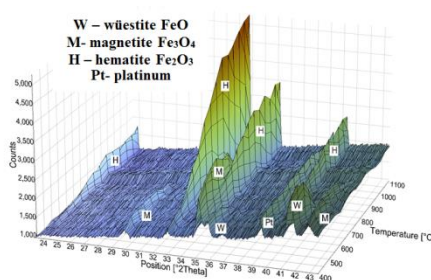


Fig. 1 a) SEM of scale



b) HT-XRD of scale

RESULTS AND DISCUSSION

The original scale is black. The colour of scale can be changed in two ways a) on dependent temperature b) chemical treatment. Ions 3^+ are very reactive in mixtures with glaze, frits and ceramic body. Fe_3O_4 is transformed to form $\gamma\text{-Fe}_2\text{O}_3$ (maghemite) and $\alpha\text{-Fe}_2\text{O}_3$ (hematite) with present oxygen.^{4,5} Nowadays, $\alpha\text{-Fe}_2\text{O}_3$ is used for several industrial applications, for instance colouring paints, plastics and enamels, thanks to its low price, low toxicity, and high thermal and chemical stability.³ The colour of the resulting glaze is different, depending on firing temperature, Tab. 1. Up to 800°C the glaze is matt and above 900°C it is glossy. The surface glazes are without defects. Spray method is better to create a compact surface.

Table 1. The color of scale during thermal and chemical exposition

Colour and treatment	Black original	Dark brown b)	Red a) b)	Yellow b)	Brown a)
Iron oxide pigment					
Final glaze					
Firing of glaze	1060°C	800°C	900°C	900°C	800°C

CONCLUSION

The study confirmed the usability of clean scales as pigments. Temperature changes the polymorphism of iron oxide and affects the final colour pigment and the color of final glaze with a high content of SiO_2 . Local vitrification formed during heat treatment with the use of transparent glazes. The resulting glass structure on ceramic body immobilizes the components coming from industrial waste and eliminates their negative impact on the environment. This effect is used in the common practice, where different oxidic pigments are used for the production of glazes.

Acknowledgments: „This work was supported by the Ministry of Education, Youth and Sports of the Czech Republic under Project No. CZ.02.1.01/0.0/0.0/17_049/0008426.“

REFERENCES

1. H.E. McGannon, Making Shaping and Treating of Steel USS, Pennsylvania, 1970.
2. H. G. Volz, Krefeld, Pigments, Inorganic, (Chap. 1), Wiley, Weinheim, 2005.
3. G. Buxbaum, Industrial Inorganic Pigments, second ed. WILEY, Weinheim, New York, 1998.
4. O. Opuchovic, A. Kareiva, Historical hematite pigment: Synthesis by an aqueous sol-gel method, characterization and application for the colouration of ceramic glazes *Ceramics International*, 41, (2015), 4504-4513.
5. A. Spinelli, A. P. Novaes de Oliveira, Synthesis of Heteromorphic Iron Oxide Red Pigment for Ceramic Application. In: 7th World Congress on Ceramic Tile Quality (2002), 245-248.

Possibility of Using Fly Ash after Denitrification by SNCR as Admixture in Alkali-activated Materials

L. Procházka¹, P. Mec²

¹Faculty of Civil Engineering, Technical University of Ostrava, Czech Republic; ²Institute of clean technologies for mining and use of energy raw materials, Technical University of Ostrava, Czech Republic

lukas.prochazka@vsb.cz

ABSTRACT

The paper deals with the possibility of using fly ash including fly ash after SNCR denitrification from power plant Třebovice as an admixture for composites based on alkali-activated blast furnace slag in order to improve selected physical and mechanical properties. Furthermore, the effect of fly ash on hydration and structure influence in thermal analysis was studied.

Keywords: Fly ash, denitrification, blast furnace slag, SNCR

Ceramic cordierite/CeO₂ for photocatalytic reduction of CO₂

M. Šihor¹, M. Valášková¹, M. Edelmannová¹, K. Kočí¹

¹institute of environmental technology, VSB - Technical University of Ostrava, Czech Republic

marcel.sihor@vsb.cz

ABSTRACT

Vermiculites are commercially available inexpensive clay minerals, but their structural properties significantly affect the properties of cordierite ceramics. In recent years, photocatalytic N₂O conversion was studied over cordierite/steatite/CeO₂ ceramics prepared from raw talc, kaolin and CeO₂ nanoparticles precipitated on vermiculite from the Paraíba region of Brazil. Based on this result the new set of ceramics cordierite/CeO₂ was prepared by precipitation of nanoparticles of ceria (CeO₂) on vermiculite from the Brazil. The samples were prepared from the mixtures containing talc (from 20 to 40 wt.%), kaolin (about 50 wt.%) and vermiculite/CeO₂ nanoparticles (from 13 to 30 wt.%) by sintering at 1300°C. The amount of CeO₂ in mixtures was from 4 to 9 wt.%. The photocatalysts properties were characterized by several characterization methods, such as X-ray powder diffraction, N₂ physisorption, diffuse reflectance UV-vis spectroscopy and photoelectrochemical measurements. The photocatalytic activity of ceramics cordierite/CeO₂ was investigated for the CO₂ photocatalytic reduction. The main reaction products were carbon monoxide moreover, hydrogen was also detected. Correlation between structural, optical and electronic properties and photoactivity have been studied in detail.

Keywords: Cordierite ceramics, CO₂, photocatalytic reduction

Acknowledgments: The work was supported from ERDF "Institute of Environmental Technology – Excellent Research" (No. CZ.02.1.01/0.0/0.0/16_019/0000853) and Large Research Infrastructure ENREGAT supported by the Ministry of Education, Youth and Sports of the Czech Republic under project No. LM2018098.

Degradation of pharmaceuticals by using three different photocatalysts

A. Smýkalová^{1,2}, B. Sokolová², K. Foniok¹, V. Matějka^{1,2}, P. Praus^{1,2}

¹Department of Chemistry, VŠB Technical University of Ostrava; Czech Republic; ²Institute of Environmental technologies, VŠB Technical University of Ostrava, Czech Republic

aneta.smykalova.st@vsb.cz

ABSTRACT

Two commercially available photocatalysts based on titanium dioxide (P25, CG300) and one photocatalyst based on exfoliated graphitic carbon nitride (g-C₃N₄) were tested for the photodegradation of paracetamol (PAR), ibuprofen (IBU) and diclofenac (DIC). For all of the photocatalysts the photodegradation was realized under the UV (368nm) as well as VIS (446nm) irradiation. An extent of the degradation was characterized using high performance liquid chromatography and UV-VIS spectroscopy.

Keywords: g-C₃N₄, TiO₂, photodegradation, pharmaceuticals.

INTRODUCTION

The presence of pharmaceuticals and their metabolites are beginning to be a problem in waters because wastewater treatment plants were not designed to remove them. For example, the number of the medical prescriptions being issued in United States is reaching approximately 4 billion dollars annually. These compounds get to waters through various sources. It is important to develop effective techniques to remove them from aquatic environment, drinking water and waters coming out of wastewater treatment plants¹.

The effort to utilize a photodegradation phenomenon for the remediation of hazardous pharmaceutical residues is reflected in a number of scientific papers dealing with this issue. Yang et al.¹ used the UVA and UVC assisted photodegradation of paracetamol over the TiO₂ photocatalyst and indicated TiO₂ as the promising material especially when UVC was used.

Graphitic carbon nitride has attracted an attention as the photocatalyst mainly with respect to its narrower band gap in comparison to TiO₂ (2.65 eV vs 3.20 eV). One of the strategies for enhancement of the photodegradation efficiency of g-C₃N₄ is exfoliation of bulk structure. The exfoliation results in the higher specific surface area of g-C₃N₄ and therefore the photodegradation activity of these structures are improved significantly².

EXPERIMENTAL

Photodegradation of the most commonly used pharmaceuticals was studied by using different photocatalysts. For the catalyst were chose commercially available TiO₂ (Precheza a.s.; CG 300), TiO₂ (Evonic; P25) and laboratory prepared exfoliated g-C₃N₄. Graphitic carbon nitride (bulk) was

synthesized by the calcination of melamine at 550°C and further exfoliated at 500°C in a muffle furnace², the resulting sample was labeled as g-C₃N₄ EX.

The above mentioned catalysts were characterized by diffusion reflectance spectroscopy (DRS) (Shimadzu UV-2600 with IRS-2600Plus), X-ray powder diffraction (XRD) (Rigaku SmartLab diffractometer equipped with Co tube), Fourier transform infrared spectroscopy (FTIR) (Nexus 470), scanning electron microscopy (SEM), transmission electron microscopy (TEM), particle size distribution and particle size.

The photodegradation tests were performed using an ultraviolet light lamp (UV lamp) and a visible light lamp (VIS lamp), with the wavelength of 368 nm and 446 nm, respectively. After the 1h long adsorption in dark a reaction mixture was sampled after 2, 4 and 6 h using a syringe and filtered using syringe filters. The changes in the PAR, IBU and DIC concentrations during the irradiation were monitored by a HPLC technique.

RESULTS AND DISCUSSION

The X-ray diffraction measurement revealed that the P25 sample is a mixture of anatase and rutile while CG300 consisted of anatase. Exfoliated graphitic carbon nitride shows diffraction lines typical for g-C₃N₄. The ability of the samples to absorb the UV-VIS light was characterized using the UV-VIS DRS. The band gap energies (E_g) were evaluated using the Tauc's plot and they are listed in Table 1. The E_g values decreased in the order CG300 > P25 > g-C₃N₄.

Table 1. The band gap energies evaluated for tested photocatalysts.

Samples	E_g (eV)
P25	3.02
CG300	3.25
g-C ₃ N ₄ _EX	2.68

General differences between intermediate products of the photodegradation of chosen pharmaceuticals were observed. Paracetamol was one of the easiest to decompose. The photodegradation process of ibuprofen produced a noticeable odor which has not been analyzed yet. During the diclofenac photodegradation a slightly pinkish solution was observed after 2-3 hours of the irradiation which vanished with longer irradiation time due to a degradation of intermediate products. The degradation efficiency of the photocatalysts increased in the order g-C₃N₄ > CG300 > P25 under the UV irradiation.

CONCLUSION

Both TiO₂ and g-C₃N₄ were indicated as the suitable photocatalysts for the degradation of paracetamol, ibuprofen and diclofenac under UVA and VIS irradiation. In the near future the degradation kinetics and intermediate products will be studied in details.

Acknowledgments: This work was financially supported by project "Institute of Environmental Technologies - Excellent Research", project No. CZ.02.1.01/0.0/0.0/16_019/0000853, by the student projects SP 2019/142 of VŠB - Technical University of Ostrava and the Czech Science Foundations (project 19-15199S).

REFERENCES

1. L. Yang, L.E. Yu, M.B. Ray. Sci. Dir. (2008) 42(13), 3480–3488.
2. L. Svoboda, P. Praus, M.J. Lima. et al. Mat.Res.Bull. (2008) 100, 323-330.

Phytotoxicity of ZnO / kaolinite nanocomposite - is the anchoring the right way to lower environmental risk?

J. Tokarský^{1,2}, K. Mamulová Kutláková², R. Podlipná³, T. Vaněk³

¹Nanotechnology centre, VŠB – Technical University of Ostrava, Czech Republic; ²IT4 Innovations, VŠB – Technical University of Ostrava, Czech Republic; ³Institute of Experimental Botany, Czech Academy of Sciences, Czech Republic

jonas.tokarsky@vsb.cz

ABSTRACT

The importance of studies on photoactive zinc oxide nanoparticles (ZnO NPs) increases with increasing environmental pollution. Since the ZnO NPs (and NPs in general) also pose an environmental risk, and since an understanding of the risk is still not sufficient, it is important to prevent their spread into the environment. Anchoring on phyllosilicate particles of micrometric size is considered to be a useful way to address this problem, however, so far mainly on the basis of leaching tests in pure water. In the present study, the phytotoxicity of kaolinite/ZnO NPs nanocomposites tested on white mustard (*Sinapis alba*) was found to be more than two times higher in comparison with pristine ZnO NPs. Also the amount of Zn accumulated in white mustard tissues and false fox-sedge (*Carex otrubae*) plants was much higher than can be expected based on the mass of ZnO NPs in the nanocomposites compared to pristine ZnO NPs. Increased phytotoxicity of the nanocomposites and higher uptake of Zn by plants from the nanocomposites in comparison with pristine ZnO NPs suggest that the immobilization of ZnO NPs on the kaolinite might not reduce the environmental risk when living organism, e.g. plants, are involved.

Keywords: zinc oxide, kaolinite, nanocomposite, phytotoxicity

INTRODUCTION

ZnO nanoparticles (NPs) exhibit photocatalytic¹, sensing², and antibacterial properties¹. However, the potential risk of pristine ZnO NPs to the environment and human health cannot be ignored^{3,4}. To avoid the risk (and also because of easier handling), many authors reported preparation of nanocomposites (NCs) – NPs anchored on phyllosilicate particles of micrometric size^{5,6} – but the stability of these NCs is commonly not reported or – in a few exceptional cases^{5,6} – it is judged solely on the basis of leaching tests in biologically blank water. So far, the only study focused on toxicity of phyllosilicate/ZnO NC (against ciliate *Tetrahymena pyriformis*) revealed an increase in toxicity of ZnO NPs in the NC. The mechanism of the toxicity is not clear⁷. No studies on the phytotoxicity of these NCs to higher plants are available. Our previous study⁶ devoted to a characterization of photoactive kaolinite/ZnO (KAZN) NCs including leaching tests in demineralized water showed that KAZN NCs could be considered stable. This result, however, is not sufficient proof of the harmlessness in real environment, particularly regarding the influence of living organisms. Therefore, phytotoxicity tests of KAZN NCs and pristine ZnO NPs on white mustard seedlings (*Sinapis alba*) and experiments monitoring the Zn accumulation in white mustard and false fox-sedge (*Carex otrubae*) have been performed in the research.

EXPERIMENTAL/THEORETICAL STUDY

KAZN NCs (10, 30, 50 wt.% of ZnO NPs) were prepared according to the previously published method⁶. Pristine ZnO NPs were purchased from Sigma Aldrich. The plants were exposed to various concentrations of KAZN NCs, pristine kaolinite, and pristine ZnO NPs (10, 100, 1000

mg/dm³), and the samples of the plants were studied using SEM (Quanta FEG 450) and AAS (GBC SensAA Dual Spectrometer) analyses. Statistical analysis was performed using STATISTICA.CZ v.12.0 software.

RESULTS AND DISCUSSION

Compared to pristine ZnO NPs (100 wt.% of ZnO), KAZN NCs exhibit higher phytotoxicity against white mustard seedlings (comparable shortening of roots was observed). The amount of Zn found in dry matter of the seedlings treated with KAZN NCs was higher (with respect to the portion of ZnO in KAZN NCs) compared to the Zn amount found in dry matter of the seedlings treated with pristine ZnO NPs. Similar results were obtained by examining the Zn accumulation in false fox-sedge. The Zn content in dry roots and dry leaflets of the false fox-sedge plants cultivated in a medium supplemented with KAZN NCs was not proportional to the percentage of Zn in the NCs (with respect to Zn content in plants cultivated in ZnO NPs-spiked medium) but higher (Fig. 1).

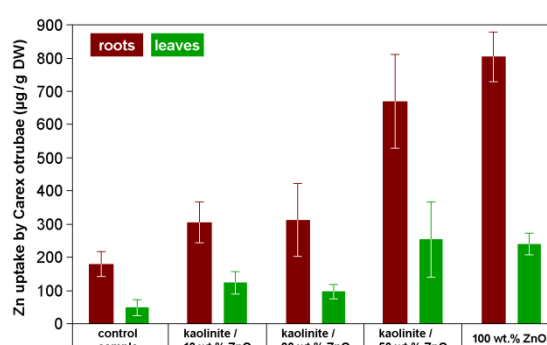


Fig. 1. Zn amount in dry matter of false-fox sedge (*Carex otrubae*) cultivated in medium supplemented by KAZN NCs and ZnO NPs (concentration 100 mg/dm³ used). is shown in Fig. 4.

Release of Zn from KAZN NCs and pristine ZnO NPs into the medium in the presence / absence of the false fox-sedge were studied. This experiment showed that the presence of the false fox-sedge increases the amount of Zn released. Detection of high Zn release rate and its accumulation in plants was confirmed by SEM analysis and EDS analysis. These analyses provided visual and quantitative evidence that ZnO NPs disappeared from the KAZN NCs during the abovementioned experiments.

CONCLUSION

With respect to the lower ZnO NPs content in KAZN NCs compared to pristine ZnO NPs, the phytotoxicity of KAZN NCs was found to be higher. Although the reason is unclear, it seems probable that lower size and larger surface area of the *in situ* prepared NPs in NCs compared to pristine NPs (i.e. properties considered positive for photocatalysis⁸) can be the cause of the observed higher phytotoxicity. Results of our study show that the KAZN NCs are unique materials and their phytotoxicity cannot be simulated using pristine ZnO NPs. The number of studies focused on NCs of the “phyllosilicate/metal oxide NPs” type continually increases and their use in practical applications is very likely in the coming years. Further research focused on toxicity of these nanocomposites is, therefore, very important and strongly encouraged.

Acknowledgments: This work was supported by the Ministry of Education, Youth and Sports of Czech Republic, grant numbers SP2019/31, 8G15003, LD14041, and LQ1602 (NPU II – IT4 Innovations Excellence in Science).

REFERENCES

1. S. Sultana, Rafiuddin, M.Z. Khan, M. Shahadat, J. Environ. Chem. Eng. 3 (2015) 886–891.
2. M.A. Iyer, G. Oza, S. Velumani, A. Maldonado, J. Romero, M.L. Munoz, M. Sridharan, R. Asomoza, J. Yi, Sens. Actuators B 202 (2014) 1338–1348.
3. V. Sharma, D. Anderson, A. Dhawan, Apoptosis 17 (2012) 852–870.
4. Z.G. Dogaroglu, N. Koleli, Clean – Soil Air Water 45 (2017) 1700096.
5. S.C. Motshekga, S.S. Ray, M.S. Onyango, M.N.B. Momba, J. Hazard. Mater. 262 (2013) 439–446.
6. K. Mamulová Kutláková, J. Tokarský, P. Peikertová, Appl. Catal. B 162 (2015) 392–400.
7. G.S. Gupta, V.A. Senapati, A. Dhawan, R. Shanker, J. Colloid Interface Sci. 495 (2017) 9–18.
8. B. Szczepanik, Appl. Clay Sci. 141 (2017) 227–239.

Application of bentonite-manganese oxide composites in removal of heavy metals

S. Dolinská^{1*}, I. Znamenáčková¹, J. Tomčová¹, V. Valovičová², L. Vaculíková², E. Plevová²

¹Institute of Geotechnics of the Slovak Academy of Sciences, Watsonova 45, 04001 Košice, Slovakia;

²Institute of Geonics of the Czech Academy of Sciences, Studentská 1768, 708 00 Ostrava-Poruba, Czech Republic

sdolinska@saske.sk

ABSTRACT

The paper is aimed on the using of non-homogeneous bentonites coated by manganese oxides for the removal of heavy metal cations from the water solutions. In the first stage Slovak natural bentonite was converted to sodium form using by Na_2CO_3 as the activating agent. After that the manganese oxides were precipitated on the surface of natural and sodium activated bentonite, respectively. The structural changes before and after the modifications of bentonites were characterized by X-ray diffraction analyses and X-ray photoelectron spectroscopy. To compare the sorption properties of the natural bentonite and modified bentonites, sorption experiments of Cd^{2+} from aqueous solutions were done.

Keywords: bentonite, composites, adsorption

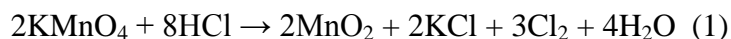
INTRODUCTION

Bentonite is one of the most popular clay rocks with exceptional adsorption properties. The main clay mineral present in bentonite is montmorillonite which belongs to the smectite mineral group. The properties of bentonite result from the crystal structure of this group. The particles of montmorillonite have negative charges on their faces due to the isomorphic substitutions in its structure. This negative charge is compensated by the presence of the cations in the interlayer space, which are not fixed and have the character of so called “exchangeable cations” (i.e. Na^+ , K^+ , Li^+ , Mg^{2+} , Ca^{2+}) [1]. This study focused on the preparation of composites containing either natural or natrified bentonite and manganese oxides. The immobilization of manganese oxides on bentonite surface could lead to the improvement of the bentonite sorption properties and also to overcome the limits to the use of pure manganese oxides as adsorbents due to the e.g. economic reasons [2]. The most common form of manganese oxides in nature are poorly crystalline materials like birnessite or vernadite [3].

EXPERIMENTAL/THEORETICAL STUDY

The bentonite from the Slovak deposit Stará Kremnička – Jelšovský potok which contained an almost monomineral fraction of montmorillonite (>90%) [4]. At first the natural bentonite was simple

chemically modified by nitrification. Nitrification salt Na_2CO_3 is used almost exclusively thanks to its financial accessibility. The composites manganese oxide + bentonite (Mn-B), manganese oxides + nitrified bentonite (Mn-NaB) and reference sample of "pure" manganese oxides (Ref-Mn) were gained using reductive precipitation of manganese oxides both in a weight ratio of 1:1 (manganese oxides : natural materials). The process of precipitation followed the reaction 1:



The effective connection of manganese oxide with the bentonite was confirmed mainly by the results of the X-ray diffraction analysis and X-ray photoelectron spectroscopy.

RESULTS AND DISCUSSION

The X – ray diffraction analysis of natural bentonite (B) confirmed montmorillonite as dominant mineral phase. The activation of montmorillonite by Na^+ cations caused structural changes which principally affected the movement of montmorillonite main (001) reflection to the right on x axis.

Reference sample of manganese oxides with the strongest reflection of d_{001} value of 0.717 nm corresponds to birnessite-type manganese oxide according to the X-ray diffraction analysis. Precipitation of manganese oxides on bentonite caused structural changes of both composites Mn-B and Mn-NaB.

The XPS spectrum of Mn-B and Mn-NaB (Fig. 1) confirm that natural bentonite surfactants were coated with manganese oxides because the same lines were present as in the sample (Ref-Mn). In addition, other calcium (Ca 2p, Ca 2s) lines from bentonite matrix were also used. The main aim of The detailed Mn 2p line measurements were made at high resolution in the 630 - 660 eV binding energy range. The presence the Mn^{4+} in the manganese-modified sample was confirmed.

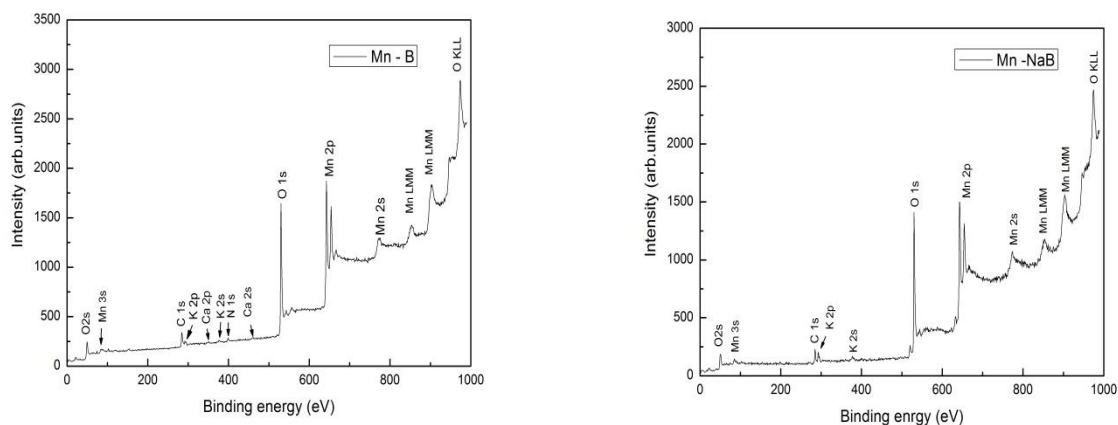


Fig. 1 X-ray photoelectron spectrum of Mn-B and Mn-NaB

The adsorption parameters were calculated through Langmuir model due to the fact that sorption data were well fitted to the linear form of the Langmuir isotherm. The obtained values of maximum adsorption capacities [mg/g] were: 63.29 (natural bentonite), 72.99 (natrified bentonite), 103.09 (Mn –B) and 108.69 (Mn-NaB).

CONCLUSION

The adsorption experiments with the modified forms of the bentonite, confirmed significant improvement of the adsorption properties of the natural materials at adsorption of Cd^{2+} after their modification by the manganese oxides. XPS measurements in manganese-modified bentonite samples was to determine the manganese chemical status.

Acknowledgments: This work was also supported by the Slovak Grant Agency for Science VEGA grant No. 2/0055/17. The research has also been done in connection with Project “Institute of Clean Technologies for Mining and Utilization of Raw Materials for Energy Use”- Sustainability program. Identification code: LO1406. The project is supported by National Programme for Sustainability I (2015-2019) and financed by the means of state budget of the Czech Republic.

REFERENCES

1. M. Galamboš, J. Kufčáková, O. Roskopfová, P. Rajec, *Journal of Radioanalytical and Nuclear Chemistry* 283 (3), (2010), 803-813.
2. D. Frías, S. Nousir, I. Barrio, M. Montes, T. López, M. Centeno, J. Odriozola, *Materials Characterization* 58 (8-9), (2007) 776-781.
3. S. Taffarel, J. Rubio. *Minerals Engineering*, 23 (14), (2010) 1131–1138.
4. J. Jesenák, V. Hlavatý. *Laboratory Device for Sedimentation of fine Bentonite Fractions*, *Scripta Facultatis Scientiarum Naturalium Universitatis Masarykianae Brunensis Geology* 28-29, (2000), 33-36.

TOPIC 6

Industrial Forum



Oral presentations (OP):**AFM-in-SEM LiteScope™: Tool for comprehensive sample surface analysis**

J. Neuman¹, Z. Novacek¹, V. Novotna¹, V. Hegrova², M. Pavera¹

¹NenoVision s.r.o., Brno, Czech Republic, ²Institute of Physical Engineering, Brno University of Technology, Brno, Czech Republic

Jan.neuman@nenovision.com

ABSTRACT

Compact AFM LiteScope™ integrable into variety of SEMs is presented. This device provides benefits of both, AFM and SEM, techniques and extends application possibilities. Moreover, it is equipped with unique CPEM™ technology providing a true correlative measurement of multiple signals at the same time, coordinates and sample conditions. Practical advantages cover precise AFM tip navigation, in-situ 3D imaging, depth/height profiling, surface roughness estimation, a variety of spectroscopic regimes or local electric conductivity measurement. Fields of application and capabilities of the device are shown on various samples and materials.

Keywords: AFM, SEM, Correlative Imaging, CPEM.

INTRODUCTION

Precise and complex analysis using multiple techniques provides deeper knowledge about the examined sample and is advantageous for successful research in many scientific fields. Atomic force microscopy (AFM) and scanning electron microscopy (SEM) are widely used techniques for imaging the nanoworld in fields of material sciences, nanotechnology, semiconductors or life sciences. AFM LiteScope™ integrated into the SEM enables to combine and to benefit from both of them [1]. LiteScope™ uses a unique technology for correlative measurement called CPEM which will be described later.

EXPERIMENTAL/THEORETICAL STUDY

AFM-in-SEM LiteScope™ is the focus of this paper. It uses the CPEM (Correlative Probe and Electron Microscopy) technology which is the key to precise complex surface sample analysis. When using this technique neither the AFM probe nor the electron beam is scanning over the sample. The movement is done by a piezo scanner with the sample. It is very advantageous that the AFM tip and electron beam have a constant shift, and images from both modalities are obtained simultaneously at the same conditions including pixel size, coordinate and scanning system (see Fig. 1). Multiple AFM signals (topography, energy dissipation, sample stiffness), SEM signals from different detectors (SE, BSE) or related techniques like EBIC, CL can be obtain using CPEM. Each signal is represented by a unique mask (color) and brings new information for further sample analysis.

RESULTS AND DISCUSSION

AFM LiteScope™ can be used for a variety of applications ranging from complex characterization of 1D, 2D and 3D nanostructures, analysis of metals and polymers to failure analysis of semiconductors, solar cells or nanodevices. However, new and innovative applications of AFM-in-SEM are yet to be discovered. Thanks to CPEM technology, complex information is obtained during a single acquisition. It is a great tool for in-situ analysis of etched structures which would be

negatively affected when exposed to air. Example of this kind of sensitive sample is in Fig. 2. where the surface of CdTe is modified by FIB. LiteScope™ can serve perfectly for fast etching dose optimization [2].

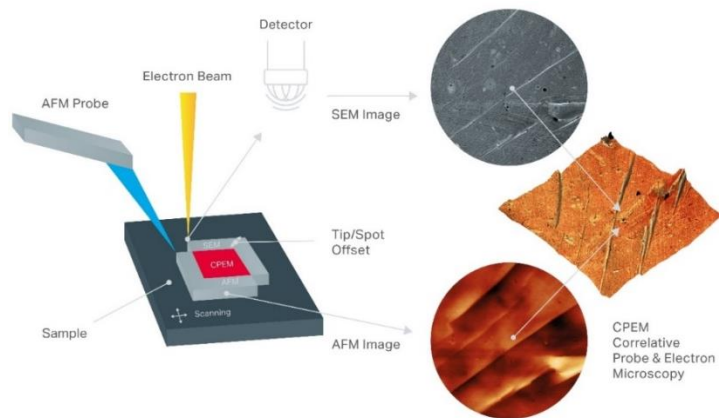


Fig. 1. The principle of CPEM (Correlative Probe and Electron Microscopy)

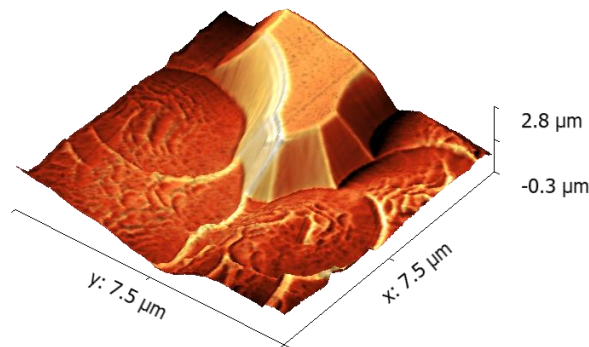


Fig. 2. Surface modification of cadmium telluride (CdTe) by the focused ion beam.

CONCLUSION

AFM LiteScope™ with CPEM technology is a strong tool for surface sample analysis revealing new details of the studied sample in one shot measurement. It gives new opportunities for applications which could not be performed on separated machines like for example in-situ analysis of samples after surface modification by various techniques or precise localization and analysis of 1D, 2D, and 3D nanostructures. Combination of AFM and SEM is very powerful and new applications are being studied bringing even more benefits for the customers.

Acknowledgment: Authors of this paper acknowledge financial support from the Technology Agency of the Czech Republic, programme Zeta, project Development of SPM Applications Suitable for Correlative Microscopy no. TJ01000434.

REFERENCES

1. NenoVision s.r.o., LiteScope™, NenoVision, 2018, www.nenovision.com/
2. O. Šik, P. Bábor, P. Škarvada, M. Potoček, T. Trčka, L. Grmela, E. Belas, Investigation of the effect of argon ion beam on CdZnTe single crystals surface structural properties, Surface and Coatings Technology, Volume 306, Part A, 2016, Pages 75-81.

Scattering-Type Scanning Near-field Optical Microscopy and Spectroscopy of Low Dimensional and nanostructured materials

A. Cernescu¹, S. Amarie¹, J. Vávra¹

¹neaspec GmbH, Eglfinger Weg 2, 855 40 Haar

jan.vavra@neaspec.com

ABSTRACT

Scattering-type Scanning Near-field Optical Microscopy (s-SNOM) is an optical microscopy and spectroscopy approach based on scanning probe technology, bypassing the ubiquitous diffraction limit of light to achieve a spatial resolution below 20 nanometers. s-SNOM employs the strong confinement of light at the apex of a sharp metallic AFM tip to create a nanoscale optical hot-spot. Analyzing the scattered light from the tip enables the extraction of the optical properties (absorption, reflectivity) of the sample directly below the tip and yields nanoscale resolved images and nanoscale spectroscopy (hyperspectral nano-FTIR) information simultaneous to topography. In this presentation we will introduce the basic principle of near-field microscopy and hyperspectral nano-FTIR for imaging and spectroscopy with 10 nanometer spatial resolution. In addition we will summarize the latest achievements in the field of near-field microscopy and spectroscopy on polymers, biomaterials and 2D materials and will focus on applications in chemical analysis and material identification at the nanoscale.

REFERENCES

1. F. Huth, et al., Nano Lett. 12, 3973 (2012).
2. C. Westermeier et al., Nat Commun. 5, 4101 (2014).
3. I. Amenabar, et al., Nature Commun. 8, 14402 (2017).

Industrial Applications of Nanotechnologies

L. Lyapeikov, A. Chepak

NANO CHEMI GROUP s.r.o., Praha; Czech Republic

lev.lyapeikov@nanochemigroup.cz; alexandra.chepak@agchemigroup.eu

ABSTRACT

Nano Chemi Group is a high-tech enterprise focusing on research, development, and commercialization of own industrial solutions based on a range of nanoproducts. We closely cooperate with renowned research institutions, universities, national laboratories, and innovative corporate giants in Europe and beyond its borders.

Thanks to tight connections and support from our reliable suppliers we have a chance to introduce materials as carbon nanoparticles, metal and alloy nanoparticles, oxide and rare earth oxide nanoparticles, compound nanoparticles to the market.

The strategy is to concentrate on present challenges of the Energy, Construction, Transportation, 3D printing, and Electronic sectors so far as the use of nanotechnology accomplish the possibility of making lots of materials stronger, lighter, durable, reactive or even better conductors of electricity among several other useful properties. That is the reason our team already achieved successful results in elastomers, polymers, and composite fields and we do believe that nanotechnology will

strongly revolutionize and improve many areas and directions of our lives. NANO CHEMI GROUP aims to bring up-to-date, effective, and beneficial solutions by delivering high-quality nano formulated products and providing substantial technical support to our customers.

Research and development of nanotechnologies and nanomaterials

Kotzianová¹, J. Klemeš¹, M. Pokorný¹, V. Velebný¹

¹Contipro a.s., Dolní Dobrouč, Czech Republic

kotzianova@contipro.com

ABSTRACT

Contipro is a Czech biotechnological company and one of the world's leading manufacturers of hyaluronic acid. In addition to manufacturing, the company also includes research with more than ten research departments including Nanotechnology. Hyaluronic acid is a natural biopolymer, which has great potential not only in cosmetics but also in a field of tissue engineering, drug delivery or wound healing. Each application has its own specific requirements which define a form of hyaluronic acid and a final structure. One of the final structures which can be prepared from both the native form of hyaluronic acid and its derivatives are nanofibers. To make nanofibers from hyaluronic acid, Contipro developed a laboratory device for electrospinning – 4SPIN LAB. So far, more than 25 different raw materials and their derivatives from the group of natural and synthetic polymers have been electrospun into a form of nanofibers. Using the 4SPIN LAB it is also possible to combine polymers with each other or add additives (API, inorganics, cosmetic ingredients etc.) and prepare composite structure with a highly defined structure. These materials have become to be substantial support for regenerative medicine and tissue engineering applications research.

SPONSORS





Malvern Panalytical je jedničkou na trhu stanovení distribuce velikosti, zetapotenciálu, molekulové hmotnosti a od loňského roku též koncentrace (nano)částic v kapalných disperzích.

Zetasizer Ultra

Dynamický (DLS) a elektroforetický rozptyl světla

Velikost částic: 0,3-10 000 nm
Zeta potenciál: > +500 mV
Koncentrace částic: 10^8 - 10^{12} Au částic/ml

Obsahuje zcela novou víceúhlovou DLS technologii pro vyšší rozlišení jednotlivých píků a stanovení koncentrace

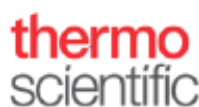


NanoSight NS300

Analýza trasování částic (ISO 19430:2016)

Velikost částic: 10-2 000 nm (záv. na mat.)
Koncentrace částic: 10^6 - 10^9 částic/ml

Rozlišení původu částic použitím fluorescenčního značení a filtrování, lasery o vlnových délkách 405, 488, 532, 638 nm.



Authorized Distributor

Thermo Scientific: stolní rastrovací elektronové mikroskopy řady **Phenom** poskytují revolučně intuitivní způsob ovládání, rychlou práci a kvalitní snímky jak z SED a BSD tak prvkové složení z EDS detektorů. Důraz je dále kladen na SW automatizaci snímání a vyhodnocení dat nejen pro průmyslové použití.

Phenom Pharos – první stolní SEM s Schottkyho zdrojem elektronů

- Rozlišení < 3 nm, zvětšení až 1 000 000x
- Vzorky až Ø 3,2 x 10 cm, mnoho příslušenství a SW
- První elektronový snímek po vložení vzorku do 25 s
- Motorizovaný stolek (X,Y), jedna optimální pracovní vzdálenost pro všechny detektory
- Optický a elektronový náhled pro rychlou orientaci a přesun kliknutím do oblasti zájmu
- Snížení nabíjení vzorku při středním či nízkém vakuu
- Jednoduchá obsluha, přívětivá cena



ANALYTICAL & MEASURING & TESTING

Blíže informace o produktech těchto firem vám sdělíme na našem stánku či je najdete na webu www.anamet.cz

Materiálová tiskárna Fujifilm Dimatix



252 10 Mníšek pod Brdy
Lhotecká 594
Tel.: 318 599 083
info@chromspec.cz

634 00 Brno
Plachty 2
Tel.: 547 246 683
www.chromspec.cz

Nový analyzátor kontaktního úhlu THETA FLEX



 **Attension**
[Together with Biolin Scientific]

CHROMSPEC
SPOL. S R.O.

252 10 Mníšek pod Brdy
Lhotecká 594
Tel.: 318 599 083
info@chromspec.cz

634 00 Brno
Plachty 2
Tel.: 547 246 683
www.chromspec.cz



EDLIN, s.r.o., Za Kralupkou 440, 277 11 Libiš, ČR
Tel. +420.603250268, zemek@edlin.cz

Systémy fy Technoorg pro přípravu TEM a SEM vzorků iontovým leštěním



IV7 UniMill pro přípravu TEM vzorků



SC-2000 pro přípravu vzorků pro SEM a EBSD

UHR naprašovačka Q150V fy Quorum

- ultrajemné naprašování pro zvětšení > 200.000x
- pracovní vakuum až 1×10^{-6} mbar
- tvorba tenkých uhlíkových vrstev
- ušlechtilé i oxidující kovy



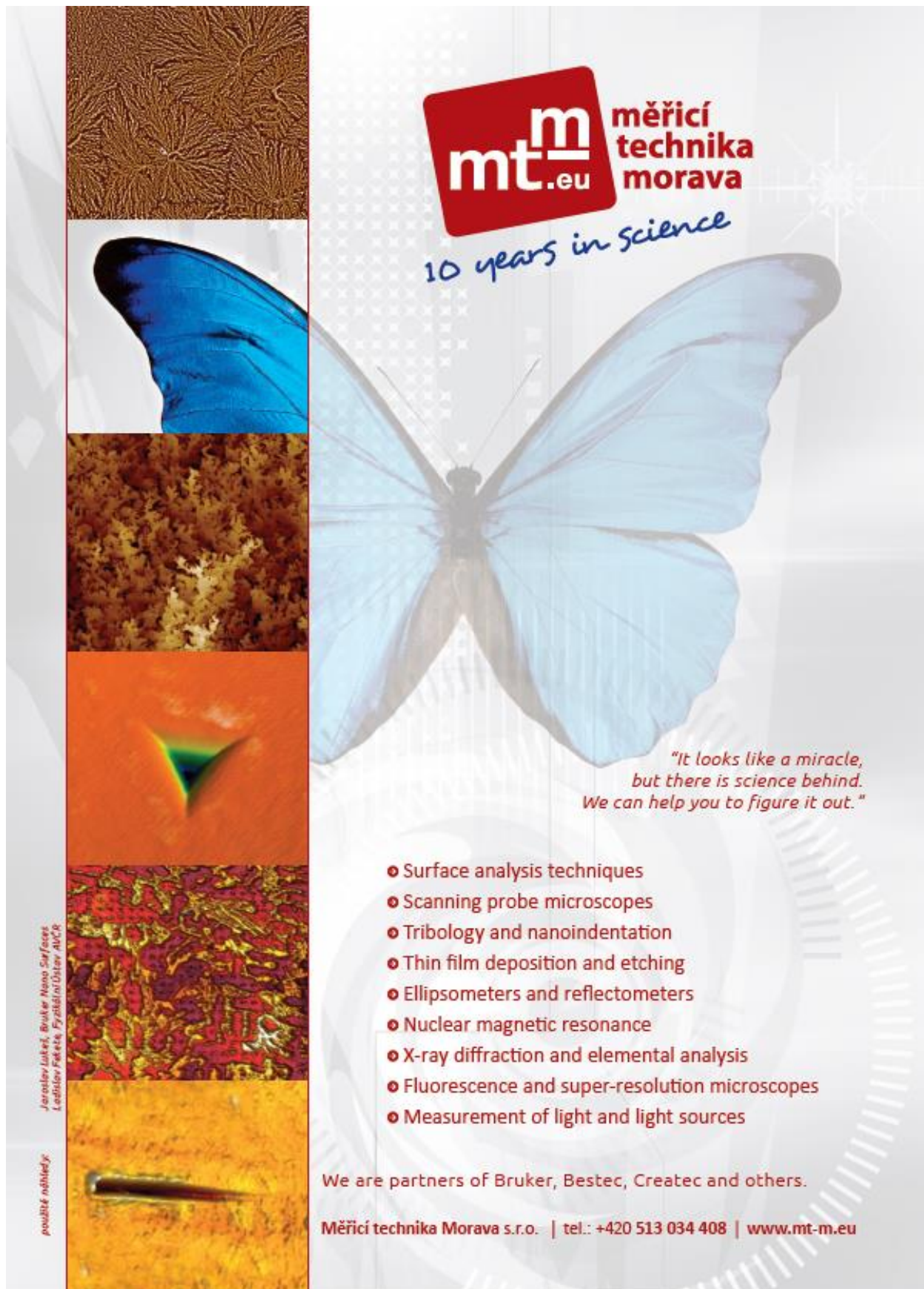
Plasmový čistič Plasma Prep III fy SPI

- použití pro SEM i TEM vzorky
- velká válcovitá komora
- volba reaktivních plynů
- tvorba RF plasmy
- pracovní rozsah 1 – 1000 W



Zařízení a služby pro elektronovou a optickou mikroskopii
Naši partneři: Quorum Ltd., Technoorg-Linda, Protochips, Graticules Optics, SPI

www.edlin.cz



mt^m.eu měřicí technika morava

10 years in science

*"It looks like a miracle,
but there is science behind.
We can help you to figure it out."*

- Surface analysis techniques
- Scanning probe microscopes
- Tribology and nanoindentation
- Thin film deposition and etching
- Ellipsometers and reflectometers
- Nuclear magnetic resonance
- X-ray diffraction and elemental analysis
- Fluorescence and super-resolution microscopes
- Measurement of light and light sources

We are partners of Bruker, Bestec, Createc and others.

Měřicí technika Morava s.r.o. | tel.: +420 513 034 408 | www.mt-m.eu

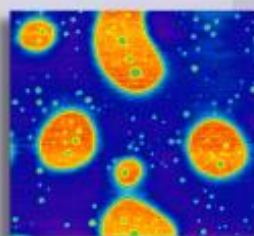
Jaroslav Lukeš, Bruker Nano Surfaces
Leobslav Pátek, Pyralis Ostrav AUCR

použití náhledy:

Dotkněte se nanosvěta

s IR-SNOM a Ramanovou spektroskopií

Touha objevovat stále nové a nepoznané provází lidstvo odnepaměti. Od okamžiku, kdy pravěký člověk poprvé spatřil plamen, uplynula dlouhá doba a z lidí jeskynních se vyvinul Homo scientificus s neustálou touhou zkoumat okolní svět. Společnost Nicolet CZ proto nabízí řadu vysoce sofistikovaných laboratorních systémů: FT-IR spektrometry schopné měřit ve všech oblastech infračerveného spektra (NIR-MIR-FAR), Ramanovy spektrometry a IR-SNOM, což je mikroskopická technika překonávající difrakční limit.



SNOM (scanning near field optical microscopy, optická skenovací mikroskopie v blízkém poli) je nová metoda, která překonává rozlišovací limit díky vlastnostem tlumených vln. Při měření se ultratenký kovový hrot ozařovaný infračerveným zářením pohybuje těsně nad povrchem vzorku, v kterém indukuje dipólový moment. Ten následně výrazně zesílí rozptylované záření, a prostorové rozlišení metody tak závisí pouze na průměru použitého hrotu, což může být i pouhých deset nanometrů. Využívá neškodné IR záření

a je vhodná např. pro studium indexu lomu, zjišťování chemické struktury, sledování mechanické deformace, krystalické fáze vzorku, orientace jednotlivých molekul, mapování povrchů (AFM) nebo rozložení náboje. Je rovněž možné zobrazovat jednotlivé molekuly proteinů či virové částice, a to vše bez poškození vzorku.

Další nedestruktivní metodou je Ramanova spektroskopie a mikroskopie. K analýze využívá laserové záření jedné vlnové délky, a to buď UV, viditelné nebo infračervené. Ve svém principu je Ramanova spektroskopie komplementární metodou k IR spektroskopii, a tak je možné kombinací těchto dvou metod analyzovat jakoukoliv molekulu. Ramanův mikroskop DXR2xi je schopný získat miliony spekter během několika desítek minut s rozlišením 0,5 mikrometru a současně získávat informace o topografii a struktuře vzorku (AFM). Své uplatnění tak nalézá nejen při studiu biologických a farmaceutických vzorků, ale také při analýze materiálů. Dokáže rovněž rozlišit jednotlivé polymorfy látek.



NICOLET CZ
MOLECULAR SPECTROSCOPY

www.nicoletcz.cz

MOLEKULOVÁ SPEKTROSKOPIE

POHLÉDNĚTE NA SVĚT NAŠÍ OPTIKOU

DLOUHÁ ŽIVOTNOST | ŠPIČKOVÝ VÝKON | ŠIROKÁ NABÍDKA PŘÍSLUŠENSTVÍ | JEDNODUCHÉ OVLÁDÁNÍ

Z NAŠÍ NABÍDKY VYBÍRÁME:

FTIR spektrometry série VERTEX

- Nejvýkonnější výzkumné spektrometry na trhu
- Maximální citlivost díky vakuu pod 0.2 hPa
- Propojení s mikroskopem, Ramanem, TGA, GC...
- Rozšíření spektrálního rozsahu od FIR/THz do VIS/UV oblasti (3–50.000 cm⁻¹)
- Časově rozlišená spektroskopie (až 110 spekter/s)



Vakuový FTIR spektrometr Vertex 80v s mikroskopem HYPERION 3000

Pokročilý Ramanův mikroskop SENTERRA II

- Až 4 excitační lasery v rozmezí 488–1064 nm
- Možnost kombinace FT-Ramana s disperzním
- Jednoduché a rychlé mapování až 100 spekter/s
- Prostorové rozlišení až 500 nm



Ramanův mikroskop SENTERRA II




www.brukeroptics.cz



NenoVision

AFM Specially Designed for SEM

LiteScope™

- Plug-and-play AFM solution for SEM microscopes
- The advantage of combined AFM and SEM techniques
- Precise AFM tip navigation with nm precision
- Advanced in-situ sample surface analysis (depth/height profiling, roughness estimation, in-situ 3D imaging, topography vs material contrast, local spectroscopy measurement)



Patented and Brand-New Correlative Probe and Electron Microscopy Technique – CPEM™

Explore variety of Applications

- Characterization of 1D, 2D, and 3D nanostructures
- Nanodevices
- Metals
- Polymers
- Solar cells
- Failure analysis of semiconductors



Characterization of 2D WS₂ layers on 1D Si nanowires



CPEM Correlative Probe & Electron Microscopy

FREE OF CHARGE MEASUREMENT

September–October 2019

Contact us and book your time slot!

www.nenovision.com



Rigaku

Leading With Innovation

XRF SOLUTIONS

Powerful, easy-to-use XRF systems: more users, more samples, more results



ZSX Primus IV



NANO Hunter II



Supermini200



Micro-Z ULS

XRF spectrometer for elemental analysis

- Tube-above optics
- Unmatched light-element performance
- Industry-leading stability and precision
- Sequential analysis
- Simultaneous available with XRD channel

Benchtop TXRF for trace analyses

- GI-XRF capability for thin film characterization
- Quantify to parts-per-billion (ppb) levels
- 600 W X-ray tube for fast measurements
- Silicon drift detector (SDD)
- 16 position autosampler
- High sensitivity for As, Se and Cd
- Perfect for nano-particle analysis

Wavelength dispersive fluorescence analyzer

- Benchtop WDXRF with minimal footprint
- No cooling water required for flexible installation
- Excellent resolution and sensitivity for light element analysis
- Standard less or quantitative analysis from Sodium to Uranium
- Ideal as a backup system for large floor-standing units in mining, metals & cement

Ultra low sulfur by D2622

- Ultra-low sulfur analysis of diesel and gasoline
- 0.3 ppm lower limit of detection (LLD)
- No He(g) purge required
- Easy-to-use benchtop analyzer

VISIT US AT BOOTH #20

Rigaku Corporation and its Global Subsidiaries

Hugenottenallee 167 | 63263 Neu-Isenburg, Germany | TEL +49 610 277 99 - 951 | www.Rigaku.com | rese@Rigaku.com

Autor: Ing. Sylva Holešová, Ph.D.

Katedra, institut: Centrum Nanotechnologií - 9360

Název: NanoOstrava 2019 – 6th Nanomaterials and Nanotechnology Meeting

Místo, rok, vydání: Ostrava, 2019, 1. vydání

Počet stran: 210

Vydala: Vysoká škola báňská-Technická univerzita Ostrava

Tisk: Ediční středisko, Vysoká škola báňská-Technická univerzita Ostrava

Náklad: 120

Neprodejné

ISBN 978-80-248-4290-5